MAGNESIUM TRANSPORT IN FERRET RED CELLS.

Lorraine M. Smith.

Thesis submitted as a requirement for the degree of Doctor of Philosophy, University of Edinburgh, 1993.

Declaration

The composition of this thesis, and the work described therein, is my own. Parts of this work have already been published and copies of the papers are included. This project was funded by the Wellcome Trust of Great Britain.

Lorraine Smith

September 1993.

Acknowledgments

I gratefully acknowledge the assistance of the following people in the completion of this thesis.

My supervisor, Dr. Peter Flatman for his guidance in this project, his teaching and friendship. I am particularly grateful to Peter for his patience and understanding during the writing of this thesis.

Dr. David Ellis for reading the manuscript and providing many useful comments and encouragement.

Dr. Iain Gow for reading parts of this thesis and providing constructive criticism and assistance with computers and printers.

Zoé Thomson and Jill Prentice for tea and sympathy when most needed.

Mum and Dad - as always.

ABSTRACT

Magnesium transport across membranes was investigated in ferret red cells. Both Mg efflux and influx were measured. Mg transport was found to have the following properties.

1. Mg efflux from unloaded, untreated ferret red cells is 44 ± 2 μmol(l cell)$^{-1}h^{-1}$ (mean ± S.E.M. n=38).

2. Mg efflux is partially inhibited by amiloride, quinidine, quinine, imipramine and divalent cations. Efflux is stimulated by SITS (4-acetamido-4'-isothiocyanato-stilbene-2,2'-disulfonic acid) and unaffected by vanadate.

3. Mg efflux is stimulated by the depletion of cell ATP. Reducing the cell ATP content reduces the Mg buffering capacity of the cells and thus increases the internal free Mg concentration ($[Mg^{2+}]_i$). This increase in $[Mg^{2+}]_i$ may account for some of the stimulation of Mg efflux.

4. Reducing external Na ($[Na_o]$) from 145 to 10 mM (Na replaced with choline chloride) stimulates Mg efflux. However Mg efflux is inhibited when $[Na_o]$ is below 10 mM. Net uptake of Mg is measured when $[Na_o]$ is maintained below 1 mM even if the extracellular medium contains only contaminant Mg (Mg is transported against its electrochemical gradient). Changes in the membrane potential are not responsible for this net uptake. These results show that the system is capable of reversing direction and mediating active transport.

5. Net Mg uptake in media with low $[Na_o]$ is stimulated when $[Mg_o]$ is greater than 1 mM. The stimulated uptake is partially inhibited by amiloride, quinidine, imipramine, NEM (N-ethylmaleimide) and cobalt. Net uptake is stimulated by vanadate and inhibited by reducing cell ATP.

6. Mg uptake observed at low $[Na_o]$ was exploited to load cells with Mg. Efflux from cells loaded in this way increases steeply when $[Mg^{2+}]_i$ is more than 1 mM.

7. Cells were also loaded with Mg using the ionophore A23187. It was possible to load the cells to more variable concentrations of $[Mg^{2+}]_i$ using the ionophore.

8. Possible models for Mg transport are discussed. There is strong evidence for a reversible Na-Mg antiport in these cells. There is also a route for Mg efflux which is insensitive to Na gradient. In response to a large Mg load Mg is lost rapidly possibly via the opening of a Mg - permeant channel.

List of abbreviations.

$[X]_o$ = the external concentration of X

cell [X] = the total intracellular concentration of X

$[Mg^{2+}]_i$ = the intracellular ionized concentration of Mg

$moles(l.cells)^{-1}$ = mole concentration per litre of cells

$moles(l.o.c.)^{-1}$ = mole concentration per litre of original cells

DGDW = double-glass distilled water

DIDS = 4,4'-diisothiocyanato-stilbene-2,2'-disulfonic acid

DMSO = dimethyl sulphoxide

DMF = dimethyl formamide

EDTA = ethylene diamine tetraacetic acid

EGTA = ethylene-bis-(ß-amino-ethyl ether) N,N'-tetra-acetic acid

NMDG = N-methyl-*D* glucamine

PCMBS = parachloromercuribenzene sulphate

SITS = 4-acetamido-4''isothiocyanato-stilbene-2,2'-disulfonic acid

TCA = trichloroacetic acid

Contents.

Contents (continued).

Contents (continued).

Contents (continued).

1. Introduction

Magnesium is the fourth most abundant cation in the human body. The normal human body contains approximately 21 - 28g of Mg. Most of this (60%) is mineralised in the crystal lattice of bone. The remainder is found mainly in the intracellular compartments of soft tissue with a small amount (1%) in the plasma and extracellular fluid (Wacker,1980; Walser,1967; Ebel and Günther, 1980).

Mg has many important roles in the body. Mg is required for the formation of the tertiary structure and insertion of many proteins in the membrane (Wacker, 1980) and Mg is essential for DNA replication as it stabilises the structure of the ribosomes (Ebel and Günther, 1980). There is also evidence that Mg regulates the stability of the cell membrane (Heaton *et al*, 1987; Tomov *et al*, 1988 and Beaven *et al*, 1990). Apart from its role in maintaining the structure of the cell, Mg also regulates much of the enzymatic activity in the cells including kinases, phosphatases, and the enzymes of glycolysis and respiration (Williams, 1993; Aikawa, 1963; Heaton, 1993). The action of Mg as a regulator of ion transport in cells has been reviewed by Flatman (1993). ATP-utilising transport (such as the fluxes of the Na-K-ATPase (Flatman and Lew, 1981; Ellory, Flatman and Stewart, 1983; Flatman, 1993) and the calcium pump (Schatzmann, 1983)), cotransport systems (such as Na-K-Cl and K-Cl cotransport (Ellory, Flatman and Stewart, 1983; Flatman, 1993)) and proteins

mediating exchange processes (such as Na-H exchange; Parker, Gitelman and McManus, 1989; Flatman, 1993) have all been shown to be sensitive to changes in [Mg]. Interestingly for many of these transport systems, both low and high Mg concentration can inhibit transport (Flatman,1993). Changes in cell [Mg] may not be large enough to suggest that it regulates by a simple `on-off' mechanism. However changes in cell [Mg] over quite a narrow range may be enough to alter the activity of many cellular enzymes.

Some Mg is bound within the cell.

Much of the total Mg in the cells is bound to proteins or sequestered in organelles (Ebel and Günther, 1980). Mg binds strongly to polyvalent anions such as some proteins and RNA. Mg may not be easily removed from some of these sites. Thus of the total cell [Mg] only a fraction of it is free to move in and out of the cell and bind to any transport or regulatory sites. Mg also binds to other species (such as phosphates) which can give up Mg more readily (Nanninga, 1961). Thus the ratio of intracellular ionized [Mg] ($[Mg^{2+}]_i$) to the intracellular bound [Mg] in the cell may change depending on the number and availability of binding sites for Mg in the cell. Changes in, for example, cell metabolism, pH, cell volume and oxygenation (for red cells; Bunn, Ransil and Chao, 1971) which can alter the availability of Mg binding sites in the cells may thus change the

concentration of $[Mg^{2+}]_i$.

Measurement of intracellular ionized [Mg].

Despite the large concentrations of Mg in the tissues (Mg is the second or third most abundant intracellular cation), little was known of its regulation and transport until relatively recently. Research into the distribution and movement of Mg was greatly aided by the development of and improvement in techniques such as atomic absorption spectrophotometry (AAS) which have enabled more precise and reproducible measurements of Mg to be made (Walsh, 1955).

AAS measures the total cell [Mg]. Measurements of $[Mg^{2+}]_i$ can only be made by knowing how much of the total cell [Mg] is bound. Flatman and Lew (1977) developed the null point method for estimating $[Mg^{2+}]_i$ using the ionophore A23187 to permeabilise the membrane to Mg. In a Ca-free medium the addition of A23187 selectively increases the membrane permeability to Mg^{2+} which is exchanged for $2H^+$. When the null point is reached and $[Mg^{2+}]$ and $[H^+]$ are in equilibrium, $[Mg^{2+}]_i$ can be calculated using the following equation

$$[Mg^{2+}]_i = [Mg^{2+}]_o * \left(\frac{[H^+]_i}{[H^+]_o}\right)^2 \qquad \textbf{1.1}$$

The null point method does not directly measure $[Mg^{2+}]_i$ and thus the estimation of $[Mg^{2+}]_i$ relies heavily on the measurement of other factors such as

internal and external pH. It is also difficult to obtain reliable results in cells which contain intracellular organelles as A23187 increases the Mg permeability of the membranes bounding the organelles as well as the cell. Mg is thus distributed according to the number of Mg binding sites in the cytoplasm and the intra-organelle space.

The null point method requires fairly large populations of cells. This makes this method more applicable to cell types which can be collected in relative abundance rather than those cells where measurements are made more appropriately on single cells. Reviews of other methods of measuring $[Mg^{2+}]_i$ are provided by Alcock (1969), Tsien (1983) and Alvarez-Leefmans, Giraldez and Gamiño (1987).

$[Mg^{2+}]_i$ can be measured using metallochromic indicators such as Eriochrome Blue (Scarpa, 1974). The absorption spectra of these dyes changes on the binding of Mg^{2+}_i. The most successful of these compounds have very low affinities for Mg^{2+}_i and so do not significantly alter the binding capacity for Mg^{2+}_i in the cell (Alvarez-Leefmans, Giraldez and Gamiño, 1987). Metallochromic dyes are also sensitive to changes in other cell constituents such as $[Ca^{2+}]$ and $[H^+]_i$ (De Weer,1976; Baylor *et al*, 1982). Therefore independent assessments of $[Ca^{2+}]$ and $[H^+]_i$ must be made to correct the measured values of $[Mg^{2+}]_i$. Experimental conditions must be set to ensure that there are no large changes in either $[Ca^{2+}]_i$ or $[H^+]_i$ during the measurement of $[Mg^{2+}]_i$. It is possible that

other intracellular factors may affect the ability of these compounds to bind Mg^{2+}_i. Metallochromic indicators provide a non-destructive measurement of $[Mg^{2+}]_i$ and are most easily used in large cells (Table 1.1).

$[Mg^{2+}]_i$ can also be measured by fluorescence (Tsien, 1989). A chelator with increased Mg-selectivity (APTRA) was formed by modifying the Mg buffering compound EDTA. From this compound the fluorescent Mg indicator, FURAPTRA, was formed (Raju *et al*, 1989). FURAPTRA (or Magfura-2) has similar spectral properties to the fluorescent Ca indicator Fura-2. The binding of Mg^{2+} causes a shift in the maximum excitation wavelength of Magfura-2. $[Mg^{2+}]_i$ can be calculated from the ratio of the fluorescent intensity of light emitted at 500 nm following excitation at wavelengths of 335 and 370 nm using the formula described for Fura-2 (Grynkiewicz *et al*, 1985).

Fluorometric probes are introduced into the cell in their membrane-permeable (acetoxymethyl ester) form. Cytosolic esterases cleave the ester groups leaving a free acid, impermeable, form of the dye inside the cell (for review see McGuigan *et al*, 1993). As with other intracellular indicators, these probes are not entirely specific to Mg^{2+}_i (Magfura-2 is more sensitive to Ca than to Mg). Measurements of $[Mg^{2+}]_i$ by these probes are also sensitive to changes in the intracellular binding of Mg^{2+}_i and diffusion of the indicator into intracellular organelles. Other fluorescent probes have also been developed (e.g. MAG-INDO-1, MAG-QUIN-1,

MAG-QUIN-2). These compounds have been developed from Ca^{2+} and H^{+} probes and are thus sensitive to these ions (London, 1991). Further modifications of these compounds are producing fluorescent probes with a greater selectivity to Mg e.g. Magfura-5 (McGuigan *et al*, 1993) although this is still affected by changes in the intracellular pH.

Recent advances in the development of Mg sensitive ligands have greatly increased the accuracy of $[Mg^{2+}]_i$ measurement by ion-selective microelectrodes. This method results in some degree of cell damage and the ligands used are not entirely exclusive to Mg. As with the metallochromic dyes and fluorometric probes, the Mg ligands are also sensitive to interference from other ions (McGuigan *et al*, 1993). Recently the development of more selective ligands for Mg and of protocols to measure changes in other ions simultaneously have improved measurements of $[Mg^{2+}]_i$ by ion-selective microelectrodes. However interference from other intracellular species cannot be ruled out and the species which most affects the measurement of $[Mg^{2+}]_i$ may vary depending on the cell type (McGuigan *et al*, 1993).

Most techniques which directly measure $[Mg^{2+}]_i$ (including ion-selective microelectrodes) do not measure the concentration of the ion but rather its activity (McGuigan *et al*, 1993). The activity of an ion (which is less than its concentration) is equal to the product of the activity coefficient and the concentration of the ion. The value of the activity

coefficient is dependent upon the ionic strength of the medium. Calibrating media must therefore mimic the composition of the cytoplasm as closely as possible.

^{31}P nuclear magnetic resonance (NMR) is another method for measuring $[Mg^{2+}]_i$ without irreversibly disrupting the cell membrane (Gupta, Benovic and Rose, 1978). The phosphates of ATP change their frequency separation, as measured by NMR, when Mg is bound. An estimate of $[Mg^{2+}]_i$ can be made from a measurement of the ratio of ATP and ATP bound to Mg (Mg-ATP) in the cell. Since NMR is an indirect measurement of $[Mg^{2+}]_i$ it relies heavily on the accurate measurement of other factors used in the calculation of $[Mg^{2+}]_i$ such as the dissociation constant for Mg-ATP.

Examples of measurements of $[Mg^{2+}]_i$ using these various techniques are given in Table 1.1.

$[Mg^{2+}]_i$ is kept below electrochemical equilibrium in many cells.

Before attempting to identify and characterise a transport system for an ion the need for such a system has to be identified. The Nernst equation can be used to predict the intracellular ionized concentration of an ion that is in equilibrium given the external concentration of that ion and the membrane potential. The value calculated for the intracellular ionized concentration assumes that the membrane is freely permeable to that ion and that its movement is independent of other ions. The Nernst equation thus

Table 1.1. Measurements of intracellular ionized [Mg].

Tissue	$[Mg^{2+}]_i$(mM)	Reference
Metallochromic indicators.		
Barnacle muscle fibres	6.0	Brinley *et al* (1977)
dialyzed squid axon	3-3.5	Brinley & Scarpa (1975)
dialyzed squid axon	3-3.5	Scarpa & Brinley (1981)
frog skeletal muscle		
Arsenazo III,	pH=6.9; 1.2	Baylor *et al* (1982)
	pH=7.1; 0.5	
dichloro-	pH=6.9; 0.29	
phosphonazoIII	pH=7.1; 0.22	
^{31}P-NMR		
frog skeletal muscle	0.6	Gupta & Moore (1980)
human erythrocytes	0.21	Bock *et al* (1985)
guinea-pig heart	2.5	Wu *et al* (1981)
pig lymphocytes	0.5	Rink *et al* (1982)
rat heart	0.5	Borchgrevink *et al* (1989)
guinea-pig erthrocytes	0.25	Jelicks *et al* (1989)
taenia of guinea-pig caecum	0.33	Nakayama & Tomita (1990)
rat heart	0.4	Nishimura *et al* (1993)

Table 1.1. (continued)

Tissue	$[Mg^{2+}]_i$ (mM)	Reference
Null Point		
human erythrocytes	0.4	Flatman (1980)
pig lymphocytes	0.8	Rink *et al* (1982)
rat hepatocytes	0.37	Corkey *et al* (1986)
Ion-selective microelectrodes		
frog skeletal muscle	3.3	Hess *et al* (1982)
ferret ventricular muscle	3.0	
frog skeletal muscle	3.8	Lopez *et al* (1984)
ferret ventricular muscle	0.4	Blatter & McGuigan (1986)
ferret ventricular muscle	0.85	Buri & McGuigan (1990)
frog skeletal muscle	0.93	Blatter (1990)
rat extensor digitorum	0.47	MacDermott (1990)
Mag-fura 2		
rat hepatocytes	0.59	Raju *et al* (1989)
rat smooth muscle	0.31	Schachter *et al* (1990)
cultured rat hepatocytes	1.1	Harman *et al* (1990)
chick embryo cardiac myocytes	0.4	Quamme & Rabkin (1990)
chicken heart cells	0.48	Freudenrich *et al* (1992)

predicts the equilibrium distribution of the ion solely on the basis of its chemical gradient and the electrical gradient imposed by its charge. Accepting these assumptions the $[Mg^{2+}]_i$ can be predicted from

$$[Mg^{2+}]_i = [Mg^{2+}]_o * \exp\left(\frac{-zEF}{RT}\right) \qquad \textbf{1.2}$$

Where E is the membrane potential (V)

R is the Gas constant (8.314 J K^{-1} mol^{-1})

F is Faraday's constant (96500 C mol^{-1})

T is temperature (311 K)

z is the charge on the ion (2)

$[Mg^{2+}]_o$ is the external ionized [Mg]

$[Mg^{2+}]_i$ is the internal ionized [Mg]

$[Mg^{2+}]_i$ is maintained below electrochemical equilibrium in most cells. Mg transport mechanisms have been studied in a number of different cell types (for review see Flatman (1984), Flatman (1991) and Beyenbach (1990)).

Squid axons and barnacle muscle fibres provide models for the study of Mg transport

Isolated squid axons provide a useful model for the study of membrane transport systems. They are large single cells and the internal and external media are easily controlled. Studies of transport processes in squid axons have, in the past, led to the

description of transport in other (including mammalian) cells. The ionized concentration of Mg in the squid haemolymph is approximately 15 mM (Caldwell-Violich and Requena, 1979). With a membrane potential of approximately -60 mV, Equation 1.2 predicts that $[Mg^{2+}]_i$ should be greater than 1 M. However, $[Mg^{2+}]_i$ in squid axon is between 2.3 and 4 mM (Baker and Crawford, 1972; De Weer, 1976). Thus $[Mg^{2+}]_i$ is maintained below electrochemical equilibrium in these cells . Further, stimulation of the axon increases Mg influx (Baker and Crawford, 1972). Thus the axon must have a transporter capable of active Mg extrusion.

Baker and Crawford (1972) measured a Mg efflux of 1 pmole cm^{-2} sec^{-1} from the axons of the squid *Loligo forbesi*. Lowering the temperature reduced Mg efflux as did the application of metabolic poisons such as cyanide or dinitrophenol (0.2 mM at pH 6.8). This suggested that Mg transport occurs through a facilitated route. The efflux was not affected by the addition of the Na-K-ATPase inhibitor, ouabain (1 mM) but 50 mM $MnCl_2$ reduced the efflux by approximately 30%. Mg efflux was reduced to approximately 20% of its control value when $[Na]_o$ was replaced by choline (the half maximal Mg efflux was measured in media containing 100 mM [Na]). Mg efflux from the axons of the squid *Loligo pealei* was also dependent on external [Na] (De Weer 1976). Replacing $[Na]_o$ with choline reduced ^{28}Mg efflux from these axons to about 27% of the control value. Mg efflux from these axons also showed a steep temperature dependence (below 12°C the Q_{10} value was

greater than 5). The rapid hydrolysis of ATP by apyrase reduced Mg efflux to approximately 6% of the control value. $LaCl_3$ (5 mM), which inhibits Ca efflux from squid giant axons (van Breemen and De Weer, 1970) and D600 (1 mM), which inhibits Ca efflux from mammalian myocardial fibres (Kohlhardt *et al*, 1972), inhibited Mg efflux with a K_m of 0.35 mM and 0.25 mM respectively.

These data suggest that Mg efflux from squid axons is not mediated by an ATP-dependent Mg pump similar to the ATPases which play a large part in the regulation of Na and Ca. However Mullins *et al* (1977) have shown that Mg efflux from the axons of *Loligo pealei* is ATP dependent. In these experiments ATP activated Mg efflux with a K_m of 0.35 mM. Results from the experiments of Baker and Crawford (1972) and De Weer (1976) indicate that Na movement across the membrane coupled to Mg efflux could account for the maintenance of $[Mg^{2+}]_i$ below electrochemical equilibrium in these cells. Such a Na-Mg exchange would have to be electroneutral as depolarisation of the membrane (by voltage step or increasing external [K]) produced no significant changes in Mg efflux. Efflux by Na-Mg exchange does not rule out a role for ATP in the regulation of the activity of the transporter. DiPolo and Beaugé (1988) replaced ATP in the dialysed axons of *Loligo pealei* with the ATP analogue ATP-γ-S. ATP-γ-S is a substrate for kinases but not for ATPases. Mg efflux, inhibited by the removal of ATP from the axon, was stimulated by ATP-γ-S. Thus it seems unlikely that

ATP provides the metabolic energy to maintain the Mg gradient in these cells.

Further evidence for the existence of Na-Mg exchange was supplied by Gonzalez-Serratos *et al* (1988) and Gonzalez-Serratos and Rasgado-Flores (1990) who demonstrated the reverse mode of this exchange in dialysed squid axons. Gonzalez-Serratos *et al* (1988) have also shown that Mg transport may be regulated by phosphorylation (by protein kinases) and dephosphorylation (by phosphatases).

$[Mg^{2+}]_i$ is maintained below electrochemical equilibrium in single fibres of barnacle muscle. As with squid axons, fibres from the barnacle muscle have a large membrane potential (approximately -50 mV). Given that the $[Mg^{2+}]_i$ is approximately 6 mM (Brinley, Scarpa and Tiffert, 1977) then Equation 1.2 predicts that the external ionized [Mg] in barnacle muscle should be less than 1 mM. External ionized [Mg] is certainly larger than this (normal saline for these cells contains approximately 40 mM [Mg]). Mg efflux from these fibres has similar characteristics to efflux from squid axons. Mg efflux from single muscle fibres of the barnacle *Balanus nubilus* was measured using ^{28}Mg and is in the range of 6 to 12 pmole cm^{-2} sec^{-1} assuming that the surface area of the fibre was a simple cylinder (Ashley and Ellory, 1972). If the cleft system of the barnacle muscle is taken into account, these values for efflux are reduced by about 15 times. Lowering the temperature reduced Mg efflux from these fibres. The Q_{10} value below 20 °C was

between 3.3 and 4. This indicates that Mg transport in these cells is not a passive process. Assessment of the metabolic requirement for transport in these cells is difficult as muscle cells contain large reserves of ATP, arginine and creatine phosphate.

Mg efflux from the barnacle muscle was not affected by the addition of ouabain (1 mM), oligomycin (an inhibitor of oxidative phosphorylation, 0.02 mM) 0.05 mM diphenylhydantoin, verapamil (a calcium channel antagonist, 1 mM), 1 mM D-600, 1 mM Na barbitone, iodoacetamide (inhibitor of ATP synthesis, 5 mM) or pCMBS (a sulfhydryl reagent, 0.2-2 mM). 1 mM NEM (another sulfhydryl reagent) irreversibly inhibited Mg efflux. Adding 100 mM $CaCl_2$, 1 mM $LaCl_3$, 2 mM $GdCl_3$, 32 mM $CoCl_2$ or 32 mM $MnCl_2$ to the medium reversibly inhibited Mg efflux. Lowering the pH from 7 to 4 reduced efflux by 30%. Mg efflux was reversibly inhibited by replacing $[Na]_o$ with choline or Li. Replacing $[Na]_o$ with sucrose also inhibited efflux but the inhibition in this case was not reversible. As with the squid axon, thermodynamic calculations predict that it is energetically possible for the Mg gradient in these cells to be maintained by a system which exchanges Na for Mg.

Montes *et al* (1988) incubated muscle fibres from the barnacle *Balanus nubilus* in Na-free media. When the external media contained high concentrations of Mg (400 mM) there was a measurable increase in the Mg content of the cells. The Mg uptake was inhibited by an increase in the external [K] from 0 to 10 mM. When the

external [K] was increased to 388 mM there was a net loss of Mg. There was, however, no significant change in the Na content of the cells and it seems that under these conditions the muscle fibres exchange Mg for K.

Although some important characteristics of Mg transport have been identified in squid axon and barnacle muscle fibres neither are mammalian tissues and thus care must be taken when extrapolating findings to mammalian systems. Also, both are excitable cells and Mg transport may be significantly different here than in other types of cells.

Mg transport in the avian heart.

$[Mg^{2+}]_i$ is below electrochemical equilibrium in heart cells. Equation 1.2 predicts that $[Mg^{2+}]_i$ should be approximately 400 mM given a membrane potential of -80 mV and an extracellular ionized [Mg] of 1 mM. $[Mg^{2+}]_i$ in heart cells is between 0.5 and 1.2 mM (Murphy *et al*, 1991). When myocytes of the chick heart were incubated in a Na-free medium ($[Na]_o$ replaced with tetraethylammonium) the $[Mg^{2+}]_i$, as measured by the fluorescent probe Magfura-2, increased considerably (Murphy *et al*, 1989 and Freudenrich *et al*, 1992). $[Mg^{2+}]_i$ also increased when the Na gradient was reversed by incubating cells, loaded to a high cell [Na], in a Na-containing medium (Freudenrich *et al*, 1992). The movement of Mg, dependent on the direction of the Na gradient, would suggest the involvement of a Na-Mg exchanger. However the rise in $[Mg^{2+}]_i$,

following a change in the Na gradient, was not affected by removing $[Mg]_o$ but was dependent on $[Ca]_o$ (Murphy *et al*, 1989 and Freudenrich *et al*, 1992). Reversing the Na gradient in these cells causes an increase in cell [Ca] by the reversal of Na-Ca exchange. The rise in cell [Ca] displaces $[Mg^{2+}]_i$ from intracellular buffers causing a rise in $[Mg^{2+}]_i$ without an increase in Mg transport (Murphy *et al*,1989). Also, lowering $[Na]_o$ causes a fall in intracellular pH. Alkanalisation and acidification of the cytoplasm are associated with a decrease and an increase in $[Mg^{2+}]_i$ respectively (Freudenrich *et al*, 1992). Thus changes in either $[H^+]_i$ or $[Ca^{2+}]_i$ can cause an increase in $[Mg^{2+}]_i$ without any change in the total cell [Mg].

Receptor-mediated Mg transport.

A large net efflux of Mg (15-20% of cell [Mg]) after the application of noradrenaline has been reported in perfused rat liver and isolated hepatocytes (Romani and Scarpa, 1990a), perfused rat heart and isolated myocytes (Romani and Scarpa, 1990b) and rat liver hepatocytes and isolated mitochondria (Romani, Dowell and Scarpa, 1991). Prolonged application of isoprenaline also provoked an efflux of Mg from isolated rat heart (Nishimura *et al*, 1993).

Noradrenaline-activated Mg efflux in liver cells (Romani and Scarpa, 1990a) and heart cells (Romani and Scarpa, 1990b) seems to be mediated through a ß-adrenergic receptor as only ß-receptor antagonists,

and not α-receptor antagonists, blocked the Mg efflux. Mg efflux was also initiated by forskolin (which activates adenylate cyclase) and by membrane permeable analogues of cAMP. Thus the activation of the ß-adrenergic receptor may cause a rise in cytosolic cAMP which will, in turn, stimulate Mg efflux. It must be noted that, in these experiments, Mg efflux was measured by the change in the $[Mg]_o$ (measured by AAS) in a medium with no added Mg. 'Zero-trans' experiments of this type are not necessarily the most appropriate for these cell groups. Some cells incubated in medium containing very low [Mg] are particularly sensitive to procedures (for example noradrenaline administration) which cause large increases in Ca (Mg normally would slow down Ca uptake by acting as a competitive blocker of Ca channels (Iseri and French, 1984)). Mg efflux on addition of noradrenaline could be as a result of fragile cells dying and releasing their Mg. However by using ^{28}Mg to measure Mg movement in isolated hepatocytes (Romani, Dowell and Scarpa, 1991) it has been shown that, in these cells, noradrenaline and forskolin can also promote a Mg efflux in a Mg-containing medium.

Noradrenaline-activated Mg efflux was inhibited by vasopressin and carbachol in liver cells (Romani and Scarpa, 1990a), heart cells (Romani and Scarpa, 1990b) and rat liver hepatocytes (Romani, Dowell and Scarpa, 1991). Romani, Dowell and Scarpa (1991) have also shown that the effects of noradrenaline, forskolin, carbachol and vasopressin on Mg efflux are correlated

with the changes they invoke in the cytosolic cAMP concentration (Mg efflux is associated with a rise in cytosolic cAMP). Recently Romani, Marfella and Scarpa (1993) have described a noradrenaline-stimulated Mg efflux from isolated rat ventricular myocytes which is dependent on external Na and Ca. Carbachol inhibits the noradrenaline-stimulated efflux and stimulates Mg influx.

In permeabilised rat hepatocytes, noradrenaline had no effect on Mg efflux (Romani, Dowell and Scarpa, 1991). However treatment with FCCP (which mobilises the Mg in mitochondria) or A23187 (which permeabilises organelles to Ca, Mg and H) both stimulated Mg efflux. Mg efflux from permeabilised rat hepatocytes was still invoked by cAMP and not cGMP, ATP or AMP. However Mg could not be mobilised from mitochondria by cytosolic ADP. Mg efflux was inhibited by the inhibitors of the adenine nucleoside translocase (atractyloside, carboxyatractyloside and bongkrekic acid).

The mechanism of noradrenaline-provoked Mg efflux proposed by Romani and Scarpa (1992) is that activation of a ß-adrenergic receptor induces a rise in cytosolic cAMP which in turn activates the exchange of ADP for MgATP at the mitochondrial membrane via the adenine nucleoside translocase. Thus the membrane Mg transporter in these cells has not been characterised. However it does seem that the Mg transporter is sensitive to changes in the $[Mg^{2+}]_i$ and following a substantial rise in $[Mg^{2+}]_i$ it can move large quantities of Mg across the cell membrane.

Mg transport in epithelia

The total body load of Mg is regulated by Mg transport across the epithelia of the gut and kidney.

Balance studies have failed to localise a main area of Mg transport along the length of the gut. There are some reports which suggest that the ileum has a much larger capacity for Mg uptake than the colon. However in considering that the time of passage is much faster through the ileum than the colon it would seem that most of the gut is capable of Mg absorption (Ebel, 1990). The mechanism of Mg absorption is also unclear. Mg may be absorbed through paracellular and transcellular routes. The mechanism may vary along the length of the gut as does the properties of the epithelium. In leaky epithelium, such as the small intestine, most transport may occur through the paracellular route. Movement of Mg through this route would depend on bulk water flow. There have as yet been no studies which have conclusively demonstrated Mg movement correlated with water flow. Transcellular transport requires interaction with a membrane protein. There is some evidence that Mg absorption is a saturating function of Mg concentration which is indicative of carrier mediated transport. The electrical potential difference (cytoplasm negative) favours passive Mg uptake across the apical membrane. An active mechanism would have to operate to move Mg across the basolateral membrane.

There appears to be some competition between Mg

and Ca absorption. Lowering the Ca content of the gut increases the absorption of Mg. Similarly when Mg is lowered, Ca absorption increases. It may be that Ca and Mg share a mechanism of uptake in the gut. Under normal conditions such a system would be able to provide an adequate uptake of Mg from a balanced diet.

Regulation of body Mg is the prerogative of the epithelium of the kidney. 80% of the plasma [Mg] is filtered at the glomerulus (Ryan, 1990 and Quamme and de Rouffignac, 1993). Some Mg is reabsorbed in the proximal tubule (the main site of Ca reabsorption) but most is absorbed in the thick ascending limb of the Loop of Henle. Very little Mg reabsorption occurs in the distal tubule and the collecting duct.

Mg reabsorption in the Loop of Henle seems to occur mainly by a paracellular route. However the Loop of Henle has a low permeability to water but the paracellular transport of Mg may be aided by cation-selective tight junctions and a favourable electrical gradient generated by the activity of Na-K-Cl cotransport at the luminal membrane and Na-K-ATPase at the basolateral membrane. Mg reabsorption is regulated according to changes in the body load (dietary deficiency causes an increase in Mg reabsorption). Mg regulation seems to be independent of Ca status and although a number of hormones (for example, calcitonin, glucagon, PTH and ADH) have been shown to have an effect on the Mg handling of the renal epithelia no specific Mg hormone has been identified.

Red cells provide a mammalian-cell model for Mg transport

Red cells are a useful model for transport studies. They are the most easily obtainable mammalian tissue especially in the case of human tissue. They have many advantages in transport studies. They have a simple geometric shape bounded by a continuous simple single membrane and (in the case of mammalian red cells) contain no intracellular organelles. Red cells can be obtained in comparatively large quantities and form a relatively homogeneous population. Due to their frequent use in transport studies many of the membrane transport systems of red cells have been well described as has their biochemistry and metabolism. Also various techniques have been developed which allow the composition of the cytoplasm to be altered.

$[Mg^{2+}]_i$ is kept below electrochemical equilibrium in human red cells

The membrane transport processes of the human red cell are, naturally, of most interest. The most widely accepted value for the concentration of $[Mg^{2+}]$ in the plasma ($[Mg^{2+}]_o$) is 0.5 mM (Walser, 1961 and Heaton, 1967). The potential across the red cell membrane is -9 mV. Using these values, Equation 1.2 predicts a $[Mg^{2+}]_i$ of approximately 1 mM for human red cells.

As has already been discussed, ion-selective microelectrodes can be used to measure $[Mg^{2+}]_i$.

However, as plasma contains much higher concentrations of Ca than the cytoplasm, it was not possible to use these ion-selective microelectrodes to measure the plasma $[Mg^{2+}]$ accurately. Recently ligands with greater specificity for Mg have been designed. Use of these ligands, in combination with microelectrodes positioned to measure $[Ca^{2+}]_o$ and $[H^+]_o$ simultaneously, has enabled corrected values for $[Mg^{2+}]_o$ to be obtained (Rouilly *et al*, 1990). Values for $[Mg^{2+}]$ in the plasma using this method have been found to be higher than those given by Walser (1961) and Heaton (1967). $[Mg^{2+}]$ in the plasma could be as high as 0.6 or 0.7 mM. Such values, used in Equation 1.2 would increase the predicted value for $[Mg^{2+}]_i$. However the results of Rouilly *et al* (1990) are not conclusive. Their measurements of $[Mg^{2+}]_o$ were made at room temperature and in media with a high pH and therefore may not be directly applicable to the $[Mg^{2+}]_o$ in the circulation. We must await verification of these results.

Recently a value for the ionised Mg in the plasma of 0.57 $mmol(litre)^{-1}$ has been reported in a study which took into account the buffering of $[Mg^{2+}]_o$ by heparin (widely used as an anticoagulant in blood collection) and the interference of silicone (lining the barrels of syringes) with the Mg ligand. (Sachs *et al*, 1993). Thus the continued use of the measurements of $[Mg^{2+}]_o$ by Walser (1961) and Heaton (1967) is not too inaccurate.

The red cell [Mg] has been measured in a variety of animals, (see review by Flatman, 1988 for a list of

values). The cell [Mg] of human red cells is approximately 2.6mmol(l cell)$^{-1}$. The proportion of the cell [Mg] which is the free, ionized form has been measured using different methods. Flatman and Lew (1977) used the null-point method to determine $[Mg^{2+}]_i$. In red cells the null-point method is more dependable as the calculation does not require an estimation of the intracellular pH. In red cells H^+ is in equilibrium with the Cl^- gradient. Thus when the membrane is made more permeable to Mg by the addition of the ionophore A23187, Cl^- and Mg^{2+} come into equilibrium. The ratio of $[Cl^-]_o/[Cl^-]_i$ (r, the chloride distribution ratio) can be determined using the isotope ^{36}Cl. Using this method, Flatman and Lew (1977) calculated the $[Mg^{2+}]_i$ in human red cells to be 0.39 mM. Gupta, Benovic and Rose (1978) and Bock, Wenz and Gupta (1985) obtained similar values for $[Mg^{2+}]_i$ using ^{31}P NMR or the null point method respectively.

Both Flatman (1980) and Gupta, Benovic and Rose (1978) have shown that $[Mg^{2+}]_i$ increases (to between 0.54 - 0.67 mM) when red cells are deoxygenated. This increase in $[Mg^{2+}]_i$ can be attributed to a reduction in the Mg binding capacity of the red cells following the binding of 2,3-diphosphoglycerate (2,3-DPG) and ATP to deoxygenated haemoglobin (Bunn, Ransil and Chao, 1971). Despite the increase, $[Mg^{2+}]_i$ is still below electrochemical equilibrium in deoxygenated human red cells.

Mg permeability in red cells has been measured using the isotope ^{28}Mg (Rogers, 1961). Although the

equilibrium rate is small it does appear that Mg can enter the cells. As $[Mg^{2+}]_i$ is below electrochemical equilibrium, red cells would be expected to slowly gain Mg as they age. This is not the case and indeed Bernstein (1959) has observed that cell fractions containing a higher proportion of older (denser) cells actually contain less Mg. Thus human red cells lose Mg as they age. More recent studies have questioned this finding. Mairbäurl and Hoffmann (1992) have measured the cell [Mg] of human red cells, separated using Percoll. The denser fractions, containing older cells, actually contained more Mg. However the $[Mg^{2+}]_i$ remained constant with age due to alterations in the Mg-binding capacity within the cells.

In the human red cell the most accurate measurements of $[Mg^{2+}]_i$, $[Mg]_o$ and membrane potential suggest that $[Mg^{2+}]_i$ is kept below electrochemical equilibrium. However the energy required to maintain this gradient is not large. If, even as Bernstein (1959) proposed, Mg is lost from cells throughout their lifespan, the cells do not require a large capacity for Mg transport.

Mg transport in human red cells

Studies by Rogers (1961) and Ginsburg *et al* (1962) using the isotope ^{28}Mg showed that many red cells, and especially human red cells, have a very low permeability to Mg. In fact the cell [Mg] changed very little when cells were incubated at 37°C or 4°C in

Mg-containing solutions over prolonged periods (Ginsburg et al, 1962 and Flatman, 1988). Despite the low rates of Mg movement across human red cell membranes and the technical difficulties in measuring such small fluxes, Mg transport has been studied in these cells.

Mg efflux from human erythrocytes was first measured by Dunn (1974). Erythrocytes from patients with renal failure have an elevated $[Mg^{2+}]_i$. Mg efflux from these cells was measured in a medium with no, or little, added Mg. Similar results were obtained when normal erythrocytes were loaded with Mg using PCMBS (parachloromercuribenzene sulphate) which increases the membrane permeability to a number of ions. The membrane permeability is restored by incubating the cells in a medium containing cysteine or dithiothreitol. When the cells contained 5.0-8.7 mM Mg and $[Mg]_o$ was 0 or 0.8 mM, a Mg efflux of 0.03-0.10 mmol(l cell)$^{-1}h^{-1}$ was measured. This efflux only occurred when there was a downhill gradient for Mg. When $[Mg]_o$ was increased, and the outward gradient for Mg was uphill, no efflux could be measured.

Mg transport in fresh and Mg-loaded human red cells has been investigated in a more systematic way by several groups.

When fresh human red cells were incubated in a medium containing no added Mg, Mg accumulated in the medium at a rate of 7.6 μmol(l cell)$^{-1}h^{-1}$ (Féray and Garay 1986). This flux is very small and was corrected to account for Mg released to the medium by cells which

had lysed. Féray and Garay (1986) measured a rate of lysis of only 0.035% This is a very low rate for red cell lysis during *in vitro* experiments. If a more reasonable value for cell lysis (say 0.2% per hour) is used in the calculation, the rate of loss from lysing cells would equal the efflux measured by Féray and Garay.

The small Mg efflux in fresh cells was sensitive to changes in temperature (activation energy, E_a, = 13200 cal/mol). The efflux was increased by decreasing the osmolality of the medium or by raising or lowering the pH. The maximal rate of Mg efflux increased in cells which had been loaded with Mg using PCMBS. A half maximal rate for Mg efflux was recorded when cell [Mg] was between 4 and 5 mmol(l cell)$^{-1}$. Raising cell [Mg] increased the magnitude of the fluxes and made it easier to resolve changes in the rate of efflux.

Féray and Garay (1986) examined some of the properties of Mg efflux from Mg-loaded human red cells. Mg efflux was not affected by changes in internal [Na] or [K]. A variety of external cations at quite high concentrations inhibited Mg efflux. The cations tested were Ca (10 mM), Sr (1mM), Ba (1 mM), Be (0.05 mM), La (0.01 mM) and Mn (1.5 mM). Mn was the most effective inhibitor of efflux although it only inhibited efflux in a Na-containing medium and not in media where Na had been replaced with K. Efflux was reduced to about 40% of the control value when cellular ATP was depleted using iodoacetamide. Féray and Garay also measured efflux in the presence of some transport inhibitors (a

full list is given in Table 1.2). Quinidine was the most effective inhibitor, reducing the efflux by 40-80%. Féray and Garay concluded that there are at least 2 routes for Mg transport in these cells. The first route is dependent on $[Na]_o$ and intracellular ATP, is inhibited by quinidine and Mn and is a saturating function of cell [Mg]. The second they described as a $[Na]_o$-independent leak pathway, although efflux through this route is far greater than the ground permeability of the red cell membrane to Mg would allow.

Féray and Garay (1988) also tested the effects of a large number of derivatives of the tricyclic antidepressants on Mg efflux from Mg-loaded human red cells. Imipramine and carpipramine were the most potent inhibitors. Féray and Garay tested the effects of these drugs on $[Na]_o$-dependent and also Na-independent Mg transport. Almost all of the drugs tested increased this second component of transport, including those drugs which inhibited $[Na]_o$-dependent efflux. Assuming that $[Na]_o$-dependent Mg efflux occurs via Na-Mg exchange and that the Mg and Na fluxes associated with the transporter are specifically and completely inhibited by imipramine, Féray and Garay (1988) predicted that internal Mg would be exchanged for external Na in the ratio of 1:3.

Lüdi and Schatzmann (1987) have also described Mg transport in human red cells. The rate of Mg efflux from fresh cells incubated in Na-containing media was 4.6 $\mu mol(l\ cell)^{-1}h^{-1}$. The cells were loaded with Mg

Table 1.2. Effects of drugs and reagents on Mg transport in red cells.

Reagent (mM)	Species	Inhibition	Reference
acetazolamide: 1	chicken	-	7
adrenalin: 0.1	chicken	-	6
amiloride: 2	human	100%	1
1	human	56%	9
1	chicken	70%	7
1	rat	60%	11
bumetanide: 0.1	human	6%	9
2	human	-	1
0.02	human	-	3
cinchonidine: 0.5	human	25%	3
cinchonine: 0.5	human	40%	3
DCCD: 1	chicken	70%	6
DIDS: 0.01	human	-	3
0.1	chicken	-	7
dothiepine: 0.1	human	80%!	5
furosemide: 1	human	-	9
1	chicken	-	7
imipramine: 0.1	human	100%!	5
iodoacetate: 1	chicken	55%	6
isoproterenol: 0.01	chicken	-	6
KCN: 1	chicken	15%	6
NEM: 1	chicken	-	7
ouabain: 0.17	human	-	1
0.1	human	-	3
0.1	chicken	-	6

Table 1.2. (continued)

Reagent (mM)	Species	Inhibition	Reference
PCMBS: 0.1	chicken	-	6
phloretin: 0.5	human	40%	3
0.1	chicken	4%	8
phloridzin: 0.1	chicken	-	8
phorbol ester: (0.1μM)	chicken	-	8
quinidine: 0.5	human	75%	3
1	rat	70%	4
0.5	rat	75%	11
0.5	human	25%	10
0.5	rat	70%	10
0.5	chicken	70%	10
quinine: 0.5	human	25%	3
SITS: 0.03	human	-	9
0.03	human	-	10
0.03	rat	4%	10
0.03	chicken	-	10
tetrodotoxin: 0.1	chicken	-	6
trifluoperazine: 0.1	chicken	-	6
0.1	human	-	10
0.1	rat	-	10
0.1	chicken	-	10
vanadate: 0.1	human	-	2

Table 1.2. (continued)

Reagent (mM)	Species	Inhibition	Reference
Ca^{2+}: 10	human	slight*	3
Sr^{2+}: 1	human	slight*	3
Ba^{2+}: 1	human	slight*	3
Be^{2+}: 1	human	slight*	3
La^{3+}: 0.01	human	slight*	3
Mn^{2+}: 100	human	80%	3
0.1	chicken	40%	6

References

(1). Lüdi & Schatzmann (1987).
(2). Frenkel, Graziani & Schatzman (1989).
(3). Féray & Garay (1986).
(4). Féray & Garay (1987).
(5). Féray & Garay (1988).
(6). Günther, Vormann & Förster (1984).
(7). Günther & Vormann (1985).
(8). Günther & Vormann (1986).
(9). Günther & Vormann (1989a).
(10).Günther & Vormann (1989b).
(11).Günther, Vormann & Höllriegl (1990).

Inhibition is the percentage of Mg efflux, in NaCl media, inhibited by that agent. (-) shows that the agent had no effect on Mg efflux. (!) indicates measurements made on $[Na]_o$-dependent Mg efflux only. The drugs shown (imipramine and dothiepine) were the most potent of a series of drugs tested (deipramine, trimipramine, clomipramine, quinupramine, caripramine, opipramol, butripyline, amitriptyline, nortriptyline, doxepine, dibenzepine, propizepine, amoxapine, maprotiline, loxapine). (*) shows slight inhibition (5-15%) of Mg efflux by these agents. Data for individual agents were not given by the authors.

using the ionophore A23187 to permeabilise the cell membrane to Mg. A23187 was washed out of the Mg-loaded cells in media containing albumin.

Mg efflux from Mg-loaded human red cells was again described as having 2 components; a $[Na]_o$-dependent and a $[Na]_o$-independent pathway. $[Na]_o$-dependent Mg efflux was unaffected by 0.17 mM ouabain or up to 2 mM bumetanide; was fully inhibited by 2 mM amiloride (a blocker of various routes of Na transport, Benos, 1982; Kleyman and Cragoe Jr, 1990) and was reduced to 5.6% of the control flux when cellular ATP was reduced by iodoacetamide. The function relating $[Na]_o$-dependent efflux and $[Mg^{2+}]_i$ was sigmoidal and very steep. The profile of the curve would suggest that more than one Mg ion binds to the transporter to initiate Mg efflux.

The $[Na]_o$-independent Mg efflux was small and showed no clear dependence on $[Mg^{2+}]_i$. $[Na]_o$-independent Mg efflux was only slightly inhibited by 2 mM amiloride and, although reduced by metabolic starvation, it was not as sensitive to changes in cell [ATP] as the $[Na]_o$-dependent efflux.

Lüdi and Schatzmann were able to measure $[Na]_o$-dependent Mg efflux from cells loaded to 1 mM $[Mg^{2+}]_i$ and incubated in a medium containing 1.5, 1.7 or 2.5 mM $MgCl_2$. Thus the Mg transporter was able to move Mg against a small electrochemical gradient. In another experiment the outward gradient for Mg was made larger by increasing $[Mg]_o$ to 5 mM when the cells contained 1.2 mM Mg. Mg efflux was measured in these experiments. Lüdi and Schatzmann (1987) concluded that

this system is capable of active Mg transport. However, when $[Mg]_o$ was between 5 and 10 mM, net Mg influx was measured. The active efflux of Mg when $[Mg]_o$ was 5 mM was inhibited and a net influx, down a Mg gradient, was measured when the cells were treated with amiloride. When the Na gradient was reversed, by loading the cells with Na using the PCMBS method and reducing the $[Na]_o$, Mg efflux was reduced but not reversed, even when the Mg gradient favoured Mg influx.

Schatzmann (1993) has investigated the irreversibility of the Mg transporter more thoroughly. Human red cells were loaded with Mg and Na using the PCMBS method. The internal and external [Mg] were arranged so that there was an inward electrochemical gradient for Mg. When there was a large inward gradient for Na ($[Na]_o$= 98 mM, cell [Na]= 6.4 mM) Mg efflux was measured. Under these conditions, therefore, the Mg transporter could mediate active outward Mg transport. When the Na gradient was reversed ($[Na]_o$=2 mM, cell [Na]=107 mM), a condition which should favour net influx by Na-Mg exchange, no significant Mg transport was measured. Further, even when there is no Na gradient across the membrane ($[Na]_o$=100 mM, cell [Na]=113 mM) and the movement of Mg out of the cell was against an electrochemical gradient ($[Mg^{2+}]_o$=1.64 mM, $[Mg^{2+}]_i$=2.74 mM), Schatzmann (1993) measured a net Mg efflux. Thus although Mg efflux is dependent on $[Na]_o$, it appears that Mg transport, against a gradient, mediated by this route does not rely on energy from the Na-gradient.

Frenkel, Graziani and Schatzmann (1989) measured Mg efflux in experiments using resealed human red cell ghosts. Mg efflux from these cells was highly dependent on cellular ATP and could proceed even in the absence of a Na gradient. However, external vanadate had no effect on Mg transport which argues against a Mg pump of the same type as the Ca-ATPase and Na-K-ATPase (the P-class ATPases). The finding that $[Mg^{2+}]_i$ affected the apparent dissociation constant for $[Na]_o$ and vice versa suggests that in resealed human red cell ghosts $[Mg^{2+}]_i$ may be exchanged for $[Na]_o$.

Günther and Vormann (1989a) have also measured Mg efflux from Mg-loaded human red cells. The cells were loaded using the ionophore A23187. $[Na]_o$-dependent Mg efflux was unaffected by 1 mM furosemide and 0.1 mM bumetanide and was substantially inhibited by amiloride. Replacing $[Na]_o$ with Li, K or choline slightly inhibited Mg efflux. Replacement of $[Na]_o$ by sucrose produced a large rise in Mg efflux which was inhibited by the anion channel blocker, 4-acetamido-4'-isothiocyanato-stilbene-2,2'-disulfonic acid (SITS, 30 μM). Incubation in sucrose media also resulted in an increase in K efflux which was similarly inhibited by SITS. SITS had no effect on Mg efflux in medium containing Na or choline (Günther and Vormann, 1989b). Günther and Vormann proposed a route for Mg transport which was independent of $[Na]_o$ but was dependent on Cl.

By testing the efficacy of several amiloride derivatives on the inhibition of Mg and K efflux from

human red cells in sucrose media, Günther, Vormann, Cragoe, Jr and Höllriegl (1989) concluded that Mg efflux and K efflux in sucrose media occur through separate routes, although both are dependent on Cl.

When human red cells are placed in a sucrose medium, Cl^- leaves the cell and the membrane potential is depolarised. Halperin *et al* (1989) have reported that when human red cells are depolarised (by incubation in high-K medium with valinomycin or by changing the nitrate concentration in the presence of DIDS) the membrane permeability of Na, K and Ca (the only ions tested in this study) is increased. The increase in permeability is irreversible and is not thought to occur through any identified transport system. Nor is it certain if the ions are transported through the same route. In considering the results of Günther and Vormann (1989b) the results of Halperin *et al* (1989) must be borne in mind. Incubation of human red cells in sucrose could depolarise the membrane sufficiently to cause the opening of a transport route similar to the one described by Halperin *et al* (1989). If this is the case then Mg transport from human red cells measured in sucrose media is through a different route than Mg transport measured in K, Li or choline medium (Günther and Vormann, 1989 a,b).

Measurements of Mg efflux from the Mg-loaded red cells have shown that there is wide variation in the maximum rate of Mg transport between cells from individual donors (Féray and Garay, 1986 and Lüdi and Schatzmann, 1987). Henrotte (1980) noted that

variability in the total cell [Mg] between donors was linked to the expression of HLA antigens (donors carrying the HLA-B35 antigen have lower cell [Mg] and a higher maximum efflux rate than donors expressing other antigens). Féray *et al* (1989) have shown an inverse correlation between the total cell [Mg] and the rate of $[Na]_o$-dependent Mg efflux in Mg-loaded cells. Thus some genetic factor may play a role in establishing the Mg load and Mg transport rate in human red cells (Henrotte, 1993). Whether this genetic factor affects the Mg transport capacity of the cell membrane is unclear. Henrotte and Franck (1990) have suggested that a plasma factor may be the determinant of the Mg transport capacity.

Mg transport has been studied in the red cells of other mammals.

Féray and Garay (1987) have measured Mg efflux from fresh red cells of the rat. Mg efflux from these cells was much larger than the flux measured in fresh human red cells (270 ± 144 μmol(l cell)$^{-1}h^{-1}$ (mean ± S.D.)). Féray and Garay identified $[Na]_o$-dependent and $[Na]_o$-independent components of Mg efflux. Quinidine inhibited both components of efflux and, although quinidine caused the cells to lyse at concentrations above 1 mM, they estimated IC_{50} values of 40 μM quinidine for the $[Na]_o$-independent component and 400 μM quinidine for the $[Na]_o$-dependent component. ATP depletion (by iodoacetamide) reduced

$[Na]_o$-dependent efflux to 40% of the control values. In Na-free media, Mn and Co were able to stimulate Mg efflux. Mg efflux into a Na-free, Mn-containing medium was inhibited by ATP depletion and quinidine but was unaffected by 1 mM ouabain, 100 μM bumetanide or 20 μM PCMBS. Increasing $[Na]_o$ inhibited Mn influx but had no effect on Mg efflux. Thus it seems that Mn, in the absence of $[Na]_o$, can be exchanged for internal Mg. Günther, Vormann and Cragoe, Jr. (1990) showed that Mn and Mg could be exchanged across the cell membrane of the rat red cell and that this occurred when Mn successfully competed with Na for binding to a Na-Mg exchanger. This mechanism was species-specific and no Mn-Mg exchange could be detected in chicken or human red cells under similar conditions.

Some properties of Mg efflux from rat red cells have also been described by Günther and Vormann (1989) and Günther, Vormann and Höllriegl (1990). Quinidine (0.5 mM) inhibited Mg efflux from Mg-loaded rat red cells when they were incubated in a Na-containing medium. $[Na]_o$-dependent efflux was unaffected by SITS or trifluoperazine. Mg efflux was reduced if $[Na]_o$ is replaced with choline or Li. Mg efflux into a sucrose medium was accompanied with a large, SITS-sensitive K efflux. Cell [Na] and $[Mg]_o$ inhibited efflux competitively and, although $[Na]_o$-dependent efflux required ATP, reducing the $[Na]_o/[Na]_i$ gradient with PCMBS reduced Mg efflux. Günther and Vormann also showed that quinidine and imipramine (which inhibited Mg efflux) do not inhibit ATPase activity in rat red

cell ghosts.

Mg transport has been identified in hamster and guinea-pig red cells (Xu and Willis, 1991; Zhao and Willis, 1993).

When guinea-pig red cells were loaded with Mg (using A23187) there was a net loss of Mg from these cells into Mg-free media (Zhao and Willis, 1993). The Mg efflux was only slightly inhibited by amiloride but was reduced substantially (from 34.5 to 5.5 mmol(l cell)$^{-1}h^{-1}$) when $[Na]_o$ was replaced with choline. Na influx was very dependent on internal [Mg] (loading the cells with 10 mM Mg in the loading medium increased the Na influx by approximately 800%). The $[Mg]_i$-dependent Na influx was inhibited by 50% by 1 mM amiloride.

When investigating the pathways for Na influx into fresh Syrian hamster red cells, Xu and Willis (1991) found that the Na influx was partly inhibited by amiloride. However the amiloride-sensitive component did not exhibit other properties of Na-H exchange. The amiloride-sensitive Na influx was inhibited by low cell [Mg] and stimulated by high cell [Mg]. The rate of Na influx, measured under a given set of conditions, corresponded with the predicted rate of Mg efflux suggesting that Na-Mg exchange is present in these cells.

Willis *et al* (1993) have shown that the rate of Na influx into hamster red cells increases when the cells are loaded with Mg. The rate of Na influx is thus influenced by the direction and size of the Mg gradient. Na influx is reduced by ATP depletion and is

strongly inhibited by amiloride.

This work on hamster red cells has provided the first demonstration of a correlation between Na movement and Mg movement in red cells. As it seems that all the amiloride-sensitive Na flux in these cells occurs through Na-Mg exchange, hamster red cells will provide a very useful model for the study of this transporter and could enable an accurate prediction of the stoichiometry of exchange.

Mg transport in chicken red cells

Although not a mammalian cell, chicken red cells have provided a model for Mg transport. The first systematic study of Mg efflux from Mg-loaded cells was performed in chicken red cells by Günther, Vormann and Förster (1984). Cells were loaded with Mg using the ionophore A23187. Mg efflux only proceeded until the cell [Mg] was at the level of control cells (Günther, Vormann and Förster, 1984). Mg efflux was unaffected by changes in intracellular or extracellular [Ca], 0.2 mM trifluoperazine, 0.1 mM adrenalin, 0.1 mM isoproternol, 0.1 mM ouabain or 0.1 mM tetrodotoxin. Reducing ATP by iodoacetate treatment inhibited Mg efflux. Mg efflux was reversibly and non-competitively inhibited by amiloride.

1 mM dicyclohexylcarbodiimide (DCCD) inhibited the efflux indicating that a membrane bound protein may be involved in transport. Loading with Mg caused an increase in Mg efflux and also an increase in protein

kinase activity (Günther and Vormann, 1986). Amiloride, which is known to inhibit some protein kinases, inhibited Mg efflux and the phosphorylation of a 230kDa membrane protein. Günther and Vormann (1986) excluded cAMP and calmodulin-dependent kinases and protein kinase C from a role in Mg transport in these cells by the finding that isoproternol, adrenalin, trifluoperazine and phorbol ester had no effect of Mg efflux.

Mg efflux from Mg loaded chicken red cells was inhibited by replacing $[Na]_o$ with choline (Günther and Vormann, 1984). The net movement of Na with Mg suggested that 2 Na are exchanged for 1 Mg. Replacing $[Na]_o$ with sucrose or Li inhibited Mg efflux from Mg-loaded chicken red cells (Günther and Vormann, 1985). Günther and Vormann (1985) measured Mg efflux in media containing PCMBS. Thus, Mg efflux from Mg-loaded chicken red cells can proceed in the absence of a Na-gradient, but requires $[Na]_o$. Replacing $[Na]_o$ with K caused an increase in the uptake of ^{28}Mg into Mg-loaded chicken red cells (Günther and Vormann, 1987). In control, non-loaded cells there was hardly any measurable ^{28}Mg uptake in Na-containing media. When $[Na]_o$ was replaced with K there is a large stimulation in ^{28}Mg influx which was inhibited by amiloride but not by furosemide.

The finding that Mg efflux was only measurable in chicken red cells which have been loaded with Mg and that cell [Mg] only falls to control levels (Günther, Vormann and Förster, 1984) suggested that Mg transport

was gated by $[Mg^{2+}]_i$. However, fresh chicken red cells (with low internal Mg) can take up ^{28}Mg particularly when $[Na]_o$ is low (Günther and Vormann, 1987) suggesting that the reverse mode of this transporter is not gated by internal [Mg].

Unlike human red cells, Mg efflux was not increased when Mg-loaded chicken red cells were incubated in sucrose media (Günther and Vormann, 1989b). Incubation in Na-free, sucrose media still produced a rise in K efflux which was inhibited by SITS and Cl^-_o. $[Na]_o$-dependent Mg efflux was inhibited by quinidine but Mg efflux into Na-free (choline or sucrose) media was not affected by quinidine. Interestingly there was no increase in K efflux following a rise in $[Ca_i]$ indicating that chicken red cells do not have the Gardos channel (Günther and Vormann, 1989b).

Mg transport in ferret red cells

Ferrets have been used extensively in the investigation of many areas of mammalian physiology (Thornton *et al*, 1979). Ferret red cells contain similar amount of Mg (3 mmol(l cell)$^{-1}$) to other species of red cells (Flatman and Andrews, 1983). Of this total cell [Mg], approximately 0.65 mM is in the free ionized form (Flatman, 1987). An $[Mg^{2+}]_o$ of 0.5 mM and a membrane potential of -9 mV predicts that, at equilibrium, $[Mg^{2+}]_i$ would be approximately 1 mM (from Equation 1.2). Thus in ferret red cells $[Mg^{2+}]_i$ is

slightly below electrochemical equilibrium. Fresh, untreated ferret red cells have a high permeability to Mg compared to many other cell types (Flatman, personal communication). Thus net Mg transport can be measured in these cells without changing their physiological Mg content and without pre-treating the cells with agents such as PCMBS and A23187. Measurements of net Mg efflux rates in ferret red cells have shown them to be remarkably reproducible (Flatman and Smith, 1990 and this thesis).

The ferret red cell membrane shows very little Na-K-ATPase activity and is very dependent on the Na-K-Cl cotransporter to regulate internal Na and K (Flatman and Andrews, 1983). As a consequence, and in contrast to most other cells, ferret red cells have a high internal [Na] (140 mM) and a low internal [K] (7 mM).

Many of the experimental tools used by transport physiologists to determine the nature of a membrane transport system have been used in this study to characterise some properties of Mg transport in fresh ferret red cells. The high internal [Na] of these cells has been exploited to investigate more thoroughly the relationship between the Na gradient and Mg transport. Some properties of Mg influx in low-[Na] media are also described. In the final section, Mg transport is described in Mg-loaded ferret red cells and the results show that the ferret red cell membrane may switch to a different mechanism for Mg transport when challenged with a large cell load of Mg.

Table 1.3. Mg transport in different cells.

As well as those mechanisms described in the Introduction, Mg transport has been studied in a variety of other cell types. Some examples are given in the table below.

Tissue	Mg transport	Reference
Prokaryotic cells		
Escherichia coli	NEM-blocked, carrier mediated	Lusk & Kennedy (1968)
Escherichia coli	Co-sensitive	Nelson & Kennedy (1971)
S-typhimunum	Co-sensitive component	Hmiel *et al* (1986)
Cardiac myocytes		
rat ventricle	carrier mediated	Page & Polimeni (1972)
guinea-pig/ferret ventricular myocardium	Na & Mg coupled transport	Fry (1986)
ferret ventricular muscle	Na-/ATP-dependent, irreversible	Buri & McGuigan (1990)
perfused rat heart	stimulated by cAMP	Romani & Scarpa (1990b)

Table 1.3. (continued)

Tissue	Mg transport	Reference
Smooth muscle		
taenia of guinea-pig caecum	Na-Mg exchange	Nakayama & Tomita (1990)
Cultured cells		
murine S49 lymphoma cells	hormone sensitive/ Mg-specific	Erdos & Maguire (1983)
Yoshida ascites tumour cells	electroneutral Mg-HCO_3 cotransport	Günther *et al* (1986)
cultured chicken heart cells	NOT Na-Mg exchange	Murphy *et al* (1989)
MDCK cells	verapamil sensitive, Mg specific	Quamme & Dai (1990)
chick embryo cardiac myocytes	verapamil-sensitive	Quamme & Rabkin (1990)
isolated hepatocytes	stimulated by noradrenaline	Romani & Scarpa (1990a)

2. Methods

Solutions and reagents.

All stock solutions were prepared in grade A volumetric borosilicate glassware using double glass distilled water (DGDW) and AnalaR grade reagents (BDH Ltd.) where possible. 2M NaCl and 2M KCl stock solutions were prepared. A stock solution (500 mM) of the free acid form of HEPES was neutralised to the required pH with NaOH. These stock solutions were used at the following concentrations in the preparation of Ferret Basic Medium (FBM): 145 mM NaCl, 5 mM KCl and 10 mM Na-HEPES buffer. The pH was measured at 38°C. The pH of the buffer and FBM was usually 7.50. The pH was sometimes adjusted within the range 7.50 to 7.67 by the addition of 1 N NaOH depending on the pH chosen for cell storage and the experimental incubations. Na-MOPS was also used as a buffer. The Na and K content of FBM and other incubation media were routinely checked by flame photometry. Osmolarity was checked using a vapour pressure osmometer and was normally 285 mOsmol kg^{-1}.

When necessary Na and K were substituted with choline chloride (recrystallised from ethanol) or N-methyl-*D* glucamine (NMDG). Substitution by NMDG required addition of sucrose to maintain the osmolarity of the medium. In Na-free media HEPES was neutralised by KOH. In Na and K-free buffers HEPES was neutralised with TRIS base.

EDTA and EGTA were neutralised with TRIS base to give a pH of 7.55 at 38°C. Both were prepared at concentrations of approximately 200 mM. The exact concentrations were checked by titration. When EGTA or EDTA bind Mg^{2+} or Ca^{2+} protons are released. The exact volume of NaOH needed to neutralise these protons was measured. An end point was reached when no protons were released with further additions of $CaCl_2$ or $MgCl_2$ and thus no further NaOH was needed to maintain pH at 7.5.

Drugs and metal ion complexes were prepared in concentrated stocks where solubility would allow. Drugs were also prepared at required concentration in the incubation medium. If concentrated stocks had to be prepared in solvents such as dimethyl sulphoxide (DMSO), dimethyl formamide (DMF) or ethanol then the concentration was adjusted so that the solvents were diluted at least 100 times in the final incubation medium.

Bumetanide (a gift from Leo Laboratories) was dissolved in water alkalinised with TRIS base.

The ionophore A23187 was dissolved at 1mg ml^{-1} in ethanol. It was added directly to cell suspensions with stirring to avoid adhesion of the molecule to the incubation vial.

Urethane (ethyl carbamate), EDTA, EGTA, Choline Chloride, NMDG, HEPES, MOPS, TRITON X-100, ionophore A23187, N-ethylmaleimide, amiloride, bovine albumin (fraction V) and SITS were obtained from Sigma Chemical Company.

Luciferin/luciferase for ATP measurements was obtained in LKB-ATP monitoring kits for use on a LKB/Wallac 1250 Luminometer. Kits were originally obtained from LKB. Recent suppliers have been Bio-Orbit.

Cell collection and Storage.

Adult ferrets were anaesthetised by an intraperitoneal administration of ethyl carbamate (urethane) solution 1.5g (kg body weight)$^{-1}$. The thoracic cavity was opened and blood collected by cardiac puncture into a syringe containing 40 μmoles Tris-EDTA (used as an anticoagulant). The whole blood was further diluted in FBM containing 40 μmoles of EDTA. The blood was spun at 3600 x g for 5 minutes in a MSC `Chilspin' centrifuge or at 2500 x g for 4 minutes in a Hereaus Biofuge 17RS. Both methods adequately separate the cells from the supernatant. The plasma, buffy coat and white cells were removed by aspiration and the red cells resuspended in FBM containing 50 μM EGTA. The red cells were washed 3 times in this medium and stored in a centrifuge tube at 5°C and 80% haematocrit.

All solutions used in this procedure were sterilised by filtration through a 0.22 μm filter unit (Millipore). The polycarbonate centrifuge tubes were sterilised by pre-rinsing in AnalaR grade ethanol and air-dried.

Red cells were normally used within 3 days of

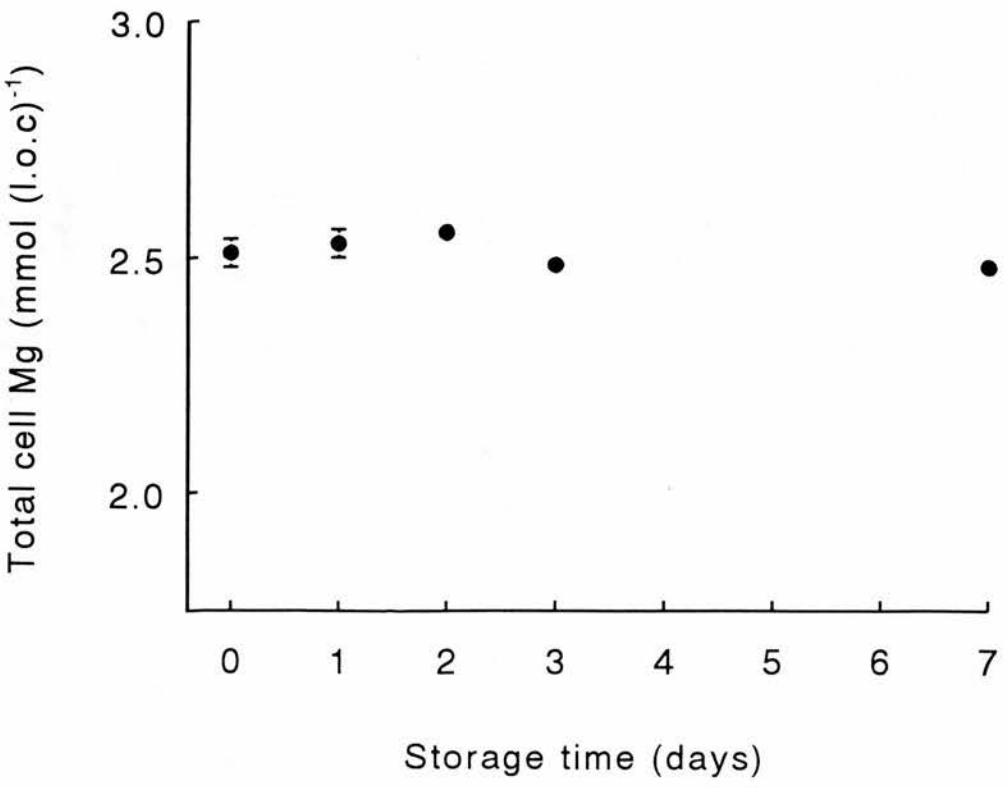

Figure. 2.1.

Time-dependent changes in the total cell [Mg] during storage. Ferret red cells were stored at about 80% haematocrit at 5°C in a polycarbonate centrifuge tube. On the days indicated 0.2 mls were removed and resuspended in FBM containing 50 μM EGTA at a mean haematocrit of 7.5%. Samples were taken to measure total cell [Mg] (pellet lysed in DGDW). Symbols show the mean of 3 determinations with S.E.M. if larger than point size.

collection. Over this time period cell [Mg] did not change (Figure 2.1). Cell [ATP] fell over this period (Figure 2.2). Unless otherwise stated all experimental media contained 11 mM *D*-glucose to maintain the cell ATP content. Cells were often incubated in FBM-glucose solution for 1 hour prior to an experiment to re-establish the ATP levels to within the control range. For cells stored for longer than 3 days this medium was supplemented with 1 mM phosphate (from a stock containing NaH_2PO_4 and Na_2HPO_4, pH = 7.49) to provide the substrates necessary for ATP regeneration. In a typical experiment the ATP content of cells which had been stored for 8 days was 0.39 ± 0.02 mmol(l cell)$^{-1}$. After a 40 minute incubation in FBM containing 11 mM glucose, 0.05 mM EGTA and 1 mM phosphate the ATP content was 0.70 ± 0.01mmol(lcell)$^{-1}$.

Cell Suspensions.

Ferret red blood cells were washed and then added to the incubation medium. The exact composition of the incubation media are given in the text and figure legends along with details of added drugs or metal ions.

The cells were incubated at about 8% haematocrit at 38°C in a circulating water bath. The suspension was stirred intermittently during the experiment to reduce lytic stress on the cells and was stirred continuously for 1 minute prior to a sample being removed to ensure homogeneity of the suspension.

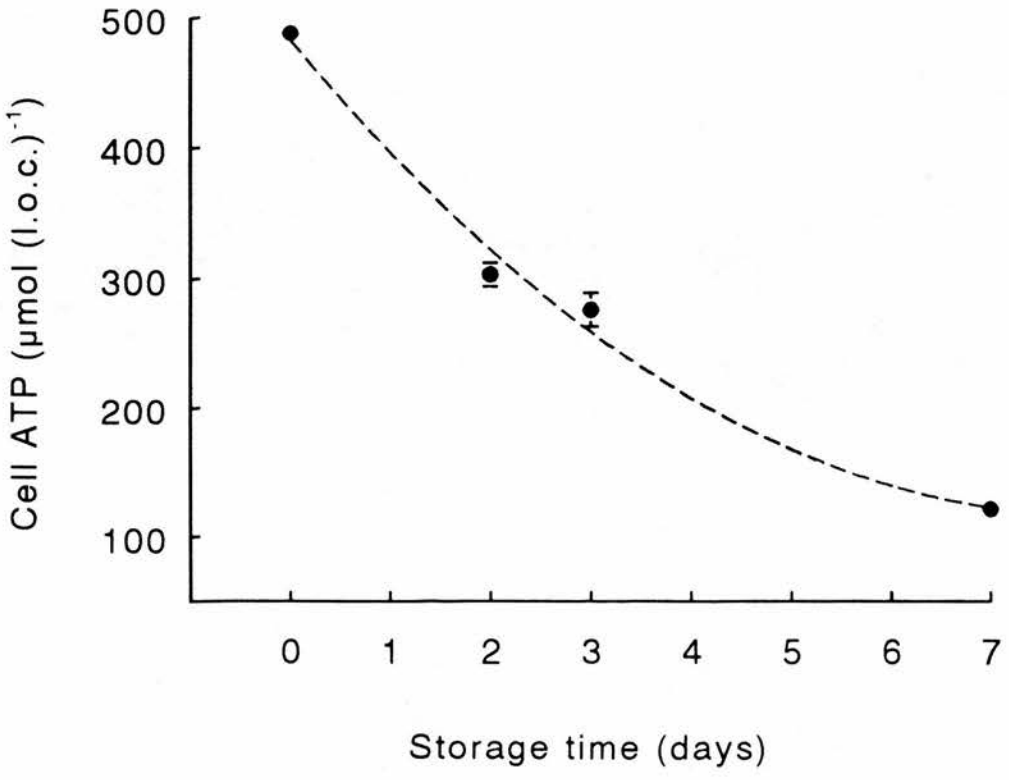

Figure 2.2.
Time-dependent changes in the cell [ATP] during storage. The data is from the same experiment as Figure 2.1. Symbols show the mean of 3 determinations of the cell [ATP] with S.E.M. if larger than point size. The data is fitted by a second order polynomial.

pH changes in red cell suspensions.

To investigate the pH dependence of Mg transport it was necessary to change the pH of the medium. Changing the pH of red cell suspensions is difficult as red cells are good buffers for protons and to some extent regulate the pH of their own environment. Figure 2.3 shows the effects of adding NaOH and HCl to a HEPES buffered medium (initially adjusted to physiological pH). Open symbols represent changes in the pH of the media and the filled symbols show pH changes in an 8% suspension of red cells. In red cell suspensions the external pH is buffered by both internal and external buffers. When the external pH is changed there is a rapid re-equilibration of protons across the membrane. Therefore it is not possible to change the external pH and not the internal pH unless the proton transporters in the membrane are inhibited chemically.

Haematocrit.

To measure the exact haematocrit of the suspension a small sample was mixed with Buffered Diluent (Van Kampen and Zijlstra cyanmethaemoglobin reagent; bought as a concentrated stock from BDH Ltd. and diluted with DGDW). The mixture was shaken well and the colour allowed to develop over 1 hour. The absorbance of the solution was measured on a Pye Unicam Spectrophotometer at wavelength of 540 nm and path length of 1 cm. Most

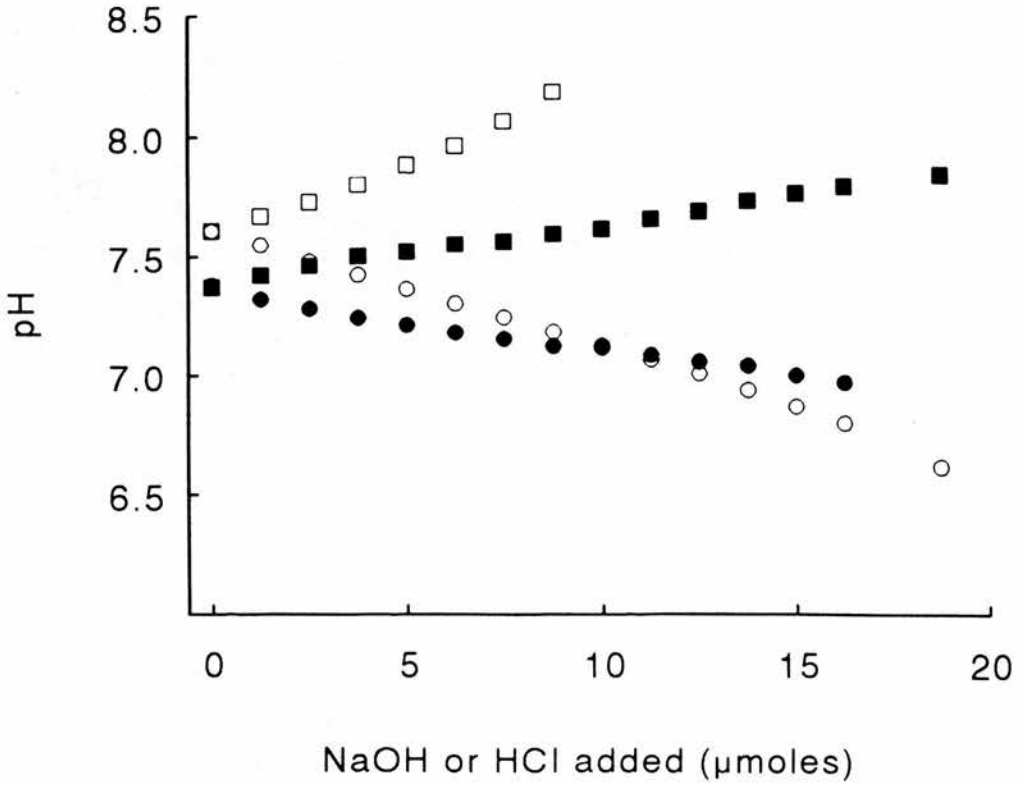

Figure 2.3.
The hydrogen ion buffering capacity of ferret red cells. 0.25M HCl (open circles) or NaOH (open squares) was added to FBM at 38°C. The external pH was measured using a Radiometer pH-electrode. Filled symbols represent similar additions of HCl and NaOH to 8% suspensions of ferret red cells in FBM.

commonly 0.1 ml of cell suspension was added to 5 ml of Buffered Diluent. The volumes of sample and reagent were varied so that in suspensions with lower haematocrits the ratio of sample volume to Diluent volume could be increased to improve the resolution of the measurement.

Haematocrit was calculated by multiplying the absorbance reading by the dilution factor and dividing by the `packed cell absorbance' i.e. the theoretical absorbance reading of a 100% suspension. The packed cell absorbance was calculated as follows;

Ferret red cells were suspended in FBM, with glucose, at about 20% haematocrit. Samples of suspension were centrifuged in sealed microhaematocrit tubes in a CHRIST Haemafuge for 5 minutes. The proportion,

$$\frac{\text{packed cell column length}}{\text{Total column length}} \times 100 \qquad \textbf{(2.1)}$$

is the haematocrit (%).

The absorbance of the suspension was also determined by mixing samples of the suspension in Buffered Diluent. The haematocrit and the corresponding absorbance of the suspension allows a proportional calculation to determine the theoretical absorbance reading for a suspension of 100% haematocrit. This was found to be 231 ± 3 (mean ± S.E.M, n=6). This value is in agreement with that of Flatman & Andrews (1983) who calculated the packed cell

absorbance for ferret red cells as 230 ± 2 (mean ± S.E.M, n=10).

Cell suspensions containing the ions Co and Mn form precipitates when added to Buffered Diluent. The haematocrits of these suspensions were measured by adding samples of the cell suspension to DGDW containing 0.5% Triton. The packed cell absorbance for cell suspensions in Triton was 284 ± 2 (mean ± S.E.M, n=10). Control experiments using suspensions not containing Co or Mn showed that the haematocrit determined using Triton solution, with the appropriate packed cell absorbance, was the same as that measured using Buffered Diluent.

Cell Lysis.

The estimation of the haematocrit by measuring the absorbance at 540 nm assumes that all the haemoglobin is contained within intact red cells. However a proportion of the cells lyse during the experiment releasing haemoglobin to the extracellular fluid (ECF). To measure the degree of cell lysis a sample of cell suspension was spun down and an aliquot of the supernatant added to Buffered Diluent. The absorbance of the sample was measured as for haematocrit measurements. Values obtained give the apparent haematocrit of the ECF based on the concentration of haemoglobin in the supernatant. This value is subtracted from the haematocrit of the total suspension to give the haematocrit of intact cells in the

suspension.

Cell lysis is a gradual process and involves the formation of a hole in the cell membrane (Bjerrum, 1979). A non-specific increase in cell permeability occurs before the hole becomes large enough to allow the release of the large haemoglobin molecule. Estimating the lysis of the cell population by the increase in the haemoglobin content of the medium can only account for the increase in the permeability of cells which have released their haemoglobin. However the cell population will include cells which have a hole in the membrane large enough to allow an increase in the non-specific leak but not large enough to allow the release of haemoglobin. Therefore corrections to efflux measurements based on the haemoglobin concentration of the external medium cannot correct for the increased rate of transport through this new, unselective route. This is not normally a cause for concern as experimental conditions are selected so that cell lysis is low (less then 2%). However there have been some instances (for example, high drug concentrations in the media, temperature above 37°C) where cell lysis has increased considerably. In such conditions it should be borne in mind that a significant part of Mg efflux, even after correction for cell lysis, may be through this route which is not normally revealed in healthy, intact cells.

Intracellular [Mg].

Intracellular [Mg] was measured using the method described by Flatman and Lew (1978) and Flatman (1980).

The cells were separated from the medium by adding 0.1 ml of the red cell suspension to a 1.5 ml reaction tube (on ice) containing 0.3 ml di -*n* - butylphthalate (density = 1.043) and 1 ml FBM (with 2 mM EDTA). When the cells are added to the ice cold FBM and EDTA mixture, membrane transport is slowed (by the reduction in temperature), the EDTA binds any Mg adhering to the cells and the extracellular fluid (ECF) is diluted 10 times. The tube was inverted, shaken and spun at 15000 x g for 30 seconds in an Eppendorf Microfuge 5415.

After centrifugation the cells (density $\approx$ 1.10) form a pellet below the oil and most of the ECF and FBM remain above. However a proportion of ECF is trapped below the oil in the cell pellet. Using ^{57}Co EDTA as an extracellular space marker it was possible to estimate this proportion. Figure 2.4 shows that increasing the spin time reduces the amount of ECF in the pellet (See figure legend for details of protocol).

In zero trans experiments, where $[Mg]_o$ is nominally zero, the 10 times dilution of the ECF and a 30 second spin time were sufficient to separate the cells. In experiments to measure Mg influx, $[Mg]_o$ was increased to concentrations above 1 mM. Under these conditions the Mg in the ECF which was trapped in the pellet would be included in the measurement of intracellular Mg and add significant error. In these

Legend to Figure 2.4.

0.1 ml samples of a red cell suspension of known haematocrit were transferred to a 1.5 ml tube containing 0.3 ml di-*n*-butylphthalate, 1 ml FBM and 2 kBq of ^{57}Co-EDTA (in 10 μl of a solution of 5 mM $CoCl_2$ and 25 mM EDTA). $^{57}CoCl_2$ chelated to (excess) EDTA cannot enter the cells and remains as an external marker. The samples were spun for varying lengths of time in an Eppendorf 5412 microcentrifuge at 12000 x g. The activity of 0.1 ml of the supernatant and the entire cell pellet obtained by cutting the end of the microtube were counted for gamma radiation in a LKB Clinigamma counter.

The percent of the cell pellet which is ECF is calculated by,

Activity in ECF = A_{ECF}
Volume of ECF counted = V_{ECF}
Specific activity of ECF = A_{ECF} / V_{ECF} μl^{-1}
Activity in pellet = A_p
Volume of cells in pellet = V_p
(= 100 x haematocrit) μl

$$\text{Percent of ECF in pellet} = \frac{A_p \times V_{ECF}}{A_{ECF} \times V_p} \times 100$$

The points shown are the mean of 2 determinations. Bars show the range if larger than point size. The curve is drawn using an exponential function: 92.exp(-8.t) + 3

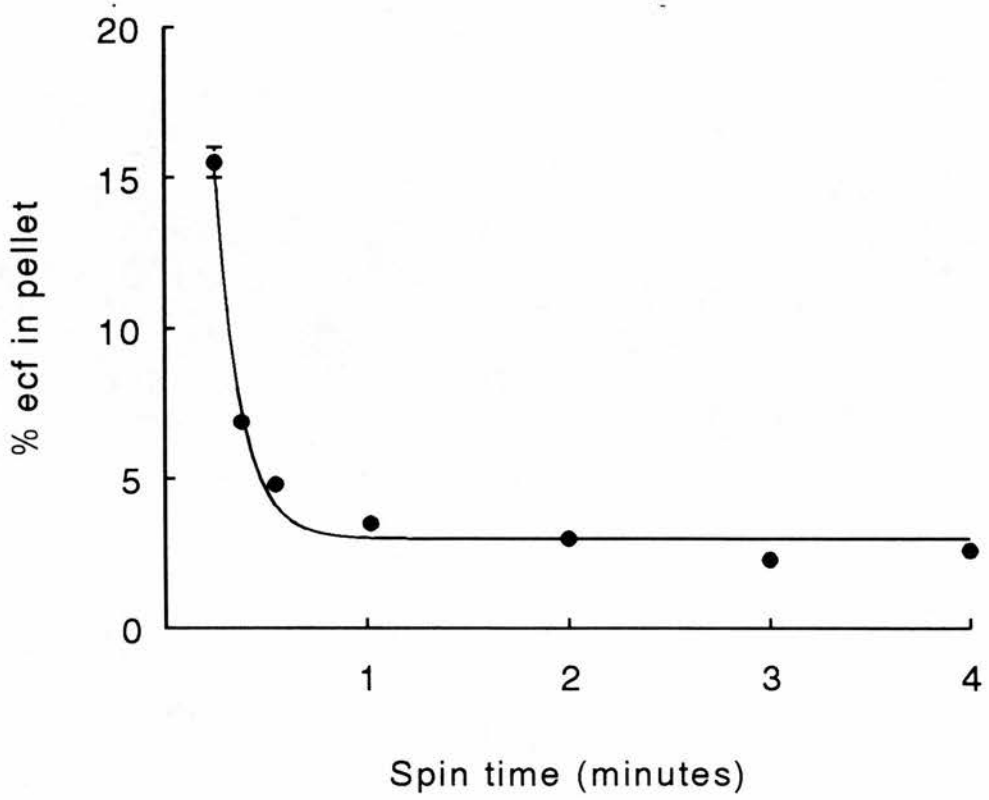

Figure 2.4.
Percentage of extracellular medium in cell pellet as a function of spin time.

experiments it was necessary to increase the spin time to 2 minutes and so reduce the trapped ECF to a reproducible 3% of the cell pellet.

After the cells were separated from the medium the oil and supernatant were removed from above the pellet by aspiration and the walls and cap of the tube were dried using a cotton swab. The cell pellet was lysed in 500 μl DGDW. 50 μl of 55% TCA was added to clear the protein from the lysate. A further addition of 640 μl DGDW was made. The final dilution volume was 1190 μl. Mg was measured by Atomic Absorption Spectrophotometry (Perkin-Elmer 2280) at a wavelength of 285 nm with background correction.

The magnesium concentration of the samples was read directly against $MgCl_2$ standards (1-50 μM) prepared in DGDW with a background matrix of 2.5% TCA. The absorbance of $MgCl_2$ standards was linear over this range (Figure 2.5). The 100 μM standard has a lower absorbance than predicted by the slope of the line drawn through the 1-50 μM standards. The bending of the function relating absorbance to concentration is predicted by the Lambert-Beer law which describes this relationship as an exponential function.

Mg concentration was calculated by:

$$(\text{AAS reading} - \text{Blank}) \times \text{Dilution Factor}$$

where the Dilution Factor =

$$\frac{\text{Volume of Cells} + \text{Dilution Volume}}{\text{Volume of Cells}}$$

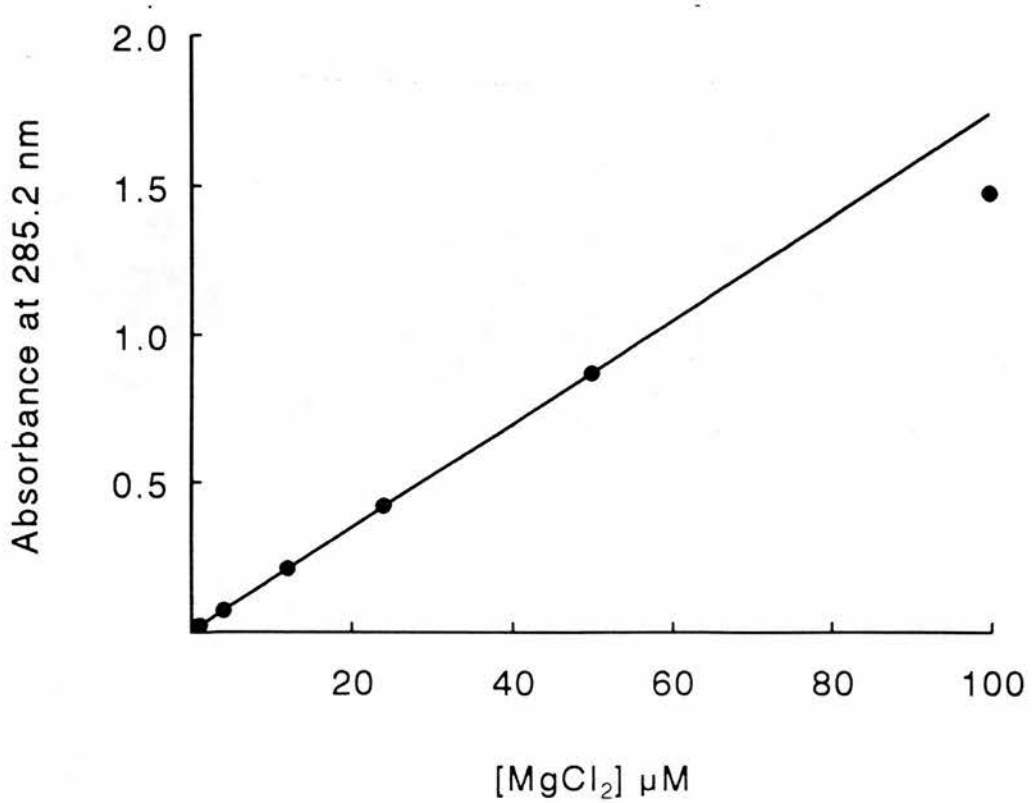

Figure 2.5.

The typical absorbance of $MgCl_2$ standards measured by atomic absorption spectrophotometry at wavelength of 285.2 nm with background correction. Standards were prepared from a 2 M $MgCl_2$ primary standard and include 2.5% TCA. For concentrations up to 50 μM the data is well fitted by a straight line. The line in the figure was drawn by linear regression analysis of absorbance values up to 50 μM. During experiments Mg samples were prepared to concentrations within the linear range (10 - 50 μM).

$$\text{or} \quad \frac{V_c + 1190}{V_c} \qquad (2.2)$$

where V_c = 100μl * Haematocrit

Mg concentration is thus expressed in the units of moles(litre of original cells)$^{-1}$ (moles(l.o.c.)$^{-1}$).

The Mg concentration is calculated on the basis of the cell haemoglobin content. To correct the measurements of [Mg] for cell lysis, the proportion of lysed cells was estimated as previously described. The corrected value for the haematocrit was substituted into the calculation of V_c.

When samples of suspension were spun through a layer of di-*n*-butylphthalate trails of cell fragments could be seen through and just above the surface of the oil. It seemed that this process of separating the cells from the medium resulted in some cell damage and haematocrit values for the total suspension and the supernatant would not give an exact measure of the number of cells forming the pellet. A further correction was thus added.

Cells were separated, processed and lysed in 500 μl DGDW as before. A sample of the lysate (200 μl) was diluted in Buffered Diluent to measure the haemoglobin of the pellet. Additions of TCA and DGDW (total volume 890 μl) were made to the remaining lysate and the Mg concentration measured by AAS.

The dilution factor for the Mg sample thus became

$$\frac{V_c + 500}{V_c} \quad * \quad \frac{V_c + 300 + 890}{V_c + 300} \qquad \textbf{(2.3)}$$

where V_c is volume of cells in the cell pellet. The apparent haematocrit of the lysate formed from the pellet under the oil (Hct_p) is

$$\frac{V_c}{V_c + 500} \qquad \textbf{(2.4)}$$

Thus cell [Mg] can be calculated using no correction factor or with a correction for cell lysis and also for the haemoglobin in the cell pellet. To assess the effectiveness of each correction step the cell [Mg] in one incubation was measured and calculated using the 3 possible dilution factors. Correcting for cell lysis increased the calculated value of cell [Mg]. The percentage increase corresponded to the percentage cell lysis measured as the haemoglobin in the ECF.

When cell [Mg] was corrected for the haemoglobin in the cell pellet the value of cell [Mg] increased but the scatter of the data also increased. The dilution factor was very dependent on the estimate of the volume of cells in the pellet. The absorbance measurements of the haemoglobin in the cell pellet could not adequately resolve the very small changes in the volume of cells. This measurement of the volume of cells could only be improved by taking larger volumes of the cell lysate to measure the volume of cells. This introduced error in the measurement of [Mg] in the sample. Thus this

correction introduced further complications to the protocol and limited the scale of experiments without improving the accuracy of the Mg measurement. Indeed this procedure increased the [Mg] in the experimental blanks. The protocol for correcting to the unit haemoglobin in the pellet was therefore discontinued and Mg samples were simply corrected for lysis.

2.8. Extracellular [Mg].

To measure extracellular Mg, samples of the ECF were isolated from the cells. Initially this was done using the method of Flatman and Lew (1978) and Flatman (1980) by adding 0.1 ml of suspension to a 0.4 ml tube containing 0.2 ml di-*n*-butylphthalate and spinning the tube for 30 seconds. 0.05 ml of the supernatant was diluted in 1.1 ml DGDW and 0.05 ml 55% TCA. The [Mg] in the sample was measured by AAS. The geometry of this separation method resulted in cell lysis through the oil layer. To avoid this damage and quantify the lysis occurring during the experiment the protocol was changed. 0.8 ml of suspension was spun in a 1.5 ml tube for 30 seconds. In a 8% suspension 0.6 ml of supernatant could be easily removed from above the pellet without causing stirring. Samples from this 0.6 ml aliquot were diluted in DGDW to measure $[Mg]_o$. Improved resolution of the measurement $[Mg]_o$ was made possible from the larger volume of supernatant now available. Increasing the volume of suspension allowed a further sample of supernatant to be transferred to

Buffered Diluent to assess the apparent haematocrit of the extracellular medium as a measure of cell lysis. Corrections to $[Mg]_o$ measurements to account for the contribution of Mg from lysed cells were made as follows;

Hct_T is the haematocrit of the main suspension
V_S is the volume of main suspension

The volume of cells (V_C) = V_S * Hct_T

Assuming that none of the cells lyse then the volume of ECF (V_{ECF}) is (V_S - V_C) = V_S*(1- Hct_T)
However if some cells lyse then the ECF contains the intracellular contents of the lysed cells (V_L)

V_L = V_S * Haematocrit of supernatant (Hct_S) **(2.5)**

Total ECF volume is the ECF volume + the intracellular volume of the lysed cells (V_{ECF} + V_L)

$$= V_S*(1-Hct_T) + V_S * Hct_S \quad \textbf{(2.6)}$$

The Mg in the ECF from the lysed cells is

$$Mg_i * \frac{\text{Volume of lysed cells}}{\text{volume of total ECF}}$$

which after substitution becomes

$$Mg_i * \frac{hct_S}{1-(hct_T-hct_S)} \quad \textbf{(2.7)}$$

The value of $[Mg]_o$ from lysed cells is subtracted from [Mg] measured by AAS to give $[Mg]_o$ corrected for cell lysis.

Mg fluxes.

Mg flux is the change in the intracellular or extracellular [Mg]. Measurement by AAS gives the concentration in μM. The calculation of cell [Mg] is based on the haemoglobin content and therefore the number of cells in the suspension. Thus measuring a flux as a change in the intracellular concentration relates the amount of Mg appearing in the medium to the number of cells in the suspension. $[Mg]_o$ is calculated as the μM concentration in the medium. To attribute any change in the $[Mg]_o$ to the number of cells in the suspension it is helpful if $[Mg]_o$ is expressed in the units $mmol(l.o.c.)^{-1}$. To do this $[Mg]_o$ (M) is multiplied by the factor:

$$\frac{1-(hct_T-hct_S)}{(hct_T-hct_S)} \qquad \textbf{(2.8)}$$

The Mg flux was determined as the change in the intracellular or extracellular [Mg] between 2 time points. The first sample was usually taken between 5 and 15 minutes after the start of the incubation. The second sample was taken after a further incubation of between 30 minutes and 2 hours. The change in the [Mg] between these 2 time points was expressed as the

flux per hour.

In initial experiments triplicate measurements of [Mg] were made at the 2 time points in one incubation. The flux was the change in the mean [Mg] between the 2 time points. To increase the statistical significance of the measurements, only one measurement of [Mg] was made at each time point in three separate incubations. The flux was then the mean flux of 3 independent measurements and could be expressed with the standard error of the mean (S.E.M.) with n = 3.

AAS Measurements; Blanks and Matrix.

Every set of Mg measurements by AAS included a group of blank samples. The value of blank samples measured by AAS gave an indication of background and contaminant Mg. The blank value was subtracted from the concentration of Mg in the experimental samples. In initial experiments Eppendorf microtubes were used and the Mg blank values were low. In a series of experiments the apparent [Mg] in the blanks became high and variable. As there had been no protocol change the plastic tubes were suspected to be the source of the contamination. Several brands of tubes and procedures were used and the background [Mg] checked. Table 2.1 shows that some brands of plastic tubes contain higher contaminant Mg than others. Pre-soaking the tubes in 5% nitric acid and drying before use reduces the background Mg to an acceptable level. However the

Table 2.1. Mg contamination of micro reaction tubes

Tubes and protocol	[Mg] μM
1. Eppendorf	0.72 ± 0.04, n=6
2. Eppendorf rinsed in nitric acid	0.03 ± 0.00, n=5
3. Eppendorf with 2.5% TCA. 1 day	0.77 ± 0.02, n=9
4. Eppendorf with 2.5% TCA. 2 days	0.97 ± 0.06, n=3
5. Eppendorf with 5% TCA. 2 days	3.56 ± 0.44, n=3
6. Tref	0.00 ± 0.00, n=2
7. Tref with 2.5% TCA. 1 day	0.01 ± 0.00, n=9
8. Alpha	0.04 ± 0.01, n=6
9. Alpha with 2.5% TCA. 1 day	0.12 ± 0.02, n=6
10. Sarstedt with 2.5% TCA. 1 day	-0.00 ± 0.00, n=9

Tubes were filled with the appropriate solution and the concentration of Mg (μM) measured by AAS. Results shown are the mean ± S.E.M. Rinsed tubes were soaked in DGDW containing approximately 5% nitric acid (AnalaR) for 1 - 2 hours and then rinsed 3 times in DGDW. Tubes for experiments were dried between chromatography paper in an oven. TCA is Aristar grade.

addition of 2.5% TCA increases the apparent [Mg]. When TCA was left in the tubes the [Mg] increased in a time dependent manner and it seemed that leaving TCA in the tubes can leach Mg out of the plastic. To overcome this problem TCA was left out of the protocol and the cell pellet was lysed in DGDW alone. $MgCl_2$ standards for AAS were prepared without the 2.5% TCA matrix. The standards were linear over the concentration range used. (Figure 2.6)

To show that the omission of TCA from the protocol did not affect the measurement of [Mg] cells from the same suspension were processed with or without the addition of TCA. In one experiment cells lysed in DGDW had an measured cell [Mg] of 2.19 ± 0.01 mM (mean ± S.E.M , n=9 measurements). If the protocol included the addition of 2.5% TCA the measured cell [Mg] was 2.20 ± 0.02 mM (mean ± S.E.M, n=9 measurements).

TCA was used in these protocols not only to precipitate the protein but also to prevent matrix interference. Matrix interference can cause error in AAS measurement and occurs when the samples and standard vary in their physical characteristics (surface tension, concentration of dissolved salts or solvents etc.). To overcome this the samples and standard are uniformly diluted to mask any variations in the composition of the sample matrix.

When measuring [Mg] in samples with different [Na] there is a large variation in the background composition against which [Mg] is measured and an obvious difference in the intensity of the AAS flame.

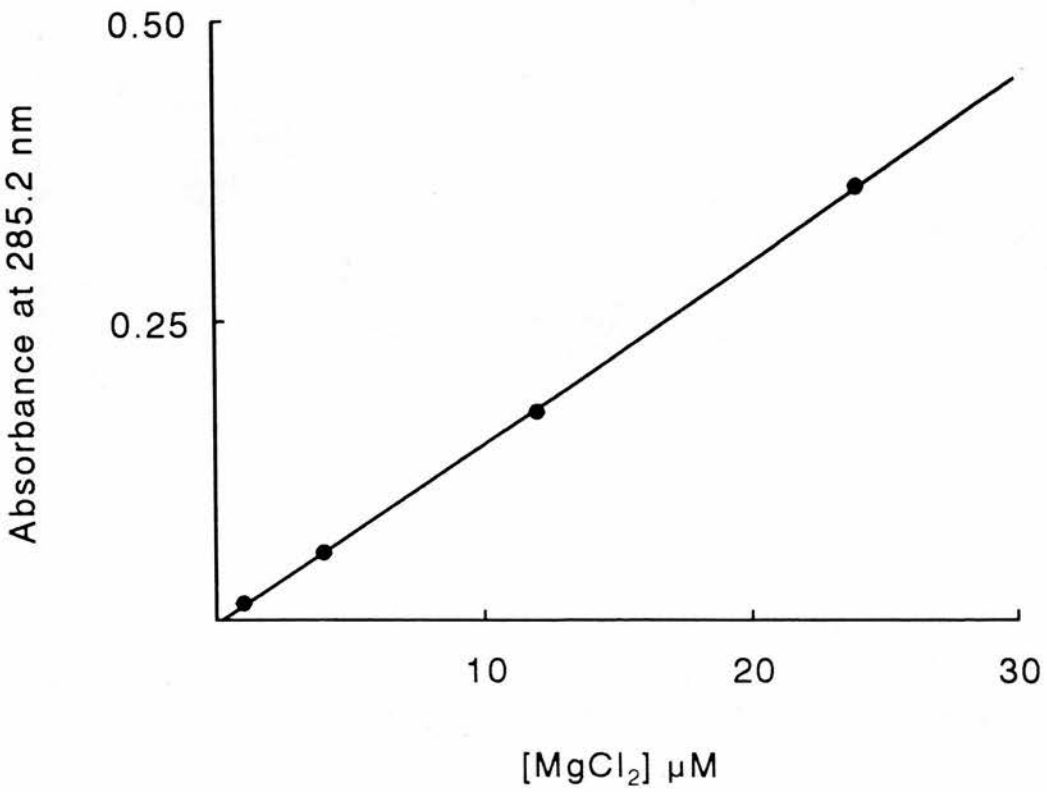

Figure 2.6.
The typical absorbance of $MgCl_2$ standards measured by atomic absorption spectrophotometry at wavelength 285.2 nm with background correction. Standards were prepared from a 2 M $MgCl_2$ primary standard. No TCA was included. The straight line was drawn through data using linear regression analysis.

Figure 2.7 shows the results of a control experiments to check that these large changes in background composition do not effect the measurement of [Mg]. Figure 2.7 shows the results of an experiment where [Mg] was measured in media each containing the same [Mg], no TCA and different [Na]. The changing background matrix had no effect on the measurement of [Mg].

Although measurements of [Mg] by AAS seem quite insensitive to changes in the composition of the background matrix it was thought prudent to investigate the effects of measuring [Mg] in a uniform matrix. $LaCl_3$ is often used as a background matrix for measuring Mg samples by AAS. To test the effectiveness of $LaCl_3$ cells were lysed in a medium containing 1% $LaCl_3$. The addition of $LaCl_3$ resulted in cell clumping and incomplete release of cellular Mg. For the same cells as above, the measured [Mg] was 0.94 ± 0.04 mM (mean ± S.E.M, n=9 measurements). $LaCl_3$ was also introduced at a later stage of the protocol. After lysing the cells in DGDW, concentrated $LaCl_3$ was added in a small volume to give a final concentration of 1 g L^{-1}. The addition of $LaCl_3$ did not change the value of measured [Mg] compared to the cells with a matrix of DGDW and added an extra step to the protocol. The addition of $LaCl_3$ was therefore not continued.

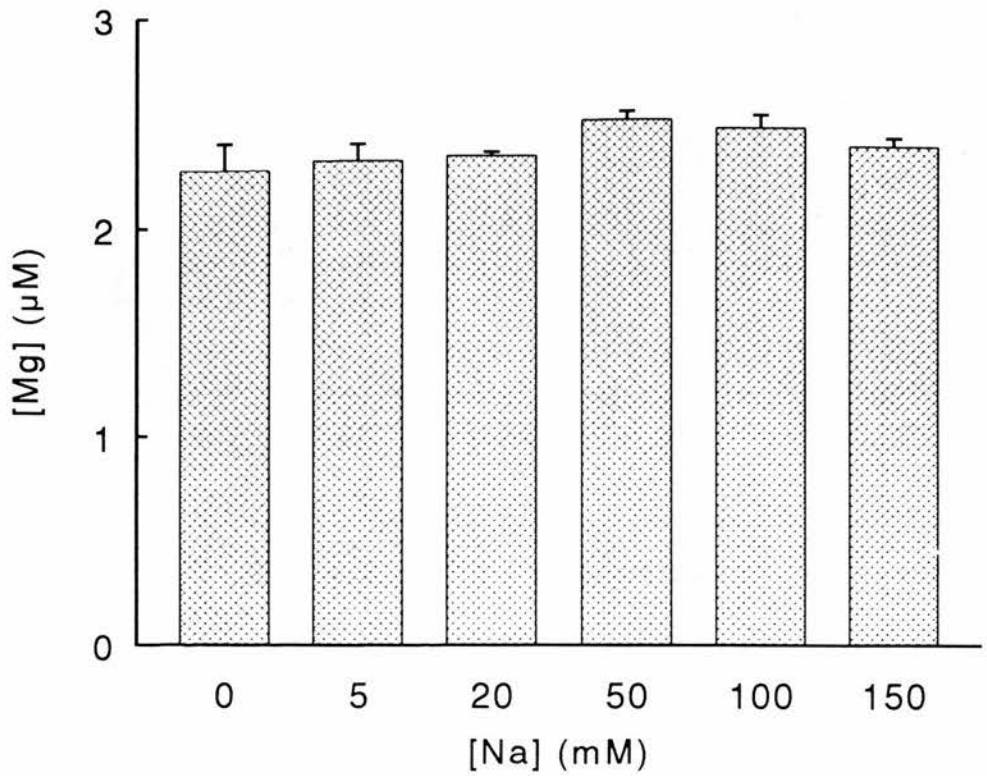

Figure. 2.7.

The effect of changing the matrix [Na] on the measurement of Mg by AAS. Media of various [Na] were prepared by mixing NaCl and choline chloride media (buffered with K-HEPES) to give the initial [Na] shown. Samples were diluted 4 times to mimic the protocol for Mg determinations. 0.1 ml of a 24 μM $MgCl_2$ stock solution was added to 1.2 ml of incubation medium to give a final [Mg] of approximately 2 μM. Samples were taken from the incubation vials and the [Mg] measured by AAS after processing. Bars show the mean of 3 measurements with S.E.M.

Sodium and potassium measurements.

To measure intracellular and extracellular [Na] the cells had first to be separated from the medium. There were 2 protocols for this used in this study. Both intracellular and extracellular samples were diluted in 1 g L^{-1} LiCl so that the concentration of the sample was less than 50 μM. [Na] was measured by AAS against 10 and 50 μM $NaNO_3$ standards containing 1 g L^{-1} LiCl.

METHOD 1. 1 ml of suspension was transferred to a 1.5 ml tube containing 0.1 ml di*n*-butylphthalate. The tube was spun for 30 seconds. A sample was taken from above the oil and diluted in LiCl. $[Na]_o$ was measured after further dilution. The end of the tube was then cut and dropped into tube containing 1 g L^{-1} LiCl. The pellet was allowed to haemolyse. The lysate was diluted in LiCl and cell [Na] was measured by AAS.

METHOD 2. The separation method was improved (and contamination from ECF reduced) by adapting the separation method used for cell [Mg] determination. 0.1 ml of suspension was added to a 1.5 ml tube containing 0.3 ml di-*n*-butylphthalate and 1 ml 145 mM choline chloride (ice-cold). The [Na] in the ECF was thus diluted. Increasing the spin time also reduced the concentration of $[Na]_o$ in the cell pellet. The supernatant was aspirated, tubes cleaned with cotton swabs and the pellet lysed in 1 g L^{-1} LiCl. The pellet was further diluted in LiCl and [Na] measured by AAS. When samples of suspension were spun down to sample

extracellular medium for $[Mg]_o$ and lysis determinations an aliquot was also diluted in LiCl to measure [Na].

To measure intracellular and extracellular [Na] the samples had to be diluted in LiCl so that the concentration was less than 50 μM. Only a small fraction of the sample (0.05 ml) was needed. The remainder of the sample was used for measurements of [K]. [K] was measured against 10 and 50 μM KNO_3 standards containing 1 g L^{-1} LiCl.

Measurement of adenosine triphosphate.

Adenosine triphosphate (ATP) was extracted and measured using a protocol modified from Brown (1982). 0.05 ml of suspension were added to a 1.5 ml tube (on ice) containing 0.35 ml of 10 mM EDTA with 0.1% Triton and 0.1 ml 2.8 M perchloric acid (PCA). The tube was vortexed and allowed to stand on ice for 5 minutes. The tube was spun for 3 minutes to precipitate the protein. The PCA was neutralised by transferring 0.3ml of the supernatant to another tube containing 0.3ml KOH buffer solution (700 mM KOH, 100 mM KCL, 200 mM HEPES). The samples were kept on ice and spun for 3 minutes before measuring ATP using the fire-fly assay.

Fire-Fly Assay.

This assay was performed at room temperature using a Luciferin-Luciferase preparation in kits manufactured by Wallac. 0.01 ml of ATP sample was added to 0.75 ml

ATP buffer solution (0.1 M TRIS, 2 mM EDTA, 4 mM Na, pH adjusted to 7.70 at room temperature using glacial acetic acid). 0.2 ml reconstituted fire-fly enzyme was added. The tube was vortexed and the light output measured on an LKB Luminometer. 0.01 ml of an appropriate ATP standard (0.2 or 2 μM in ATP Buffer) was added and the light output re-measured. ATP concentration was calculated from the ratio of sample reading to (sample + standard) reading.

Cell Water Content.

An estimate of changes in cell volume was made by measuring the water content of the cells.

Labelled glass vials were heated in an oven at 105 °C for 1 hour and cooled under vacuum. The vials were weighed to 0.1 mg on a Sartorius balance when at room temperature. 1 ml of an approximate 10% red cell suspension was transferred to a 1.5 ml tube containing 0.2 ml di-*n*-butylphthalate. The tube was spun at about 14000 x g for 3 minutes, the supernatant and oil removed by aspiration and the walls dried using a cotton swab. 0.05 ml of packed cells were transferred to the pre-weighed vial using a Gilson Pipetman positive displacement pipette. The weight of glass vial with cells was noted.

The vial and cells were heated in the oven at 105 °C for approximately 18 hours. The vials were cooled under vacuum and weighed. The vials were heated, cooled and weighed until a constant weight was

attained. The difference between the dry weight and wet weight of the cells is the cell water which is expressed as a percentage of the wet weight.

The amount of ECF in the cell pellet was calculated using ^{57}Cobalt-EDTA as an extracellular marker. The protocol for this measurement is similar to that described in the legend to Figure 2.4. The trapped ECF accounted for 3% of the cell pellet. To correct for this the cell water content was multiplied by the factor EC/(1-EC) where EC is the fraction of cell pellet which is ECF.

The cell water content of untreated ferret red cells in a number of experiments was 68.1 ± 0.8 % wet weight (mean ± S.E.M.,n=19 measurements).

Measurements of membrane potential.

Red cells have a high Cl^- conductance and Cl^- is distributed across the membrane according to the predicted Donnan equilibrium. Thus the membrane potential is usually close to the chloride equilibrium potential. The distribution of Cl^- across the membrane is thus a useful measurement of the membrane potential.

When the balance of ionic species across the membrane is disturbed Cl^- redistributes itself according to its new equilibrium potential. The chloride distribution ratio ($[Cl]_o/[Cl]_i$) thus increases when the cell is hyperpolarised and decreases when the cell is depolarised.

Measurement of membrane potential by the Cl^-

distribution ratio is not always appropriate. If there are large changes in cell permeability the distribution of Cl^- may no longer be the best measure of the membrane potential. The membrane potential will be determined by the concentration of the permeant species. Thus when measuring changes in the membrane potential in treated cells it is important to consider the possible permeability changes in the cells which may occur as a result of the experimental protocol.

Under normal conditions the movement of Cl^- across the membrane is several orders of magnitude faster than the movement of other species and therefore Cl^- distribution dominates the membrane potential. Under those conditions where Cl^- no longer dominates the potential it is possible to measure changes in the membrane potential by the distribution of H^+ across the membrane. There are a number of reagents which can greatly increase the permeability of the membrane to H^+. Under these conditions the ratio $[H^+]_i/[H^+]_o$ gives an accurate measure of membrane potential. This technique has the advantage that the membrane potential can be measured as changes in the intracellular and extracellular pH. It is also sensitive enough to measure very rapid changes in the membrane potential.

In these experiments changes in membrane potential were monitored by (i) changes in the chloride distribution ratio or (ii) changes in the distribution of H^+ using a proton ionophore to increase H^+ permeability.

Chloride distribution ratio.

The chloride distribution ratio was measured using the technique of Flatman and Lew (1980). 1ml of cell suspension was transferred to a 1.5 ml tube containing ^{36}Cl. The tube was vortexed and incubated for 5 minutes at 38 °C to allow ^{36}Cl to equilibrate. The tube was spun briefly to remove any suspension from the cap of the tube and 0.2 ml of di-*n*-butylphthalate added. The sample was spun for 2 minutes at 14000 x g to separate the cells from the medium. 0.05 ml of supernatant was added to 0.9 ml DGDW and 0.05 ml TCA. The tube was vortexed, spun for 3 minutes and 0.7 ml of the supernatant added to 3 ml Rialuma scintillation cocktail in a scintillation vial. Samples were counted for beta emission on a LKB 1218 Rackbeta liquid scintillation counter.

The cell pellet was cleaned by aspirating the remaining FBM and oil. The walls of the tube were cleaned using a cotton swab. 0.05 ml of cells were transferred to a tared 1.5 ml tube using a positive displacement pipette. The weight of the cells was noted. The cells were then lysed in 0.9 ml DGDW and 0.05 ml 55% TCA. After vortexing and spinning for 3 minutes, 0.7 ml of the sample was counted in 3 ml Rialuma using the same parameters as for $[^{36}Cl]_o$.

The chloride distribution ratio is given as

$$[Cl]_o/[Cl]_i$$

and is calculated by

$$\frac{(cpm_o / 50) * weight * water\ content * (1-EC)}{cpm_i - weight * EC * (cpm_o / 50)} \qquad (2.9)$$

where $cpm_o / 50$ is the extracellular counts per minute per μl.

cpm_i is the intracellular counts per minute

weight is the weight of the cell pellet in mg

water content is the water content of the cells

EC is the fraction of cell pellet which is ECF

The value of the Cl^- distribution ratio for untreated ferret red blood cells was 1.32 ± 0.02 (mean ± S.E.M., n=9).

H^+ distribution.

H^+ distribution was measured using the method of Macey, Adorante and Orme (1978). Red cells were washed twice and suspended at about 8% haematocrit in an unbuffered medium (145 mM NaCl, 5 mM KCl). When using cells stored in the fridge it was sometimes necessary to adjust the starting pH to a more physiological value by adding a small amount of 1.3 M tetraethylammonium. 0.2 mM of the proton ionophore carbonyl cyanide m-chlorophenylhydrazone (CCCP) were added (stock solution = 50 mM in DMSO). The pH of the suspension was measured using a Ross semimicro combination pH electrode. Cells were lysed in 0.2% TRITON X-100 (from stock of 20% in DGDW) and the pH remeasured after reaching a steady value.

Loading cells with Mg using A23187.

The intracellular [Mg] of ferret red cells was changed using two methods. The intracellular [Mg] of ferret red cells increases when they are incubated in media with a low [Na] and high [Mg]. This phenomenon was exploited to load the cells with Mg. The protocol for this is described in Chapter 5.

A23187 is a carboxylic acid antibiotic which increases the membrane permeability to Ca and Mg (Reed and Lardy, 1972). When A23187 is added to a cell suspension the intracellular [Mg] changes to a concentration which is at electrochemical equilibrium with the extracellular [Mg] (Flatman and Lew, 1977). Thus by changing $[Mg]_o$ it is possible to control the cell [Mg].

Cells were suspended at about 8% haematocrit in FBM with added $MgCl_2$. Concentrations of Mg between 0 and 2 mM were used in the extracellular medium. Figure 2.8 shows the changes in the cell [Mg] when cells were incubated in 1 or 0.6 mM $MgCl_2$ and 5 μM A23187. The time taken for [Mg] to equilibrate is dependent on $[Mg]_o$. The higher the concentration of $[Mg]_o$ the more time is needed for cell [Mg] to reach a plateau. Equilibration of Mg was usually allowed to proceed for 5 minutes.

Before fluxes can be measured from Mg-loaded cells the ionophore must be removed from the cell membrane. A23187 has a high capacity for Mg transport and any residual ionophore will mask the movement of Mg through

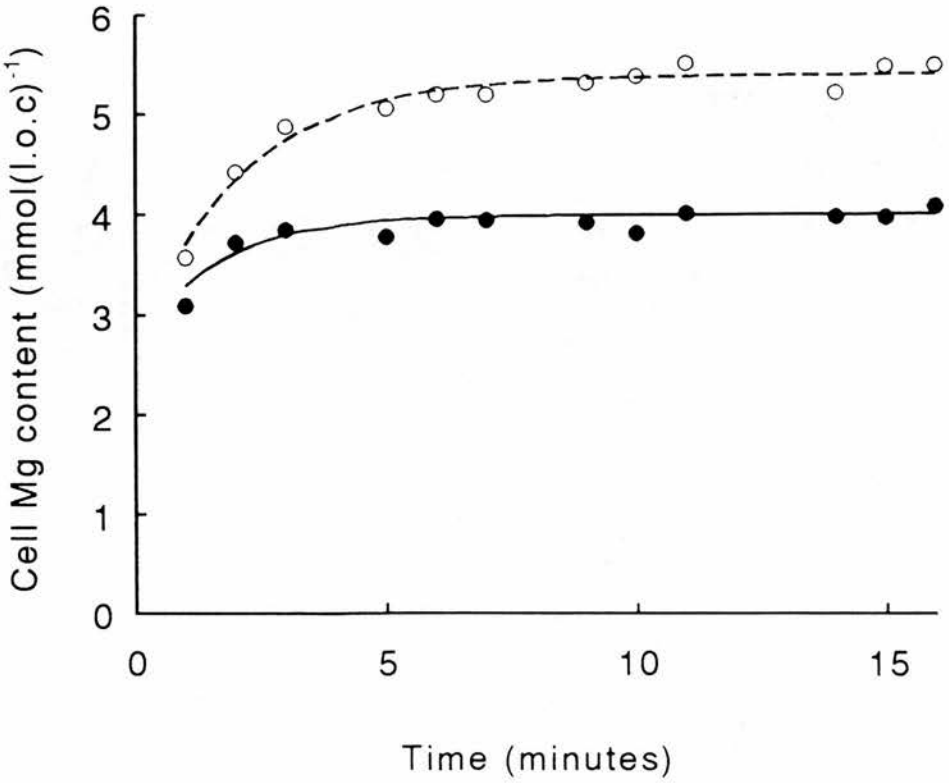

Figure 2.8.

The time dependent increase in the cell Mg content of cells incubated with the ionophore A23187 and different external [Mg]. Ferret red cells were incubated at about 7% haematocrit in FBM with 11 mM glucose, 0.05 mM EGTA and either 1 mM (open circles) or 0.6 mM (filled circles) $MgCl_2$. 5 μM A23187 was added at time zero. Cell [Mg] was measured at the times indicated. The lines show exponential fits of the data (A*(1-exp(k*t))+B). The parameters of the curve fit were: (open circles) A, 2.74; B, 2.64; k, -0.49; (filled circles) A, 1.32; B, 2.67; k, -0.64.

other routes.

Loaded cells are washed in FBM containing Bovine serum albumim (BSA) to remove the ionophore. To prepare a standard protocol for the removal of the ionophore it is necessary to assay the efficiency of the washing procedure. Other studies have done this by measuring Mg efflux from untreated cells and comparing this to efflux from cells which have seen the ionophore but have control cell [Mg]. A washing protocol devised using this test does not take into account the effects of high cell [Mg]. At high concentrations of Mg it may be more difficult to remove A23187 since the ionophore can form precipitates with Mg inside the cells. Once these precipitates are inside the cells they cannot be washed away with BSA-containing media. The ionophore inside the cells would leach into the membrane and mediate Mg flux. Thus a test for A23187 removal which uses cells with control cell [Mg] may not be the most appropriate.

Cells were loaded with Mg using the ionophore and an external [Mg] of 1 mM. The loaded cells were washed 1, 2, 3 or 4 times in FBM containing BSA. The cells were then washed and incubated in FBM. Figure 2.9 shows cell [Mg] in these cells measured during the 3 hour incubation in FBM. The symbols show the different number of washes in BSA-containing medium. Mg efflux is very sensitive to the number of washes. The rate of efflux was reduced by increasing the number of washes from 3 to 4. In other experiments Mg efflux was measured from cells which had been washed 5 times in

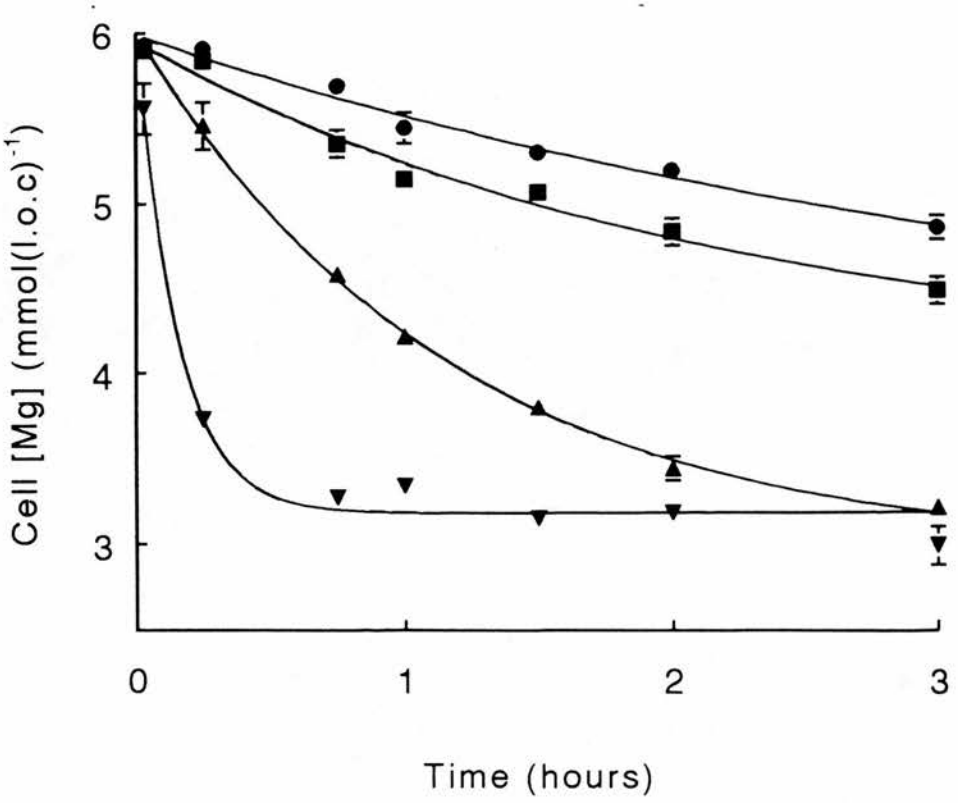

Figure 2.9.

Mg efflux from Mg-loaded cells. Cells were incubated in FBM with 5 μM A23187 and 1 mM $MgCl_2$ for 10 minutes. They were then washed in FBM containing 2 mg/ml BSA and/or 1 mM $MgCl_2$ as shown in the table below. The cells were also given a final wash in FBM. Triplicate measurements of cell [Mg] were made at the time points indicated. The data was fitted using exponential functions.

	Number of washes			
	(1)	(2)	(3)	(4)
inverted triangles	BSA/Mg			
triangles	BSA/Mg	BSA		
squares	BSA/Mg	BSA/Mg	BSA	
circles	BSA/Mg	BSA/Mg	BSA	BSA

BSA-containing media. After this extra wash the rate of efflux increased. This suggests that it is possible to cause some cell damage and alter the cell permeability by overwashing. It was therefore decided to wash the cells 4 times in BSA-containing media before measuring fluxes.

The rate of efflux from loaded cells was used as an assay for the removal of the ionophore. EDTA was added to the incubation medium to make this test more sensitive. EDTA binds $[Mg]_o$ and thereby produces a large outward gradient for Mg. Mg transport through the ionophore is very sensitive to this gradient. Therefore Mg efflux from cells containing residual ionophore is much faster than from cells which contain no ionophore and the cell [Mg] falls below the initial Mg level.

The ratio of cells to medium in each wash is also important in the removal of the ionophore. Figure 2.10 shows an experiment where cell [Mg] was measured over 1 hour in cells which had been loaded with A23187 and 1 mM $[Mg]_o$. All groups of cells had been washed the same number of times but the ratio of cells to medium varied.

The results from Figures 2.9 and 2.10 assisted in the formation of a standard protocol for loading with Mg using the ionophore and the subsequent washing steps. This protocol is described in Table 2.2. Cells were incubated at approximately 10% haematocrit in FBM with added $MgCl_2$ (0 - 2 mM). The incubation (loading) was allowed to proceed for 5 minutes. The cells were

Legend to Figure 2.10

Cells were loaded with Mg as described for Figure 2.9. The table below shows the ratio of medium to cells (Ratio), the concentration of BSA (mg/ml) in each wash and the number of washes. Wash 1 was warm while the others were cold. All washes contained BSA and washes 1 and 2 also contained 1 mM $MgCl_2$. After washing the cells were suspended in FBM (with 20 mM HEPES) with 0.2 mM $MgCl_2$ and 1 mM EDTA. Triplicate measurements of cell [Mg] were made at the time points indicated.

	Ratio	BSA	Washes
inverted triangles	10	2	4
triangles	20	2	4
squares	100	2	1
	10	2	3
circles	20	4	4

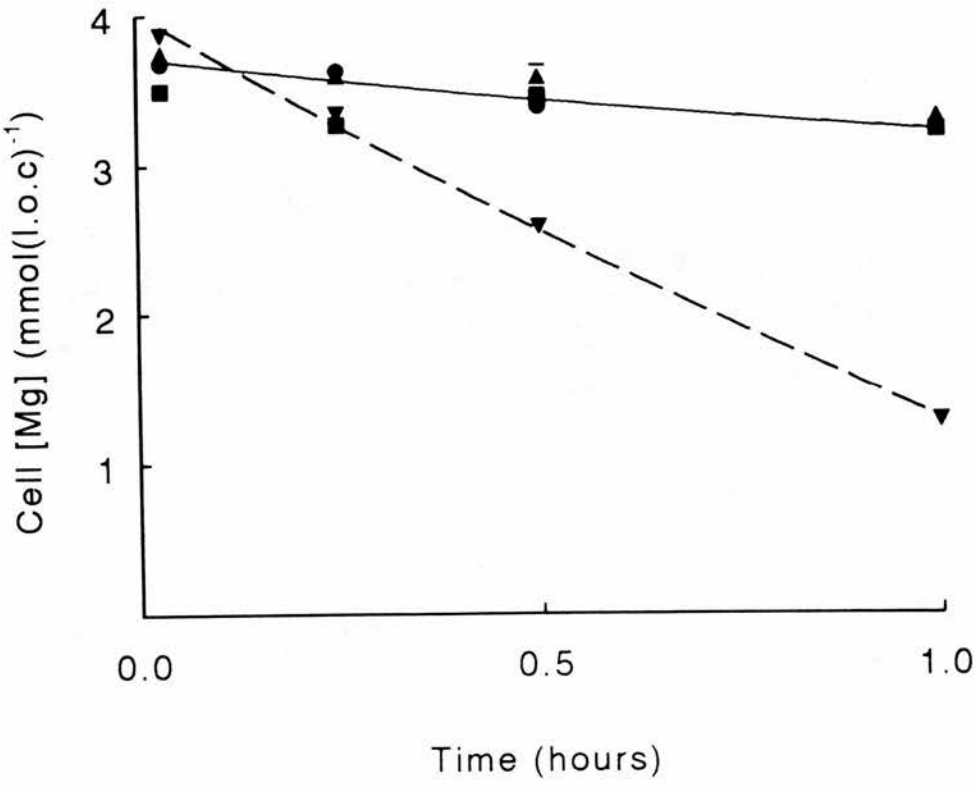

Figure 2.10.
Mg efflux from Mg-loaded cells.

then spun down and washed twice in a 20 times volume of FBM containing 2 mg/ml BSA and $MgCl_2$ (the initial wash media contained the same [Mg] as the loading medium). All washes were ice-cold except the second wash. The cells were incubated at 38 °C for 5 minutes in this wash medium before spinning down. The third and fourth washes contained BSA but no added $MgCl_2$. The cells were then washed a further time in the incubation medium (with no BSA). In some experiments BSA was also included in the loading medium.

The precipitation of A23187 in the cells and hence the ability to remove it from the cells is dependent on a number of factors including the haematocrit of the suspension (and hence the concentration of ionophore in the cells), the length of time the cells are incubated with the ionophore and the cell [Mg]. These factors are difficult to control exactly. In all experiments using the ionophore there is no certainty that the ionophore has been completely removed. A fluorimetric assay for A23187 has been described (Simonsen & Lew 1980). The protocol described in the paper of Simonsen and Lew was used to assay residual A23187 in ferret red cells. Using this assay it has thus far not been possible to measure residual ionophore. The very small concentrations of ionophore remaining in the cells after washing may be outwith the resolution of this assay.

In all experiments where the cells had been loaded using A23187 the final incubation medium contained EDTA. Thus if there was any residual ionophore in the

Table 2.2. Protocol for loading cells with Mg using the ionophore A23187

Load medium FBM
11 mM glucose
0.05 mM EGTA
1 mM $MgCl_2$.

Cells are incubated in LOAD medium at 38°C. 10 μM A23187 (from a stock of 1 mg/ml in AnalaR grade ethanol) are added with continuous stirring and the cells are incubated with the ionophore for 5 minutes.

Wash media The cells are washed 5 times in 20 volume washes.

Wash 1: FBM, 2 mg/ml BSA, 1 mM $MgCl_2$ (ice-cold wash)

Wash 2: FBM, 2 mg/ml BSA, 1 mM $MgCl_2$ (the cells are incubated in this wash for 5 minutes at 38 °C).

Wash 3: FBM, 2 mg/ml BSA (ice-cold wash).

Wash 4: FBM, 2 mg/ml BSA (ice-cold wash)

Wash 5: FBM

Incubation medium

For flux measurement the cells are suspended in a medium containing (mM) : NaCl (131); KCl (5), Na-HEPES (20 with 14 mM Na); glucose (11); EGTA (0.05); EDTA (1); $MgCl_2$ (0.2).

cells during efflux measurements, efflux would occur at a much higher rate and the cell [Mg] would fall below the control (unloaded) concentration. Inclusion of EDTA in all incubation media for cells loaded using the ionophore provided an internal check for the complete removal of the ionophore.

Mg buffering in ferret red cells.

Mg binds to many substances inside a red cell. Flatman and Lew (1980) have described 3 buffer systems for oxygenated human red cells. The capacities and affinities of these three systems can probably be attributed to Mg binding sites on proteins, nucleotides (including ATP) and organic phosphates. Of the total cell [Mg] (measured by AAS) some is bound inside the cell and some is in the free ionized form. The fraction of the total cell [Mg] which is free depends on the concentration of the buffers inside the cell. Measurements in ferret red cells have shown that the concentration of certain intracellular Mg buffers varies depending on the state of the cell. For example depletion of the cell [ATP] by incubation in medium containing 2-deoxyglucose alters the buffering capacity of the cells (these experiments are described in Chapter 3). A measurement of the buffering capacity in the cells allows the determination of the $[Mg^{2+}]_i$ for every measurement of total cell [Mg].

Mg buffering curves for ferret red cell were produced using the method described by Flatman and Lew

(1980). Ferret red cells were incubated at approximately 8% haematocrit in FBM with added $MgCl_2$. 5 concentrations of $MgCl_2$ (mM; 0.1, 0.3, 0.6, 1.0, 1.5) were most commonly used. The initial cell [Mg] and haematocrit were measured. 10 μM A23187 was added and the Mg was allowed to equilibrate for at least 5 minutes. After this time the final cell [Mg] and the exact $[Mg]_o$ were measured.

The intracellular concentrations of bound and free Mg are at all times dictated by the Law of Mass Action:

$$[Mg]_b = \sum_{j=1}^{n} \left(\frac{[Mg^{2+}]_i * C_j}{[Mg^{2+}]_i + K_j} \right) \qquad \textbf{(2.10)}$$

(where C_j and K_j are the capacity and affinity of the jth buffer respectively).

When the ionophore is added to the medium, intracellular and extracellular ionized Mg ($[Mg^{2+}]$) equilibrate. The ionophore mediates the electroneutral exchange of Mg for 2 protons. It is possible to express Mg:2H exchange as

$$\left(\frac{[Mg]_i}{[Mg]_o} \right) = \left(\frac{[H^+]_i}{[H^+]_o} \right)^2 \qquad \textbf{(2.11)}$$

Since H^+ and Cl^- are equilibrated by an anion shuttle equation **(2.11)** becomes

$$\left(\frac{[Mg]_i}{[Mg]_o} \right) = \left(\frac{[Cl^-]_o}{[Cl^-]_o} \right)^2 = r^2 \qquad \textbf{(2.12)}$$

Measurements of total cell [Mg] give the concentration

in mmol(l.o.c.)$^{-1}$. To express in mmol(cell water)$^{-1}$ the concentration is divided by the cell water content. The ionized and bound concentrations can be calculated from equation **(2.12)** thus

$$[Mg]_b = [Mg]_T - r^2 * [Mg]_o \qquad \textbf{(2.13)}$$

where

$[Mg]_T$ is the total cell [Mg] (mmol(l cell water)$^{-1}$)

$[Mg]_b$ is the intracellular bound [Mg]

$[Mg]_o$ is the extracellular ionized [Mg]

The intracellular ionized [Mg] is obtained by subtracting the intracellular bound [Mg] from the total cell [Mg].

Mg buffering curves usually express bound [Mg] as a function of ionized [Mg]. A buffering curve composed of data from several typical experiments is shown in Figure 2.11. The same data is also shown in Figure 2.12. In Figure 2.12 total cell [Mg] (mmol(l.o.c.)$^{-1}$) is shown as a function of ionized [Mg]. Using this curve it is possible to obtain an estimate of $[Mg^{2+}]_i$ from the measured value of total cell [Mg].

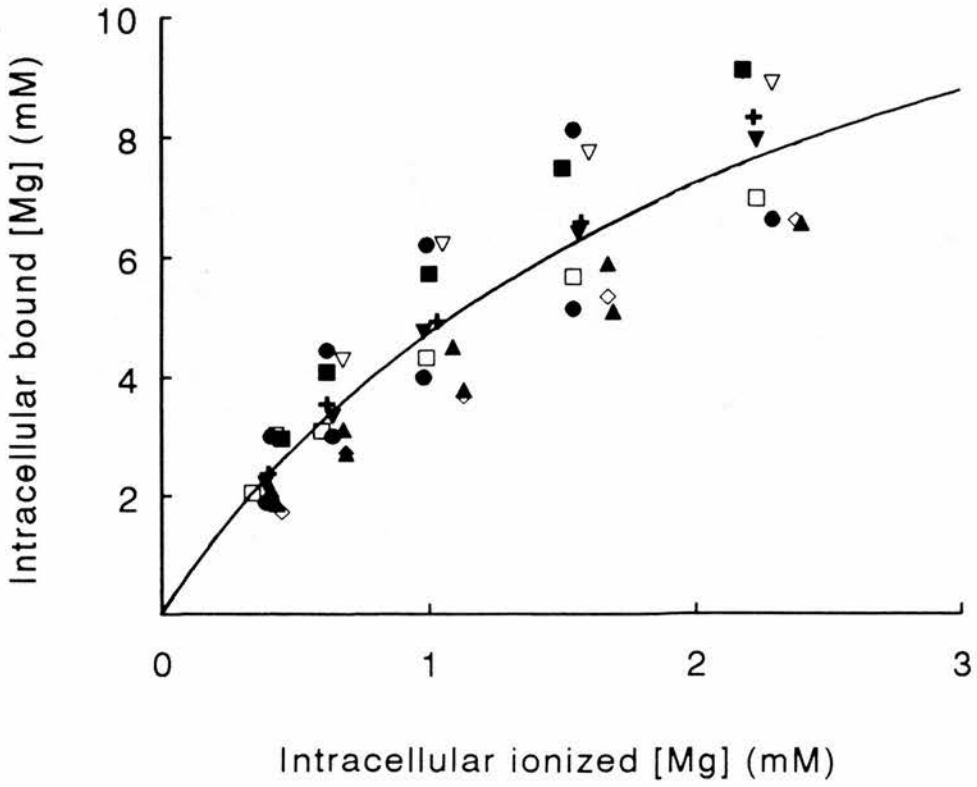

Figure 2.11.

Mg buffering curve for fresh ferret red cells. The Mg buffering in ferret red cells was measured using the protocol described in the text. Bound [Mg] is shown as a function of the intracellular ionized [Mg]. Symbols represent different experiments using cells from different animals. The line shown is the best fit of all the data and is drawn assuming 1 site ligand binding. The parameters of the curve fit with standard error are; Capacity, 14.82 ± 2.07 and K_d, 2.14 ± 0.50.

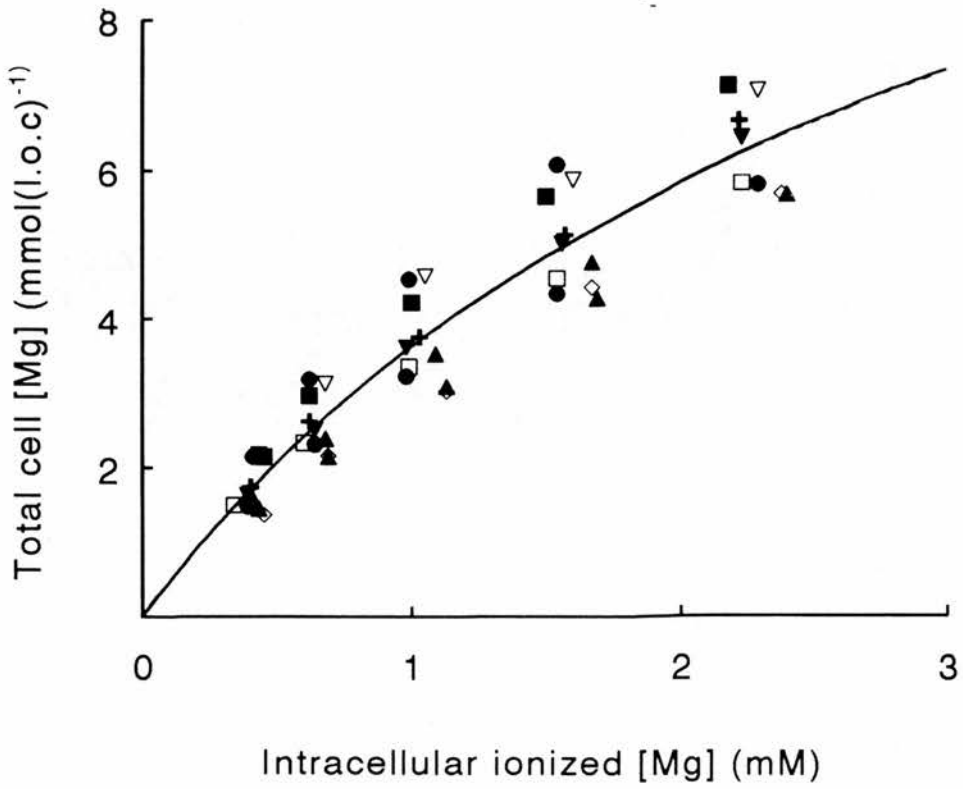

Figure 2.12.

Mg buffering curve for fresh ferret red cells. The data shown is from the same experiments as Figure 2.11. Total cell [Mg] (mmol(l cell)$^{-1}$) is shown as a function of intracellular ionized [Mg]. The line shown is the best fit of all the data and is drawn assuming 1 site ligand binding. The parameters of the curve fit with standard error are; Capacity, 14.41 ± 2.04 and K_d, 2.98 ± 0.64.

3. Magnesium Efflux

Measurement of Mg efflux

When ferret red cells are incubated in a medium to which no Mg has been added there is a measurable net efflux of Mg from these cells. A great advantage of ferret red cells over many other species of red cells in studies of Mg transport is that ferret red cells do not require loading with Mg to enable Mg efflux to be measured. Efflux can be measured as a change in either the intracellular or extracellular [Mg]. Mg efflux is linear over time periods of up to 5 hours (the maximum time period studied). Figures 3.1 and 3.2 show data from a typical experiment. The measurements of intracellular and extracellular [Mg] are corrected for cell lysis which in this experiment did not exceed 0.7% (this amount of cell lysis is typical for cells incubated for long time periods in FBM). Figure 3.1 shows the changes in the cell [Mg] over 5 hours. Mg efflux from these cells (given by the slope of the line) was 39 ± 7 μmol(l.o.c.)$^{-1}$h^{-1}. Figure 3.2 shows data from the same experiment where efflux was measured as a change in the extracellular [Mg]. Efflux determined by this method was 38 ± 6 μmol(l.o.c)$^{-1}$h^{-1}. These data demonstrate that it is possible to measure these small fluxes by changes in either the intracellular or extracellular [Mg] and that the loss of Mg from inside the cell can be detected as a corresponding increase in the extracellular [Mg]. The

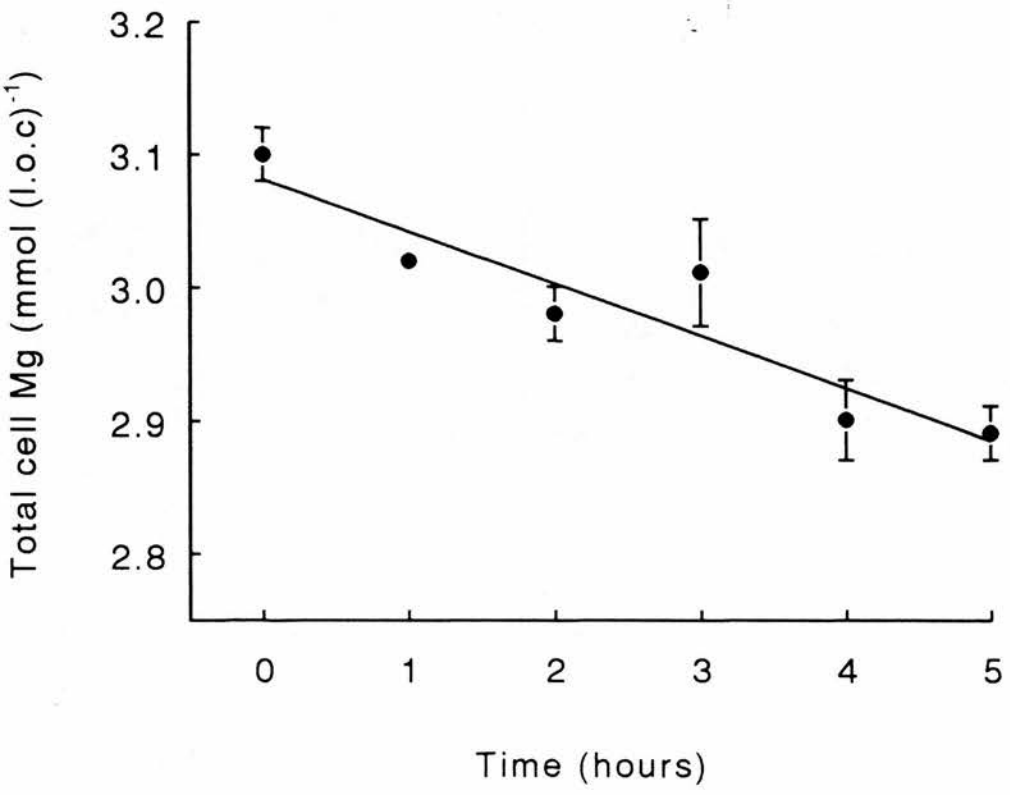

Figure 3.1

Cell [Mg] (mmol(l.o.c)$^{-1}$) as a function of time. Figure shows the result of one experiment. Ferret red cells were suspended (at 9% haematocrit) in FBM with 11 mM glucose and 0.05 mM EGTA. Triplicate measurements of cell [Mg] were made as indicated and points show the mean value with S.E.M. (if larger than point size). The data are corrected for lysis which in this experiment did not exceed 0.8%. The slope of the line (drawn using linear regression analysis) gives a value for Mg efflux which from this data is 39 ± 7 μmol(l.o.c.)$^{-1}$h^{-1}.

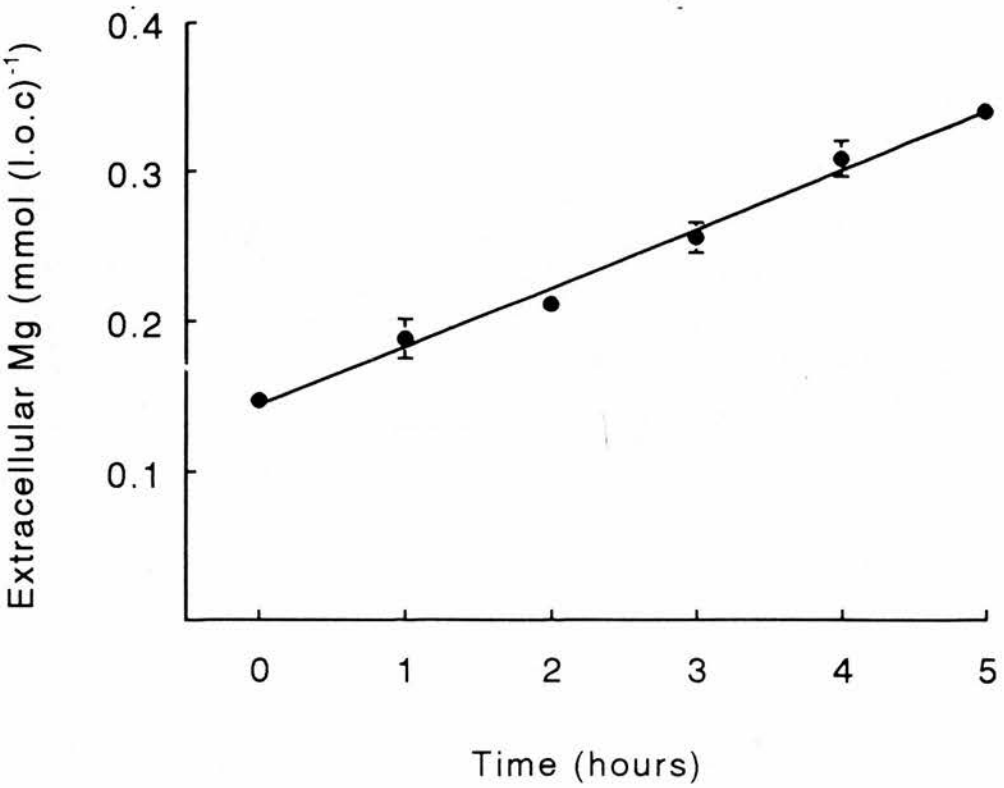

Figure 3.2

$[Mg]_o$ (mmol(l.o.c.)$^{-1}$) as a function of time. $[Mg]_o$ was measured as a molar concentration in the extracellular medium and expressed in the units mmol(l.o.c.)$^{-1}$ for comparison with changes in cell [Mg]. Data is from the same experiment as Figure 3.1. Triplicate measurements of $[Mg]_o$ were made as indicated and points show the mean value with S.E.M. (if larger than point size). Data is corrected for cell lysis. The slope of the line gives a Mg efflux of 38 ± 6 μmol(l.o.c.)$^{-1}h^{-1}$.

correlation between the loss of cell Mg and the increase in $[Mg]_o$ was demonstrated in several experiments. The ratio of the change in cell [Mg] to the change in $[Mg]_o$ was 1.05 ± 0.23 (mean ± S.E.M. n = 5 independent experiments).

Measurement of Mg fluxes as a change in the cell [Mg] requires the detection of very small changes in the cell [Mg]. For example, the efflux shown in Figure 3.1 represents only a 1% change in the cell [Mg] over 5 hours. Measuring changes in the cell [Mg] especially over shorter time periods (fluxes were often measured over 30 minutes) produces more scattered data. Mg efflux was therefore usually measured as a change in the [Mg] of an extracellular medium to which no Mg had been added. If lysis remains low throughout the experiment (less than 1%) this method gives reproducible measurements. Measurements of extracellular [Mg] require a less complicated protocol than measurements of cell [Mg] and using this simpler, less time consuming protocol allowed a wider investigation of the properties of Mg transport. The major drawback with looking at changes in the [Mg] of the medium, and the necessity of a very low extracellular [Mg], is that it was not possible to investigate the effects of extracellular [Mg] (including physiological concentrations) on Mg efflux.

Mg efflux estimated from changes in $[Mg]_o$ was measured in cells from a number of ferrets. The mean efflux from cells stored overnight at 4°C was 41 ± 2 μmol (l.o.c.)$^{-1}h^{-1}$ (mean ± S.E.M., n = 22 ferrets).

Table 3A.

Comparison of Mg efflux from animals of different sex and strain. Mg efflux was measured the days after cell collection. Mg efflux was measured as a change in $[Mg]_o$ and was corrected for cell lysis. Values given are the mean flux with S.E.M. with the number of different ferrets in brackets.

Table 3B.

The effects of storage on Mg efflux from ferret red cells. Red cells were stored at 80% haematocrit at 5°C for the time periods indicated. Efflux was measured as described for Table 3A. For longer storage times only data from single ferrets are available.

Table 3. Mg fluxes in ferret red cells

Table 3A.

	Mg efflux (μmol(l.o.c.)$^{-1}h^{-1}$)	
	Female	Male
Albino	43 ± 4 (n = 10)	45 ± 2 (n = 3)
Fitch	40 ± 3 (n = 6)	32 ± 2 (n = 3)

Table 3B

Days in storage	Mg efflux (μmol(l.o.c.)$^{-1}h^{-1}$
1	41 ± 2 (n = 22)
2	42 ± 8 (n = 3)
3	52 ± 13 (n = 3)
8	39
10	30
21	45

Table 3A lists flux rates from different batches of cells according to the sex and strain of the donor. Data show that there is no obvious difference in the fluxes measured in these groups. Data were also monitored to check for any seasonal variation in the efflux rates. Ferrets undergo physiological and metabolic changes throughout the year most noticeably around the beginning of the breeding season. To check for any possible effect on Mg transport, Mg efflux rates were monitored throughout the year. No seasonal changes in the Mg transport rate were evident (data not shown).

Table 3B shows the effect of storage on Mg transport rates. Table 3B shows that differences in the length of time for which the cells are stored has no effect on Mg transport rates. The length of time that cells can be stored in the fridge depends on the efficiency of the semi-sterile technique used during cell collection. Although Mg efflux is unaffected by storage times of up to 21 days, the experiments described in this study used cells normally within 1-3 days (and a maximum of 8 days) after collection.

The temperature dependence of Mg efflux.

Figure 3.3 shows the effects of changing the incubation temperature on the rate Mg efflux from ferret red cells. FBM is pH-buffered by Na-Hepes. The pH of the medium at different temperatures was checked and adjusted (by the addition of HCl) to compensate for

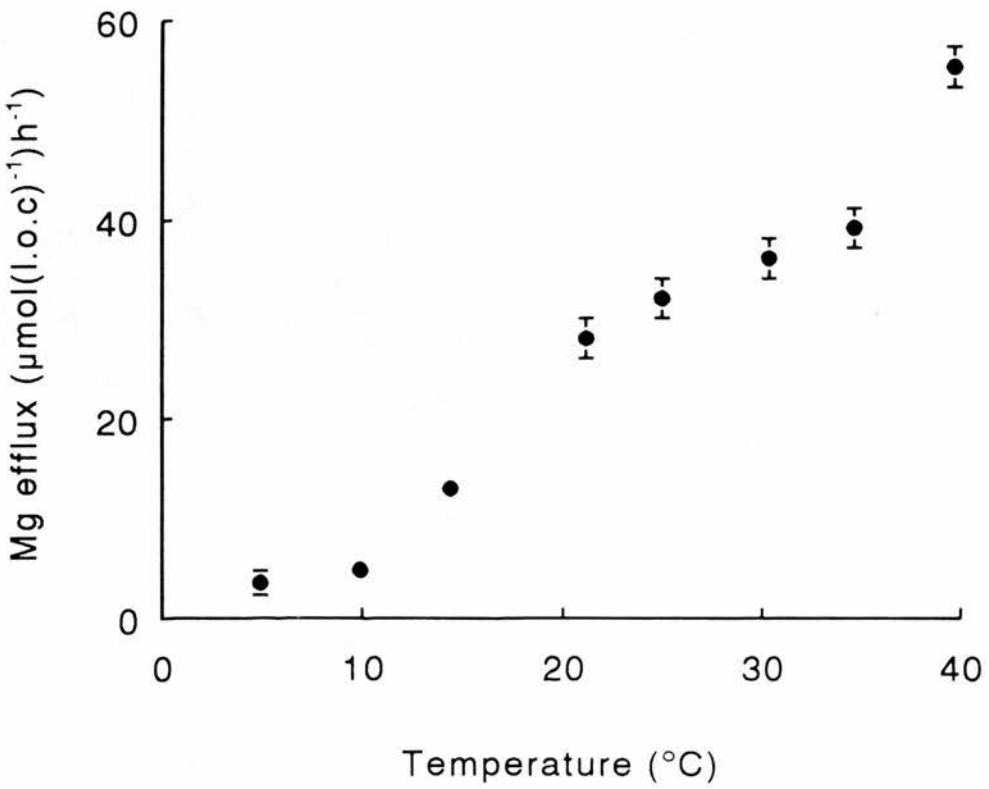

Figure 3.3.

The temperature dependence of Mg efflux. Figure is the result of 1 experiment. 1N HCl was added to the incubation medium to adjust the pH to 7.5 at each temperature. Mg efflux was measured as a change in $[Mg]_o$ and was corrected for cell lysis (< 0.9%). The time over which the fluxes were measured was varied to allow adequate resolution of flux measurements. Between 5 and 15°C fluxes were measured over 2 hours, 20 - 25°C over 1 hour and 30 - 40°C over 30 minutes. Points show the mean of 3 measurements of efflux with S.E.M (if larger than point size).

the temperature coefficient of HEPES buffer. Fluxes at low temperatures are slower than those measured at higher temperatures. To maintain the resolution of the flux measurement at low and high temperatures, the length of the flux period was increased and decreased respectively (see figure legend for details).

Figure 3.3 is a typical result from one experiment. Mg efflux increased as the temperature was raised from 5 to 40°C. Mg efflux was less sensitive to changes in temperature between 20 and 40°C than to changes in temperature below 20°C. This pattern of temperature dependence is quite unusual when compared to the temperature dependence of many other transport systems (Housley and Stanley, 1982). The Mg ion has a large shell of hydration and exchanges the water of its hydration shell very slowly (Hille, 1984). The mobility and binding of the Mg ion is thus much slower than would be predicted from the size and charge of the unhydrated ion. These features of the physical chemistry of the Mg ion may be a factor in the unusual temperature dependence of this ion.

Data from temperature dependence studies can be manipulated to give an Arrhenius plot. From the slopes of the lines of an Arrhenius plot it is possible to estimate the activation energy for membrane transport over a given temperature range. The activation energy (Ea) is described by $-m \times R$, where m is the slope of the line and R is the Gas constant. Arrhenius plots often yield discontinuous lines. A break in the line of an Arrhenius plot indicates a distinct change in the

activation energy of transport and is usually associated with a change in the physical properties of the membrane lipid (Houslay and Stanley, 1982).

The Arrhenius plot of the data from the experiment of Figure 3.3 is shown in Figure 3.4 and shows a temperature break at 20°C. The slopes of the lines either side of this break give values for the activation energies of 94 kJ mol^{-1} for 5-20°C and 24 kJ mol^{-1} for 21-40°C.

Further examination of the data in Figures 3.3 and 3.4 suggests that the rate of increase of Mg efflux may again change abruptly when the temperature is greater than 35°C. The temperature dependence was examined and the activation energy calculated over 3 intervals as follows.

for 5 to 21°C, Ea was 94 $kJmol^{-1}$
21 to 35°C, 17
35 to 40°C, 164

Other similar experiments confirmed that at temperatures above 35-39°C there was a large increase in the activation energy. However a break in the Arrhenius plot at temperatures above 35°C is mainly due to the measurement of very large fluxes at temperatures around 40°C. In all experiments increasing the temperature above 39°C also increased cell lysis. An increase in the non-specific permeability of the cells prior to lysis at these high temperatures cannot be discounted.

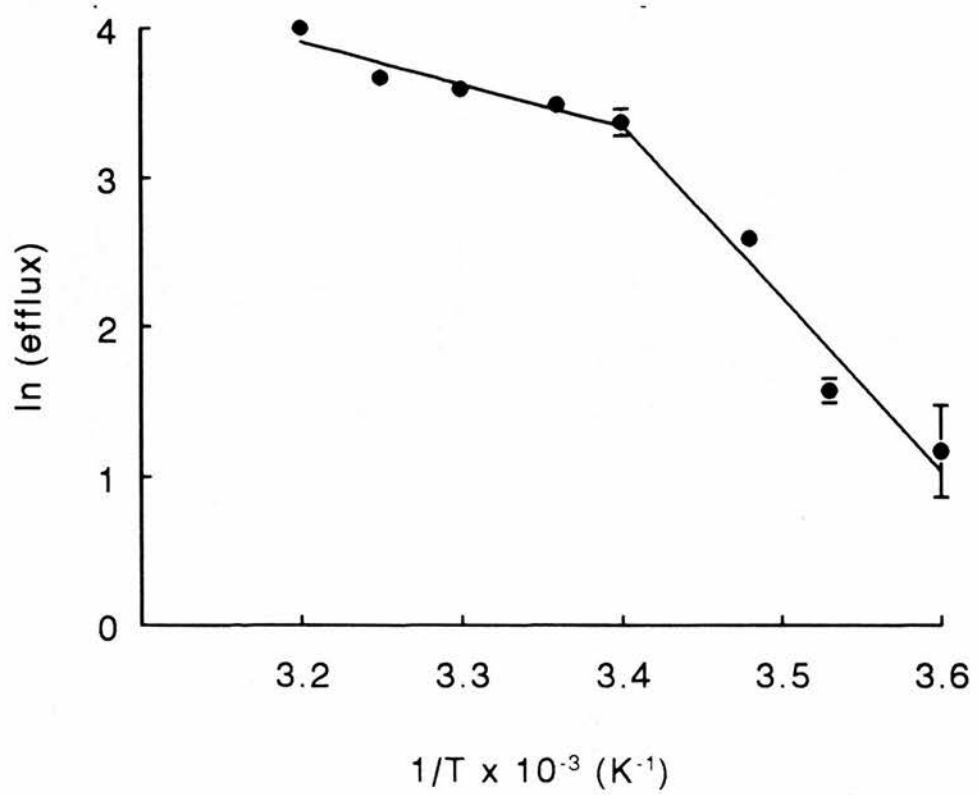

Figure 3.4.

Arrhenius plot of the data in Figure 3.3. The lines were drawn using linear regression analysis and are described by the Arrhenius equation $\ln(K) = -E_a/R.T + \ln(A)$. The activation energy for Mg efflux (calculated from the slopes of the lines) is 24 $kJmol^{-1}$ for 20 - 40°C and 94 kJ mol^{-1} for 5 - 20°C.

The ATP dependence of Mg efflux.

The hydrolysis of ATP provides the energy for many cellular reactions including the activity of many membrane transporters. To test whether cellular ATP is a requirement for the operation of a transporter, the rate of transport is measured in cells which have been chemically treated to change the cell [ATP]. The [ATP] of ferret red cells is reduced by incubating them in media in which glucose is replaced with 2-deoxyglucose. 2-deoxyglucose substitutes for *D*-glucose on the glucose transporter. It is sufficiently similar to *D*-glucose to undergo phosphorylation by hexokinase (Whittam, 1964). 2-deoxyglucose 6-phosphate however cannot participate further in the reaction sequence and the synthesis of ATP is inhibited. The phosphorylation of 2-deoxyglucose also utilises ATP and the ATP content falls. The reduction occurs quite rapidly. After a 1 hour incubation the ATP content of ferret red cells is 4 ± 1% (mean ± S.E.M., n=4 experiments) of control concentrations. The effect of reducing the ATP concentration on Mg efflux in ferret red cells is shown in Figure 3.5. In this typical experiment the ATP content fell from 656 ± 7 to 26 ± 1 μmol(l.o.c.)$^{-1}$ (mean ± S.E.M.,n=6) after 2 hours in a medium with 2-deoxyglucose. Figure 3.5 shows that Mg efflux is higher in cells with a low [ATP]. Extending the depletion time to 3 hours produced no further significant fall in the ATP content but Mg efflux

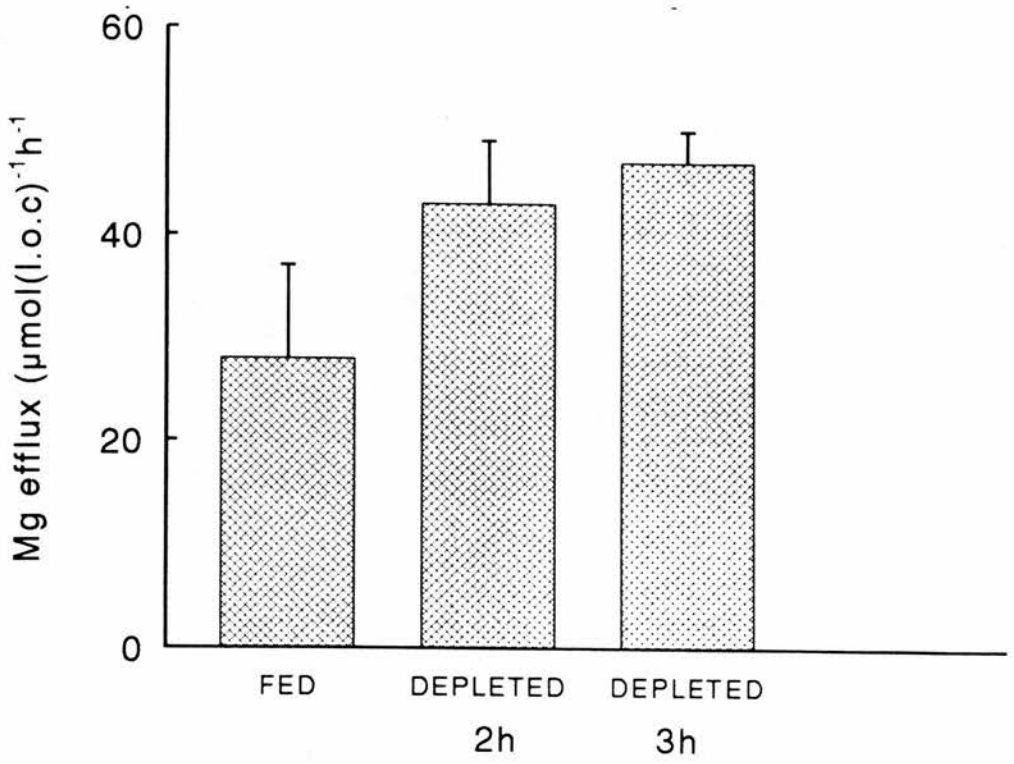

Figure 3.5.

ATP dependence of Mg efflux. Ferret red cells were incubated in FBM with 11 mM glucose for 30 minutes (FED) or in FBM with 11 mM 2-deoxyglucose for 2 or 3 hours (DEPLETED). Mg efflux was then measured as a change in $[Mg]_o$ (corrected for cell lysis) over 30 minutes. FED cells had a cell [ATP] of 656 ± 7 μmol(l.o.c.)$^{-1}$. DEPLETED cells had a cell [ATP] of 26 ± 1 and 21 ± 1 μmol(l.o.c)$^{-1}$ after 2 and 3 hours respectively. Bars show the mean efflux of 3 separate incubations in 1 experiment with S.E.M.

slightly increased.

These results show that Mg efflux can proceed when the ATP content of the cells is below 30 μmol(l.o.c.)$^{-1}$. This suggests that the hydrolysis of ATP does not directly provide the energy for Mg transport in these cells.

Mg is buffered inside the cell so that the concentration of the free ionized ion ($[Mg^{2+}]_i$) is only a fraction of the total cell [Mg]. The $[Mg^{2+}]_i$ in the cell changes according to the capacity and affinity of the intracellular Mg buffers. The Mg buffering capacity was determined from the equilibrium concentrations of internal Mg when the incubation medium contains A23187 and a range of [Mg], using the method of Flatman and Lew (1980), (see METHODS).

The relationship between total and ionized [Mg] in ferret red cells was examined. The results of these experiments are shown in Figure 3.6. The filled symbols and solid line show the relationship between total [Mg] and $[Mg^{2+}]_i$ in 3 independent populations of cells with control levels of ATP. The open symbols and dashed line show the same relationship in cells with a reduced [ATP]. The shift in the curve following [ATP] depletion indicates that ATP is a major site for Mg binding in ferret red cells. Thus reducing the cell [ATP] not only increases Mg efflux but also increases $[Mg^{2+}]_i$. For example, in the experiments shown in Figure 3.6, the cell [ATP] fell to 3% of the control value and $[Mg^{2+}]_i$ increased from approximately 0.7 mM to 1 mM.

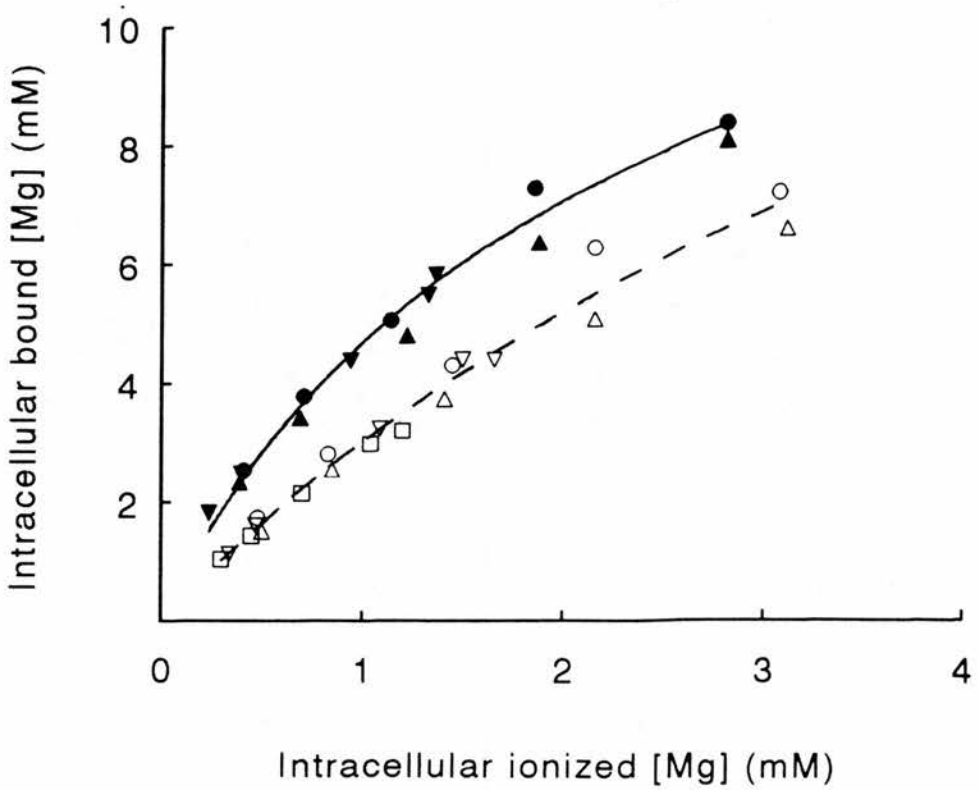

Figure 3.6.

Mg buffering in fed and depleted cells. The bound and free $[Mg]_i$ of ferret red cells were measured using the method of Flatman and Lew (1980) and Flatman (1988). The different symbols represent independent experiments. Cells were incubated in FBM with either 11 mM glucose (filled symbols and solid line) or 11 mM 2-deoxyglucose (open symbols and dashed line) for 1 hour. The mean cell [ATP] was (μmol(l.o.c.)$^{-1}$) 0.64 ± 0.04 (filled symbols, n=3 experiments) and 0.03 ± 0.01 (open symbols, n=4 experiments). The lines were drawn assuming 1 site ligand binding with capacities and dissociation constants (filled symbols), 14 and 2; (open symbols), 18 and 5 mM respectively.

The pH dependence of Mg efflux.

The effect of changing the external pH on Mg efflux in ferret red cells is shown in Figure 3.7. This shows the results of 2 independent experiments where the initial external pH had been changed by the addition of either HCl or NaOH as shown in the METHODS. The ability of red cells to buffer the external medium is shown in Figure 3.7 where the horizontal bars represent the drift in pH over the time period studied. The drift in pH is larger when the cells are suspended in a medium which is initially more alkaline. Alkaline conditions favour glycolysis which produces lactate and protons (Murphy, 1960). In this way cells in an alkaline environment produce excess H^+ and the pH is lowered. Acidity inhibits glycolysis and the cells in the more acidic environment do not produce protons preventing a drift to a more acidic pH. Figure 3.7 shows that lowering the external pH causes a small rise in Mg efflux. Thus H^+ may directly stimulate Mg efflux. Alternatively, as H^+ displaces Mg from intracellular binding sites, Mg efflux may be stimulated by a small increase in $[Mg^{2+}]_i$.

The effects of some transport inhibitors on Mg efflux.

The sensitivity of Mg transport in other red cells to a number of transport inhibitors has been described

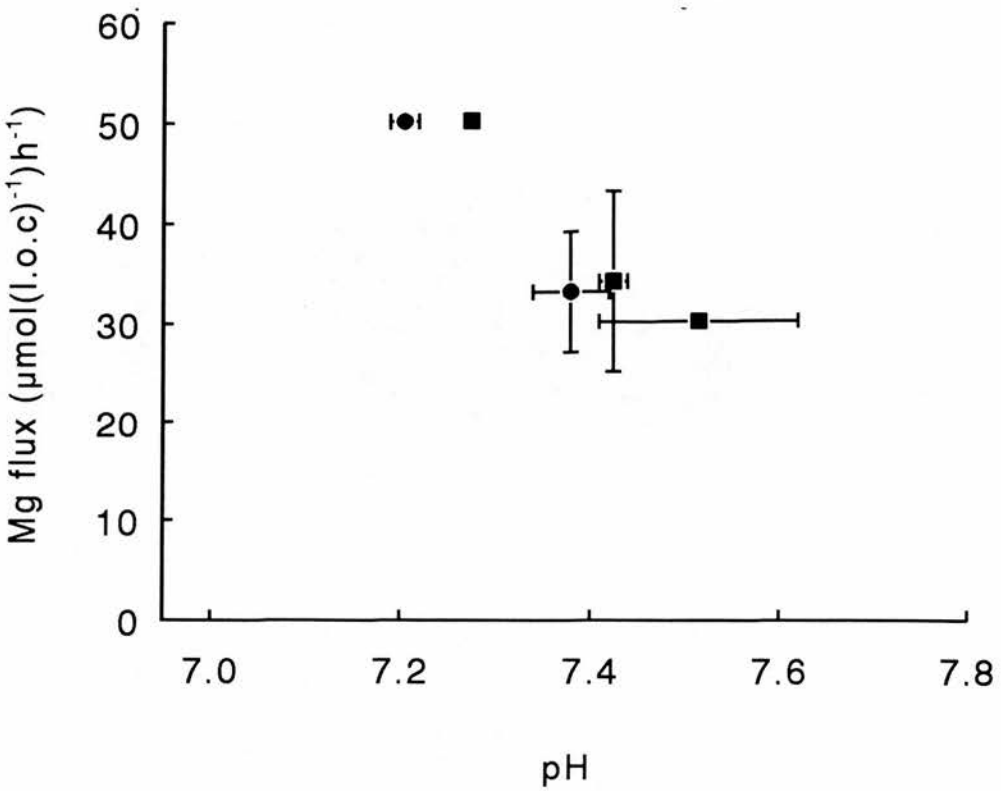

Figure 3.7.

The pH dependence of Mg efflux. Figure shows the results of 2 independent experiments. The pH of the incubation medium was adjusted to the required starting value with either HCl or NaOH (1N stocks). Efflux was measured as changes in the $[Mg]_o$ (with S.E.M.), corrected for cell lysis. Points show the mean flux between triplicate measurements of $[Mg]_o$ at 5 minutes and 2 hours 5 minutes after the start of the incubation.

in the Introduction. A selection of drugs was tested on Mg transport in ferret red cells. The results of these experiments are shown in Figure 3.8.

Ouabain (0.5 mM), bumetanide (0.5 mM), nitrobenzylthioinosine (10 nM) and α-cyano 4-hydroxycinnamate (0.3 mM) have no effect on Mg efflux from ferret red cells.

As ferret red cells have very little capacity for transport via the Na-K-ATPase (Flatman, 1983) it is not surprising that ouabain had no effect on transport in these cells. However, Flatman (1983) has also shown that ferret red cells have a high capacity for transport through the Na-K-Cl cotransport system. Indeed, most of K transport in ferret red cells (97%) occurs through the Na-K-Cl cotransporter. As bumetanide (a potent and specific inhibitor of Na-K-Cl cotransport) has no effect on Mg efflux, this indicates that Mg efflux does not occur through this route and nor is it coupled to the movement of Na, K or Cl through the cotransporter.

Nitrobenzylthioinosine blocks nucleoside transport in nucleoside-permeable sheep erythrocytes (Jarvis, McBride & Young 1982). Nitrobenzylthioinosine also blocks nucleoside efflux from human red cells with an increased permeability to ATP following a brief pulse of hypoxia (Bergfeld and Forrester, 1989). Nitrobenzylthioinosine had no effect on Mg efflux and thus Mg efflux, in these cells, is not coupled to the transport of nucleosides.

α-cyano 4 hydroxycinnamate blocks the transport of

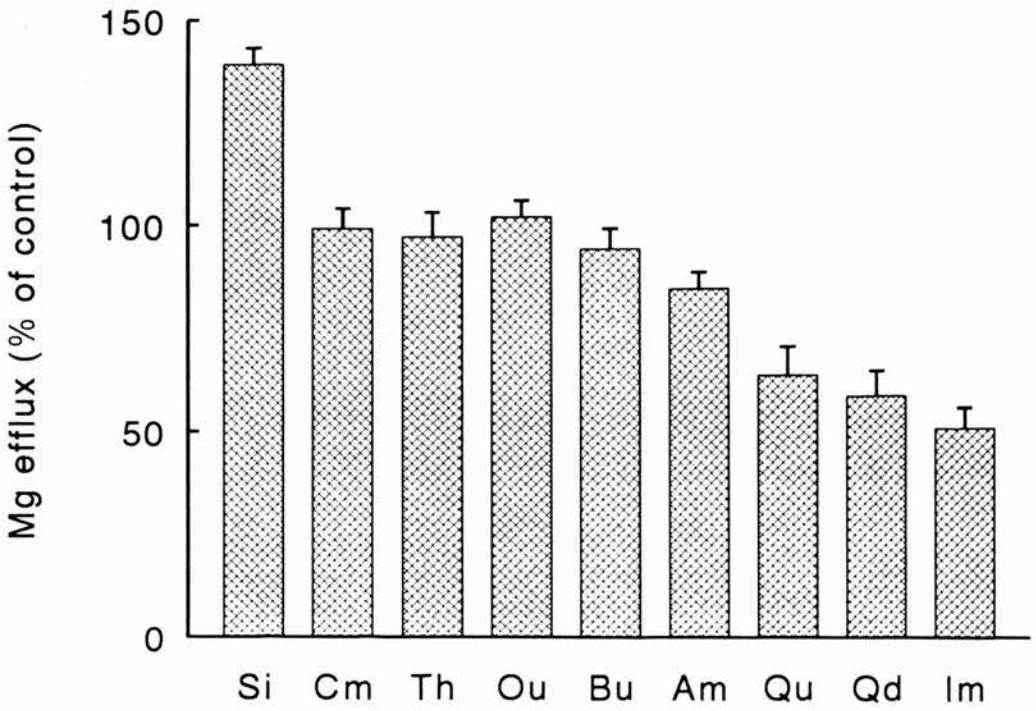

Figure 3.8.

Effect of transport inhibitors on Mg efflux. Bars show the mean flux with S.E.M. in separate experiments. A control flux (no drug added) was measured in each experiment. Efflux is the change in $[Mg]_o$, corrected for lysis (< 1.2%) and is expressed as a percentage of its control. The drug concentration and number of flux measurements were as follows: Si (SITS, 0.1 mM, n=3); Cm (α-cyano 4 hydroxycinnamate, 0.3 mM, n=3); Th (nitrobenzyl thioinosine, 10 nM, n=3); Ou (ouabain, 0.5 mM, n=4); Bu (bumetanide, 0.5 mM n=4); Qu (quinine, 0.5 mM n=4); Qd (quinidine, 0.5 mM, n=2); Im (imipramine, n=3); Am (amiloride, 0.5 mM, n=4 experiments, using cells from different animals).

lactate and pyruvate in human red cells (Halestrap, 1976). This compound had no effect on Mg transport in ferret red cells. Therefore, Mg efflux from ferret red cells is independent of the transport of these metabolic intermediates.

4-acetamido-4-isothiocyanatostilbene-2,2-disulphonic acid (SITS, 0.1mM)), a potent but non-specific inhibitor of the band-3 anion exchanger, stimulated Mg efflux by approximately 30%. When SITS is added to a suspension of ferret red cells the cells depolarise and the membrane potential becomes 0 mV. These results suggest that Mg efflux is sensitive to changes in the membrane potential. This is a feature common to electrogenic membrane transporters.

The effect of 0.1 mM bepridil on Mg efflux is shown in Figure 3.11. Bepridil, an antianginal agent, blocks Na-Ca exchange and Na and Ca channels in cardiac myocytes (Gill *et al*, 1992). Bepridil inhibited Mg efflux in ferret red cells although it is not as potent an inhibitor as amiloride.

Amiloride, quinine, quinidine and imipramine all inhibit Mg efflux from ferret red cells (Figure 3.8). These drugs inhibit Mg transport in red cells from a number of different species (see INTRODUCTION). No drug tested completely blocked Mg efflux although, of those tried in this study, the most potent was imipramine which reduced Mg efflux to half its control value at a concentration of 0.5 mM. The dose-dependent effects of all these drugs are difficult to ascertain as, at concentrations greater than 1 mM, they cause

considerable cell lysis. As well as being the most potent inhibitor of Mg efflux from ferret red cells, imipramine was also the most lytic drug (when imipramine was increased to 1 mM, cell lysis was greater than 6%). The dose-dependent effects of amiloride and quinidine were investigated as these drugs offer the best compromise between inhibitory and lytic effects. In the experiment shown in Figure 3.8, 1 mM amiloride reduced efflux to 67 ± 5% of control (mean ± S.E.M., n=5) and 1 mM quinidine reduced efflux to 42 ± 5% of control (mean ± S.E.M., n=6). The cell lysis in these experiments was 2% in the presence of amiloride and 0.8% in the presence of quinidine.

Dose dependent inhibition by amiloride and quinidine

The dose-dependent effects of amiloride on Mg efflux are shown in Figure 3.9. The different symbols used in Figure 3.9 represent the results of 3 independent experiments using cells from different ferrets. The control fluxes of each experiment are given in the figure legend. In all of these experiments the addition of amiloride at low concentrations stimulated Mg efflux. When the amiloride concentration was 1μM, Mg efflux was 117 ± 3% of the control (mean ± S.E.M.,n=4 experiments). There is a net inhibition of Mg efflux when the concentration of amiloride is increased above 0.1 mM. When the amiloride concentration is greater than 2 mM there is

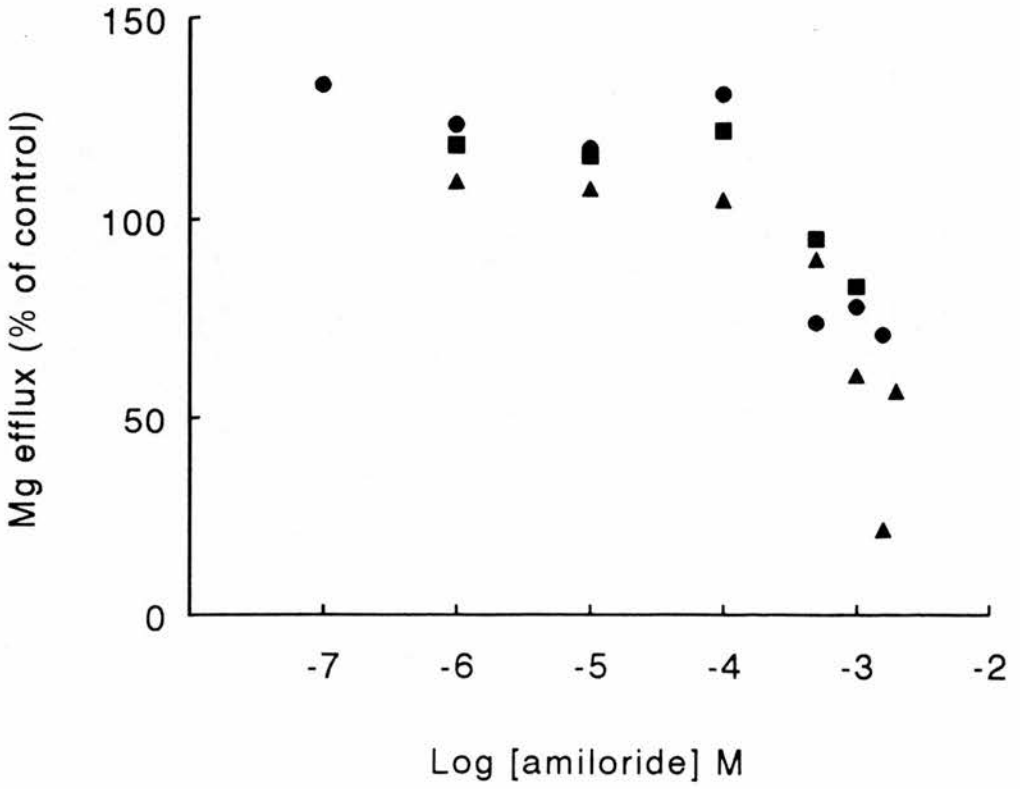

Figure 3.9.

Mg efflux as a function of amiloride concentration. Symbols show the data of 3 independent experiments using cells from different animals. Efflux is expressed as a percentage of the control flux (no drug added). A control flux was measured in each experiment. Efflux is the change in $[Mg]_o$, corrected for lysis (< 2.2%) either between triplicate measurements of $[Mg]_o$ in 1 cell suspension (●,■) or between single measurements of $[Mg]_o$ in 3 cell suspensions at 10 and 130 minutes after the start of the incubation. Control fluxes were 30, 34 and 45 (μmol(l.o.c.)$^{-1}$h^{-1}) for ●, ■ and ▲ respectively.

an apparent reversal of the inhibitory effect of amiloride and Mg efflux increases. This increase in Mg efflux was seen in all the experiments illustrated in Figure 3.9. Mg efflux at amiloride concentrations above 2 mM is not shown in this figure as the scatter in the data makes the interpretation of the K_i difficult. Figure 3.10 shows the results of another experiment where Mg efflux was measured in media containing different concentrations of amiloride. All the concentrations of amiloride used are shown and the figure illustrates the typical pattern when the amiloride concentration is above 2 mM. In Figure 3.10, increasing the amiloride concentration from 2 to 3 mM increased the efflux by 20% (relative to the efflux at the concentration where amiloride had its greatest inhibitory effect). At 4 mM amiloride the efflux was increased by 50%. Cell lysis also increased considerably when the drug concentration was increased. When the medium contained 2 mM amiloride, cell lysis was 3% and increasing amiloride to 3 and 4 mM increased cell lysis to 4 and 6% respectively. However, the magnitude of Mg efflux at high amiloride concentrations, and the amiloride concentration at which inhibitory action of the drug was apparently reversed, were not reproducible between experiments.

The dose-dependent inhibition of Mg efflux reveals 2 components of Mg efflux: one which is inhibited by amiloride and appears to have a typical pattern of dose-dependent inhibition and another which seems to increase as the concentration of amiloride is

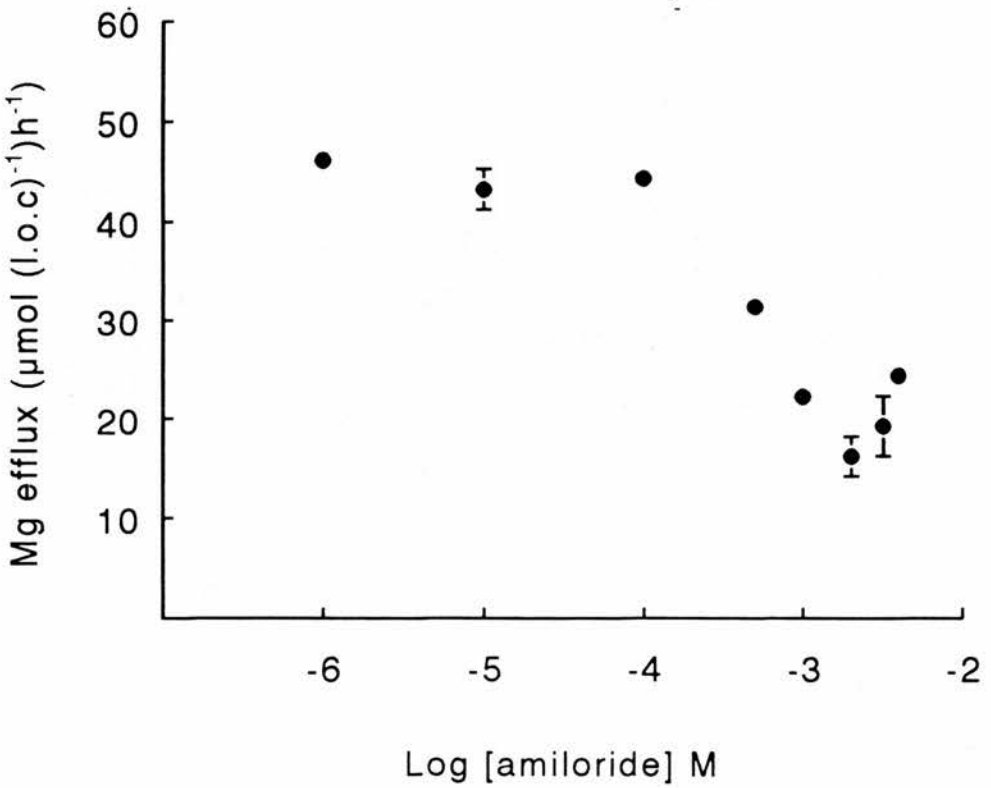

Figure 3.10.

Mg efflux as a function of amiloride concentration. Figure shows the result of 1 experiment and highlights the pattern of the dose-dependency curve at high amiloride concentrations. Efflux was measured as a change in triplicate measurements of $[Mg]_o$, corrected for cell lysis, at 10 and 130 minutes after the start of 1 incubation. The control flux (no drug added) was 39 ± 5 μmol(l.o.c.)$^{-1}h^{-1}$ (mean ± S.E.M of the slope of the line). The amiloride concentration (mM) and corresponding cell lysis (%) were: 0.5, 0.2; 1, 2.1; 2, 3.7; 3, 4.1; 4, 5.7 respectively.

increased. The addition of these components could, theoretically, predict the pattern shown in Figure 3.10 where a small initial stimulation of efflux at low concentrations of the drug is followed by a dose-dependent decrease in flux as the drug concentration is increased and further increases in the drug concentration cause an increase in Mg efflux. Analysis of the exact shape of the amiloride-dose-dependency curve is hampered by the large variation in the fluxes measured at high drug concentrations.

An apparent reversal of the inhibitory effects of amiloride at high amiloride concentrations could indicate a transport system for Mg which is progressively revealed by the addition of the drug. Alternatively high concentrations of amiloride may result in a greater proportion of the cells being in a 'pre-haemolytic' state where their membranes have become more permeable to Mg through a non-selective route. Although the data presented here are corrected for cell lysis it must be reiterated that this correction can only account for cells which have released their haemoglobin. Any increase in the permeability not associated with the release of haemoglobin is not considered in the correction factor. Thus a drug-induced pre-haemolytic leak cannot be discounted.

Due to effects of high concentrations of amiloride on Mg efflux it is not possible to determine whether amiloride can completely block the Mg efflux pathway.

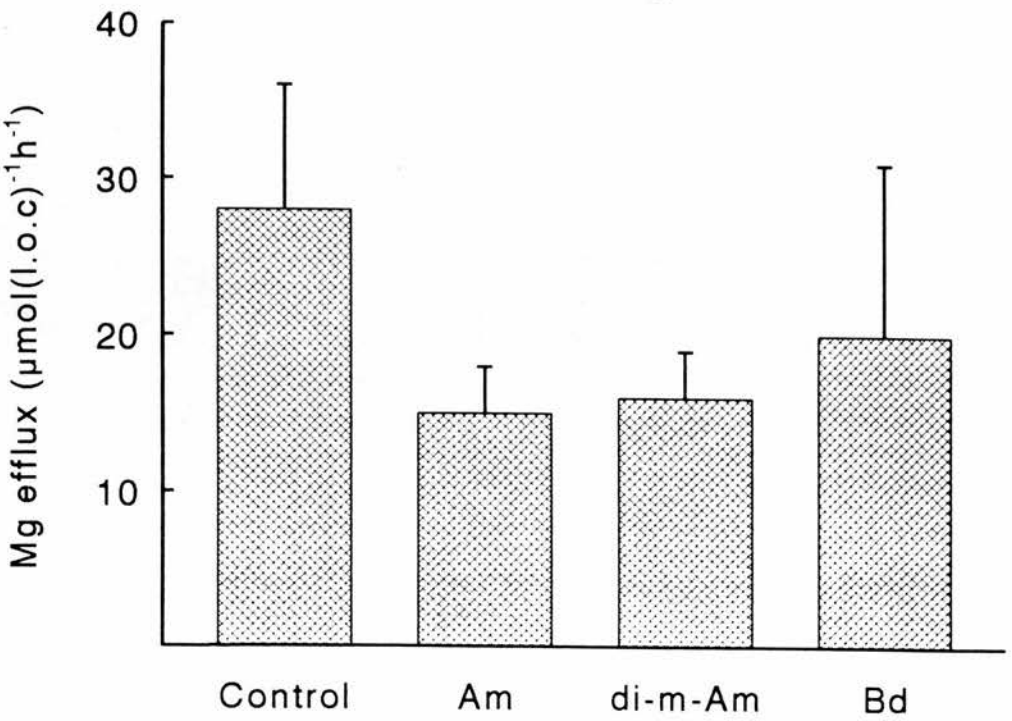

Figure 3.11.

The effects of amiloride, dimethylamiloride and bepridil on Mg efflux. Figure shows the result of an experiment using cells from 1 animal. Efflux was measured as a change in single measurements of $[Mg]_o$ at 10 and 40 minutes after the start of 3 separate incubations. Bars show the mean efflux with S.E.M.. The media contained no added drug (Control), 1 mM amiloride (Am), 1 mM dimethylamiloride (di-m-Am) or 0.1 mM bepridil (Bd).

Thus the possibility that there is also a component of Mg efflux which is insensitive to amiloride cannot be excluded.

Inhibition of efflux is quantified by the concentration of drug which inhibits half of the maximum flux (K_i). Ignoring the increase in efflux after administration of low doses of the drug then the following estimates of K_i can be made from Figures 3.9 and 3.10. If it is assumed that amiloride can inhibit all of the Mg flux then the K_i is 1 mM. If only 56% of the Mg efflux is amiloride sensitive (the maximum level of inhibition seen) then the K_i is 0.5 mM.

Amiloride inhibits several mechanisms of Na transport. Several amiloride analogues with varying specificity to different Na transport mechanisms have now been developed (Simchowitz and Cragoe, Jr, 1986). Some of these analogues have been tested on Mg efflux from Mg-loaded human, chicken and rat red cells (Günther, Vormann, Cragoe, Jr and Höllriegl, 1989). Figure 3.11 shows the effects of 1 mM amiloride and the same concentration of the amiloride analogue dimethylamiloride on Mg efflux from ferret red cells. Figure 3.11 shows that both amiloride and dimethylamiloride inhibit Mg efflux but that the analogue (which is a more potent inhibitor of Na-H exchange than amiloride) is not as effective as amiloride in inhibiting Mg efflux.

The dose-dependent effects of quinidine on Mg efflux were also investigated. Figure 3.12 shows the results of 4 separate experiments where various doses

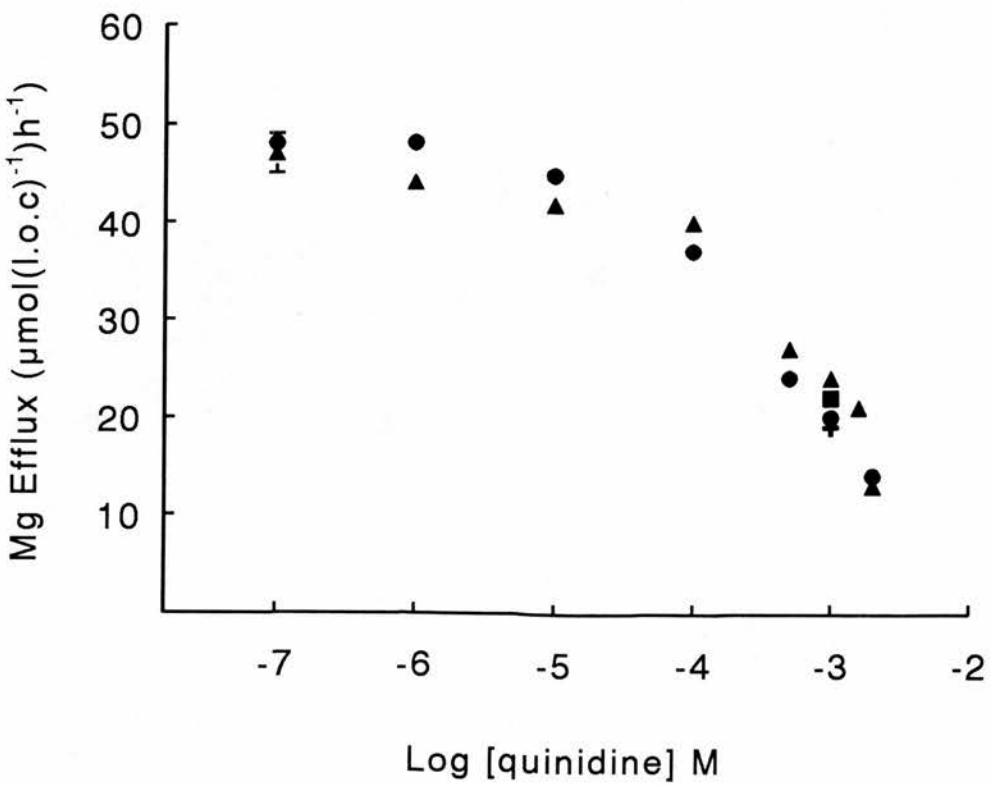

Figure 3.12.

Mg efflux as a function of quinidine concentration. Data shown are the results of 4 separate experiments using cells from different animals. Efflux was measured as a change in triplicate measurements of $[Mg]_o$, corrected for lysis (< 0.6%), at 10 and 130 minutes after the start 1 incubation. Points show the mean flux with S.E.M. if larger than point size. Control fluxes (μmol(l.o.c.)$^{-1}h^{-1}$) for each experiment were (circles), 45 ± 2; (triangles), 42 ± 3; (square), 47 ± 2; (cross), 63 ± 6.

of quinidine were added to the medium. Values for the control fluxes for each experiment are given in the figure legend. Similarly to the effects of amiloride, low concentrations (0.1 μM) of quinidine increased the control values of efflux and concentrations above 2 mM caused an increase in the rate of Mg efflux. Increasing the quinidine concentration above 2 mM also increased cell lysis from 0.6% to a mean value of 3%. This leads to the same problems in determining a true value for the maximum inhibition by quinidine and the K_i as encountered with the amiloride data. If it is assumed that 100% of the Mg efflux is quinidine-sensitive, the K_i for efflux inhibition is 1 mM. If only 70% of the total flux is quinidine sensitive then the K_i becomes 0.4 mM. These values fall within the ranges quoted for other cell types. However the inability to completely inhibit the transporter or define a drug insensitive component in any species makes kinetic analysis of these data difficult.

Inhibition of Mg efflux by metal ions, calcium and vanadate

The effects of a variety of ions on Mg efflux are shown in Figure 3.13.

0.04 mM $CuSO_4$, an inhibitor of Na flux in carnivore red cells (Sha'afi and Hajjar, 1971) stimulates Mg efflux by approximately 20%.

Calcium, manganese, nickel and cobalt all

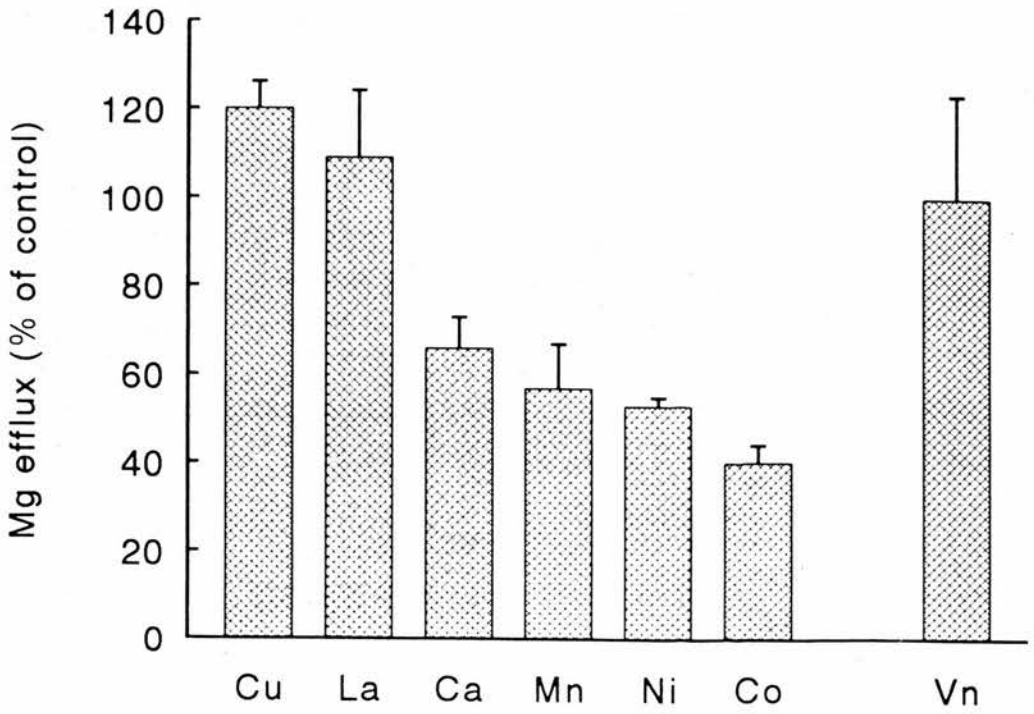

Figure 3.13.

Effect of some metal ions and vanadate on Mg efflux. Bars show the mean flux with S.E.M. A control flux (no ion added) was measured in each experiment. Efflux was measured as a change in $[Mg]_o$, corrected for cell lysis (< 1%), and is expressed as a percentage of its control. EGTA was excluded from incubation media containing Ca, Mn, Ni or Co. The additions to the media and the number of flux measurements were: Cu (0.04 mM $CuSo_4$, n=3); La (0.05 mM $LaCl_3$, n=3); Vn (0.2 mM, n=3); Ca (1 mM $CaCl_2$, n=3); $NiCl_2$ (1 mM, n=2); Co (1 mM $CoCl_2$, n=16); Mn (1 mM $MnCl_2$, n=5) and Vn (0.2 mM Na_3VO_4, n=3).

inhibited Mg efflux in ferret red cells (Figure 3.12). Cobalt was the most effective inhibitor and reduced Mg efflux to 40% of the control flux when the external concentration of $CoCl_2$ was 1 mM.

The hydrated Mg ion is large and exchanges water molecules in its hydration shell very slowly (Hille, 1984). Thus the effective size of the Mg ion and its behaviour in solution is similar to the transition ions. This may allow the transition ions to compete for Mg binding sites more effectively than Ca. Mn, Ni and Co are also effective inhibitors of the influx and efflux modes of Na-Ca exchange in squid axon. La^{3+} is also an effective blocker of Na-Ca exchange in a number of cell types including squid giant axons, cardiac myocytes and vesicular preparations (for review see Kaczorowski *et al*, 1989). La^{3+} has an ionic radius similar to that of Ca and inhibits many reactions involving Ca. La^{3+} also inhibits other routes for Ca movement apart from Na-Ca exchange and is assumed to act as a competitive inhibitor for Ca transport. However La^{3+} had no effect on Mg transport in ferret red cells. If Mg transport is through Na-Mg exchange then the Na antiports for Ca and Mg movement are separate transporters. La^{3+} also blocks the Ca pump in human red cells (Schatzmann 1983) and thus a transporter similar to the Ca-pump cannot provide a mechanism for Mg efflux.

Vanadate in the form $VO_3(OH^{2-})$ blocks all known P-type ATPases including the Na, Ca and H pumps (for review see Nechay et al, 1986). Vanadate had no effect

on Mg efflux in ferret red cells. Mg efflux in these cells is therefore not mediated by a P-type ATPase Mg pump. This agrees with the measurement of Mg efflux in ATP-depleted ferret red cells (Figure 3.5) which suggested that Mg efflux does not use ATP hydrolysis as a primary energy source.

Dose-dependent inhibition of Mg efflux by $CoCl_2$.

All the divalent cations tested inhibited Mg flux in ferret red cells. The most effective was Co. The maximum inhibition of Mg efflux, in the presence of any of the divalent ions tested, was 60%.

The dose dependent inhibition of Mg efflux by $CoCl_2$ is shown in Figure 3.14. The shape of this curve has many features similar to those for the dose dependent inhibition of Mg efflux by amiloride and quinidine (Figures 3.9, 3.10, 3.11). Low doses of Co produced an apparent stimulation of Mg efflux. Increasing the concentration of Co inhibited Mg efflux. $[Co]_o$ could be increased up to 5 mM before there was an increase in Mg efflux and a significant amount of cell lysis. The shape of the curve in Figure 3.13 suggests that there is a fraction of the Mg efflux which cannot be inhibited by Co.

The K_i for the inhibition of efflux by Co was estimated from this data as 0.7 mM when it is assumed that all Mg flux is sensitive to Co and 0.3 mM if only 70% of the flux is Co sensitive.

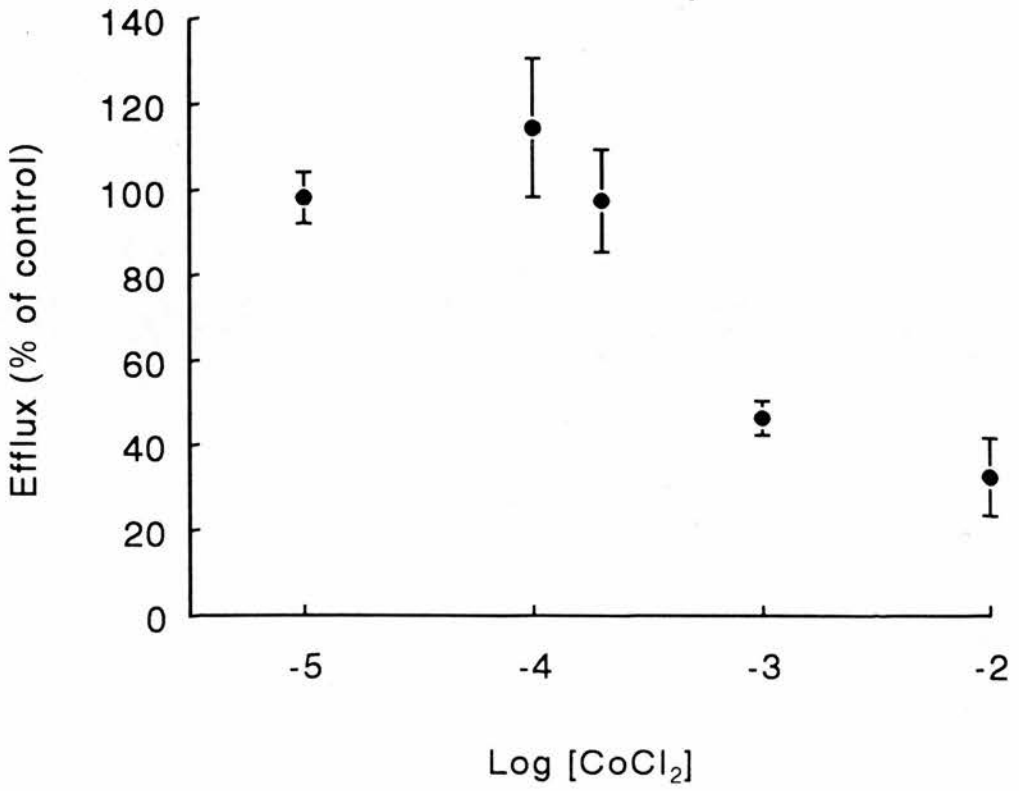

Figure 3.14.

Mg efflux as a function of $CoCl_2$ concentration. Figure is the result of one experiment. Efflux was measured as a change in $[Mg]_o$, corrected for cell lysis (< 0.6%), at 5 and 35 minutes after the start of 3 separate incubations. The control flux (no Co added) was 77 ± 13 μmol(l.o.c.)$^{-1}$h^{-1}). Points show efflux expressed as a percentage of its control flux with S.E.M. EGTA was not included in the incubation media. Samples of the suspension were diluted in 0.5% TRITON X-100 solution for haematocrit and cell lysis measurements.

Incubation in low-[Na] media: effects on $[Mg]_o$, cell [Na] and cell [K].

The $[Na]_o$-dependence of Mg efflux from human, rat and chicken red cells has been described (Lüdi & Schatzmann, 1987; Féray & Garay, 1986; Féray & Garay, 1987; Günther & Vormann, 1985) In all these species reducing $[Na]_o$ inhibits Mg efflux.

In initial experiments to investigate the $[Na]_o$ dependence of Mg efflux in ferret red cells, efflux was measured as a change in $[Mg]_o$ over 2 hours. The result from one typical experiment is shown in Figure 3.15. Figure 3.15 shows that Mg efflux was stimulated when $[Na]_o$ was reduced from 145 mM to 1 mM. In this experiment $[Na]_o$ was replaced with choline chloride. Similar results were obtained when $[Na]_o$ was replaced with *n*-methyl-d-glucamine (NMDG). Therefore the stimulation of Mg efflux was not due to the pharmacological effects of choline.

The striking anomaly between the $[Na]_o$-dependence of Mg efflux in the red cells of ferrets and other species prompted a more thorough examination of Mg efflux in low-[Na] media. The time dependent changes in $[Mg]_o$ over the 2 hour incubation period are shown in Figure 3.16. When the medium contained 145 mM NaCl (filled circles) the increase in $[Mg]_o$ was linear over 2 hours. The increase in $[Mg]_o$ was unaffected by the addition of 0.01 mM bumetanide (open circles). When

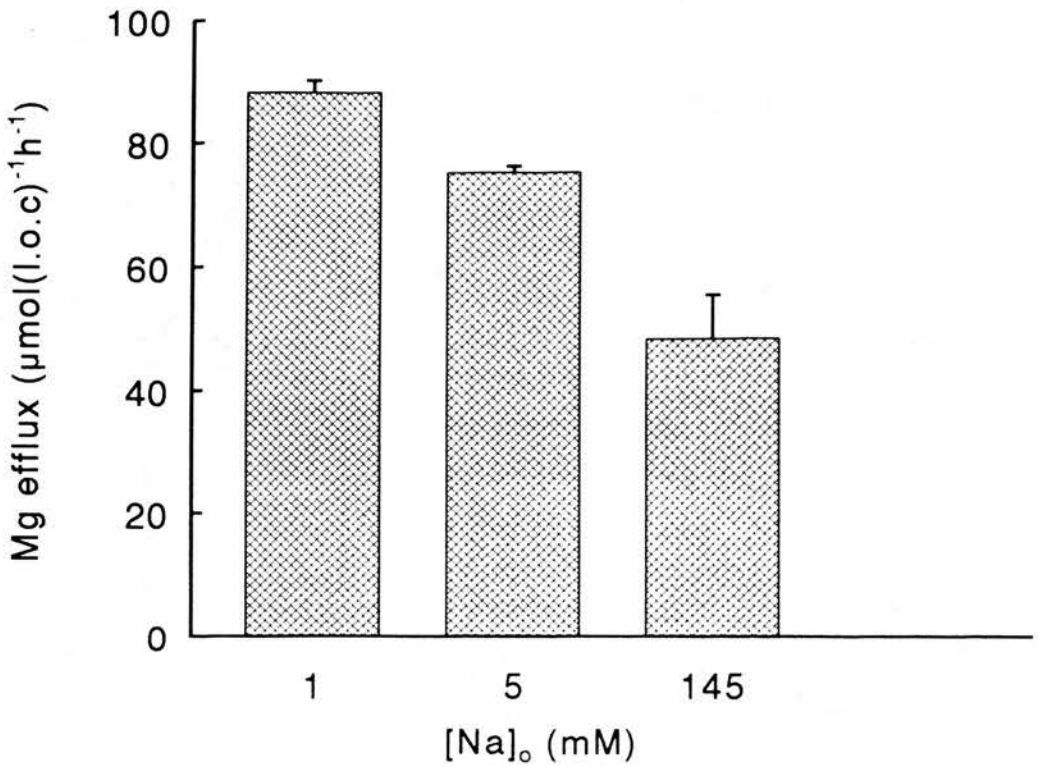

Figure 3.15.

$[Na]_o$-dependence of Mg efflux: efflux measured over a long time interval. Bars show the combined results of 2 separate experiments, using cells from different animals, with the range. Cells were incubated in medium of (mM): KOH, 5; Tris-EGTA, 0.05; glucose, 11; HEPES, 7.4; the initial NaCl concentration and sufficient choline chloride to maintain the sum, [NaCl] + [choline chloride] = 145 mM. Efflux was measured as a change in $[Mg]_o$, corrected for cell lysis, between triplicate measurements of $[Mg]_o$ at 10 and 130 minutes after the start of the incubation.

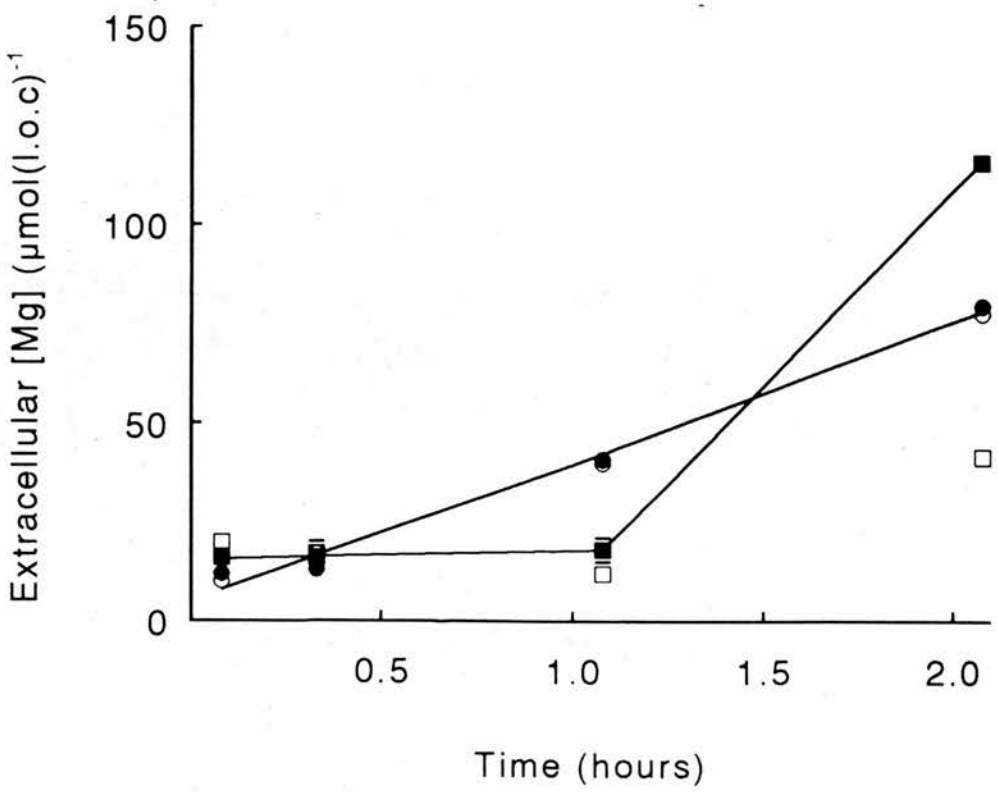

Figure 3.16.

$[Mg]_o$ as a function of time. Cells were incubated in either FBM (circles) or (mM); choline chloride, 145; KOH, 5; HEPES, 7.4, pH = 7.55 (squares). Bumetanide was also added to the medium as indicated (open symbols). Triplicate measurements of $[Mg]_o$ were made (and corrected for lysis, < 1.9%) at the times indicated. Points show the mean value with S.E.M. if larger than point size.

$[Na]_o$ was replaced with choline chloride the efflux of Mg from these cells was inhibited over the first hour of the incubation (filled squares). In this experiment the Mg efflux over the first hour of the incubation (calculated from the slope of the line) was 34 ± 1 μmol(l.o.c.)$^{-1}h^{-1}$ in 145 mM NaCl and 2.2 ± 0.5 μmol(l.o.c.)$^{-1-1}$ in choline chloride medium. Bumetanide had no effect on Mg efflux over the first hour in choline chloride. After 2 hours in choline chloride medium there was a large rise in $[Mg]_o$. This increase in $[Mg]_o$ was inhibited by bumetanide (open squares).

Figure 3.16 shows that reducing $[Na]_o$ inhibits Mg efflux, but only over the initial phase of the incubation. In Figure 3.15 the efflux was measured as a change in $[Mg]_o$ over 2 hours and thus incorporates not only the initial inhibition of flux but also the large rise in $[Mg]_o$ after 1 hour in low-[Na] media.

During the experiment shown in Figure 3.16 changes in the cell [Na] and [K] were also measured. Figure 3.17 shows the changes in cell [Na] which coincide with the changes in the $[Mg]_o$. The circles show cell [Na] measured when $[Na]_o$ was 145 mM. There was no significant change in cell [Na] over 2 hours (filled circles). Bumetanide had no effect on cell [Na] in this medium (open circles). When $[Na]_o$ was replaced with choline chloride the cell [Na] fell. In this experiment cell [Na] fell from 100 to 33 mmol(l.o.c.)$^{-1}$ over 2 hours (filled squares). Bumetanide inhibited the fall in cell [Na] (open squares). In the

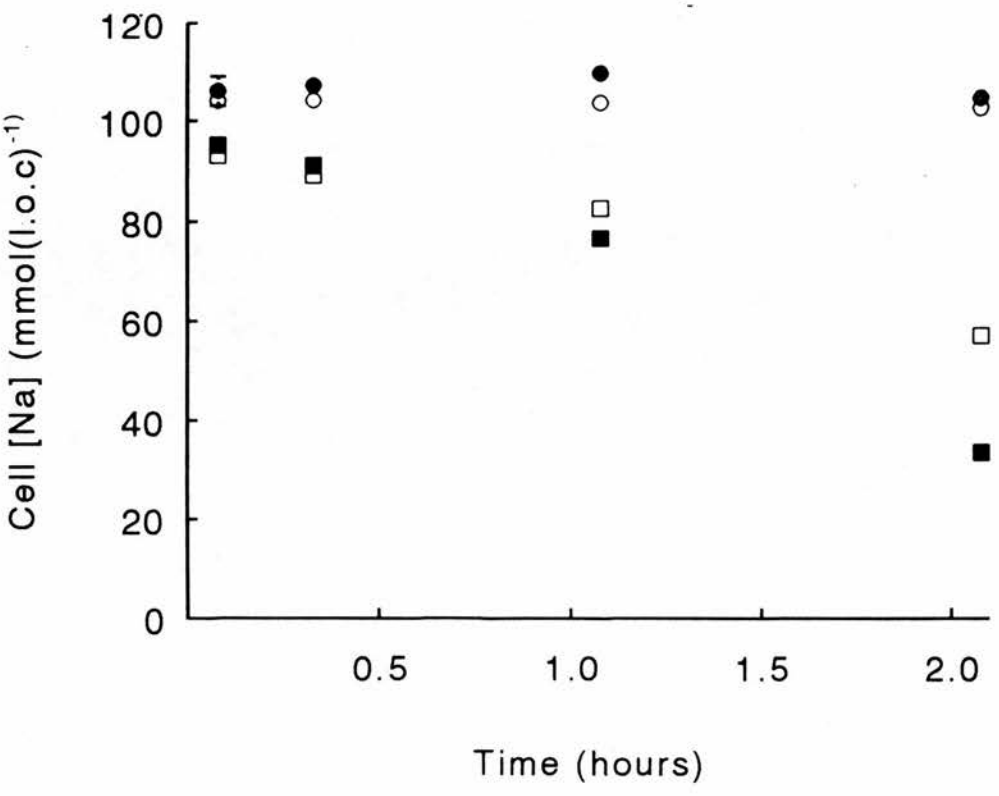

Figure 3.17.
Cell [Na] as a function of time. Figure shows data obtained from the same experiment as Figure 3.16. Points show the mean of 3 determinations of $[Na]_i$ with S.E.M. if larger than point size. Cells were incubated in FBM (circles) or media with Na replaced with choline (squares). Bumetanide was also added to the media as indicated (open symbols).

experiment shown, the cell [Na] only fell to 58 mmol(l.o.c.)$^{-1}$ after 2 hours when bumetanide was present. This indicates that a significant amount of Na efflux (down the large outward gradient for Na) occurs through the Na-K-Cl cotransporter.

Figure 3.18 shows the corresponding changes in the cell [K] during the same experiment. When the medium contained 145 mM NaCl there was little change in the cell [K] content over 2 hours (filled circles). Bumetanide had no effect on cell [K] in this medium (open circles). When [NaCl] was replaced with choline chloride the cell [K] fell rapidly. In this experiment the cell [K] had fallen from 5.6 to 3.4 mmol(l.o.c.)$^{-1}$ within the first 5 minutes of incubation. After 1 hour the cell [K] was 1.4 mmol(l.o.c.)$^{-1}$. After the second hour of the incubation the cell [K] increased. This re-uptake of K, following prolonged incubation in choline chloride media, was seen in several experiments. The addition of bumetanide to the choline chloride medium inhibited the loss of cell [K] and there was no re-uptake of K over the second hour of the incubation (open squares).

When $[Na]_o$ is replaced by choline chloride the outward gradient for Na becomes large and Na leaves the cells driven by this gradient. Although there are several routes for Na movement a significant amount of Na efflux, in these cells, occurs through the Na-K-Cl cotransporter. Although there is no change in the K gradient in low-[Na] media, the movement of Na out of the cells, through the Na-K-Cl cotransporter drives K

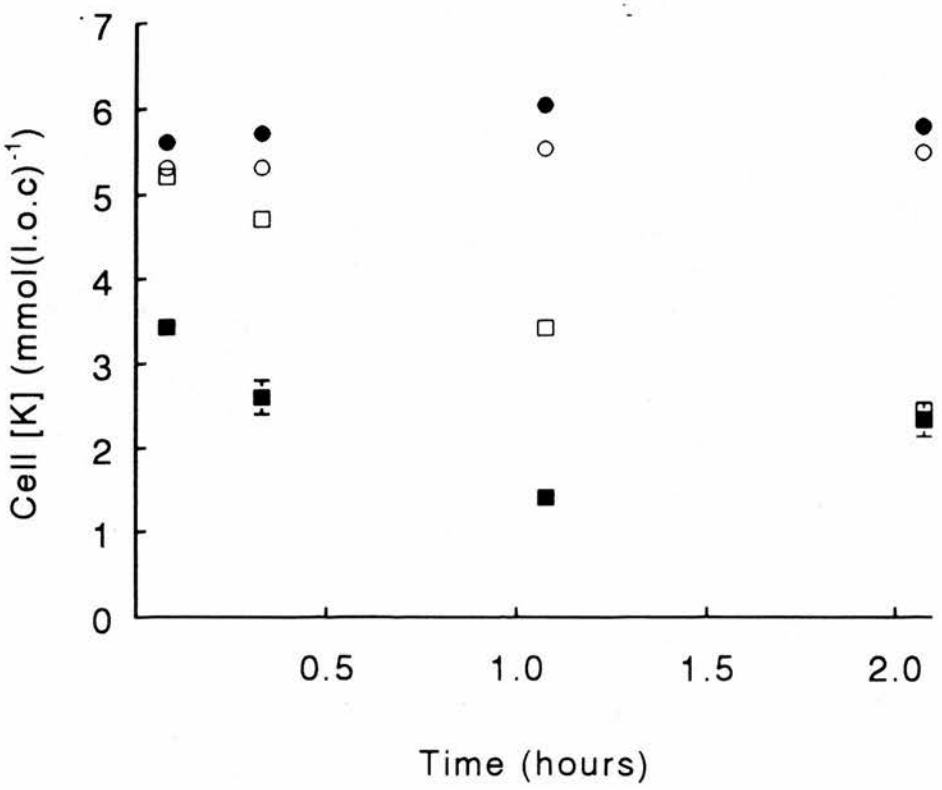

Figure 3.18.
Cell [K] as a function of time. Figure shows data obtained from the same experiment as Figures 3.16 and 3.17. Points show the mean of 3 determinations of $[K]_i$ with S.E.M. if larger than point size. Cells were incubated in FBM (circles) or media with Na replaced with choline (squares). Bumetanide was also added to the media as indicated (open symbols). The initial cell [K] was 5.6 mmol(l.o.c.)$^{-1}$.

out of the cells. The Na-K-Cl cotransporter moves Na and K in equimolar amounts (Flatman, 1989). In the experiment shown in Figures 3.17 the cell [Na] fell from 100 to 33 mmol(l.o.c.)$^{-1}$ over 2 hours (when no bumetanide was added). This is equivalent to a decrease in cell [Na] of 147 to 48 mM (if the cell water is assumed to be 68%). Ferret red cells contain only 7 mM cell [K]. As the Na-K-Cl cotransporter requires internal [K] to operate, the cell must take up K by another route to allow the Na-K-Cl cotransporter to continue operating.

In a low-[Na], bumetanide-free medium, the cell [K] increased after 2 hours incubation. This increase in cell [K] coincided with the large rise in $[Mg]_o$. The increase in cell [K] and $[Mg]_o$ at this time point was seen in several experiments. Examples of these experiments are shown in Figures 3.19 and 3.20. Figure 3.19 shows measurements of $[Mg]_o$, cell [Na] and cell [K] in cells incubated in media where NaCl had been substituted by choline chloride. In Figure 3.20 NaCl was replaced with n-methyl-*D*-glucamine.

Cell volume measurements were made in a number of experiments and showed that over the 2 hour incubation in low-[Na] media the cell water content falls from 68% ± 1 to 61% ± 1 (mean ± S.E.M.,n = 7) representing a mean fall in cell volume of 7%. Therefore the incubation in low-[Na] media (with the loss of cell [Na] and [K]) is associated with a small cell shrinkage. There is an increase in cell lysis when ferret red cells shrink (experimental observation). A

3.19 (i)

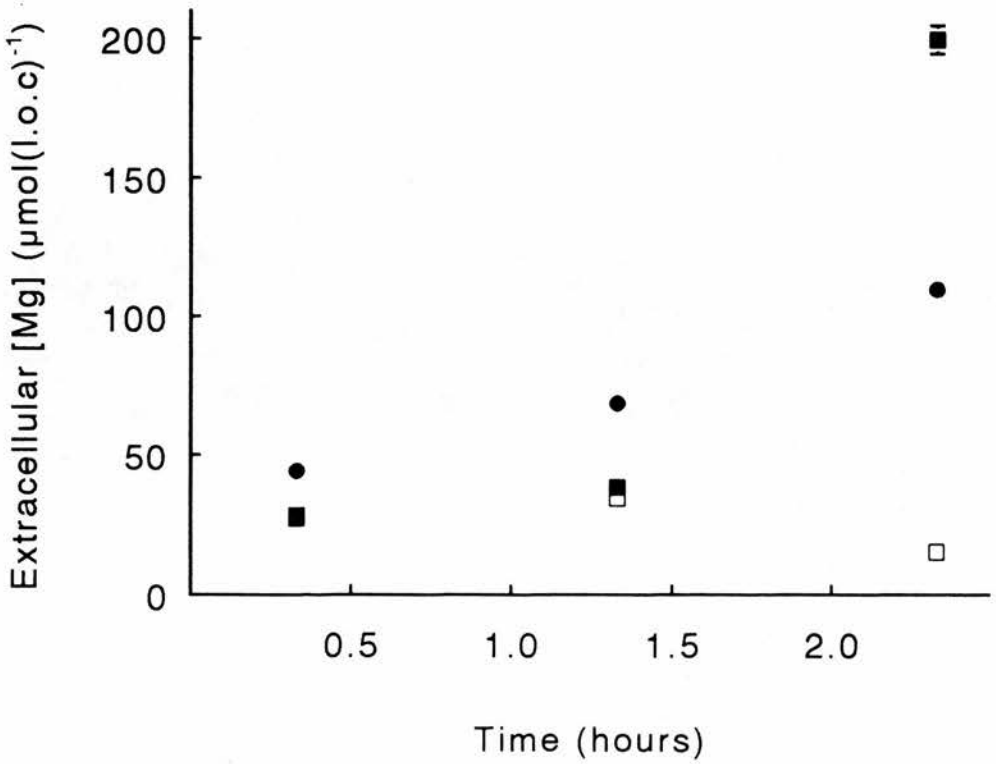

Figure 3.19.

$[Mg]_o$ (i), cell [Na] (ii) and cell [K] (iii) as a function of time. Figures 19i, 19ii and 19iii are the results of 1 experiment. Cells were incubated in either FBM (circles) or media in which Na was replaced with choline (squares). The composition of the media is described in the legend of Figure 3.16. Bumetanide (0.05 mM) was added as indicated (open symbols). Triplicate measurements of $[Mg]_o$, $[Na]_i$ and $[K]_i$ were made at the time points indicated and points show the mean value with S.E.M. if larger than point size.

3.19 (ii)

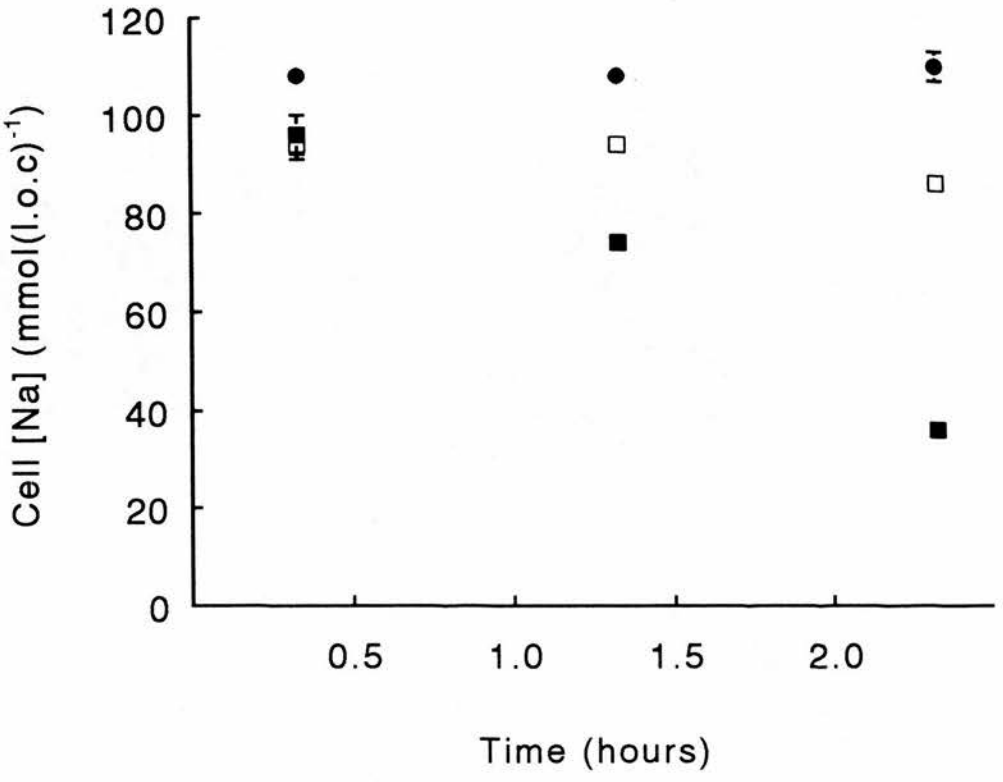

3.19 (iii)

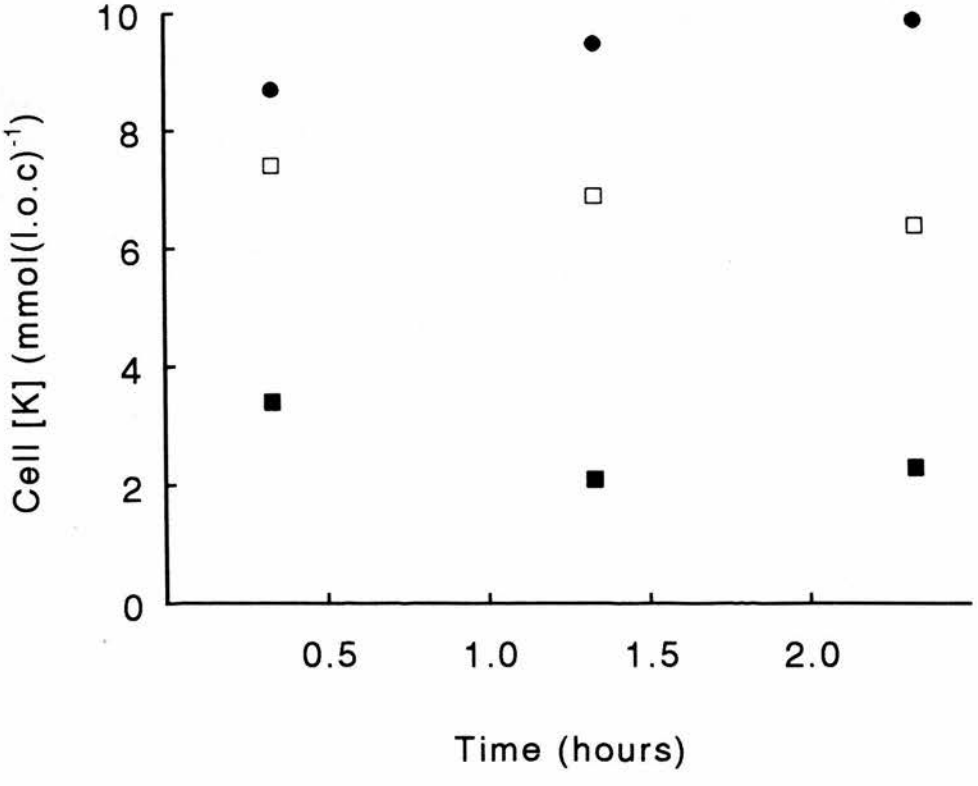

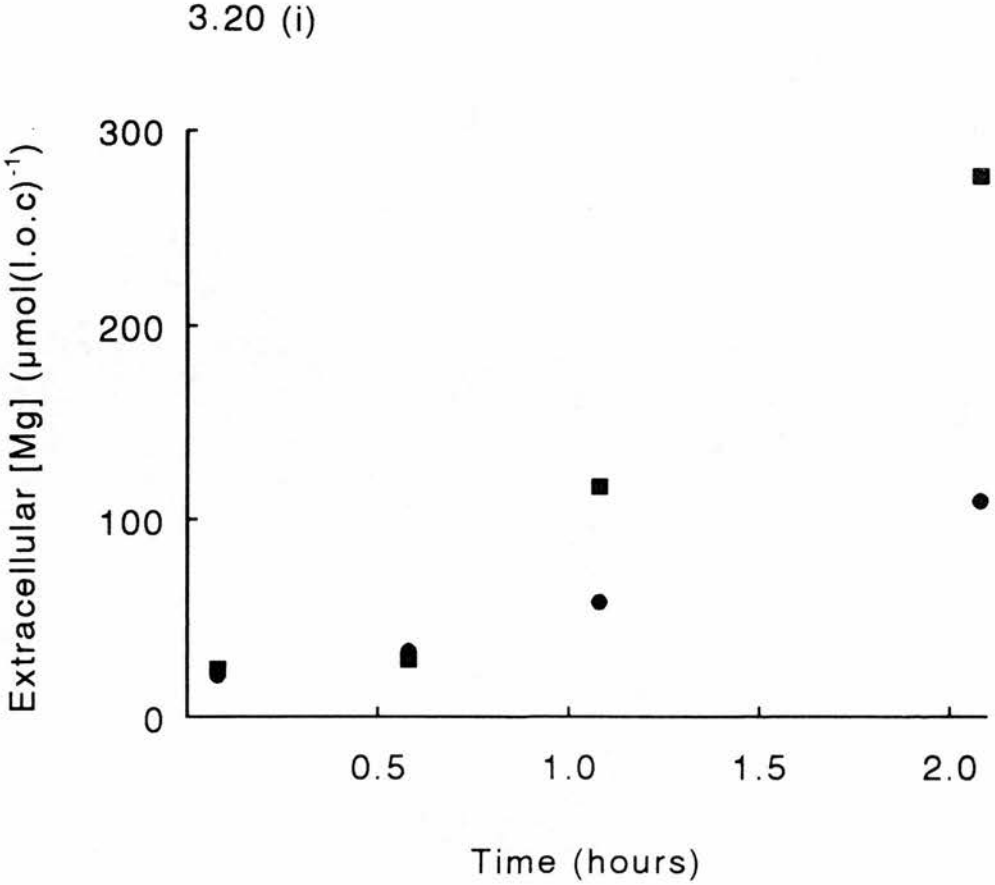

Figure 3.20.

$[Mg]_o$ (i), cell [Na] (ii) and cell [K] (iii) as a function of time. Figures 20i, 20ii and 20iii are the results of 1 experiment. Cells were incubated in either FBM (circles) or a medium in which Na had been replaced with *N*-methyl-D-glucamine (squares). The low-[Na] medium contained 145 mM *N*-methyl-D-glucamine, 5 mM KOH, 20 mM sucrose, 11 mM glucose, 0.05 mM EGTA and 7.4 mM HEPES (pH=7.55 at 38 °C). Triplicate measurements of $[Mg]_o$, $[Na]_i$ and $[K]_i$ were made at the times indicated and the points show the mean value with S.E.M. if larger than point size.

3.20 (ii)

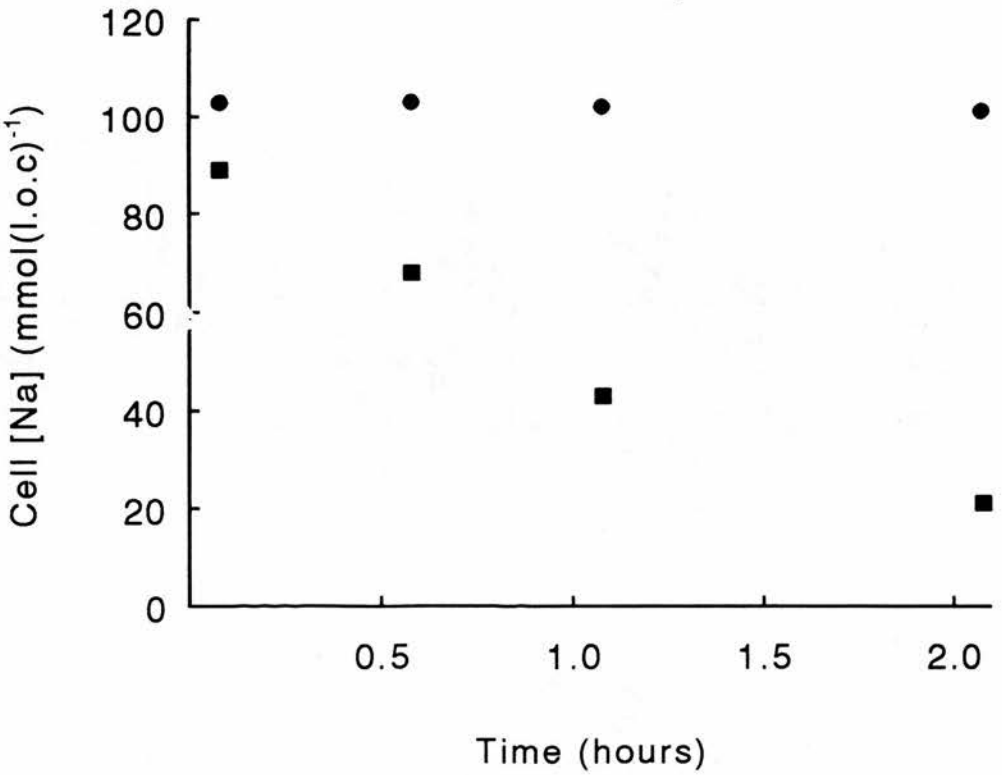

3.20 (iii)

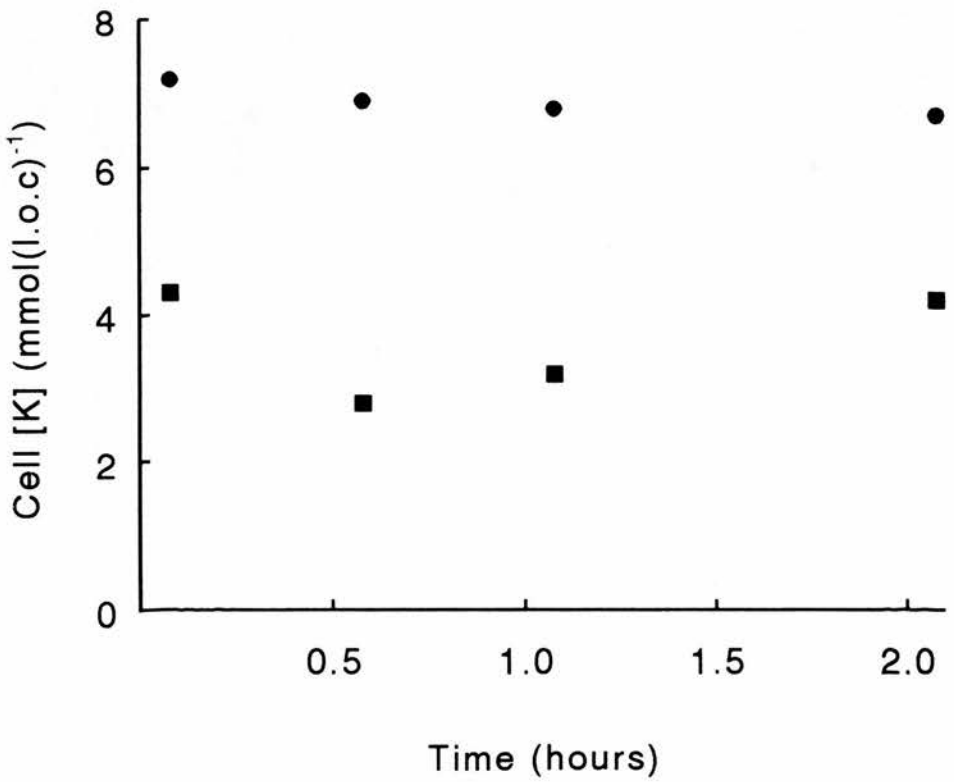

non-specific increase in the membrane permeability prior to complete lysis could account for the re-uptake of K (into K-depleted cells) and increase in Mg efflux after incubation in low-[Na], bumetanide-free media. Cell volume changes may, alternatively, open a membrane channel which can mediate the movement of Mg and K. The opening of channels in response to some extreme event has been shown in other cell species. For example Halperin, Brugnara, Tosteson, Van Ha and Tosteson (1989) showed that a depolarisation of membrane potential in human red cells triggered the opening of a non-specific cation channel which increased the membrane permeability to Na, K and Ca.

The decrease in cell volume after a 2 hour incubation in low-[Na] media is associated with a change in the membrane potential. Changes in the membrane potential were monitored by measuring the chloride distribution ratio (r). The chloride distribution ratio in cells which had been incubated in FBM was 1.31 ± 0.04 (mean ± S.E.M., n=3 independent experiments). After a 2 hour incubation in low-[Na] media (Na replaced with choline chloride) the chloride distribution ratio was 1.69 ± 0.09. Thus a long incubation in low-[Na] media causes not only a small decrease in cell volume but also (slightly) hyperpolarises the membrane potential.

To test whether the increase in $[Mg]_o$ is dependent on a rise in cell [K] ferret red cells were incubated in media in which both [Na] and [K] had been replaced with choline chloride. The time dependent changes in

$[Mg]_o$, cell [Na] and cell [K] were measured under these conditions. The results from one of these experiments are shown in Figure 3.21. Mg efflux was inhibited over the first hour of the incubation when both $[Na]_o$ and $[K]_o$ were replaced with choline chloride (triangles) In low-$[Na]_o$ media there was a rise in $[Mg]_o$ and cell [K] after 2 hours incubation (squares). However, when both $[Na]_o$ and $[K]_o$ were replaced with choline chloride there was no increase in $[Mg]_o$ or cell [K] after 2 hours (triangles).

The loss of cell [Na] was the same whether $[Na]_o$ or both $[Na]_o$ and $[K]_o$ were replaced with choline chloride. Cell volume changes were monitored throughout this experiment by estimating the packed cell volume of samples from the suspension. Cells in both media reduced in volume slightly and by the same amount.

Figure 3.21 shows that the increase in Mg efflux after a long incubation in media with low-[Na] depends on the K-depleted cells being able to take up K. In low-$[Na]_o$ media the Mg transporter may exchange Mg for K. This need not necessarily mean that Mg and K are exchanged on a coupled transporter. The incubation conditions may alter the permeability of the membrane sufficiently to allow the equilibrium of K to become an important factor in determining the membrane potential. Mg efflux is sensitive to changes in the membrane potential (Figure 3.8, the effect of SITS). Alternatively, the experimental conditions may mean that K is the ion which moves across the membrane most

3.21 (i)

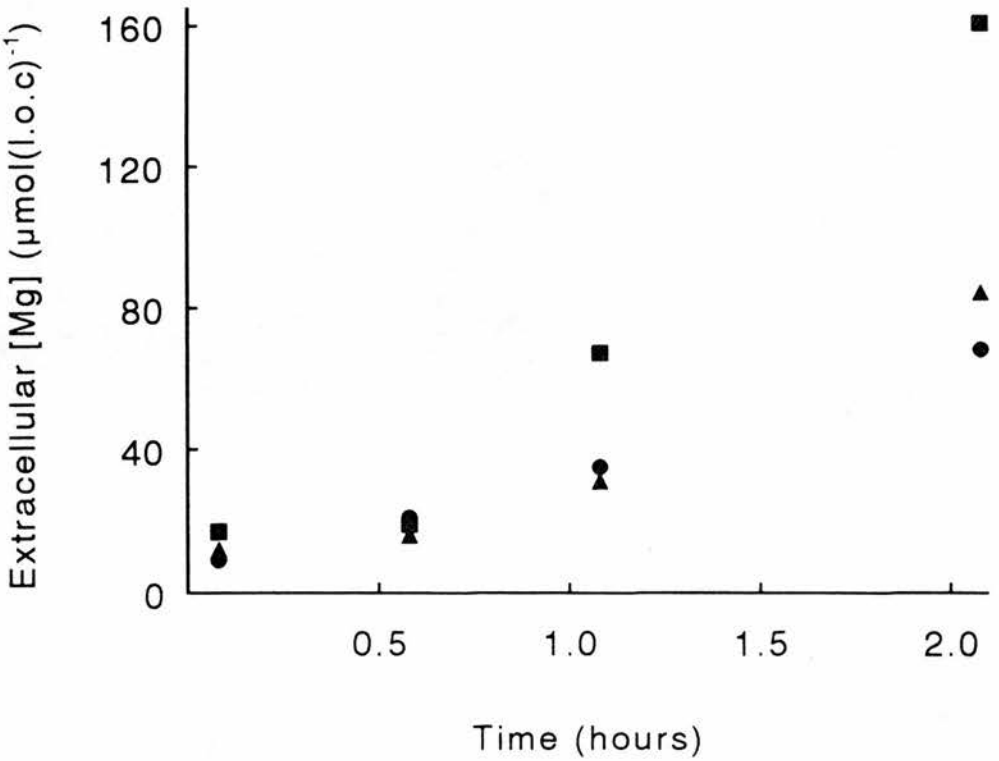

Figure 3.21.

$[Mg]_o$ (i), cell [Na] (ii) and cell [K] (iii) as a function of time. Figures 21i, 21ii and 21iii are the results of 1 experiment. Symbols represent the incubation of cells in different media as follows (mM): *circles*, NaCl, 145; KCl, 5; TRIS-HEPES, 10; *squares*, choline chloride, 145; KCl, 5; TRIS-HEPES, 10; sucrose, 20; *triangles*,choline chloride, 150; TRIS-HEPES, 10; sucrose, 20. All media also contained 0.05 mM EGTA and 11 mM glucose. Triplicate measurements of $[Mg]_o$, cell [Na] and cell [K] were made at the times indicated and the points show the mean value with S.E.M. if larger than point size.

3.21 (ii)

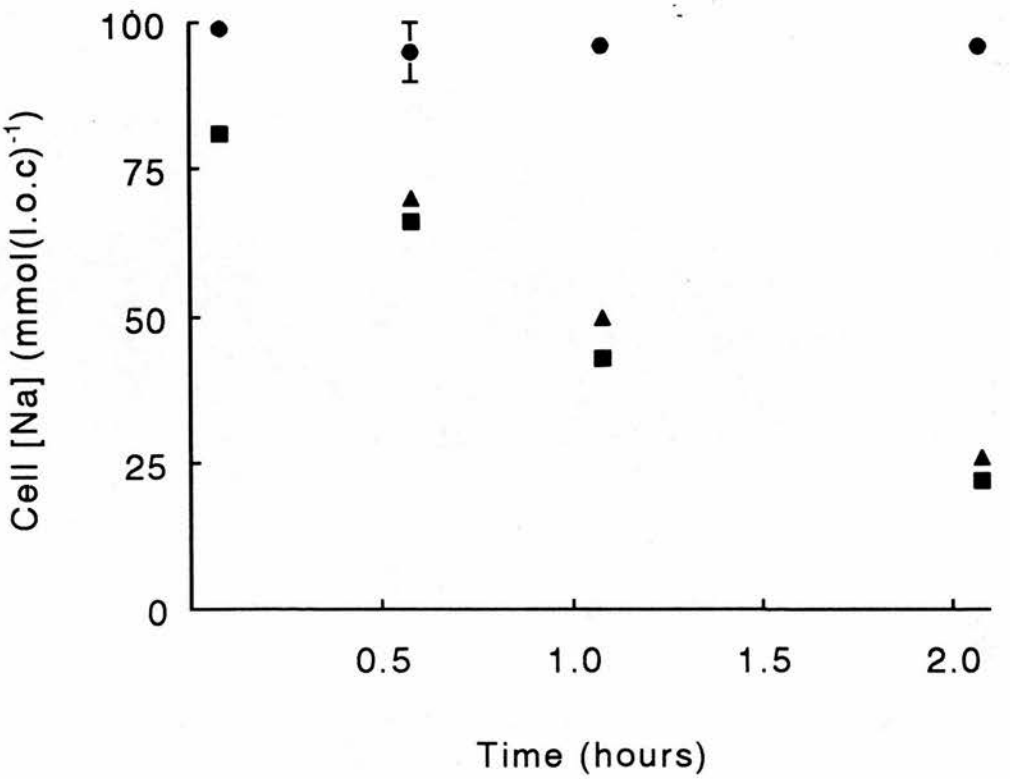

3.21 (iii)

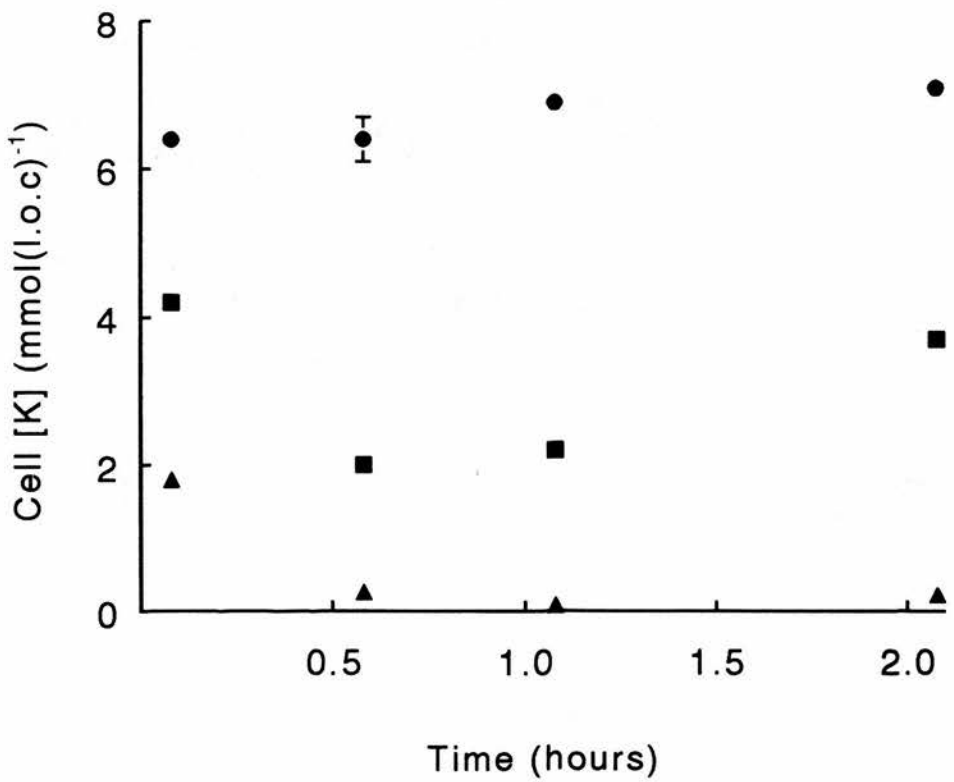

easily to compensate for the positive charge carried out of the cell during Mg efflux.

Figures 3.16 - 3.19 show that bumetanide reduces the loss of cell [Na] and cell [K] from ferret red cells and so prevents large changes in cell volume. To limit changes in the intracellular ion content as much as possible during the measurement of the $[Na]_o$-sensitive Mg efflux, bumetanide was added to the media and the fluxes were measured over the first 40 minutes of the incubation.

External [Na] dependence of Mg efflux.

The $[Na]_o$ dependence of Mg efflux is shown in Figure 3.22. Net Mg efflux was measured as change in the $[Mg]_o$ over a 30 minute period within 40 minutes of the cells being added to the medium. Figure 3.22 is a typical result of several independent experiments and there are some important features in this figure which should be noted.

(1). When the $[Na]_o$ was reduced from 145 to 20 mM, Mg efflux was stimulated by 67%. In 3 other separate experiments reducing $[Na]_o$ to 10 mM increased the Mg efflux by 71 ± 6% (mean ± S.E.M. n = 3) relative to efflux in 145 mM Na. Thus, Mg efflux is inhibited at physiological $[Na]_o$. This suggests that Na_o effects either the binding or release of Mg from transporting sites. Such cooperative interaction is a feature of cotransported ions.

(2). Bumetanide was added at all $[Na]_o$

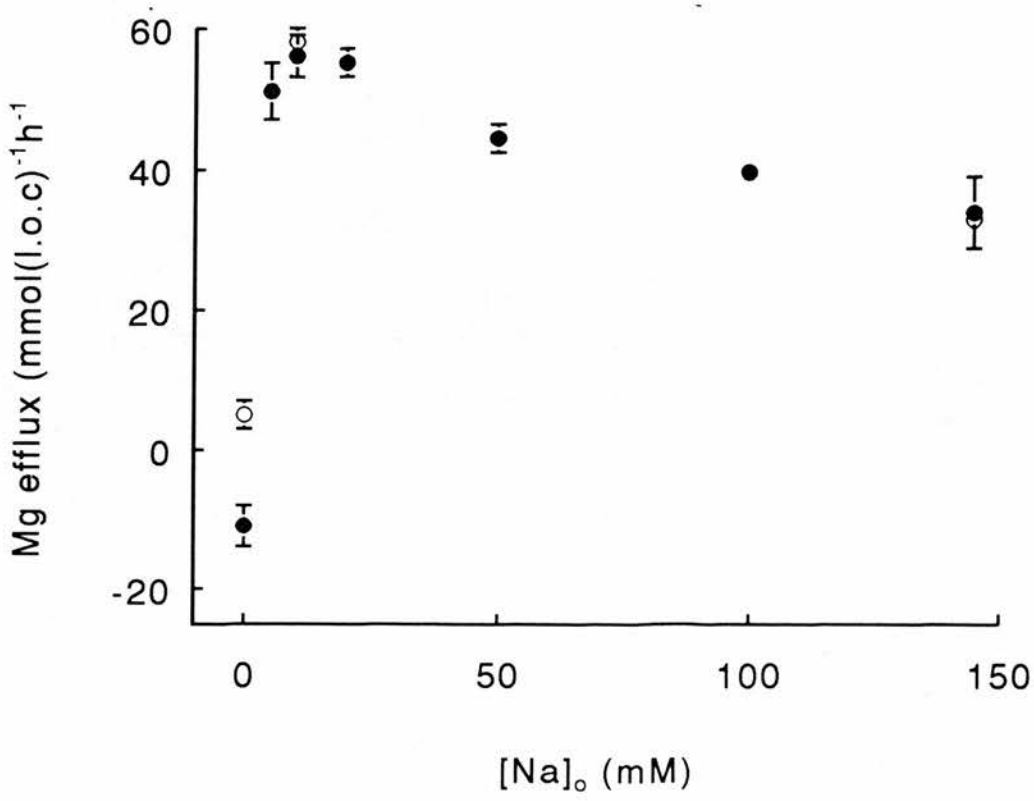

Figure 3.22.

Mg efflux as a function of $[Na]_o$. Figure shows the result of 1 typical experiment. Cells were incubated in medium containing (mM): KOH, 5; Tris-EGTA, 0.05; glucose, 11; Hepes, 7.4; the initial [NaCl] shown and sufficient choline chloride to maintain the sum, [NaCl] + [Choline chloride] = 145 mM. Efflux was the change in cell [Mg] at 10 and 40 minutes after the start of 3 separate incubations. Points show the mean efflux, corrected for cell lysis, with S.E.M. if larger than point size. The media usually contained 0.01 mM bumetanide (filled circles). Open circles show efflux when no bumetanide was added.

concentrations (filled circles). Mg efflux was also measured in media containing no bumetanide and either 145 or 20 mM NaCl. At these $[Na]_o$, bumetanide had no effect on Mg efflux.

(3). When $[Na]_o$ was reduced to below 20 mM Mg efflux was inhibited both in the presence and absence of bumetanide. Assuming that the Mg efflux measured when $[Na]_o$ is 20 mM is a maximum value for efflux, then the K_{Na} for Mg efflux is 2 mM. When $[Na]_o$ was less than 5 mM the degree of inhibition of Mg efflux varied between individual experiments.

(4). Mg influx was measured when the cells were incubated in a nominally Na-free medium but only when bumetanide was present in the incubation medium. The role of bumetanide in revealing this net influx was investigated by measuring the intracellular [Na] and [K] during this experiment. These results are shown in Figures 3.23 and 3.24.

Figure 3.23 shows the changes in cell [Na] at the beginning (open bars) and end (filled bars) of the 30 minute period over which Mg efflux was measured. When $[Na]_o$ was reduced, the cell [Na] decreased over the 30 minute incubation. The magnitude of the Na loss was dependent on the $[Na]_o$ and hence on the gradient for Na efflux. Bumetanide was included in all of these conditions. When no bumetanide was added to the medium (hatched bars) there was a greater fall in cell [Na] over the 30 minute incubation. Figure 3.24 shows a similar pattern for the changes in the cell [K] during incubation in media with reduced $[Na]_o$. Cell [K] fell

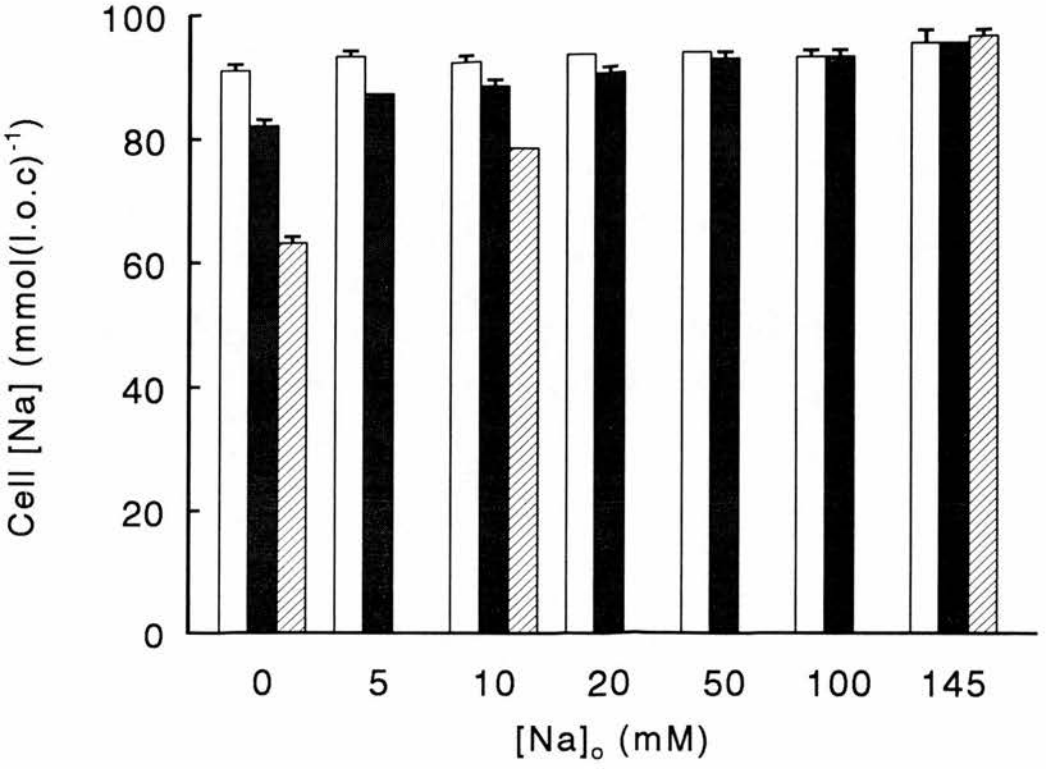

Figure 3.23.

Cell [Na] as a function of $[Na]_o$. Data are from the same experiment as Figure 3.22 and the media are as described in the legend to Figure 3.22. Cell [Na] was measured at 5 (open bars) and 35 minutes (filled bars) after the start of the incubation in a medium containing 0.01 mM bumetanide. Hatched bars show the cell [Na] after 35 minutes in a medium with no bumetanide. Bars show the mean of 3 measurements of cell [Na] with S.E.M.

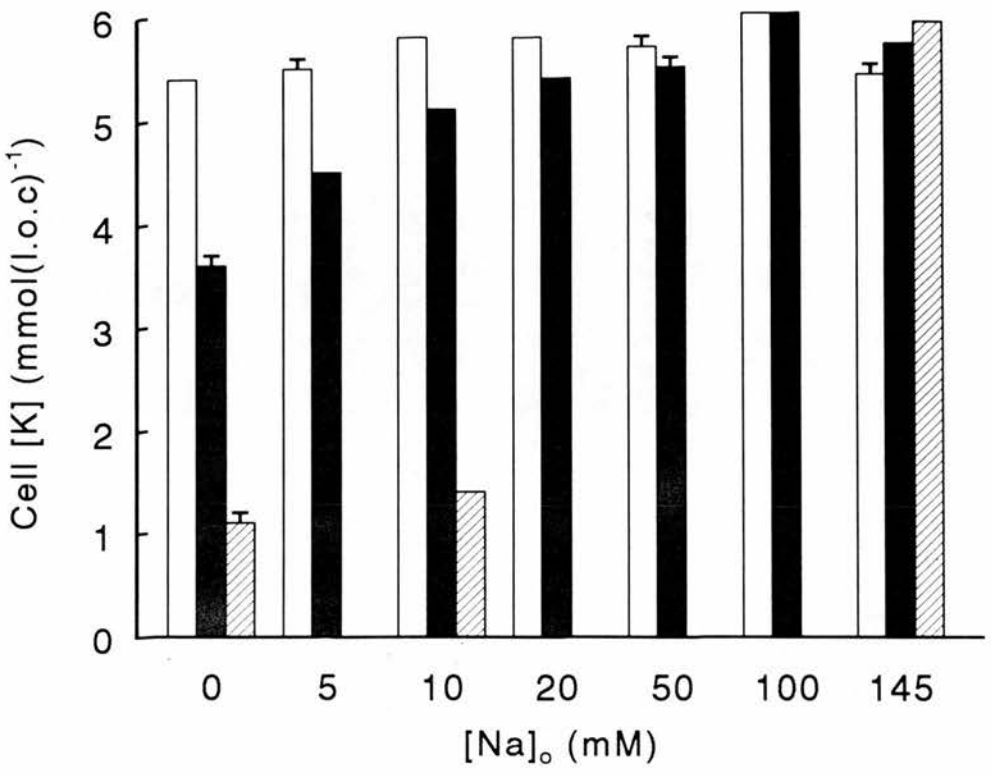

Figure 3.24.

Cell [K] as a function of $[Na]_o$. Data are from the same experiment as Figures 3.22 and 3.23. The media are as described in the legend to Figure 3.22. Cell [K] was measured at 5 (open bars) and 35 minutes (filled bars) after the start of the incubation in a medium containing 0.01 mM bumetanide. Hatched bars show the cell [K] after 35 minutes in a medium with no bumetanide. Bars show the mean of 3 measurements of cell [K] with S.E.M.

over 30 minutes and the amount lost from the cells was dependent on $[Na]_o$. Cell [K] fell to much lower levels when there was no bumetanide in the medium (hatched bars).

In the experiment shown in Figures 3.22, 3.23 and 3.24, measurements of the $[Na]_o$ in nominally Na-free media were made at the beginning and end of the flux period. The initial $[Na]_o$ was 0.2 mM. After 30 minutes the $[Na]_o$ was 1.4 mM in media which contained bumetanide and 2.8 mM in media with no bumetanide. As bumetanide has no direct effect on Mg efflux (see Figure 3.8) it seems to reveal Mg uptake by maintaining a low $[Na]_o$. This suggests that Mg efflux can be reversed but only at very low concentrations of $[Na]_o$.

Figure 3.25 shows the $[Na]_o$-dependence of Mg efflux and also shows the effects of adding 0.1 mM EDTA and 1 mM $CoCl_2$ to the media. Figure 3.25 shows the combined results of 3 independent experiments. Mg efflux was stimulated by reducing $[Na]_o$ from 145 mM to 10 mM and was inhibited when $[Na]_o$ was less than 10 mM (filled circles). Bumetanide had no effect on Mg efflux when $[Na]_o$ was 145 or 2 mM but in nominally Na-free media bumetanide inhibited Mg efflux (open circles).

0.1 mM EDTA had little effect on Mg efflux in 145 mM NaCl. As $[Na]_o$ was reduced, Mg efflux was increasingly stimulated by EDTA (squares). EDTA had its greatest stimulatory effect on Mg efflux when $[Na]_o$ was very low (a condition which normally inhibited Mg efflux). EDTA is a potent chelator of Mg and

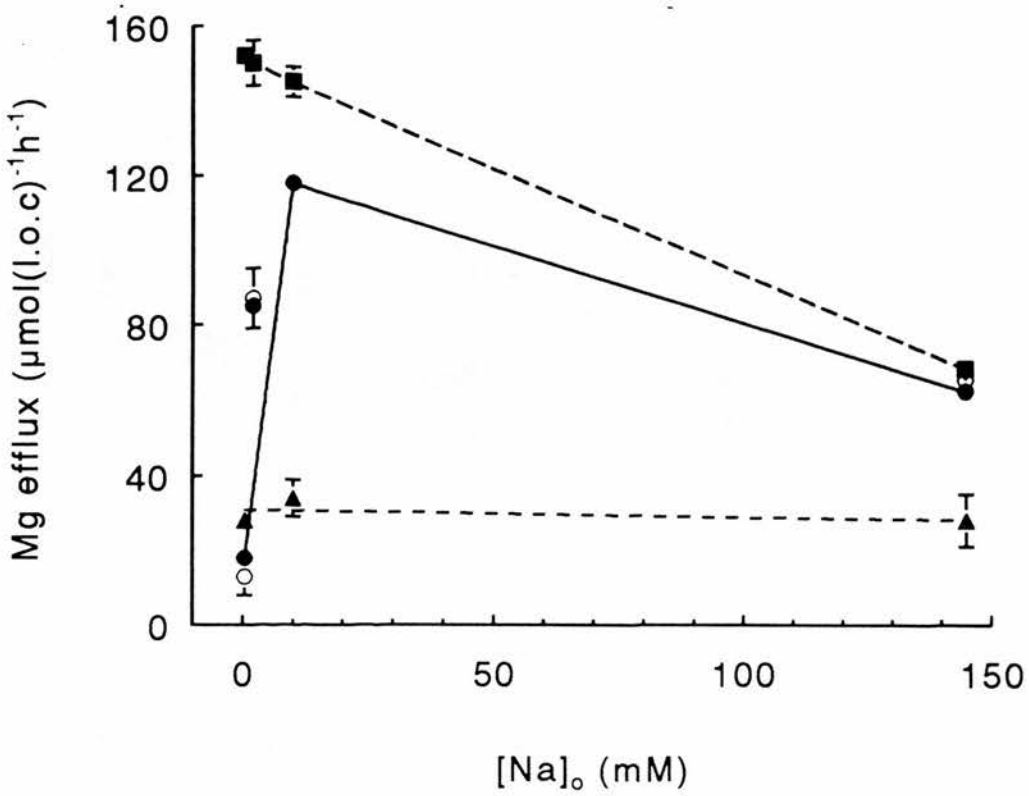

Figure 3.25.

$[Na]_o$-dependence of Mg efflux; the effects of EDTA and $CoCl_2$. Figure shows data from 3 separate experiments. Cells were incubated in medium containing (mM): KOH, 5; Tris-EGTA, 0.05; glucose, 11; Hepes, 7.4; the initial [NaCl] shown and sufficient choline chloride to maintain the sum, [NaCl] + [Choline chloride] = 145 mM. In each experiment efflux was determined by making single measurements of $[Mg]_o$ in 3 cell suspensions at 5 and 35 minutes after the start of the incubation. Points show the mean efflux (corrected for lysis) with S.E.M. if larger than point size. Symbols: *filled circles*, control; *open circles*, 0.01 mM bumetanide; *squares*, 0.1 mM Tris-EDTA; *triangles*, 1 mM $CoCl_2$.

effectively maintains $[Mg^{2+}]_o$ at 10^{-8} M (calculated using the method described by Flatman and Lew (1980) with the dissociation constants for Mg^{2+} and H^+ given by Sillén and Martell (1971) corrected for temperature and ionic strength). The buffering of $[Mg]_o$ by EDTA creates a large outward gradient for Mg.

The effects of EDTA can be most readily explained by consideration of Mg transport through a Na-Mg antiport. Under all conditions there is efflux and influx of Mg through this transporter, the measured *net* flux depending on the favoured direction of Mg movement under any given conditions. In media containing 145 mM [NaCl] there is a small inward gradient for Na. These conditions favour Na uptake and Mg efflux. There is little, if any, Mg uptake and the measurement of the increase in $[Mg]_o$ is an accurate evaluation of net Mg efflux. EDTA has no effect on Mg efflux under these conditions suggesting that **(1)** the transporter is insensitive to changes in the outward Mg gradient under these conditions, **or (2)** the release of Mg from the external binding site is not a rate limiting step **or (3)** the influx of Mg (or recycling) is not a requirement for transport.

As $[Na]_o$ is lowered, the Na gradient allows more Mg influx through Na-Mg exchange. Under these conditions net Mg efflux, measured as the accumulation of Mg in the medium, is reduced. This could be due to either a decrease in unidirectional efflux, an increase in unidirectional influx or both. Assuming that $[Mg]_o$ is not required for Mg efflux, EDTA will have no effect

on unidirectional Mg efflux. However EDTA will inhibit unidirectional influx by removing the $[Mg]_o$ available to be transported into the cell. The Mg efflux measured in media with low-[Na] and EDTA is the total unidirectional efflux under these conditions. It then follows that the difference in net Mg efflux measured in the presence or absence of EDTA is the net Mg influx mediated by the reversal of Na-Mg exchange.

1 mM $CoCl_2$ inhibited Mg efflux at all concentrations of $[Na]_o$ (triangles). This effect of Co reveals a component of efflux which is insensitive to changes in $[Na]_o$. In this experiment 1 mM Co inhibited approximately 60% of the Mg efflux in 145 mM NaCl. Treatment with Co, as well as other agents such as amiloride and quinidine (Figures 3.9 and 3.11), reveals a route for Mg efflux which is insensitive to these agents as well as to changes in $[Na]_o$. Mg efflux through this route accounts for approximately 40% of the efflux measured in 145 mM $[Na]_o$. The Mg permeability through this route can be calculated using Equation 3.1.

Given that 16 μmol(l.o.c.)$^{-1}h^{-1}$ (40% of the mean Mg efflux) moves through the drug-insensitive route for Mg transport, then this pathway has a permeability (P) of $7 * 10^{-10}$ cm^{-2} sec^{-1}.

$$J = P * V * [c_1 - c_2 * e^V] / [e^V - 1] \qquad \textbf{3.1}$$

where V is $[z * F * (E_2-E_1)]/[R * T]$

F = Faraday constant (96500 C mol^{-1})

z = valancy

R = Gas constant (8.314 $Jdeg^{-1}mol^{-1}$)

T = absolute temperature (K)

E_2, E_1 = potential either side of the membrane

c_2, c_1 = concentrations .. ..

(in moles cm^{-3})

J = flux (moles cm^{-2} sec^{-1})

Active Mg uptake.

The operation of a Na-Mg exchange transporter can only be clearly demonstrated by showing that the movement of Mg is linked to the movement of Na. There are many routes for Na transport across the membrane and it is therefore very difficult to identify the Na flux corresponding to the very small Mg efflux in these cells. The identification of these fluxes will only be possible with the identification of potent and specific inhibitor of this Mg transport system.

If Na-Mg exchange is a major route for Mg transport then it should be possible to change the direction of Mg transport by altering the direction of the Na gradient. This has been attempted in human red cells (Lüdi and Schatzmann,1987; Schatzmann, 1993) but human red cells require loading with Na to change the

Na gradient significantly. Ferret red cells have a high cell [Na] (Flatman, 1983) and a small inward Na gradient which can be reversed by simply lowering $[Na]_o$. The reversal of Mg transport at low $[Na]_o$ has already been demonstrated (Figure 3.22).

Attributing transport to an antiport assumes that the movement of one (or more) of the transported species down a gradient provides sufficient energy for the system to transport the other species. The energy harvested from or required for the movement of an ion can be estimated thermodynamically from Equation 3.2.

$$\Delta G_{1\rightarrow 2} = zF(E_2 - E_1) + RT \ln (c_2/c_1) \quad (Jmol^{-1}) \qquad \textbf{(3.2)}$$

where F = 96500 ($C\ mol^{-1}$)

z = valency

R = 8.314 ($Jdeg^{-1}mol^{-1}$)

T = absolute temperature (K)

E_2, E_1 = potential either side of the membrane

c_2, c_1 = concentrations .. ..

ΔG is calculated for the movement of each ion. If $\Delta G<0$ then the reaction occurs spontaneously. If $\Delta G>0$ then an energy input is required for ion movement across the membrane. The values for ΔG ($kJmol^{-1}$) give an indication of the energies required or harvested from the transport of the ions. Equation 3.2 predicts the energy involved in moving ions according to thermodynamic principles. It does not take into

account the kinetic factors which may influence the movement of ions. For example, Equation 3.2 cannot predict changes in affinity of binding sites, the requirement for the binding of an ion to an activation site or the activation energy of the transporter.

Equation 3.2 was used to set experimental conditions so that there was an outward gradient for Na as well as Mg. Under these conditions any influx of Mg would be against a gradient and would thus be active transport. Results from 3 such experiments are shown in Tables 3C, 3D and 3E.

Table 3C shows data from an experiment where ferret red cells were incubated in a medium with a very low [Na] (0.13 mM). This created a large outward gradient for Na which could yield 17 $kJmol^{-1}$. The initial $[Mg]_o$ was 0.23 mM. After 30 minutes the cell [Mg] had increased and $[Mg]_o$ had decreased. The energy required for this net influx of Mg was 2.4 $kJmol^{-1}$. Tables 3D and 3E show the data from 2 similar experiments. In these experiments the initial $[Na]_o$ was raised to 10 mM which reduced the energy available from the outward Na gradient to 6 $kJmol^{-1}$. $[Mg]_o$ was also reduced in this experiment thus increasing the energy input needed to drive Mg influx (3.1 $kJmol^{-1}$ in Table 3D and 3.6 $kJmol^{-1}$ in Table 3E). Despite these stringent conditions, the cell [Mg] increased over the 30 minute incubation. The experiments illustrated in Tables 3C, 3D and 3E demonstrate that ferret red cells can take up Mg against a gradient if sufficient energy is available from the outward movement of Na down a

chemical gradient.

Equation 3.2 was used to calculate the change in the membrane potential necessary to make the influx of Mg, measured in Tables 3C, 3D and 3E, a passive process. For the influx of Mg to occur down a gradient then ΔG must be less than zero. For the experiments shown in Tables 3C, 3D and 3E, Mg influx would only become a passive process when the membrane potential was greater than -14, -25 and -27 mV respectively. The membrane potential was not measured in these experiments. However the membrane potential was measured in a number of rather more extreme conditions. For example, when ferret red cells were incubated in low-[Na] media, with no bumetanide, for 45 minutes the change in the membrane potential (as measured using the proton ionophore, CCCP) was less than 1 mV. Thus it is unlikely that during the short incubations in Tables 3C, 3D and 3E the membrane potential changes sufficiently to drive Mg influx.

Equation 3.2 was used to calculate the energy requirements for the movement of Mg under physiological conditions. For ferret red cells in vivo the cell [Na] is 145 mM, the $[Na]_o$ is 150 mM and the membrane potential is -9 mV. Thus there is a small inward gradient for the movement of Na. Equation 3.1 predicts that the movement of Na down this gradient yields 1 $kJmol^{-1}$. Assuming that $[Mg]_o$ is 0.5 mM (Walser, 1961 and Heaton, 1967 and see Introduction). then the energy requirement for Mg efflux is 1 $kJmol^{-1}$. Thus there is just sufficient energy in the inward Na

Legend to Tables 3C, 3D and 3E.

Measurement of active Mg influx in ferret red cells. Each table shows the result of an independent experiment using cells from a different animal. In Tables 3C and 3D the cells were stored overnight and washed twice in the incubation medium before the start of the experiment. In Table 3E the cells were stored for 2 days and washed only once prior to the experiment. The wash and incubation medium for each experiment is as described in the tables. The exact concentration of Mg in the medium was measured by AAS. Mg influx was measured as a change in the cell [Mg]. ΔG was calculated from Equation 3.2 using the external and internal [Na] and [Mg] as shown in the tables. Intracellular ionized $[Mg^{2+}]_i$ was obtained from a Mg buffering curve using the measured value of the cell [Mg]. (Mg buffering was measured in each group of cells). Cell [Na] was 145 mM and the membrane potential was assumed to be -9 mV. Different protocols were used to measure Mg influx. In Table 3D triplicate measurements of cell [Mg], $[Mg]_o$, cell [Na] and cell [K] were made at 10 and 40 minutes after the start of 1 incubation. In Tables 3C and 3E single measurements were made at 10 and 40 minutes after the addition of the cells to 3 separate incubations. Results show the mean measurement with the S.E.M. if this is significant at 2 decimal places.

Table 3C. Active uptake of Mg (1).

Medium. 145 mM choline chloride
5 mM K in 7 mM K-HEPES
11 mM glucose
0.05 mM EGTA
0.1 mM bumetanide

0.23 mM $MgCl_2$ (measured value)

Energy in ion gradients

assuming membrane potential = -9 mV

ΔG_{Na} = -17.3 $kJmol^{-1}$
1→2

ΔG_{Mg} = 2.4 $kJmol^{-1}$
2→1

Results.

Haematocrit 6 %

Mean cell [Mg] (total) 3.54 ± 0.13 $(mmol(l.o.c.)^{-1})$

Free [Mg] (value from buffer curve) 0.67mM

	initial	final
$[Mg]_o$ (mM)	0.23	0.17
$[Na]_o$ (mM)	0.13	0.70 ± 0.03

Mg uptake: 1.10 ± 0.04 $mmol(l.o.c.)^{-1}h^{-1}$

Table 3D. Active uptake of Mg (2).

Medium. 10 mM NaCl
135 mM choline chloride
5 mM K in 7 mM K-HEPES
11 mM glucose
0.05 mM EGTA
0.1 mM bumetanide

0.11 mM $MgCl_2$ (measured value)

Energy in ion gradients

assuming membrane potential = -9 mV

ΔG_{Na} = -6.1 $kJmol^{-1}$
1→2

ΔG_{Mg} = 3.1 $kJmol^{-1}$
2→1

Results

Haematocrit 7%

Mean cell [Mg] (total) 2.43 ± 0.03 $(mmol(l.o.c.)^{-1})$

Free [Mg] (value from buffer curve) 0.7 mM

	initial	final
$[Mg]_o$ (mM)	0.11	0.11
$[Na]_i$ $(mmol(l.o.c.)^{-1})$	98 ± 1	93 ± 2
$[K]_i$ $(mmol(l.o.c.)^{-1})$	6.0 ± 0.1	5.8 ± 0.1

Net Mg uptake 0.14 ± 0.02 $mmol(l.o.c.)^{-1}h^{-1}$)

Table 3E. Active uptake of Mg (3).

Medium. 10 mM NaCl
135 mM choline chloride
5 mM K in 7 mM K-HEPES
11 mM glucose
0.05 mM EGTA
0.1 mM bumetanide

0.11 mM $MgCl_2$ (measured value)

Energy in ion gradients.

assuming membrane potential = -9 mV

ΔG_{Na} = -6.1 $kJmol^{-1}$
1→2

ΔG_{Mg} = 3.6 $kJmol^{-1}$
2→1

Results

Haematocrit 8 %

Mean cell [Mg] (total) 2.92 ± 0.02 $(mmol(l.o.c.)^{-1}$

Free [Mg] (value from buffer curve) 0.86 mM

Mg uptake: 0.12 ± 0.02 $mmol(l.o.c.)^{-1}h^{-1}$.

gradient to drive the efflux of Mg in oxygenated ferret red cells.

Assuming that all Mg transport occurs via Na-Mg exchange in ferret red cells, then at equilibrium

$$\Delta G_{Mg} = \Delta G_{Na} \qquad (3.3)$$
$$2\rightarrow1 \qquad 1\rightarrow2$$

where $\Delta G_{Na} = n[zFE + RT\ln(c_2/c_1)]$

Substituting and simplifying equation 3.2 gives

$$\left(\frac{[Mg^{2+}]_o}{[Mg^{2+}]_i}\right) \leq \left(\frac{[Na_o^{+}]}{[Na_i^{+}]}\right)^n \exp\left(\frac{EF(2-n)}{RT}\right) \qquad (3.4)$$

where E (membrane potential) = 10 mV (-0.01 V)

F = 96500 ($Jmol^{-1}volts^{-1}$)

R = 8.314 ($Jdeg^{-1}mol^{-1}$)

T = 310 K

n is the ratio of Na ions to Mg ions transported in each cycle of the transporter.

Equation 3.4 predicts that if Na-Mg exchange transports 3 Na ion and 1 Mg ion then it would reverse direction when Na_o was 17 mM. If the ratio was 2 Na for 1 Mg or 1 Na for 1 Mg then reversal would occur at 7.5 mM and 0.6 mM $[Na]_o$ respectively. A reversal of Na-Mg exchange at 0.6 mM $[Na]_o$ most closely fits the data shown here (see Figures 3.22 and 3.25).

These thermodynamic predictions require too many

assumptions and cannot be exclusively accepted as a model for the Mg transporter at this time. However it is interesting to note that if the Mg transporter does require $[Na]_o$ below 0.6 mM before it can reverse direction it would explain why the addition of bumetanide and short flux time periods (limiting the loss of cell [Na] and preventing a rise in the $[Na]_o$) are necessary before net Mg influx can be measured. These data do suggest that reducing $[Na]_o$ to provide sufficient energy can allow Mg transport to reverse direction and mediate net active Mg influx.

4. Magnesium Influx.

Mg efflux from ferret red cells is inhibited, and a net influx of Mg is revealed, when the cells are incubated in media with very low (< 1 mM) [Na] (Figure 3.22). Thus it seems that it is possible to reverse Na-Mg exchange even when the medium contains micromolar concentrations of Mg. However Mg influx and Mg efflux may occur through different transporters or, if both influx and efflux occur through the same route, the conditions which favour Mg influx may alter the properties of the transporter. This chapter describes some properties of Mg influx into ferret red cells.

The $[Mg]_o$ dependence of Mg influx.

Mg influx measured in media with very low $[Na]_o$ and low $[Mg]_o$ is very small and not always easily detected. It is thus difficult to examine the properties of Mg influx under these conditions. Even in experiments where $[Mg]_o$ is raised to 0.1-0.3 mM the measurement of influx still relies on the detection of very small changes in the cell [Mg]. Measurement of Mg influx depends on $[Na]_o$ being kept below 1 mM throughout the experiment. As ferret red cells contain a high concentration of Na, cell lysis and Na leak from the cells can raise $[Na]_o$ sufficiently to prevent Mg influx. It is especially difficult to measure Mg influx using this method, in a batch of cells which have an increased permeability to Na (as a result of

chemical treatment, storage or as an inherent property). To provide a more useful model for the study of Mg influx, the effect of raising $[Mg]_o$ was examined.

The effects of increasing $[Mg]_o$ on Mg influx are shown in Figure 4.1.

When $[Na]_o$ was reduced from 145 mM to 5 mM (open circles) Mg influx was stimulated at all $[Mg]_o$. Mg influx appears to occur through a saturable pathway. Fitting the data with the line shown, assuming simple Michaelis-Menten kinetics, gives a maximum influx rate of 0.88 $mmol(l.o.c.)^{-1}h^{-1}$ and a K_m (for the activation of Mg influx by $[Mg]_o$) of 0.37 mM.

Although simple Michaelis-Menten kinetics generates a good curve fit for the data in Figure 4.1, closer examination of the data shows that Mg influx is slightly inhibited when $[Mg]_o$ is increased from 5 to 10 mM. The inhibition of Mg influx at high $[Mg]_o$ was seen in several similar experiments. The largest inhibition of Mg influx by increasing $[Mg]_o$ was measured in an experiment where the Mg influx was reduced from 0.63 ± 0.08 to 0.45 ± 0.03 $mmol(l.o.c.)^{-1}h^{-1}$ (mean ± S.E.M.,n=3 measurements of influx in 1 experiment) when $[Mg]_o$ was increased from 5 to 10 mM. The data from these experiments suggests that high $[Mg]_o$ inhibits Mg influx when $[Na]_o$ is low. $[Mg]_o$ may compete with $[Na]_o$ for binding sites and at high concentrations $[Mg]_o$ may inhibit the operation of the transporter by impeding the binding or release of Na from an external binding site.

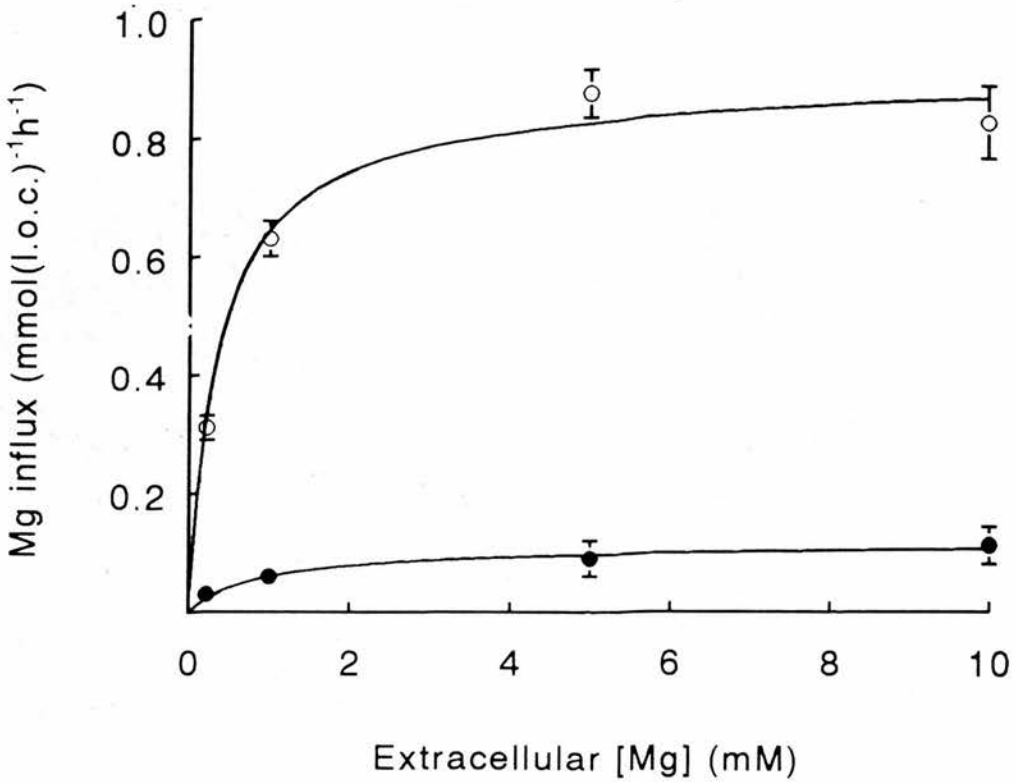

Figure 4.1.

Mg influx as a function of $[Mg]_o$. Cells were incubated in media containing (mM);glucose, 11 ; EGTA, 0.05; bumetanide, 0.1; KOH, 5; HEPES, 8; KCl, 5; the $[MgCl_2]$ shown and either 145 mM NaCl (filled circles) or 5 mM NaCl and 145 mM choline chloride (open circles). Influx was measured as a change in the cell [Mg] at 10 and 40 minutes after the start of 3 separate incubations in 1 experiment. Points show the mean influx ± S.E.M. if larger than point size. Lines were drawn assuming Michaelis-Menten kinetics with parameters (maximum influx (mmol(l.o.c.)$^{-1}$h^{-1}), 0.11 and 0.88; K_m (mM), 0.87 and 0.37 for cells in 145 mM and 5 mM Na respectively.

When the external medium contained 145 mM Na and 5 mM Mg, Mg influx occurred at a much slower rate than in 5 mM $[Na]_o$ (filled circles). The data, under these conditions, were also fitted using simple Michaelis-Menten kinetics. The parameters of the curve fit give a maximum influx of 0.113 $mmol(l.o.c.)^{-1}h^{-1}$ and a K_m (for the activation of Mg influx by $[Mg]_o$) of 0.87 mM. The curve fits generated for Mg influx from media containing 5 or 145 mM $[Na]_o$ show that the apparent affinity of the transporter for $[Mg]_o$ increases when $[Na]_o$ is reduced.

A proportion of Mg influx in either 5 or 145 mM $[Na]_o$ will be through a 'leak' pathway. As $[Mg]_o$ is increased, the influx of Mg through this `leak' pathway will also increase. A 'leak' pathway has been identified in Mg efflux experiments. Approximately 40% of efflux, which could not be inhibited by a variety of reagents, was also insensitive to changes in the $[Na]_o$ (Figure 3.25). The permeability of this `leak' pathway to Mg was calculated from efflux data and was estimated as $7*10^{-10}$ $cm^{-2}sec^{-1}$ (Equation 3.1). Assuming that this route is operating under the conditions used to measure Mg influx, then an increase in $[Mg]_o$ to 10 mM should increase the movement of Mg through the 'leak' pathway to approximately 0.53 $mmol(l.o.c.)^{-1}h^{-1}$. This influx is sufficient to account for the Mg influx when the cells are incubated in 145 mM Na and 10 mM Mg. The calculation of the Mg permeability can only provide a rough estimate of the Mg movement through this pathway. What is clear is

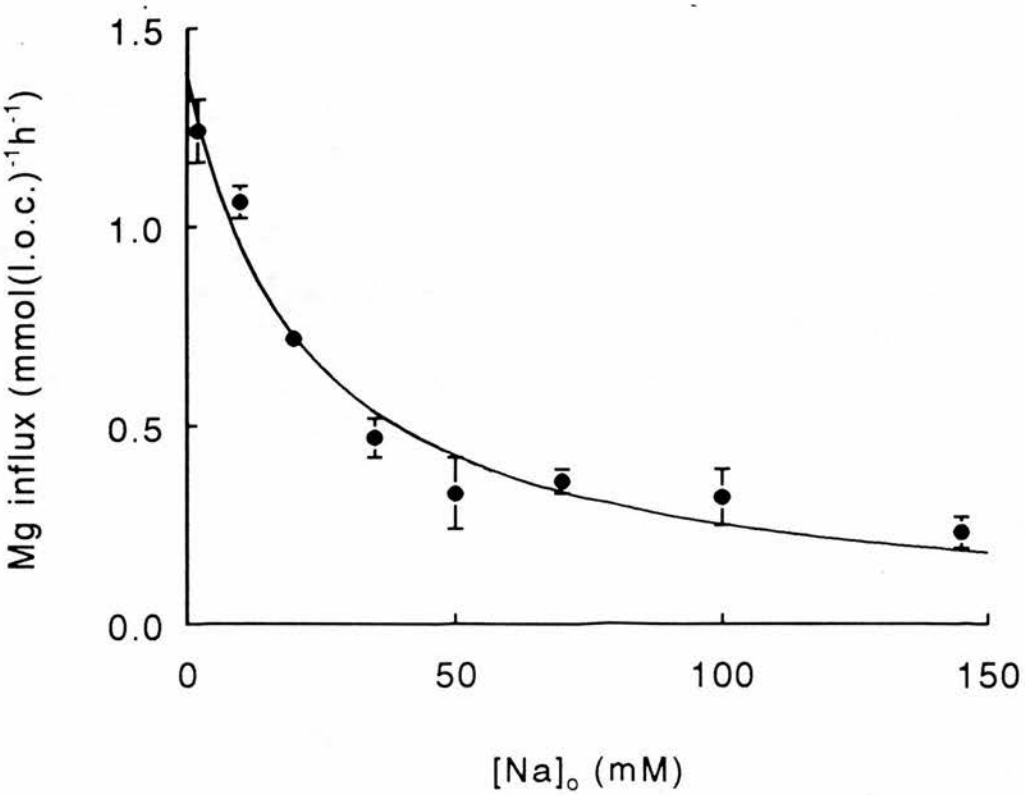

Figure 4.2.

Mg influx as a function of $[Na]_o$. Cells were incubated in a media containing (mM); KOH, 5; HEPES, 8; glucose, 11; EGTA, 0.05; bumetanide, 0.1; $MgCl_2$, 5; the $[Na]_o$ shown and sufficient choline chloride so that the sum [NaCl] + [Choline-Cl] was 145. Mg influx was measured as a change in the cell [Mg] at 10 and 40 minutes after the start of 3 separate incubations in 1 experiment. Points show the mean influx ± S.E.M. if larger than point size. Lines were drawn assuming Michaelis-Menten kinetics (Na binds to an external site to inhibit Mg influx) with parameters, (maximum Mg influx) 1.39 $mmol(l.o.c.)^{-1}h^{-1}$; K_m, 22 mM.

that the $[Na]_o$-insensitive route for Mg efflux can mediate Mg influx when $[Mg]_o$ is increased. In 145 mM $[Na]_o$ a substantial part, if not all, Mg influx will be through this 'leak' pathway. However in 5 mM $[Na]_o$, Mg movement through this route will make only a minor contribution to the total Mg influx.

Figure 4.1 shows that a small Mg influx was measured when $[Na]_o$ was 145 mM and $[Mg]_o$ was 0.2 mM. This measurement is unusual. In 5 independent experiments a small decrease in cell [Mg] was measured in media containing 145 mM $[Na]_o$ and a $[Mg]_o$ between 0.2 and 0.4 mM (the net efflux was 0.06 ± 0.04 $mmol(l.o.c.)^{-1}h^{-1}$, mean ± S.E.M, n=5 experiments). When the medium contained 145 mM [Na] and 1 mM [Mg] there was little change in the cell [Mg] (the net influx was 0.01 ± 0.02, mean ± S.E.M., n=5 experiments). These experiments indicate, when the medium contains 145 mM $[Na]_o$, $[Mg]_o$ must usually be greater than 1 mM for Mg influx to be measured.

Figure 4.1 shows that a maximum rate of Mg influx can be measured in media with either 5 or 145 mM $[Na]_o$ when $[Mg]_o$ is 5 mM. In subsequent experiments 5 mM $[Mg]_o$ was selected as an appropriate condition for the measurement of Mg influx.

The $[Na]_o$ dependence of Mg influx.

Figure 4.2 shows the $[Na]_o$-dependence of Mg influx when the medium contained 5 mM Mg. Mg influx increased as $[Na]_o$ was reduced. The data of Figure 4.2 are

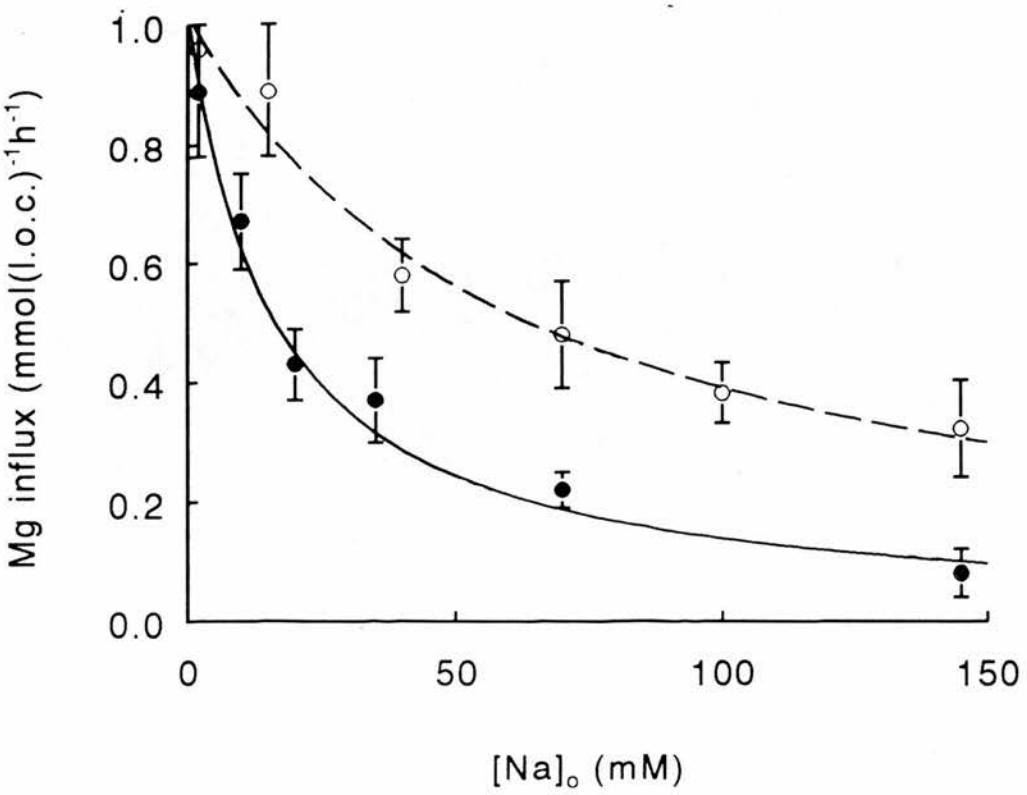

Figure 4.3.

Mg influx as a function of $[Na]_o$. Media was the same as described in legend to Figure 4.2 but contained either 2 mM (filled circles) or 10 mM (open circles) Mg. Mg influx was measured as a change in the cell [Mg] at 10 and 40 minutes after the start of 3 separate incubations in 1 experiment. Points show the mean ± S.E.M. if larger than point size. Lines were drawn assuming Michaelis-Menten kinetics (Na binds to an external site to inhibit Mg uptake) with parameters (maximum influx, mmol(l.o.c.)$^{-1}$h^{-1} and K_m, mM) 1.03 and 16 when $[Mg]_o$ was 2 mM; 1.02 and 62 when $[Mg]_o$ was 10 mM.

fitted with a line assuming simple Michealis-Menten kinetics. The curve fit parameters give a value for the K_m (the inhibition of Mg influx by $[Na]_o$) of 22 mM.

Another example of the $[Na]_o$-dependence of Mg influx is shown in Figure 4.3. In this experiment, $[Mg]_o$ was 2 mM (filled circles) or 10 mM (open circles). Both sets of data were fitted with a line assuming Michaelis-Menten kinetics. The curve fit parameters give values for K_m (the inhibition of Mg influx by $[Na]_o$) of 16 mM when $[Mg]_o$ is 2 mM and 62 mM when $[Mg]_o$ is 10 mM. The curve-fit parameters of Figures 4.2 and 4.3 show that when $[Mg]_o$ is increased, the affinity of the transport site for $[Na]_o$ decreases.

The time dependence of Mg influx.

Figure 4.4 shows the changes in the cell [Mg] when ferret red cells were incubated for up to 2 hours in media with 5 mM Mg and either 145 mM Na (filled circles) or 5 mM Na (open circles). Figure 4.4 shows the data of 1 experiment. The results of several independent experiments, using the same protocol, were remarkably consistent with the results shown in Figure 4.4.

When ferret red cells were incubated in media containing 145 mM Na and 5 mM Mg, Mg influx occurred at a steady rate for up to 2 hours. The line shown in Figure 4.4 was drawn using linear regression analysis and has a slope of 0.26 ± 0.02 $mmol(l.o.c.)^{-1}h^{-1}$ (mean ± S.E. of the mean slope, n=6 points). Assuming a

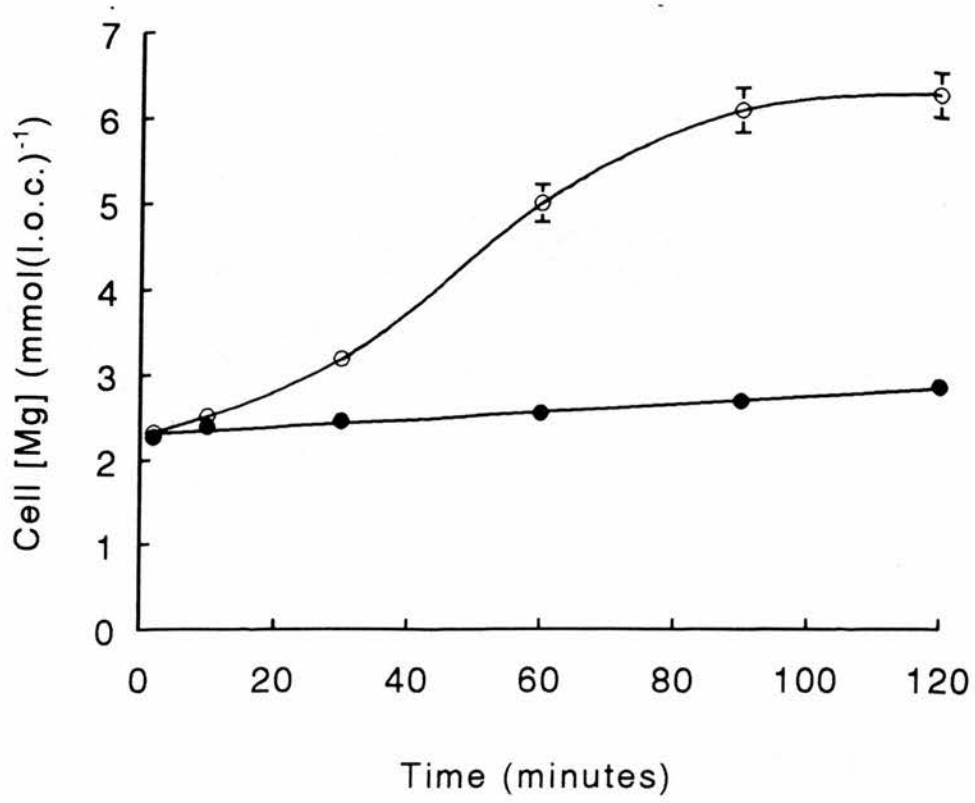

Figure 4.4.

Time dependent Mg influx. Cells were incubated in a media containing (mM); glucose, 11; EGTA, 0.05; bumetanide, 0.1; $MgCl_2$, 5; KOH, 5; HEPES, 8 and either 145 NaCl (filled circles) or 5 NaCl and 140 choline chloride (open circles). Points show the mean of triplicate measurements of cell [Mg] (± S.E.M. if larger than point size) in 1 incubation. Lines were drawn using linear regression analysis (filled circles, slope = 0.26) or by eye (open circles). The initial cell [Na] and [K] (mmol(l.o.c.)$^{-1}$) were 98 and 6.4 respectively. After 2 hours cell [Na] and [K] were 100 and 6.3 (in 145 mM $[Na]_o$) and 40 and 5.6 in 5 mM $[Na]_o$.

membrane permeability of $7 * 10^{-10}$ cm^{-2} sec^{-1} for Mg (calculated from efflux data) then Equation 3.1 predicts that, when $[Mg]_o$ is 5 mM, Mg influx should be 0.26 $mmol(l.o.c.)^{-1}h^{-1}$. Mg influx in media with 145 mM $[Na]_o$ and high $[Mg]_o$ is remarkably consistent with the movement of Mg into the cells through the same `leak' pathway for Mg efflux which is insensitive to $[Na]_o$ and a variety of transport inhibitors.

Reducing $[Na]_o$ to 5 mM stimulated Mg influx. The time dependent changes in the cell [Mg] are shown in Figure 4.4 (open circles). Mg influx, under these conditions, is a complicated function of the incubation time. A mathematical model for this pattern of influx is difficult to determine and the line through the points, under these conditions, was drawn by eye.

The rate of Mg influx from media containing 5 mM Mg and 5 mM Na is continually changing over the 2 hours of incubation. There are insufficient data in Figure 4.4 to determine the true shape of the curve over the initial stage of the incubation. The curve was tested in another experiment where the cell [Mg] was measured at 5 minute intervals for the first 40 minutes of the incubation. Although stimulated by incubation in 5 mM Na, the rate of influx over the first 30 minutes is still quite slow. Measurement of changes in cell [Mg] over the 5 minute time intervals produced quite scattered data and was not able to improve the resolution of the shape of this part of the curve.

The rate of Mg influx increased considerably after 30 minutes incubation in media with 5 mM Na and 5 mM

Mg. The rate of Mg influx was highest between 30 and 60 minutes incubation. After 60 minutes the rate of influx slowed and the cell [Mg] reached a plateau value after 2 hours incubation. The time-dependent pattern of loading and the maximum cell [Mg] attained were reproduced in several independent experiments. In one experiment the incubation was continued beyond 2 hours. Cell [Mg] did not increase further with prolonged incubation but the rate of cell lysis increased. Thus the plateau level represents the maximum cell [Mg] to which the cells in this population can load under these conditions.

The cell [Mg] at electrochemical equilibrium was measured in these cells (Figure 4.4) by adding 10 μM A23187 after 2 hours incubation. Mg was allowed to equilibrate for 10 minutes in the presence of the ionophore before measurements of the cell [Mg] were made. The cell [Mg] was 11.57 ± 0.13 mmol(l.o.c.)$^{-1}$ and 12.73 ± 0.14 mmol(l.o.c.)$^{-1}$ (mean ± S.E.M.,n=3 measurements) for cells incubated in 145 mM and 5 mM Na respectively. Thus the maximum [Mg] attained by these cells after 2 hours incubation in 5 mM $[Na]_o$ and 5 mM $[Mg]_o$ is not a result of the cell [Mg] reaching electrochemical equilibrium.

If the plateau cell [Mg] in Figure 4.4. represents Mg equilibrium through Na-Mg exchange then the cell [Mg] at equilibrium will depend on the stoichiometry of exchange. If 1 Na is exchanged for 1 Mg (n=1) then Equation 3.4 predicts that Mg would be at equilibrium (under the conditions for measuring Mg influx) when

$[Mg^{2+}]_i$ is 203 mM. Such a $[Mg^{2+}]_i$ is unattainable for the cells. Increasing the stoichiometry of Na-Mg exchange to 2:1 or 3:1 increases the calculated value for cell [Mg] at equilibrium to the absurdly high values of 3920 and 75572 mM respectively.

These values were calculated assuming that cell [Na] remained constant throughout the incubation. However, this is not the case. In the experiment shown in Figure 4.4, cell [Na] fell to 40 $mmol(l.o.c.)^{-1}$ (57 mM) after 2 hours incubation. Using this value for the cell [Na] in Equation 3.4 predicts that at equilibrium $[Mg^{2+}]_i$ is 83mM, 650 mM and 5100 mM when Na-Mg exchange stoichiometry is assumed to be 1:1, 2:1 and 3:1 respectively. Thus even taking into consideration the reduction of cell [Na] during the incubation cannot account for the plateau value of cell [Mg] by influx mediated by Na-Mg exchange.

The distribution of Mg at equilibrium either through a channel or Na-Mg exchange will be affected by the membrane potential. In the time-dependence experiments the cells are incubated in media with a low-[Na] and a high-[Mg] for quite long periods. Such treatment may cause perturbations in the membrane potential. To allow cell [Mg] to equilibrate at 6.23 $mmol(l.o.c.)^{-1}$, Equation 3.4 predicts that the membrane potential would have to change to +86 mV if transport was through a 1:1 Na-Mg exchange. For cell [Mg] to equilibrate at 6.23 $mmol(l.o.c.)^{-1}$ through a channel, the Nernst equation predicts that the membrane potential would have to change to +11 mV. Both of

these calculations require that an estimate of the $[Mg^{2+}]_i$ from the total cell [Mg] be made using the Mg-buffering curve for ferret red cells (Figure 2.12). The membrane potential was not measured in these experiments but it has been measured under a number of different conditions in separate experiments. For example, in Na-free media the membrane potential hyperpolarises by only a few millivolts. In Na-free media with SITS the membrane potential fell to 0 mV. No larger changes in the membrane potential were measured under a variety of incubation conditions. Thus changes in the membrane potential, sufficient to allow equilibrium through 1:1 Na-Mg exchange or a channel, are unlikely.

The plateau level of cell [Mg] in Figure 4.4 may be the result of changes in the general Mg permeability of the membrane. An initial increase in the Mg permeability would be followed, after 2 hours incubation, by a reduction in the Mg permeability. Changes in the membrane permeability to Mg would be most readily assessed using the Mg isotope ^{28}Mg. Unfortunately this isotope is not available in this laboratory and it was not possible to directly measure the time course of changes in the cell Mg permeability.

Alternatively, the plateau concentration of cell [Mg] after 2 hours in 5 mM Na and 5 mM Mg may be the result of Mg influx and Mg efflux operating at a steady state. It is difficult to determine what effects the incubation conditions have on the kinetics of Mg efflux and Mg influx. For example, $[Mg]_o$ may inhibit the

movement of Mg down the electrochemical gradient into the cell and $[Mg^{2+}]_i$ may stimulate the active transport of Mg out of the cell.

The plateau value of cell [Mg] in Figure 4.4 may also be the result of several different factors acting simultaneously. The conditions in this experiment are set to increase Mg influx by reversing Na-Mg exchange. If ferret red cells have a heterogeneous capacity for Na-Mg exchange then different cells within the population will take up Mg at different rates. The shape of the curve in Figure 4.4 suggests that increasing $[Mg^{2+}]_i$ stimulates Mg influx (perhaps by opening Mg channels). An increase in the Mg permeability will cause a large influx of Mg as the experimental conditions have created a large inward Mg gradient. This model is further complicated by the observation that ferret red cells are very fragile when loaded to high cell [Mg]. Thus as $[Mg^{2+}]_i$ increases, and cells are recruited into the high Mg permeability group, the large increase in $[Mg^{2+}]_i$ may cause the cells to lyse. This model predicts that the plateau value for cell [Mg] in Figure 4.4 is the result of a difference in the rate at which cells can take up Mg through Na-Mg exchange, an increase in Mg permeability following a rise in $[Mg^{2+}]_i$ (occurring at different times in different fractions of cells) and the lysis of cells with a high capacity for Na-Mg exchange which load to high levels of $[Mg^{2+}]_i$ very quickly.

Measurement of Mg influx.

To investigate some of the properties of Mg influx a standard protocol for the measurement of these fluxes was devised. Mg influx was usually measured as a change in the cell [Mg] within 40 minutes of the start of incubation. This ensured that Mg influx was independent of large changes in cell [Na], cell [K] and cell volume and that increases in cell [Mg] were reasonably linear with time.

Mg influx from a medium containing 145 mM Na and 5 mM Mg was 0.15 ± 0.03 $mmol(l.o.c.)^{-1}h^{-1}$ (mean ± S.E.M, n=16 ferrets). Although quite small, Mg influx from media containing 5 mM Mg and 145 mM Na is very reproducible between independent experiments using cells from different ferrets. The magnitude of these fluxes was not affected by the sex or strain of the donor or the length of time for which the cells were stored.

The Mg influx when the medium contains 5 mM Na and 5 mM Mg showed a greater degree of variation. The mean Mg influx was 1.50 ± 0.21 $mmol(l.o.c.)^{-1}h^{-1}$ (mean ± S.E.M., n=16 ferrets, in the same experiments as for influx measured in 145 mM Na and 5 mM Mg). The large standard error reflects the wide distribution in the magnitude of Mg influx (range was 0.55 - 3.55 $mmol(l.o.c.)^{-1}h^{-1}$). Measurements of Mg influx in individual experiments were very reproducible. However there was considerable variation in the magnitude of fluxes measured in cells from different animals. The

magnitude of influx could not be correlated with the sex or strain of the donor. The magnitude of the influx also varied when measured in cells from one animal but on different days after cell collection. There was no correlation between storage time and magnitude of influx. Although cells lose ATP in storage (Figure 2.2) this was not the factor affecting influx. In a separate control experiment the Mg influx was measured in cells from storage (cell [ATP] was 0.27 $mmol(l.o.c.)^{-1}$ and influx was 0.73 ± 0.08 $mmol(l.o.c.)^{-1}h^{-1}$, mean ± S.E.M., n=3 measurements of influx). After a 1 hour incubation in FBM containing 11 mM glucose and 1 mM phosphate the cell [ATP] had risen to 0.70 $mmol(l.o.c.)^{-1}$ and the influx was 0.92 ± 0.02 $mmol(l.o.c.)^{-1}h^{-1}$).

The effects of some transport inhibitors, metabolic inhibitors and sulfhydryl reagents on Mg influx.

The effects of some transport inhibitors on net Mg uptake from a medium containing 5 mM Na and 5 mM Mg are shown in Table 4.1 (i). Each group represents experiments performed on the same day using cells from the same animal. Due to the variation in the size of the control fluxes, each flux is given as a percentage of the control flux in its group. Table 4.1 (ii) shows the effects of some metabolic inhibitors and sulfhydryl reagents on Mg influx. Data are given in the same format as Table 4.1 (i).

Legend to Table 4.1.

The effect of some transport inhibitors (i) and metabolic inhibitors and sulfhydryl reagents (ii) on Mg influx. Cells were incubated in media containing (mM); NaCl, 5; choline chloride, 140; KOH, 5; HEPES, 8; glucose, 11; EGTA, 0.05; $MgCl_2$, 5 and the reagents shown. In all groups (except B and D) 0.1 mM bumetanide was added to the media (including controls). In Group G cells were preincubated (for 30 minutes) in media containing either PCMBS or L-cysteine. (*PCMBS + L-cysteine) indicates that an incubation in a medium containing PCMBS was followed by an incubation in a medium containing L-cysteine. Mg influx was measured as a change in the cell [Mg] within 40 minutes of the cells being added to the medium. Data show the mean of 3 separate measurements of influx in 1 experiment with S.E.M. The groups represent experiments using cells from different ferrets and show the mean influx with the control flux for that group. The mean influx for each condition is also given as a percentage of the appropriate control.

Table 4.1. (i).

Inhibitor	Mg influx ($mmol(l.o.c.)^{-1}h^{-1}$) Mean ± S.E.M.	% of control flux
Group A		
Control	2.50 ± 0.05	100 ± 2
Quinidine (0.5 mM)	0.56 ± 0.02	22 ± 1
Imipramine (0.5 mM)	0.47 ± 0.06	19 ± 2
Amiloride (1 mM)	0.55 ± 0.07	22 ± 3
Group B		
Control	3.55 ± 0.14	100 ± 4
Ouabain (0.5 mM)	3.57 ± 0.23	101 ± 7
SITS (0.1 mM)	3.53 ± 0.22	99 ± 6
Group C		
Control	0.94 ± 0.02	100 ± 2
Vanadate (0.05 mM)	1.37 ± 0.05	146 ± 5
Vanadate (0.20 mM)	2.78 ± 0.05	296 ± 5
Group D		
Control	1.30 ± 0.05	100 ± 4
Bumetanide (0.1 mM)	1.34 ± 0.05	103 ± 4
Group E		
Control	3.55 ± 0.14	100 ± 4
Glibenclamide (5 μM)	3.57 ± 0.09	101 ± 3

Table 4.1. (ii).

Reagent	Mg influx (mmol(l.o.c.)$^{-1}h^{-1}$) Mean ± S.E.M.	% of control flux
Group F		
Control	2.25 ± 0.13	100 ± 6
NEM (1 mM)	0.79 ± 0.01	35 ± 2
Group G		
Control	1.07 ± 0.04	100 ± 4
*PCMBS (50 μM)	1.11 ± 0.02	104 ± 2
*L-cysteine (4 mM)	1.83 ± 0.12	171 ± 11
*PCMBS + L-cysteine	2.11 ± 0.05	197 ± 5
Group H		
Control	0.73 ± 0.08	100 ± 11
Okadaic acid (10^{-6} M)	0.95 ± 0.09	130 ± 8
Group I		
Control	1.14 ± 0.05	100 ± 4
Phorbol ester (1 μM)	1.09 ± 0.19	96 ± 17
Calphostin C (1 μM)	0.68 ± 0.21	60 ± 18

0.1 mM bumetanide and 0.5 mM ouabain had no effect on Mg influx. 1 mM amiloride, 0.5 mM quinidine and 0.5 mM imipramine all inhibited Mg influx with a similar efficacy. 5 μM glibenclamide, an inhibitor of ATP-dependent K channels (Schmid-Antomarchi *et al*, 1987) had no effect on Mg influx.

Interestingly SITS, which stimulated Mg efflux, had no effect on Mg influx. Also vanadate, which had no effect on Mg efflux, stimulated Mg influx. The effect of vanadate on Mg influx was dose-dependent.

The sulfhydryl reagent NEM (*N*-ethylmaleimide), which stimulates passive K transport in red cells of a number of different species (Wiater and Dunham, 1983), inhibited Mg influx in ferret red cells.

In other studies PCMBS (*p*-chloromercuribenzene -sulphonate) has been used to temporarily increase the red cells permeability to Na and Mg (Féray and Garay, 1986: Lüdi and Schatzmann, 1987). The effects of PCMBS are usually reversed by incubating the cells in a medium containing L-cysteine. A 30 minute pre-incubation in a medium with 50 μM PCMBS had no effect on Mg influx in ferret red cells (Group G). However a pre-incubation in a medium with 4 mM L-cysteine increased Mg influx considerably. A 30 minute pre-incubation in media with PCMBS followed by an incubation in media containing L-cysteine similarly increased Mg influx.

Okadaic acid, a potent inhibitor of protein phosphatases 1 and 2A (Cohen *et al*, 1990) stimulated Mg influx (group H). Phorbol ester (4ß-phorbol 12ß-

12ß-myristate 13α-acetate), an activator of protein kinase C (Nishizuka, 1984) which stimulates Mg influx into S49 lymphoma cells (Grubbs and Maguire, 1986) had no effect on Mg influx (Group I). Calphostin C, a potent and specific inhibitor of protein kinase C (Kobayashi *et al*, 1989) inhibited Mg influx (Group I).

The results of Table 4.1 (ii) suggest that although protein phosphatases and kinases may be involved in Mg transport, they are not the key regulators of Mg transport in ferret red cells.

As well as the results shown in Table 4.1 (i) and (ii), the effect of some of these reagents on Mg influx was also measured in media containing 145 mM Na and 5 mM Mg. The control fluxes under these conditions were (mmol(l.o.c.)$^{-1}$h^{-1}), Group A; 0.15, Group B; 0.16, Group D; 0.16, Group E; 0.23, Group F; 0.21, and Group G; 0.17. Only quinidine and NEM had any effect on Mg influx in 145 mM Na and 5 mM Mg. Mg influx in media containing 0.5 mM quinidine was 0.01 ± 0.03 mmol(l.o.c.)$^{-1}$h^{-1} (control group A) and in media containing 1mM NEM it was 0.44 ± 0.08 mmol(l.o.c)$^{-1}$h^{-1}. (control group F). Influx was measured as the mean of 3 independent determinations of flux and is given with the S.E.M.

The dose-dependent inhibition of Mg influx by amiloride.

The dose dependent effects of amiloride on Mg influx are shown in Figure 4.5. The control flux in

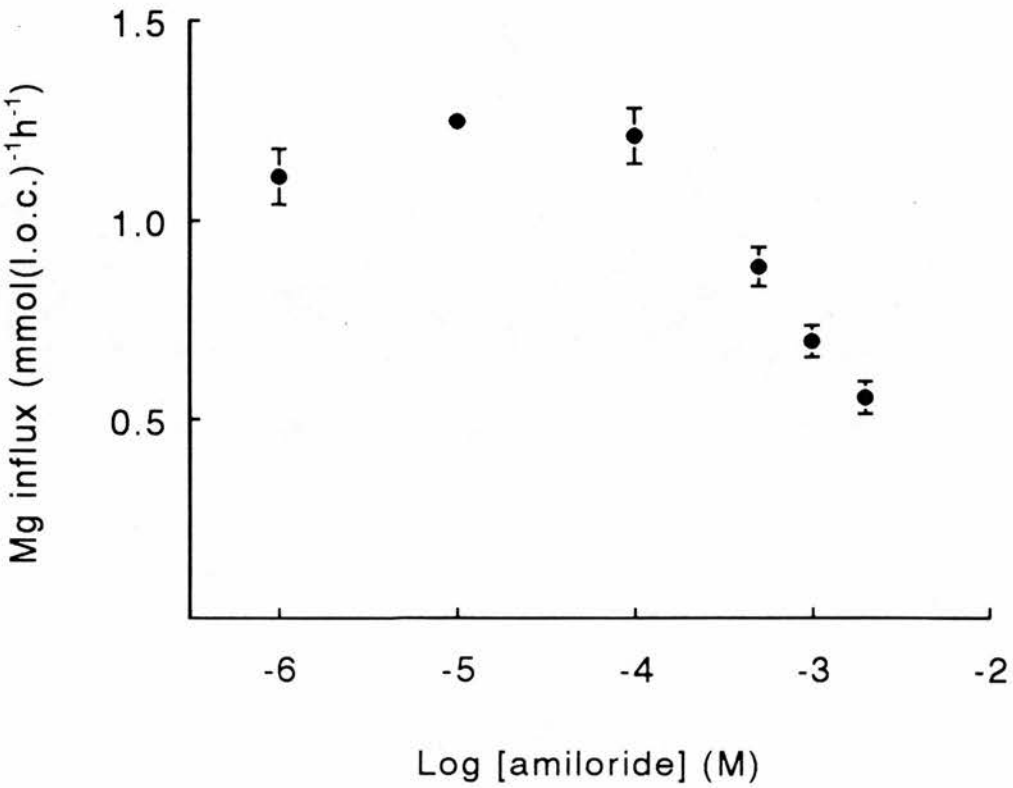

Figure 4.5.

Mg influx as a function of amiloride concentration. The media contained (mM); NaCl, 5; choline chloride, 140; KOH, 5; HEPES, 8; glucose, 11; bumetanide, 0.1; $MgCl_2$, 5 and the amiloride concentrations shown. Influx was measured as a change in the cell [Mg] (corrected for cell lysis) at 10 and 40 minutes after the start of 3 separate incubations in 1 experiment. Points show the mean influx ± S.E.M. where larger than point size. The control flux (no amiloride added) was 1.18 ± 0.01 mmol(l.o.c.)$^{-1}h^{-1}$.

this experiment was 1.18 mmol(l.o.c.)$^{-1}h^{-1}$. Thus, at concentrations below 0.1 mM, amiloride slightly stimulated Mg influx. Amiloride concentrations above 0.1 mM inhibited Mg influx. When the amiloride concentration was increased to above 2 mM there was an apparent stimulation in Mg influx and also an increase in the rate of cell lysis. These properties are very similar to the dose-dependent effects of amiloride on Mg efflux (Figures 3.9 and 3.10). As with the data on Mg efflux it was not possible to resolve the effects of amiloride at concentrations above 2 mM due to the large amount of cell lysis under these conditions. The K_i for the inhibition of Mg influx by amiloride was estimated as 1.3 mM, if it is assumed that all of the Mg influx is inhibited by amiloride, or 0.5 mM if only 60% of Mg influx is sensitive to amiloride.

Substitution of various groups on the amiloride molecule has led to the development of a series of amiloride analogues with varying specificities for different routes of Na movement (Simchowitz and Cragoe Jr., 1986). Three of these amiloride analogues were tested for possible effects on Mg uptake. Benzamil hydrochloride and amiloride 5-(N,N,-hexamethylene) had no effect on Mg influx. Amiloride-HCl-(N,N)-dimethyl was only slightly more effective at inhibiting Mg influx than the unsubstituted amiloride but was not as potent an inhibitor of Mg influx as imipramine.

The ATP dependence of Mg influx.

Cell [ATP] is reduced when red cells are incubated in a medium in which glucose has been replaced with 2-deoxyglucose. The effects, on Mg influx in ferret red cells, of reducing cell [ATP] by this method are shown in Figure 4.6. Ferret red cells were incubated in media containing either 11 mM glucose (Fed cells) or 11 mM 2-deoxyglucose (Depleted cells). The cell [ATP] in the fed cells was 0.61 mmol(l.o.c.)$^{-1}$ and after 3 hours in the depletion medium the cell [ATP] had fallen to 0.02 mmol(l.o.c.)$^{-1}$. Mg influx was measured in media containing 145 mM Na and 5 mM Mg (filled bars) and also in media containing 5 mM Na and 5 mM Mg (hatched bars). Mg influx measured with either 145 mM Na or 5 mM Na was reduced following depletion of cell [ATP].

Figure 4.7 shows another experiment where Mg influx was measured following the depletion of cell [ATP]. The cell [ATP] in the fed cells was 0.63 mmol(l.o.c.)$^{-1}$. After 1 hour in 11 mM 2-deoxyglucose the cell [ATP] had fallen to 0.08 mmol(l.o.c.)$^{-1}$. After another 2 hours in the depletion medium the cell [ATP] was 0.03 mmol(l.o.c.)$^{-1}$. Depletion of cell [ATP] inhibited the Mg influx in media containing 5 mM Mg and either 145 mM Na (filled bars) or 5 mM Na (hatched bars).

Figure 4.7 is shown to highlight the differences in the magnitude of Mg influx measured in 5 mM Na and 5 mM Mg in fed cells. In Figure 4.6 this influx is 0.77

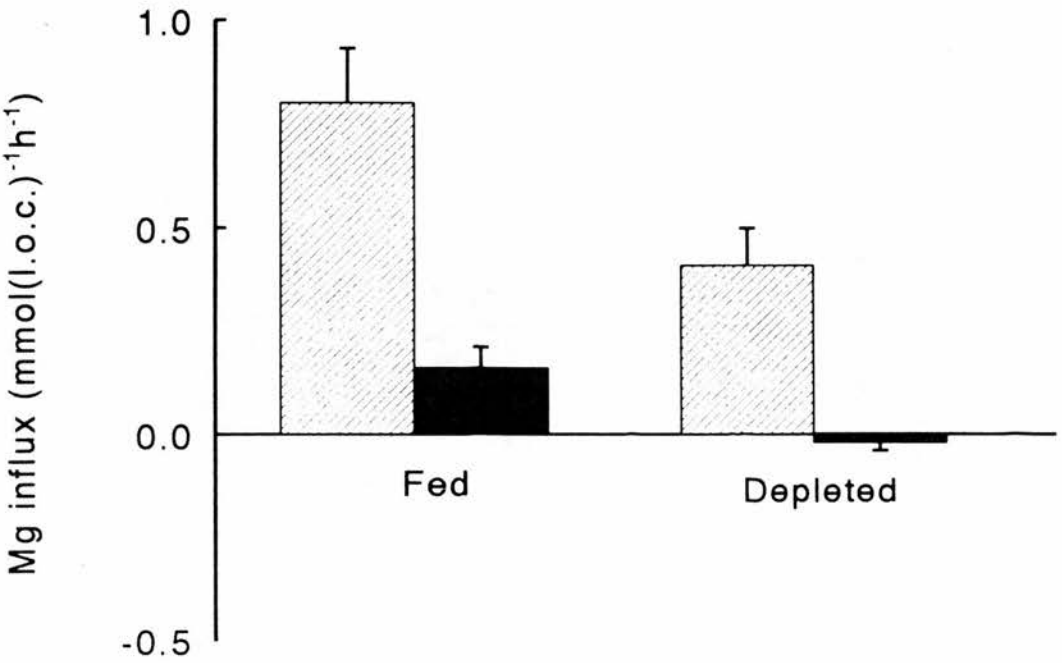

Figure 4.6.

The ATP dependence of Mg influx. Cells were incubated at 38 °C in FBM containing 0.05 mM EGTA and 11 mM glucose for 1 hour (Fed cells) or 11 mM 2-deoxyglucose for 3 hours (Depleted cells). Cells were transferred to a medium containing (mM); EGTA, 0.05; bumetanide, 0.1; $MgCl_2$, 5; KOH, 5; HEPES, 8 and either 145 mM NaCl (filled bars) or 5 mM NaCl and 140 mM choline chloride (hatched bars). Influx was the change in cell [Mg] at 10 and 40 minutes after the start of 3 separate incubations in 1 experiment. Bars show mean influx ± S.E.M. The cell [ATP] (mmol(l.o.c.)$^{-1}$) was 0.61 (Fed cells) and 0.02 (Depleted cells).

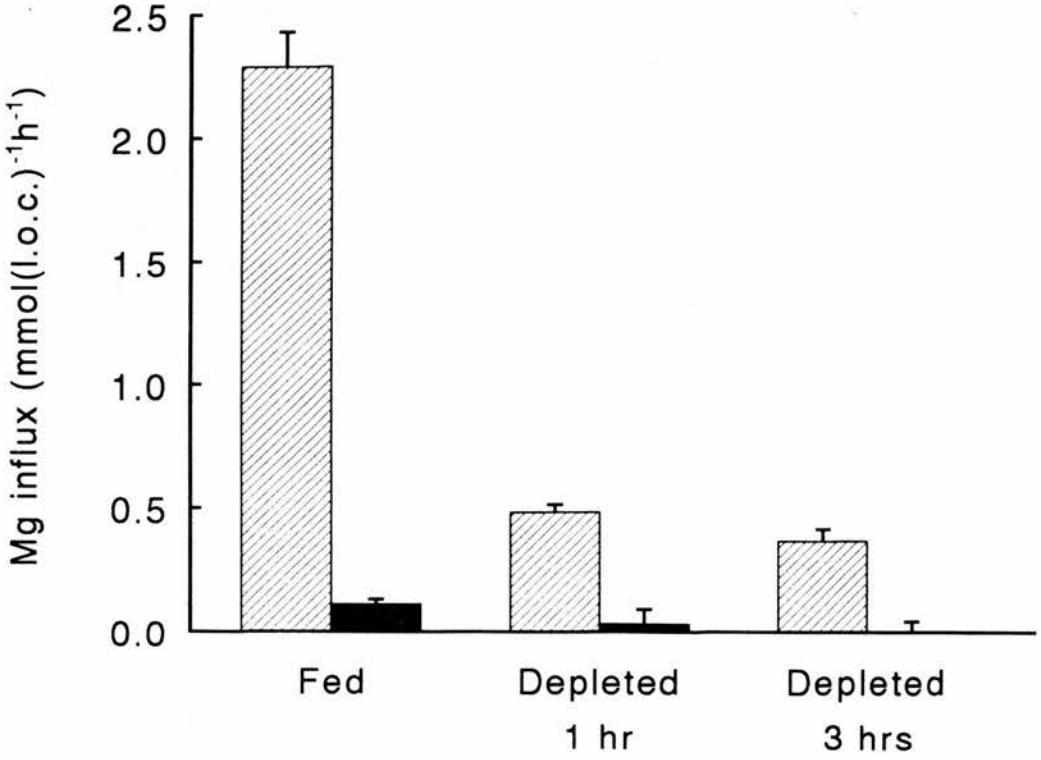

Figure 4.7.

The ATP dependence of Mg influx. Influx was measured in cells taken directly from storage in fridge at 5°C (Fed cells) or in cells which had been incubated in FBM with 11 mM 2-deoxyglucose for 1 or 3 hours (Depleted cells). Influx was measured as a change in cell [Mg] at 10 and 40 minutes after the start of 3 separate incubations (in media as described in legend to Figure 4.6) in 1 experiment. The bars show the mean influx in 145 mM Na (filled bars) or 5 mM Na (hatched bars) ± S.E.M. The cell [ATP] (mmol(l.o.c.)$^{-1}$) was 0.63 (Fed cells), 0.08 (Depleted, 1 hour) and 0.03 (Depleted, 3 hours).

mmol(l.o.c.)$^{-1}h^{-1}$ and in Figure 4.7 it is 2.29 mmol(l.o.c.)$^{-1}h^{-1}$. Depletion of cell [ATP] reduced the influx in Figure 4.6 by 65% and the influx in Figure 4.7 by 84%.

Mg influx appears to be dependent on cell [ATP]. This is in striking contrast to the effects of the depletion of cell [ATP] on Mg efflux (Figure 3.5) This does not necessarily indicate that the influx and efflux of Mg require different supplies of metabolic energy. ATP may have a direct effect on Mg transport by stimulating Mg influx when cell [ATP] is high but reducing the Mg permeability of the cell when cell [ATP] is low.

ATP need not exert its influence on Na-Mg exchange but may regulate some other route for Mg transport. It has already been suggested that the conditions used for measuring Mg influx (low-$[Na]_o$ and high-$[Mg]_o$) may reveal another, high capacity, route for Mg movement (Figure 4.4). Cells which have a higher Mg permeability under these conditions are more sensitive to changes in cell [ATP] (compare Figures 4.6 and 4.7) suggesting that it is this other route which is regulated by cell [ATP]. There is some evidence that ion movement through channels can be regulated by phosphorylation (Levitan, 1985). An increase in cell [ATP] may increase the movement of Mg through membrane channels and depletion in cell [ATP] may reduce the membrane capacity for Mg transport through these channels.

5. The $[Mg^{2+}]_i$ dependence of Mg efflux.

To study the effects of $[Mg^{2+}]_i$ on Mg transport it is necessary to change the internal [Mg]. Other studies of Mg transport have increased the Mg permeability of cells by the use of chemical agents, most commonly the divalent cation ionophore A23187 or the mercurial PCMBS. The results shown in Chapter 4 have shown that ferret red cells take up Mg when incubated in a medium with a low [Na] and high [Mg] content. Using these results it has been possible to devise a protocol which allows ferret red cells to load with Mg without the use of chemical agents. In this protocol the cells are incubated in a medium with a low [Na] and a high [Mg]. They are then incubated in a medium with physiological [Na] and high [Mg] to allow the reestablishment of any Na lost during the initial incubation. A full protocol is described in Table 5.1. This chapter describes some experiments in which ferret red cells were loaded with Mg by (**1**) increasing the Mg permeability of the cells using A23187 or (**2**) reversing the direction of Na-Mg exchange. Comparison of the properties of Mg efflux from cells loaded using either method provides a control to test whether the main factor affecting Mg transport is $[Mg^{2+}]_i$ or some artifact of the loading technique.

Loading cells with Mg using A23187

A23187 allows the rapid equilibration of Mg across the cell membrane and the final cell [Mg] can be controlled by adjusting the external [Mg] in the presence of the ionophore (Figure 2.8). Loading cells using A23187 results in a uniform distribution of Mg throughout the cell and the cell population (Simonsen, Gomme and Lew, 1982). The major drawback with the use of A23187 is the difficulty in ensuring its complete removal from the cell membrane once Mg loading is complete. A23187 allows large movements of Mg across the membrane and any residual ionophore will add considerable error to the estimation of Mg fluxes through a transporter. It is therefore necessary to ensure that all the ionophore has been removed before measuring Mg fluxes. Removal of the ionophore requires several washing steps and is aided by adding BSA to the wash medium. The METHODS section describes the standard protocol used for loading ferret red cells with Mg and then washing away the ionophore.

A quantitative fluorimetric assay for residual A23187 in red cells has been described by Simonsen and Lew (1980). It has thus far not been possible to measure residual A23187 in ferret red cells using this assay. It may be that this assay is not sensitive enough to measure the small amount of A23187 remaining in the cells after the washing procedure.

Residual ionophore can also be assessed using a biological assay. Cells containing residual ionophore

incubated in medium with the Mg-chelator EDTA lose Mg at a high rate and the cell [Mg] falls below the control concentration. Cells which have not been exposed to A23187 lose little Mg when incubated in EDTA-containing medium. This was a very sensitive test for the effectiveness of washing out the ionophore and was used to develop the washing protocol described in the METHODS section. The efflux medium for cells loaded using A23187 always contained EDTA.

Ferret red cells were loaded using A23187 and an $[Mg]_o$ of 1 mM. Under these conditions the cell [Mg] increased to 5.18 ± 0.18 mmol(l.o.c.)$^{-1}$ (mean ± S.E.M.,n = 15 experiments) with values ranging from 4.0 to 6.2 mmol(l.o.c.)$^{-1}$. Each experiment used cells from a different donor. The initial cell [Mg] and concentration of internal Mg buffer varied slightly between experiments as did the experimental conditions during loading (for example, the haematocrit of the loading suspension, the stock [$MgCl_2$]). Despite these differences, the final cell [Mg] after loading was remarkably reproducible.

Loading with the ionophore resulted in no significant change in the concentration of other cell constituents. For example, in one experiment the cell [ATP] in control and loaded cells was 0.21 ± 0.01 and 0.25 ± 0.01 mmol(l.o.c.)$^{-1}$) respectively. The cell [Na] was 110 ± 2 and 108 ± 1 mmol(l.o.c.)$^{-1}$ (mean ± S.E.M., n = 3 measurements) in control and loaded cells respectively.

Mg buffering curves have been measured in groups

of cells which had been loaded using A23187. There was no difference in the buffering curves for these cells and the composite buffering curve for untreated unloaded ferret red cells (Figure 2.11). Thus any residual ionophore in these experiments does not contribute to the buffering of $[Mg^{2+}]_i$.

Mg efflux from Mg-loaded cells

Ferret red cells were loaded with Mg by incubation in FBM with 1 mM $MgCl_2$ and 5 μM A23187. The loaded cells were washed according to the protocol given in the METHODS section and were incubated in a medium containing Mg-EDTA (0.2 mM $MgCl_2$, 1 mM EDTA; $[[Mg^{2+}]_o \approx 3*10^{-7}M$). Figure 5.1 shows the changes in the cell [Mg] over 3 hours. The data in Figure 5.1 are fitted using an exponential function with a rate constant of $0.231h^{-1}$. Since the rate constant is low, the fall in cell [Mg] can also be fitted with a linear function over 3 hours which gives a rate of efflux of 0.38 $mmol(l.o.c.)^{-1}h^{-1}$. This is approximately 10 times the rate of Mg efflux from fresh ferret red cells. If the incubation had been allowed to proceed it would have taken approximately 5 hours for the cell [Mg] to return to the control concentration.

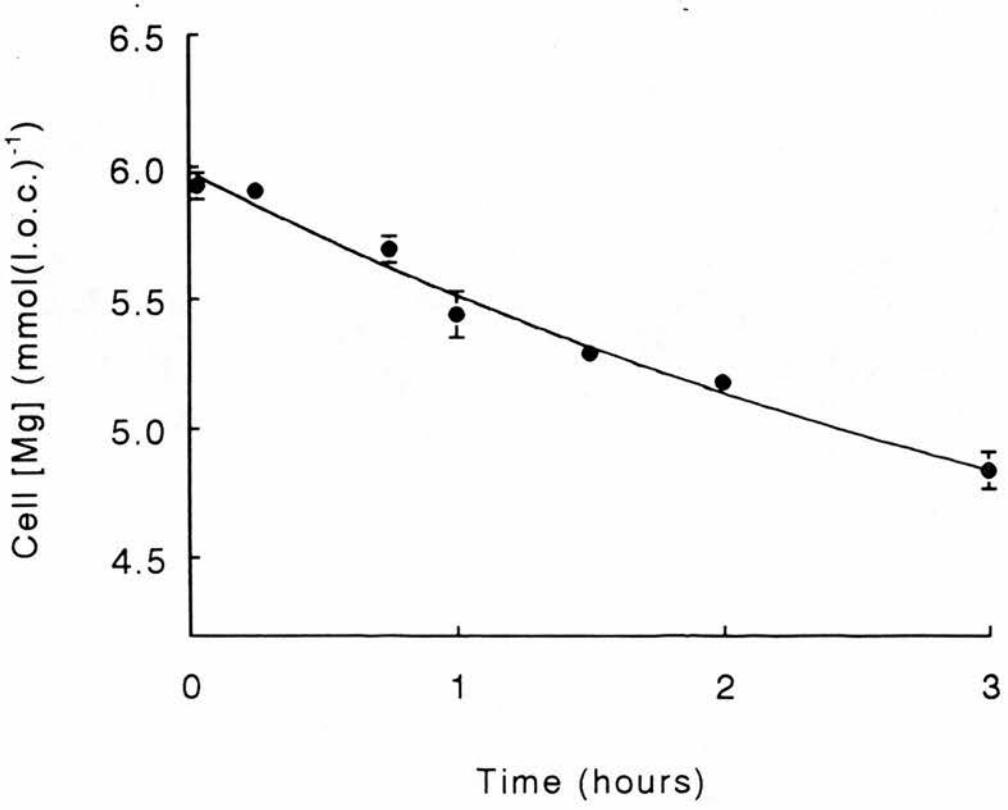

Figure 5.1.

Cell [Mg] as a function of time. Cells were loaded by incubation them in FBM containing 5 μM A23187 and 1 mM $MgCl_2$ (cell [Mg] = 5.73 mmol(l.o.c.)$^{-1}$). The ionophore was washed out using the protocol given in Table 2.2. Mg-loaded cells were incubated in FBM containing (mM); glucose, 11; Tris-EGTA, 0.05; $MgCl_2$, 0.2; EDTA, 1. Triplicate measurements of the cell [Mg] (corrected for cell lysis) were made at the time points indicated. Points show the mean of 3 measurements of cell [Mg] with S.E.M. if larger than point size. Line was drawn using an exponential function
(2.29 * exp(-0.23 * t) + 3.70).

Loading cells with Mg using A23187 and a range of $[Mg]_o$.

Ferret red cells were loaded with Mg by incubating them in FBM containing A23187 and a range of different $[Mg]_o$. When the cells were treated with the ionophore and an $[Mg]_o$ of between 0.3 and 2 mM, the final cell [Mg] was between 1.90 and 7.64 $mmol(l.o.c.)^{-1}$. The cells were washed according to the protocol in the METHODS section and suspended in a medium containing 0.2 mM $MgCl_2$ and 1 mM EDTA ($[Mg^{2+}]_o \approx 3*10^{-7}M$). Mg efflux was measured as a change in the cell [Mg] over 30 minutes and was corrected for cell lysis. The intracellular ionized [Mg] corresponding to the (total) cell [Mg] was obtained from a Mg buffering curve (a buffering curve was constructed for each batch of cells). Figure 5.2 shows Mg efflux as a function of intracellular ionized [Mg].

It is also possible to express the efflux shown in Figure 5.1 as a function of $[Mg^{2+}]_i$. The difference in the cell [Mg] between any 2 time points can be expressed as a flux per hour. If a Mg buffering curve is constructed for these cells it is possible to estimate the $[Mg^{2+}]_i$ corresponding to the mean cell [Mg] between these 2 time points. However the rate of efflux in Figure 5.1 is slow and the small difference in cell [Mg] between time points limited the resolution of changes in the efflux rate. For this set of data it was thought better to smooth the function mathematically. The data in Figure 5.1 was fitted by

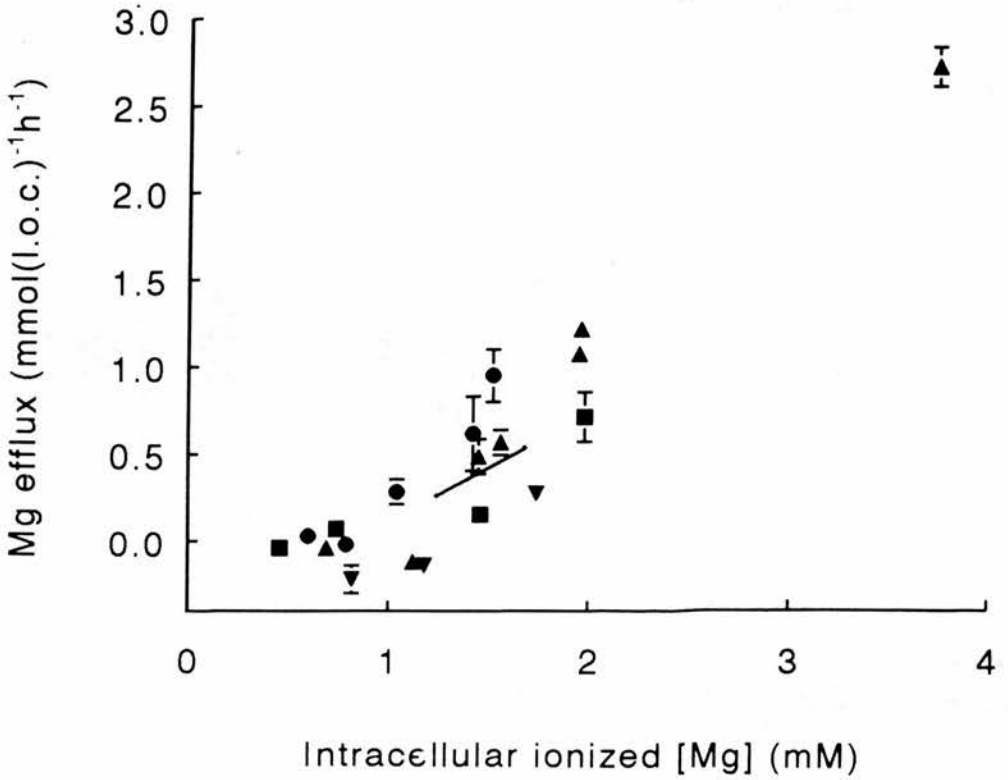

Figure 5.2.

Mg efflux as a function of intracellular ionized [Mg]. Cells were loaded with Mg by incubation in FBM with 5 μM A23187 and a range of $[Mg]_o$ (0.3-2 mM). The ionophore was washed out using the protocol given in Table 2.2. Mg-loaded cells were incubated in media as described for Figure 5.1. Mg efflux was a change in the cell [Mg] over 30 minutes in 4 separate experiments (shown by different symbols). Points show the mean of 3 determinations of efflux ± S.E.M. if larger than point size. Line shows the derivative of the exponential function fitted to the data of Figure 5.1.

an exponential function. The derivative of this function is the rate (or efflux) at every time point. The cell [Mg] at various time points was obtained from Figure 5.1 and the corresponding $[Mg^{2+}]_i$ measured from a Mg buffering curve. Transforming the data in this way gives the line shown in Figure 5.2. The line in Figure 5.2 is drawn over the range of $[Mg^{2+}]_i$ measured in the experiment of Figure 5.1.

Figure 5.2 shows that the line representing the data of Figure 5.1 is a reasonable fit of the data from experiments using either (A23187) loading technique even if extrapolated to higher concentrations of $[Mg^{2+}]_i$. This demonstrates that the relationship between Mg efflux and $[Mg^{2+}]_i$ can be obtained either from changes in cell [Mg] over long time periods or by loading to different starting [Mg] and measuring efflux over shorter time periods. Both these methods produce similar results. Loading with Mg using different $[Mg]_o$ has the advantage that a wider range of $[Mg^{2+}]_i$ can be investigated. A shorter incubation time also reduces the possibility of changes in the concentration of other cellular constituents which may affect Mg permeability.

The $[Na]_o$ dependence of Mg efflux from Mg-loaded cells

Cells were loaded using 1 mM $[Mg]_o$ and A23187. The cells were washed free of the ionophore as described in the METHODS section. The cells were then

incubated in media with different [Na] and 0.2 mM $MgCl_2$. Figure 5.3 shows that when $[Na]_o$ was 145 mM there was a net efflux of Mg from these cells. Reducing $[Na]_o$ inhibited Mg efflux and when $[Na]_o$ was approximately 70 mM the direction of Mg transport was changed. Below 70 mM $[Na]_o$ it was possible to measure net Mg influx. The $[Na]_o$ at which reversal occurs is based on the curve fit shown in Figure 5.3. Although the curve provides a good fit of the data, quite large changes in the curve fit parameters produced little change in the shape of the curve. The curve fit is not sensitive enough to accurately predict the binding constants for the transporter. However even when the data were fitted using a wide range of values for maximum efflux and uptake, the dissociation constant for Na was always low. This suggests that Mg influx involves a high affinity Na binding site.

Estimates of $[Mg^{2+}]_i$ were made from the measurements of the cell [Mg] and a Mg buffering curve. In both experiments shown in Figure 5.3 measurements of $[Mg^{2+}]_i$ and $[Mg]_o$ were made when the $[Na]_o$ was 10 mM. For the experiment shown as circles, $[Mg^{2+}]_i$ was 1.8 mM and $[Mg^{2+}]_o$ was 0.2 mM. In the experiment represented by squares, $[Mg^{2+}]_i$ was 2.0 mM and $[Mg^{2+}]_o$ was 0.2 mM. Thus in both experiments the influx of Mg occurred against a chemical gradient for Mg.

The membrane potential of these cells was not measured and thus the electrical gradient for the movement of Mg is not known. However for Mg to move passively into the cells down an electrical gradient

Legend to Figure 5.3

The $[Na]_o$ dependence of Mg efflux from Mg-loaded cells. Cells were loaded by incubation in FBM with 5 μM A23187 and 1 mM MgCl. The ionophore was washed out using the protocol given in Table 2.2. Loaded cells were incubated in (mM): KOH, 5; Tris-EGTA, 0.05; glucose, 11; HEPES, 7.4; bumetanide, 0.01; $MgCl_2$, 0.2 ; the initial NaCl concentration shown and sufficient choline chloride to maintain the sum [NaCl] + [choline chloride] = 145 mM. Mg influx was a change in cell [Mg] over 1 hour (corrected for cell lysis) in 2 separate experiments. Points show the mean of 3 separate measurements of influx with S.E.M. if larger than point size (circles) or the mean flux between triplicate measurements of cell [Mg] at the beginning and end of the time period (squares). Line was drawn assuming Michaelis-Menten kinetics (Na binds to an external Na site to inhibit Mg influx). The curve fit parameters are: maximum influx; 3 $mmol(l.o.c.)^{-1}h^{-1}$, maximum Mg efflux; 0.2 $mmol(l.o.c.)^{-1}h^{-1}$, dissociation constant; 4.5 mM. The initial cell [Mg] of the loaded cells was 4.85 (circles) and 5.70 (squares) $mmol(l.o.c.)^{-1}$.

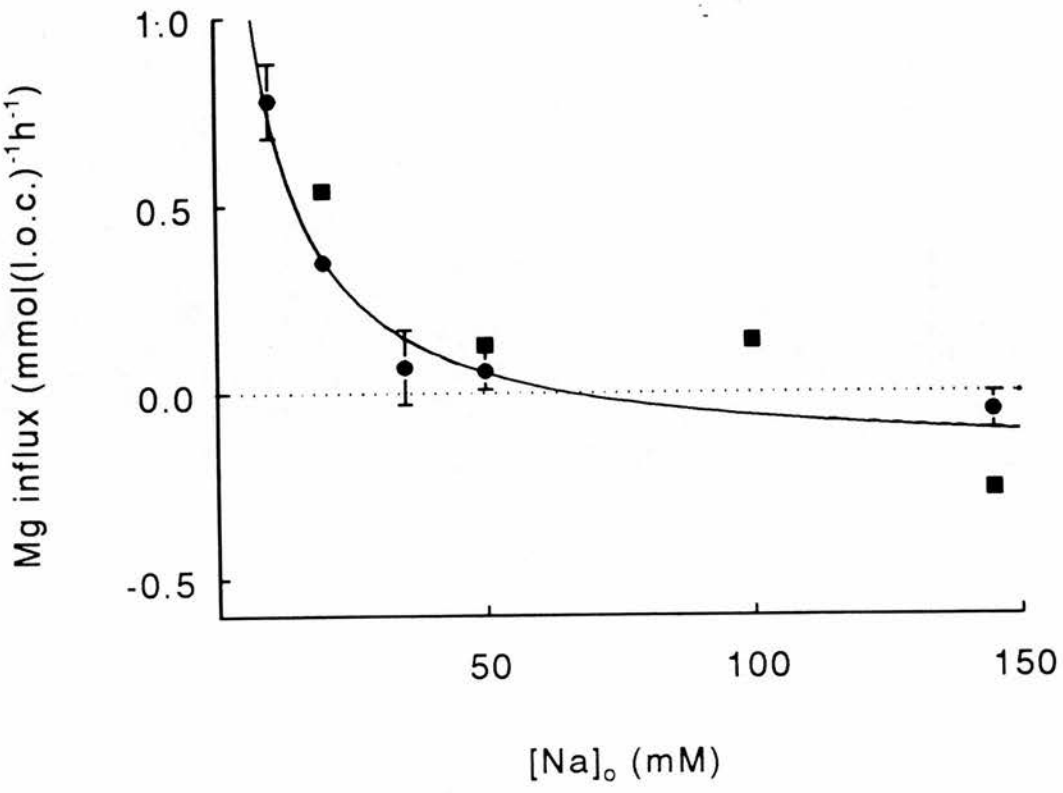

Figure 5.3.
The $[Na]_o$-dependence of Mg efflux from Mg-loaded cells.

the membrane potential would have to be -29 mV. The membrane potential of ferret red cells has been measured under a number of other extreme conditions but no hyperpolarisation of this magnitude has ever been measured. Indeed, prolonged incubation in media with low [Na] resulted in only a very small change in the membrane potential. It seems unlikely that the membrane potential would have changed sufficiently to account for the uptake of Mg at low $[Na]_o$ seen in Figure 5.3.

Effects of amiloride on Mg transport in Mg-loaded cells.

Cells were loaded with Mg by incubating them in a medium containing 1 mM [Mg] and A23187. After washing the cells, according to the protocol in Table 2.2, they were re-incubated in medium containing 0.2 mM $MgCl_2$ and either 145 or 20 mM [Na]. Changes in the cell [Mg] were measured over 30 minutes. The results of this experiment are shown in Figure 5.4. In 145 mM $[Na]_o$ an efflux of 0.29 $mmol(l.o.c.)^{-1}h^{-1}$ was measured. In 20 mM $[Na]_o$ this efflux was reversed and a net influx of Mg of 1.16 $mmol(l.o.c.)^{-1}h^{-1}$ was measured. The cell [Mg] was 5.65 $mmol(l.o.c.)^{-1}$ corresponding to $[Mg^{2+}]_i$ of 2 mM. This experiment provides further evidence for the reversal of net Mg transport (and movement against a chemical gradient) when $[Na]_o$ is reduced.

Figure 5.4 also shows the effect of adding 1 mM amiloride to the medium. Amiloride inhibited both the Mg efflux in 145 mM $[Na]_o$ and the net Mg influx in 20

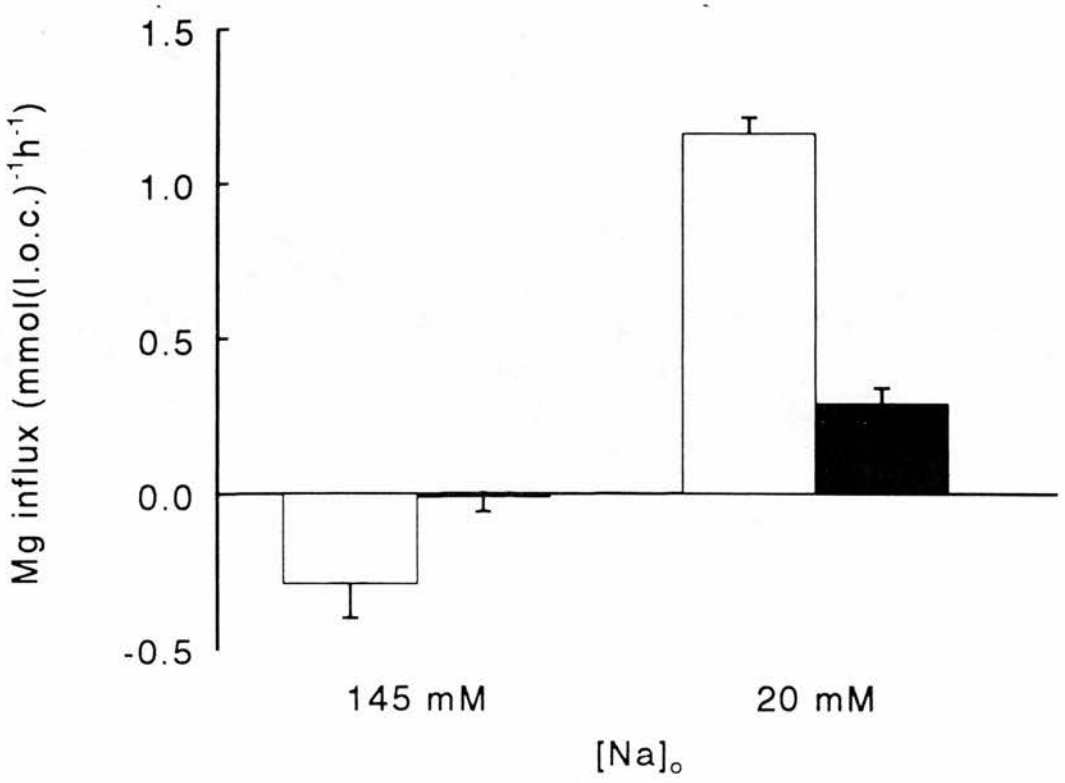

Figure 5.4.

$[Na]_o$ dependence of Mg influx. Cells were loaded (cell [Mg] = 5.65 mmol(l.o.c.)$^{-1}$) by incubation in FBM with 5 μM A23187 and 1 mM MgCl. Ionophore was washed out using the protocol given in Table 2.2. Loaded cells were incubated in (mM): KOH, 5; Tris-EGTA, 0.05; glucose, 11; HEPES, 7.4; bumetanide, 0.01; $MgCl_2$, 0.22 and either 145 mM NaCl or 20 mM NaCl and 125 mM choline chloride. Bars show the mean influx (corrected for cell lysis) over 30 minutes in 3 separate incubations. Filled bars show influx when media contained 1 mM amiloride. $[Mg]_o$ at the end of the incubation was 0.24mM in 145mM [Na] and 0.19mM in 20mM [Na].

mM $[Na]_o$. Amiloride inhibited Mg efflux by 97% and Mg influx by 75%. Thus in these cells nearly all Mg efflux and most of Mg influx occurs through an amiloride sensitive route.

The effect of reducing $[Mg^{2+}]_i$ on Mg influx.

Figure 5.5 shows the effects of removing most of the cell [Mg] on Mg influx. Figure 5.5 shows the result of 1 experiment where the influx of Mg (measured as a change in the cell [Mg]) was measured in media containing 5 mM Mg and either 145 mM Na (filled bars) or 5 mM Na (open bars). Mg uptake was measured in 3 groups of cells. In one group the cells had been incubated in FBM with 2 mM EDTA and 5 μM A23187 for 10 minutes. The ionophore had then been washed away. This treatment reduced the cell [Mg] to 0.14 $mmol(l.o.c.)^{-1}$. In the second group the cells were pretreated by incubating them in a medium containing 0.3 mM [Mg] and 5 μM A23187. Cell [Mg] in this group was 2.24 $mmol(l.o.c.)^{-1}$. In the third group influx was measured in cells which had not been incubated in media containing A23187 (cell [Mg] was 2.55 $mmol(l.o.c.)^{-1}$).

Figure 5.5 shows that, despite the large difference in the cell [Mg] of the EDTA treated cells and the control group, there was no difference in Mg influx from media with 145 mM $[Na]_o$ or 5 mM $[Na]_o$. Mg influx does not appear to be sensitive to the increase in the inward Mg gradient, generated by the reduction in cell [Mg] to approximately 5% of the control

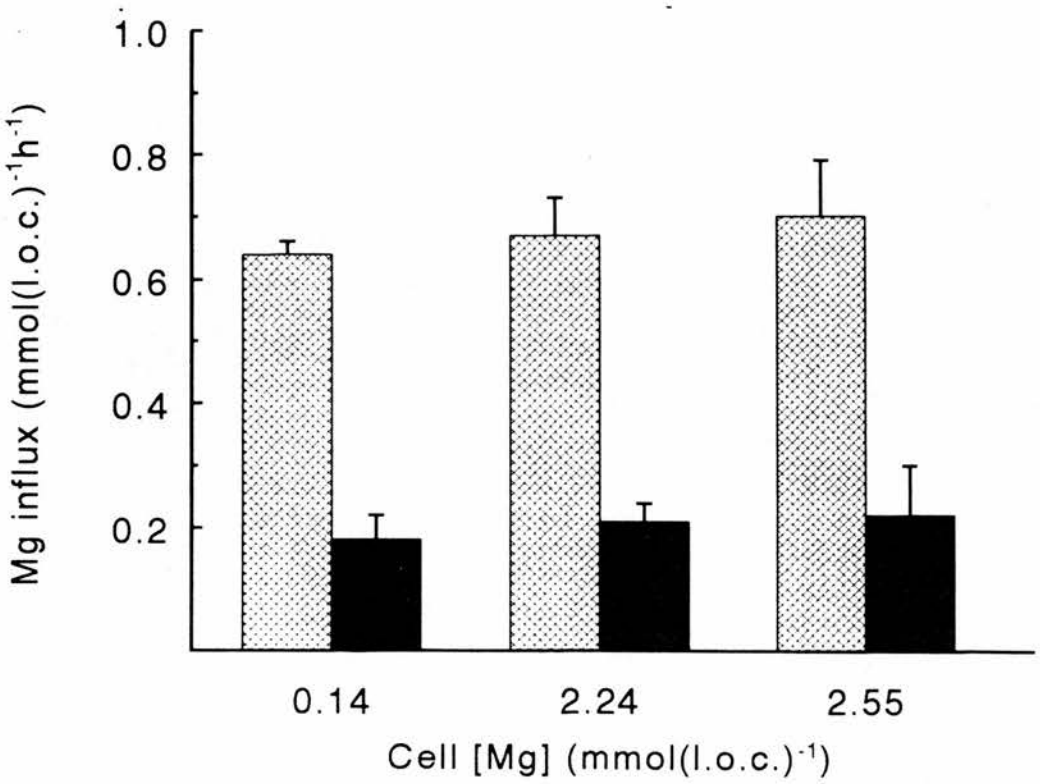

Figure 5.5.

Mg influx as a function of cell [Mg]. Cells were incubated in FBM with 5 μM A23187 and either 1 mM EDTA (cell [Mg] = 0.14) or 0.3 mM $MgCl_2$ (cell [Mg] = 2.24). Ionophore was washed out using the protocol given in Table 2.2. Cells were incubated in (mM) KOH, 5; Tris-EGTA, 0.05; glucose, 11; HEPES, 7.4; bumetanide, 0.01; $MgCl_2$, 0.22 and either 5 mM [Na]/140 mM choline (hatched bars) or 145 mM [Na] (solid bars). Influx was the change in cell [Mg] at 10 and 40 minutes after the start of 3 separate incubations. Bars show the mean influx ± S.E.M. Control group (cell [Mg] = 2.55) were not incubated in media containing A23187.

concentration. Neither does a reduction in cell [Mg] inhibit Mg influx. This does not rule out the possibility that Mg transport is dependent on internal Mg. The transporter may have a high affinity internal binding site for Mg.

An increase in Mg permeability following Mg loading by incubation in a media containing 5 mM Mg and 5 mM Na.

It has been shown (Chapter 4 and Figure 5.5) that cell [Mg] increases when ferret red cells are incubated in a medium containing 5 mM Na and 5 mM Mg. This property was exploited to enable the investigation of the effects of an elevated cell [Mg] on Mg transport in cells which had not been treated with chemical agents.

Figure 5.6 shows the results of an initial experiment, using the loading protocol devised from the Mg influx experiments, which confirmed that the Mg permeability of the cells was affected by increasing the cell [Mg].

Untreated cells (cell [Mg] = 2.30 mmol(l.o.c.)$^{-1}$) were incubated in media containing 145 mM NaCl and 5 mM $MgCl_2$. Mg influx over 30 minutes was 0.13 mmol(l.o.c.)$^{-1}h^{-1}$ (Flux **A**). This value agrees with values for Mg influx, measured under similar conditions (Chapter 4). The cells were then loaded to 3.27 mmol(l.o.c.)$^{-1}$ when incubated in a medium containing 5 mM [Mg] and 5 mM [Na] (LOAD). The loaded cells were then incubated in FBM and the cell [Mg] fell (EFFLUX).

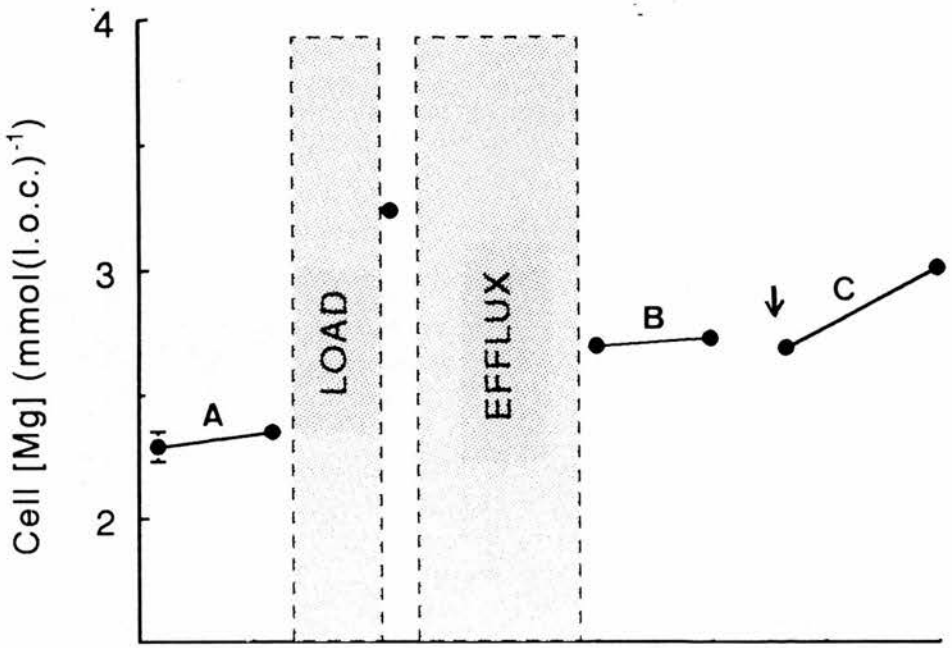

Figure 5.6.

Changes in Mg permeability after incubation in 5 mM $[Na]_o$ and 5 mM $[Mg]_o$. Cells were incubated in FBM with 5 mM Mg. Mg influx, over 30 minutes (Flux A), was 0.13 mmol(l.o.c.)$^{-1}h^{-1}$). The cells were then loaded with Mg by incubation in media containing 5 mM Mg and 5 mM Na (LOAD; protocol is given in Figure 5.7). Cells were then incubated in FBM for 1 hour (EFFLUX). Mg influx over the following 30 minutes (Flux B) was 0.05 mmol(l.o.c.)$^{-1}h^{-1}$. 5 mM Mg was then added to the medium (↓). The influx over the next 30 minutes (Flux C) was 0.63 mmol(l.o.c.)$^{-1}h^{-1}$.

The rate of efflux over the first hour was approximately 0.59 mmol(l.o.c.)$^{-1}$h^{-1}. After 60 minutes the flux rate was much reduced and, after a further 30 minutes incubation (Flux **B**; 0.05 mmol(l.o.c.)$^{-1}$h^{-1}), the cell [Mg] was 2.73 mmol(l.o.c.)$^{-1}$. 5 mM [$MgCl_2$] was added to the medium (↓). The influx of Mg over the next 30 minutes was 0.63 mmol(l.o.c.)$^{-1}$h^{-1} (Flux C). Thus a small change in the cell [Mg] (2.30 to 2.73 mmol(l.o.c.)$^{-1}$) resulted in a large change (x 5) in the rate of Mg influx.

A protocol for loading ferret red cells with Mg by incubation in a media with low-[Na] and high-[Mg].

A standard protocol for loading cells with Mg by incubation in a media with high-[Mg] and low-[Na] is shown in Figure 5.7. The protocol involves steps which allow the cell [Na] and [K] to be maintained.

The cells were incubated in a medium containing 5 mM NaCl and 5 mM $MgCl_2$. $[Na]_o$ was substituted with choline chloride and the medium also contained bumetanide to reduce the loss of cell [Na] (and [K]) through the Na-K-Cl cotransporter. Loading was allowed to proceed for 1 hour. Time dependent uptake studies (Figure 4.1) have shown that increasing the incubation time does not result in a further increase in the cell [Mg]. The cells were then washed and resuspended in FBM containing 5 mM $MgCl_2$. The cells were incubated in this (RECOVERY) medium for 30 minutes. The purpose of

Legend to Figure 5.7.

Protocol for loading cells with Mg by incubation in a medium containing 5 mM Na and 5 mM Mg. After 1 hour incubation in LOAD medium, the cells were washed and resuspended in RECOVERY medium. Changes in the cell [Mg], [Na] and [K] following incubation in LOAD and RECOVERY media are given in Table 5.1. The final washes reduced $[Mg]_o$. The haematocrit was approximately 10% in the incubations and washes used at least 10 volumes of medium.

Figure 5.7.

Protocol for Mg-loading by incubation of cells in low-[Na]/high-[Mg] media.

1. Cells washed x1 and suspended in LOAD media;

5 mM NaCl
140 mM choline chloride
7 mM HEPES containing 5 mM K^+
11 mM glucose
5 mM $MgCl_2$
0.1 mM bumetanide
0.05 mM EGTA

2. Cells incubated in LOAD medium at 38 °C for 1 hour.

3. Cells washed x1 and suspended in RECOVERY media;

FBM:(mM) NaCl, 145; KCl, 5; Na-HEPES, 10.
11 mM glucose
5 mM $MgCl_2$
0.05 mM EGTA

4. Cells incubated in RECOVERY medium at 38 °C for 30 minutes.

5. Cells washed three times in ice-cold FBM supplemented with

Wash 1. 1 mM EDTA
Wash 2. 0.05 mM EGTA
Wash 3. 0.05 mM EGTA.

this incubation was to allow some time for the re-equilibration of Na and other cellular constituents. The cells were then washed twice in FBM. The first wash contained 1 mM EDTA to aid the removal of $[Mg]_o$, especially any Mg which may be sticking to the cells. The second wash contained only EGTA and removed the EDTA from the medium.

The cell [Mg], [Na], [K] and water content were measured at different stages of the loading procedure. The mean values from 2 separate experiments are given in Table 5.1. The results from Table 5.1 show that some [Na] and [K] are lost from cells during the loading step. Incubation in the recovery medium allowed some re-uptake of [Na]. Overall there were no large changes in cell [Na], [K] or water during the loading procedure.

Figure 5.8 shows a buffering curve for cells which have been loaded using this protocol. In this experiment there was only a slight increase in the Mg buffering capacity of cells which had been incubated in media with low-[Na] and high-[Mg]. This was probably due to an increase in the cell [ATP] (the LOAD medium contained glucose).

After 1 hour in LOAD medium the cell [Mg] content had increased. Some Mg was lost during the RECOVERY and washing stages of the protocol. In 12 separate experiments the cell [Mg] increased to 4.03 ± 0.18 $mmol(l.o.c.)^{-1}$. This represented an increase in the total cell [Mg] of 53 ± 6%. This percentage increase was independent of the initial cell [Mg]. After 1 hour

Table 5.1.

Changes in cell [Mg], [Na], [K] and cell water during incubation in low-[Na]/high[Mg] media.

	1	2	3	
[Mg]	2.55	3.72	3.58	mmol(l.o.c.)$^{-1}$
[Na]	104	89	95	mmol(l.o.c.)$^{-1}$
[K]	5.9	5.7	5.7	mmol(l.o.c.)$^{-1}$
Cell Water	65.20		63.64	%

1. measurements made in control (unloaded) cells.
2. measurements after incubation in LOAD medium.
3. measurements after incubation in RECOVERY medium.

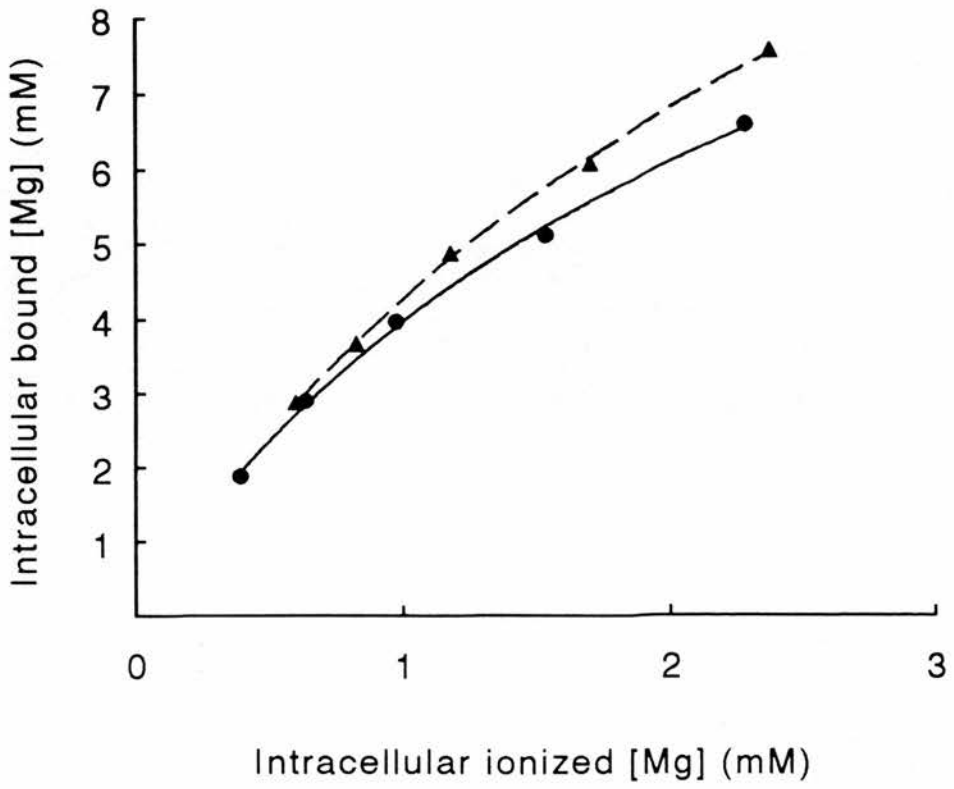

Figure 5.8.

Mg buffering in control and Mg-loaded cells. Mg buffering was measured using the protocol described in METHODS. Intracellular bound [Mg] is shown as a function of intracellular ionized [Mg] in control, untreated cells (circles) and Mg-loaded cells from the same donor (triangles). Cells were loaded using the protocol given in Figure 5.7. Cell [ATP] was 0.32 and 0.27 mmol(l.o.c.)$^{-1}$ for control and Mg-loaded cells respectively. The lines were drawn using Michaelis-Menten kinetics assuming 1 ligand binding with capacities (mM) and dissociation constants (mM): 13 and 2, (control); 16 and 3 (Mg-loaded) respectively.

in the LOAD medium the cell [Mg] had reached a maximum. This maximum load does not represent the equilibrium of Mg across the membrane. Possible reasons for this limit to loading have been discussed in Chapter 4.

Incubation in low-[Na] and high-[Mg] allows ferret red cells to be loaded with Mg to a reproducible level. However the range of $[Mg^{2+}]_i$ which can be studied using this technique is quite narrow.

Mg efflux from Mg-loaded cells.

Cells loaded using the protocol given in Figure 5.7 were incubated in medium containing 0.2 mM $MgCl_2$ and 1 mM EDTA ($[Mg^{2+}]_o \approx 3*10^{-7}$M). Changes in the cell [Mg] were measured over time. Figures 5.9 and 5.10 show the results of two typical experiments. The data are fitted with an exponential function. In 6 experiments the rate constant for efflux, given by the fitted exponential, was 2.35 ± 0.26 h^{-1} (mean ± S.E.M., n=6). The rate of efflux from these cells is approximately 10 times that from cells loaded with Mg using the ionophore method.

The changes in the cell [Mg] over time can be manipulated to show the relationship between efflux rate and $[Mg^{2+}]_i$ (Figure 5.2). For cells loaded with Mg using the ionophore, Mg efflux was still quite slow and the changes in the efflux were more accurately determined by the derivative of the fitted exponential function. For the cells loaded by incubation in low-[Na] and high-[Mg] the rate of efflux is much

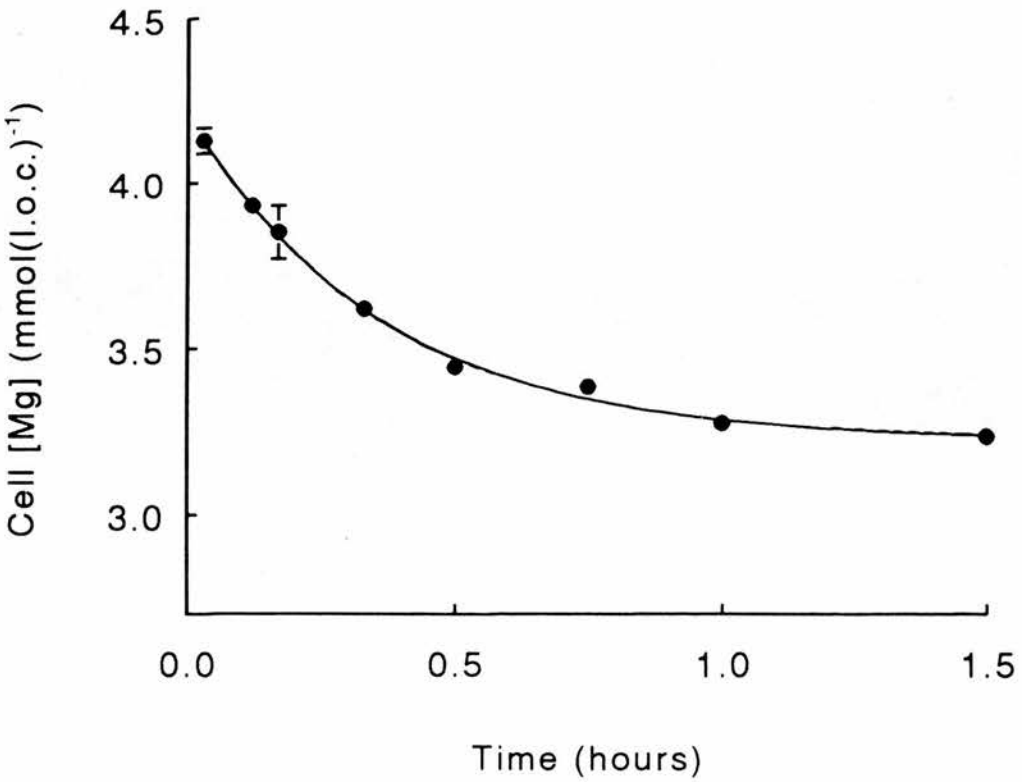

Figure 5.9.
Cell [Mg] as a function of time. Cells were loaded with Mg using the protocol given in Figure 5.7. Mg-loaded cells were incubated in media containing (mM): NaCl, 139; NaOH, 6; KCl, 5; HEPES, 20; glucose, 11; Tris-EGTA, 0.05; $MgCl_2$, 0.2; EDTA, 1. Points show the mean of 3 measurements of cell [Mg] (corrected for cell lysis), in 1 experiment, with S.E.M. if larger than point size. Line was drawn using an exponential function (0.99*exp(-3*t) + 3.22).

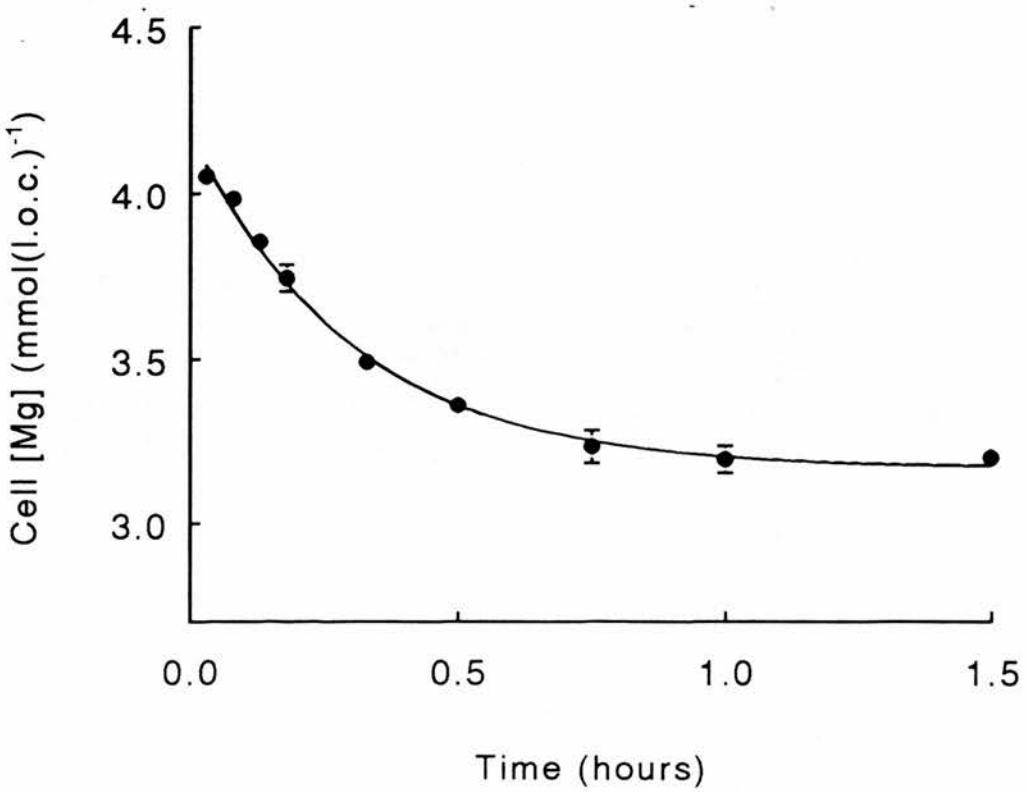

Figure 5.10.
Cell [Mg] as a function of time. Figure shows data from a similar experiment to that shown in Figure 5.9. Cells were loaded with Mg using the protocol given in Figure 5.7. Mg-loaded cells were incubated in media as described in the legend to Figure 5.9. Points show the mean of 3 measurements of cell [Mg] (corrected for cell lysis), in 1 experiment, with S.E.M. if larger than point size. Line was drawn using an exponential function (1.02*exp(-3*t) + 3.16).

faster and the relationship between Mg efflux and $[Mg^{2+}]_i$ can be determined from the raw data.

The efflux is the change in the cell [Mg] between 2 time points expressed as a flux per hour. The mean cell [Mg] over the flux period was used to find the corresponding $[Mg^{2+}]_i$ from a buffer curve. Buffer curves were produced for the cells in each experiment. Efflux as a function of $[Mg^{2+}]_i$ from 6 separate experiments transformed in this way is shown in Figure 5.11.

The effect of amiloride on Mg efflux from cells loaded with Mg by incubation in media with low-[Na] and high-[Mg].

Figure 5.12 shows the changes in the cell [Mg] with time in cells which have been loaded with Mg by incubation in media containing 5 mM Na and 5 mM Mg (solid line). The dashed line in Figure 5.12 shows the changes in cell [Mg] when the medium contained 1 mM amiloride. Both sets of data are fitted by an exponential function. The rate constant for Mg efflux is 1.9 h^{-1} and 1.3 h^{-1} in the control and amiloride-containing media respectively.

These data show that Mg efflux from these Mg-loaded cells was only slightly inhibited by amiloride. This is in contrast to the large inhibition of Mg efflux from cells which were loaded with Mg using the ionophore method (Figure 5.4). This indicates that the 2 methods of loading the cells with Mg may reveal

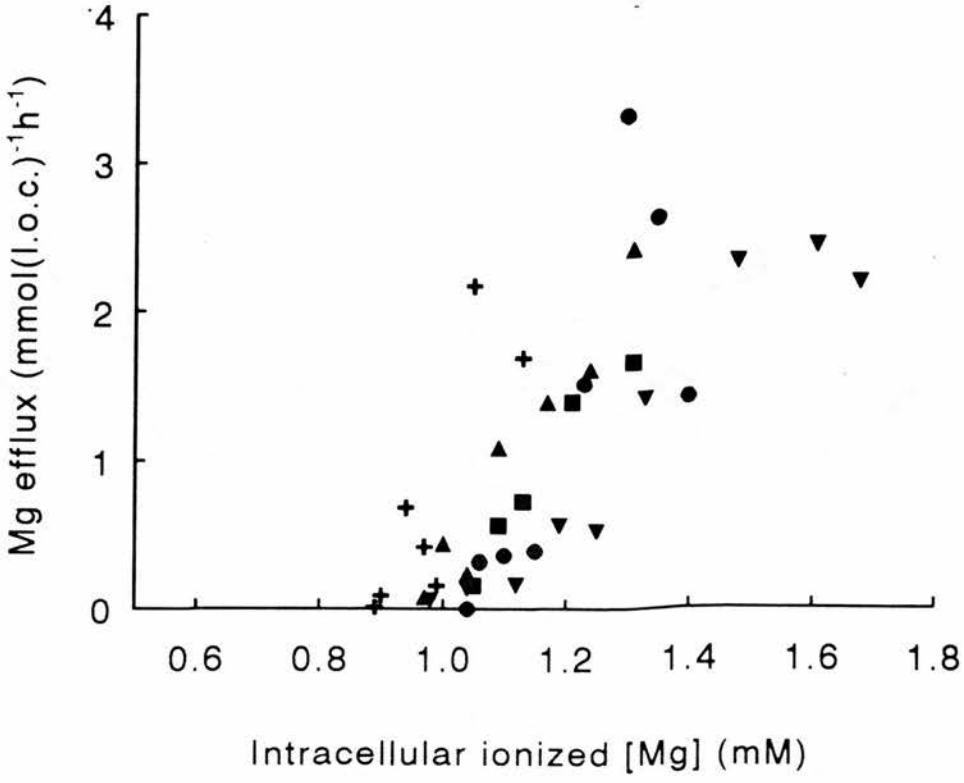

Figure 5.11.
Mg efflux as a function of intracellular ionized [Mg]. Cells were loaded with Mg using the protocol given in Figure 5.7. Mg-loaded cells were incubated in media as described in the legend to Figure 5.9. Changes in cell [Mg] over short time intervals were expressed as a flux per hour. The mean cell [Mg] over each time interval gave the intracellular ionized [Mg] from Mg buffering curves (Mg buffering measured in each experiment). Symbols represent the data from 5 separate experiments and includes the data from Figures 5.9 and 5.10 (triangles and circles respectively).

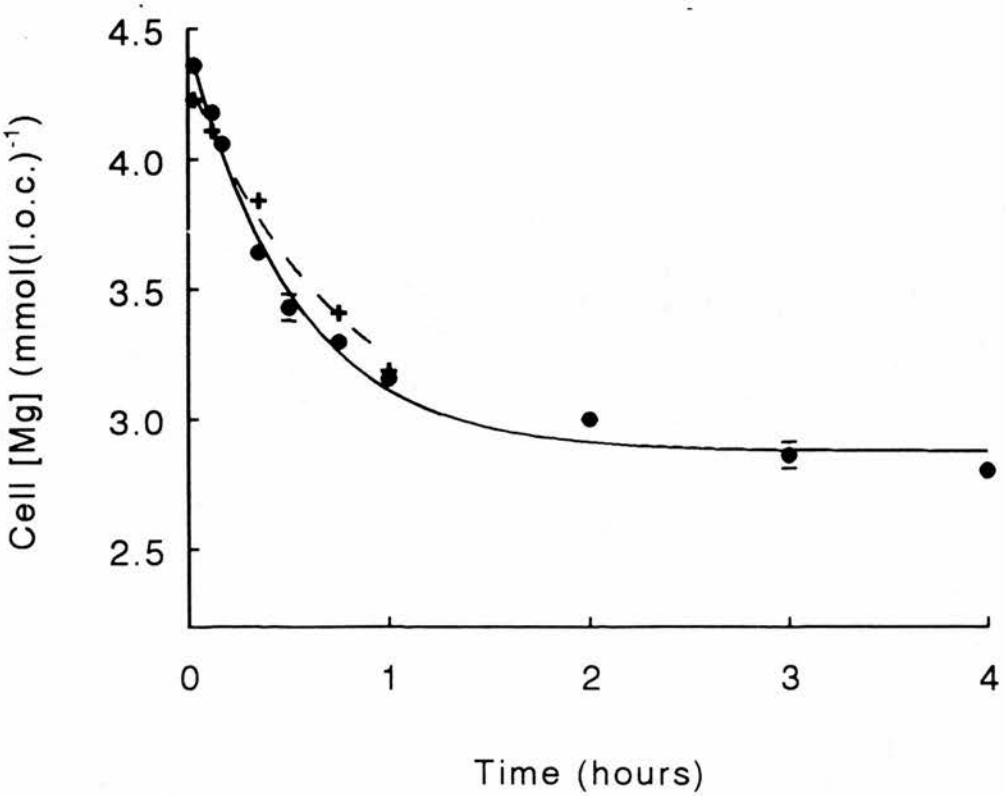

Figure 5.12.

Cell [Mg] as a function of time. Cells were loaded with Mg using the protocol given in Figure 5.7. Mg-loaded cells were incubated in media as described in the legend to Figure 5.9. Points show the mean of 3 measurements of cell [Mg], in 1 experiment, (corrected for cell lysis) with S.E.M. if larger than point size. Crosses show efflux from Mg-loaded cells when the media contained 1 mM amiloride. Lines were drawn using exponential functions: 1.59*exp(-1.9*t) + 2.87 (circles) and 1.46*exp(-1.3*t) + 2.85 (crosses).

different routes for Mg transport.

Comparison of Mg efflux from cells loaded with Mg using either the ionophore method or by incubation in media with low-[Na] and high-[Mg].

Consider the Figures 5.2 and 5.11 which show Mg efflux as a function of $[Mg^{2+}]_i$ in cells loaded using the ionophore method and incubation in media with low-[Na] and high-[Mg] respectively. It is not clear what form of function should be used to fit these data. The range of values in both cases is not large enough to accurately predict the shape of the function at concentrations of $[Mg^{2+}]_i$ around the physiological concentration. The simplest model is one in which Mg efflux proceeds at a low rate until $[Mg^{2+}]_i$ reaches some threshold value. Above this value, Mg permeability is greatly increased and Mg efflux is a linear function of $[Mg^{2+}]_i$. The data in Figures 5.2 and 5.11 were fitted by linear regression analysis and Figure 5.13 shows the lines which were fitted to the data. The solid line represents the fit of the data in Figure 5.2 (ionophore method) and the dashed line represents the fit of the data in Figure 5.11 (incubation in low-[Na] and high-[Mg]).

Although the simplest model may not be the most accurate, these lines allow direct comparison of the efflux rates at high $[Mg^{2+}]_i$ after loading using the different methods. Figure 5.13 shows that when cells

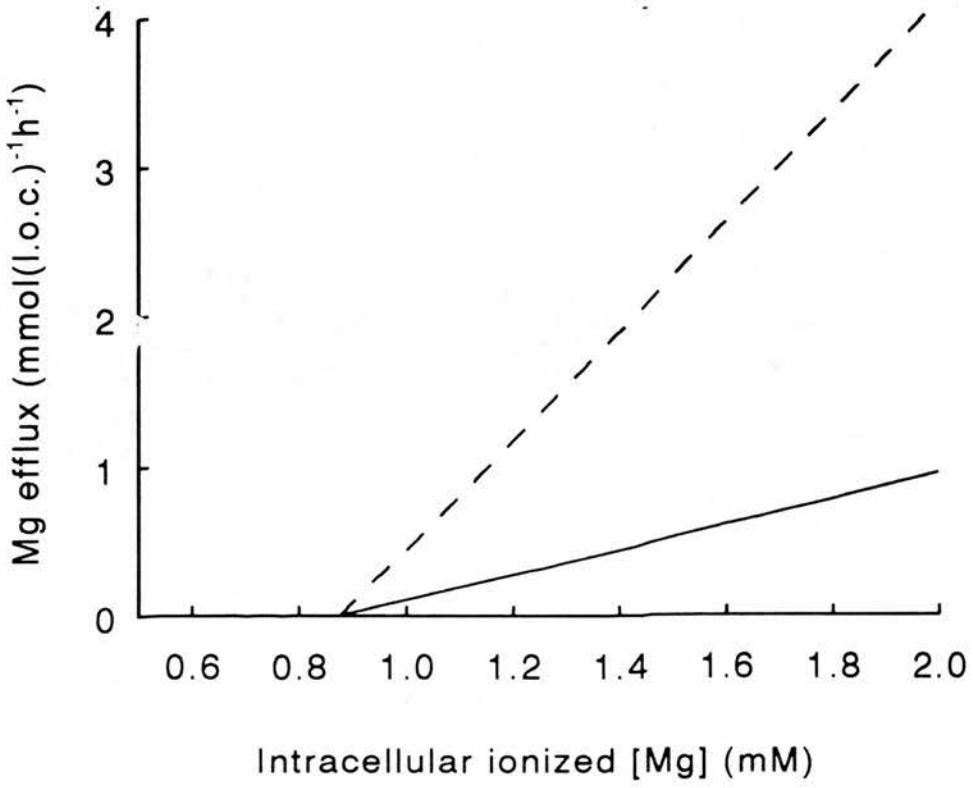

Figure 5.13.
Mg efflux as a function of intracellular ionized [Mg]. Data in Figures 5.2 and 5.11 were fitted with straight lines using linear regression analysis. The solid line shows the fit of the data from cells loaded using the ionophore (Figure 5.2; y = 0.84*x - 0.73, r = 0.9). The broken line shows the fit of the data from cells loaded with Mg using the protocol given in Figure 5.7 (Figure 5.11; y = 3.60*x - 3.15, r = 0.8).

are loaded with Mg using the ionophore method there is a significant increase in the rate of efflux when the $[Mg^{2+}]_i$ is greater than 0.9 mM. When the cells are loaded by incubation in low-[Na] and high-[Mg], Mg efflux also increases when $[Mg^{2+}]_i$ is greater than 0.9 mM. However in these cells the Mg efflux when $[Mg^{2+}]_i$ is above 0.9 mM is a much steeper function of $[Mg^{2+}]_i$ than when cells were loaded using the ionophore method. This could suggest that the procedure for loading the cells by incubation in media with low-[Na] and high-[Mg] causes a large increase in the Mg permeability.

i. The effect of incubation in media with low-[Na] on Mg efflux from Mg-loaded cells.

Figure 5.14 shows the results of an experiment which aimed to investigate the effect of a long incubation in a medium with low-[Na] on the Mg permeability.

The cells were loaded with Mg using the ionophore-method and were then incubated in FBM containing 0.2 mM $MgCl_2$ and 1 mM EDTA. Figure 5.14 shows the changes in the cell [Mg] over 2 hours (circles). Another group of the same cells was incubated in a medium containing 5 mM NaCl for 1 hour. The exact composition of the incubation medium, the subsequent washing steps and incubation were the same as given in the protocol in Figure 5.7, but $MgCl_2$ was

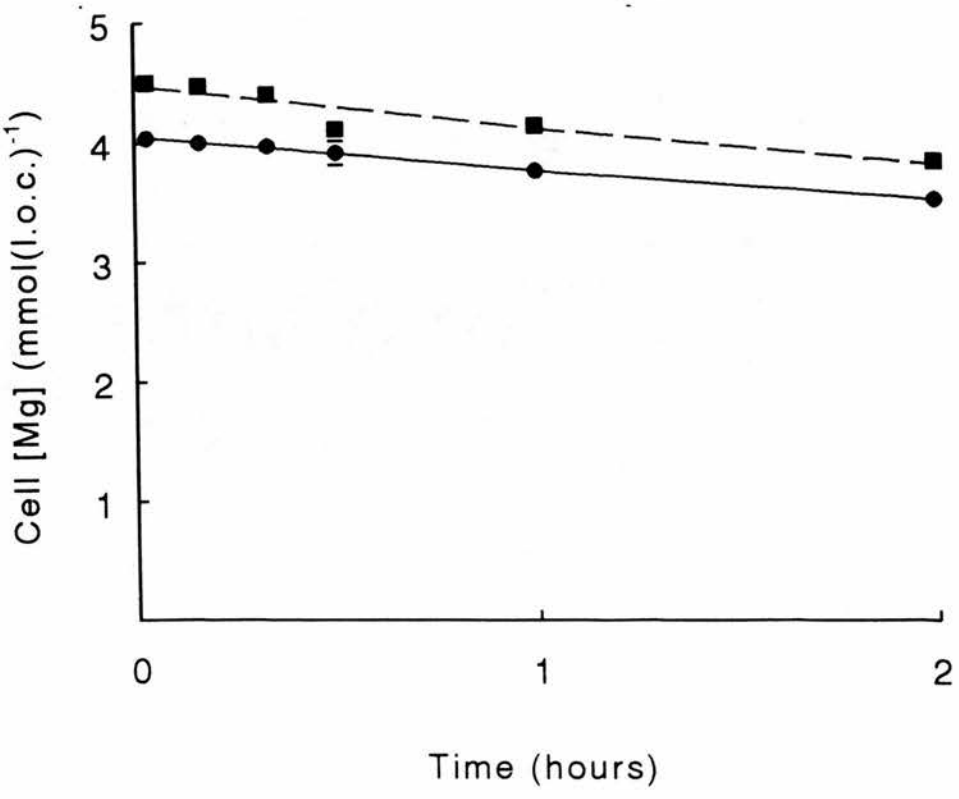

Figure 5.14.

Cell [Mg] as a function of time. Cells were loaded with Mg using the ionophore (circles, protocol given in Table 2.2). Another batch of cells from the same donor were incubated in the media described in Figure 5.7 but which contained no added Mg. The cells were then loaded with Mg using the ionophore (squares). Mg-loaded cells were incubated in media as described in the legend to Figure 5.9. Points show the mean of 3 measurements of cell [Mg] (corrected for cell lysis) with S.E.M. if larger than point size. Lines were drawn using exponential functions: 4.82*exp(-0.06*t) - 0.78 (circles) and 5.30*exp(-0.07*t) - 0.82 (squares).

not added to any of the media. These cells were subsequently loaded with Mg using the ionophore method. The changes in the cell [Mg] over 2 hours in these cells are also shown in Figure 5.14 (squares). There is little difference in the rate of Mg efflux from cells loaded using the ionophore method and those cells incubated in low-[Na] media prior to loading using the ionophore method. Even if the cell [Mg] is increased, following a pre-incubation in a low external [Na], there is no large increase in the Mg permeability. Thus the increase in Mg permeability, following incubation in media with low-[Na] and high-[Mg], cannot be due to the effects of low $[Na]_o$ alone.

ii. The specificity of the increase in Mg permeability following Mg-loading.

As ^{86}Rb was readily available in this laboratory, the specificity of the increase in permeability was tested by measuring the bumetanide-resistant ^{86}Rb flux in cells which had been incubated in media with low-[Na] and high-[Mg]. The bumetanide-resistant ^{86}Rb flux gives a measure of the rate of ^{86}Rb movement through routes other than the Na-K-Cl cotransporter. In a control group of cells, the bumetanide-resistant ^{86}Rb equilibrium rate constant was 0.13 h^{-1}. In a group of cells which had been loaded with Mg by incubation in a media with low-[Na] and high-[Mg], the rate constant for the equilibrium of ^{86}Rb was 0.04 h^{-1}. Thus, as the increase in Mg movement is not accompanied

by an increase in the permeability to ^{86}Rb, the Mg permeability cannot occur through a route which is entirely non-specific. This result rules out the possibility that the cells are simply made very leaky (as a step towards cell lysis) by the loading procedure. If the loading procedure opens a channel for Mg, then the ^{86}Rb experiments do not exclude the possibility that K moves through this route as the channel may discriminate between K^+ and the much larger Rb^+ (Hille, 1984).

iii. Differences in the rate of Mg efflux following Mg-loading using different protocols may be a result of cell heterogeneity.

In considering the difference in Mg efflux from cells loaded using either the ionophore method or by incubation in a medium with low-[Na] and high-[Mg] (Figure 5.14) the effects of these procedures on the whole cell population must also be considered. When the cells are loaded with Mg using the ionophore method, all the cells in the population are loaded uniformly. However the conditions set for loading by incubation in a medium with low-[Na] and high-[Mg] were selected to exploit the ability of ferret red cells to reverse the direction of Mg transport in low-$[Na]_o$. The sigmoidal appearance of the pattern of Mg uptake when the cells are incubated in a media with low-[Na] and high-[Mg] (Figure 4.4) suggests that there may be a

heterogeneous capacity for this route of Mg uptake throughout the cell population. Thus the rate of initial uptake in each cell will be dependent on the amount and activity of a (Na-Mg) transporter in the membrane. Experiments using cells loaded with Mg using the ionophore method have indicated that an increase in the Mg permeability follows an increase in $[Mg^{2+}]_i$ above a threshold value. A heterogeneous capacity for a (Na-Mg) transporter in media with low-[Na] and high-[Mg] will result in cells reaching this threshold at different times and thus the cell population will consist of cells with a range of $[Mg^{2+}]_i$ and Mg permeabilities. As measurements of efflux and $[Mg^{2+}]_i$ are made relative to the haemoglobin concentration of the total cell suspension the overall effect of a heterogeneous loading will be that high rates of efflux will apparently occur at lower $[Mg^{2+}]_i$.

Some evidence that cells within a population of cells behave differently when loaded with Mg by incubation in media with low-[Na] and high-[Mg] was obtained from an experimental observation. After the cells had been incubated in the media with low-[Na] and high-[Mg], transferred to a centrifuge tube and spun, a very dense button of cells formed at the bottom of the centrifuge tube. These cells were very difficult to resuspend and were very dark in colour. Following the wash in the RECOVERY medium there was considerable cell lysis (the only point in this protocol where lysis was noticeable by eye). During subsequent washes no button of cells formed in the tube and cell lysis was low.

Flatman (1988) has shown that ferret red cells lyse when the cell [Mg] is increased to high concentrations using the ionophore. The cells in the button could be a fraction of the population which have a high capacity for Na-Mg exchange, reach the threshold $[Mg^{2+}]_i$ quickly, increase their $[Mg^{2+}]_i$ to even higher levels (following an increase in the Mg permeability) and lyse during resuspension in the RECOVERY medium. Interestingly this dense button of cells was only seen when the media had a low-[Na] and high-[Mg]. The loading procedure was repeated but this time no $MgCl_2$ was added to the LOAD or RECOVERY media. After incubation in low-[Na] there was a pellet of denser cells. However this button of cells was much smaller, not so dark and much easier to resuspend than when the LOAD and RECOVERY media had contained Mg.

Changes in the density of the cells were investigated using Percoll gradients. Ferret red cells lie in a uniform band between 1.098 and 1.115 g ml^{-1}. After incubation in low-[Na] media all the cells still fell within this range of densities. However there did appear to be a slightly denser band at the lower end of this range (darker band of cells between 1.100 and 1.115 g ml^{-1}). Thus low-[Na] incubation does seem to cause some of the cells to slightly increase in density although the increase in density is not sufficient to allow a clean separation of the denser fraction of cells.

iv. At least some of the Mg efflux from cells, loaded using the ionophore-method, occurs through the same route as Mg uptake in media with low-[Na] and high-[Mg].

A group of cells was treated following the protocol for Mg loading by incubation in media with low-[Na] and high-[Mg] (Figure 5.7). Another batch of cells from the same animal was loaded using the ionophore-method. Both experiments were performed simultaneously. Figure 5.15 is an example of the result of one such experiment which shows some unusual features. When the cells were loaded using the ionophore-method the rate of the subsequent efflux was unusually slow. Incubation in a medium with low-[Na] and high-[Mg] did not result in substantial Mg loading in these cells. Thus in this batch of cells, neither the route for Mg influx, in a medium with low-[Na] and high-[Mg], nor the route for Mg efflux, following loading using the ionophore-method, were operating. This does not necessarily imply that the route is absent in these cells. It may be that Mg transport is regulated by some cellular or metabolic species and that cellular events prior to this experiment switched off the cellular capacity for this transport system. It is interesting to note that whatever factor has prevented Mg influx, when the conditions were set to stimulate the reverse mode of a Na-Mg exchanger, has also inhibited the large rise in Mg efflux following Mg loading using the ionophore method.

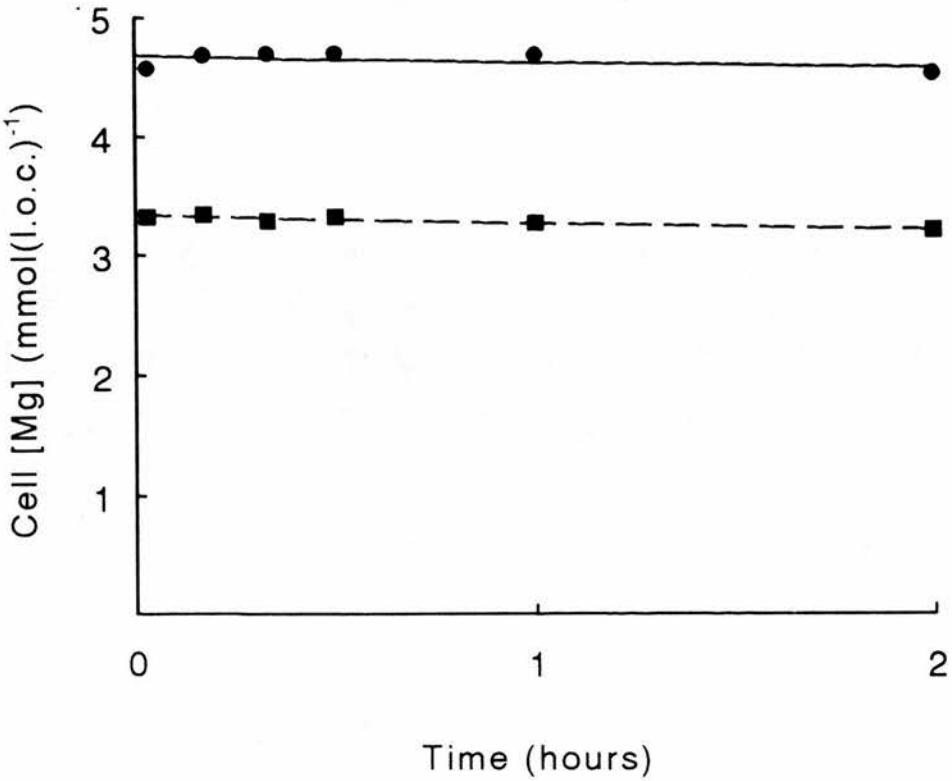

Figure 5.15.

Cell [Mg] as a function of time. The initial cell [Mg] was 2.62 mmol(l.o.c.)$^{-1}$. Cells were loaded with Mg using the ionophore (circle, protocol given in Table 2.2) or by incubation in 5 mM Na and 5 mM Mg (squares, protocol given in Figure 5.7). Mg-loaded cells were incubated in a medium as described in the legend to Figure 5.9. Points show the mean of 3 measurements of cell [Mg] (corrected for cell lysis). S.E.M. is smaller than point size. Lines were drawn using linear regression analysis: y = -0.09*x + 4.69 (circles), y = -0.09*x + 3.34 (squares).

6. Discussion.

Mg efflux from fresh, intact ferret red cells can be measured as a change in either the intracellular or extracellular [Mg] if the external medium is initially Mg free (Figures 3.1 and 3.2). Mg efflux from ferret red cells measured under these, zero-trans, conditions is approximately 10 times the Mg efflux from fresh human red cells measured under similar conditions. The Mg efflux from ferret red cells, although still small (occurring at approximately 40 μmol(l cell)$^{-1}$h^{-1}) is nevertheless large enough to be measured reproducibly if care is taken. The examination of these fluxes has led to the elucidation of a number of important properties of Mg transport in ferret red cells containing a physiological cell [Mg].

Ferret red cells can take up Mg against a gradient when $[Na]_o$ is low.

Mg efflux has a complicated dependence on $[Na]_o$. Mg efflux is stimulated when $[Na]_o$ is reduced from 145 mM (the physiological concentration) to 10 mM (Figure 3.23). Reducing $[Na]_o$ below 10 mM inhibits Mg efflux. Mg efflux is reduced to half its maximum value when $[Na]_o$ is 2 mM.

Ferret red cells contain a high intracellular [Na] and thus reduction of $[Na]_o$ below 10 mM produces a large gradient for the movement of Na out of the cells. At low $[Na]_o$, Mg efflux is a steep function of $[Na]_o$

and is very sensitive to small changes in $[Na]_o$. When the loss of Na from cells, incubated in nominally Na-free media, is limited (by measuring fluxes over short time intervals in media containing bumetanide) then net Mg influx can be measured (Figure 3.23). Mg influx can occur when the external medium (nominally Mg-free) contains as little as 2 μM Mg. Although Mg influx has only been measured in experiments where bumetanide was added to the medium it is unlikely that bumetanide directly stimulates Mg influx. Examination of $[Na]_o$ in the presence and absence of bumetanide indicates that bumetanide only affects Mg transport when it significantly alters the cell and external [Na] (Figure 3.24). Further, high concentrations of bumetanide have no effect on the rate of Mg efflux at $[Na]_o$ above 10 mM (Figure 3.23) or the rate of Mg influx in low-[Na] media (Table 4.1).

Several independent experiments have confirmed that net active Mg influx can be measured when $[Na]_o$ is reduced to such a level that the energy yield from the outward movement of Na is sufficient to drive active Mg influx (Tables 3C, 3D and 3E). Measurements in other experiments indicate that it is highly unlikely that disturbances in the membrane potential would be sufficient to drive Mg influx down an electrical gradient. This apparent reversal of the direction of Mg transport following a reduction in $[Na]_o$ is clear evidence for the coupling of Mg transport to the movement of Na. The simplest model for such a transport system is Na-Mg exchange. Indeed, the data

of Figures 3.23 and 3.26 predict a model for Mg transport in which 1 Na ion is exchanged for 1 Mg ion (calculated using Equation 3.4). Given the experimental conditions of Figures 3.23 and 3.26, such a transporter would have a high affinity for $[Na]_o$ and reverse direction, mediating Mg influx, when $[Na]_o$ is 0.6 mM.

The stoichiometry of a postulated Na-Mg exchange has been estimated in other studies. Günther, Vormann and Förster (1984) estimated that 1 Mg is exchanged for 2 Na in Mg-loaded chicken red cells. Féray and Garay (1988) predicted that in Mg-loaded human red cells, 3 Na are exchanged for 1 Mg. Thus far all predictions of a stoichiometry for Na-Mg exchange are circumstantial. Günther, Vormann and Förster (1984) used amiloride to inhibit Mg efflux. Amiloride does not completely block Mg transport and inhibits other routes of Na transport which are independent of Mg movement. Féray and Garay (1988) used imipramine as a blocker of Mg transport. The ability of this drug to completely and specifically block Mg transport must also be questioned. As Mg fluxes are very small, and the total Na transport capacity of the membrane is very high, the identification of the Na fluxes accompanying Mg movement will only be achieved with the discovery of a specific and potent inhibitor of Mg transport. Recently Willis, Xu and Zhao (1992) have identified Na-Mg exchange in hamster red cells which appears to be completely inhibited by amiloride. These cells may provide a useful model for determining the

stoichiometry of Na-Mg exchange.

Several studies of Mg transport in a variety of red cell species have shown that Mg efflux is inhibited when $[Na]_o$ is reduced. The apparent affinity of $[Na]_o$ for the *$[Na]_o$-dependent Mg efflux* in human red cells is 20 mM (Féray and Garay, 1986) or 23 mM (Lüdi and Schatzmann, 1987). In chicken red cells it is 25 mM (Günther and Vormann, 1985). These values were calculated using cells which had been loaded with Mg. In rat red cells, where the Mg-loading procedure results in only a small increase in the cell [Mg], the apparent affinity of the *$[Na]_o$-dependent Mg efflux* is 11 mM (Féray and Garay, 1987). The findings of this study show that in ferret red cells (with physiological cell [Mg]) the apparent affinity for $[Na]_o$ (2 mM) is much lower than that observed in other red cells. The large disparity in the values obtained for the apparent external Na affinity of the Mg transporter may be due to the differences in the cell [Mg] in these different studies (an increase in cell [Mg] decreasing the apparent affinity of an external Na-binding site). Alternatively, different cells, in different experimental conditions, may move Mg through routes which have different affinities to $[Na]_o$.

Mg influx.

When the external [Mg] is increased to produce a large inward Mg gradient, Mg influx becomes sufficiently large to enable influx to be reliably

detected by changes in the total cell [Mg].

Mg influx is stimulated when $[Na]_o$ is reduced from 145 mM to 5 mM (Figure 4.1). Thus, at least some Mg influx occurs through the $[Na]_o$-dependent route that can mediate active Mg efflux. Unlike Mg efflux, where the control measurements of efflux were remarkably consistent, there is considerable variation in the magnitude of Mg influx in 5 mM $[Na]_o$ and 5 mM $[Mg]_o$. These conditions reveal a route for Mg transport which has a variable capacity. The route for influx may be the same as the route for Mg efflux and the experimental conditions, used for measuring Mg influx, may alter the activity of the transporter. Alternatively, the experimental conditions may reveal another, separate, route for Mg movement. The sigmoidal appearance of the time-dependent-Mg-influx curve (Figure 4.4) suggests that, under the conditions used to measure Mg influx, an initial rise in $[Mg^{2+}]_i$ causes an increase in the membrane permeability. An increase in the Mg permeability combined with a large inward Mg gradient results in a large influx of Mg. The increase in Mg permeability is not a non-specific membrane leak as there is no increase in the bumetanide-resistant ^{86}Rb equilibrium rate constant. It is not solely a change in $[Mg^{2+}]_i$ which triggers a change in the membrane permeability to Mg. A reduction in cell [Na] concomitant with the increase in $[Mg^{2+}]_i$ seems to be a more effective trigger for changes in the membrane permeability. Further, when ferret red cells are incubated in choline chloride media, their cell

increases (Flatman, personal communication). The rate of influx into ferret red cells is very sensitive to changes in the cell [ATP] (Figures 4.6 and 4.7) A combination of these factors may be the key to the changes in the Mg membrane permeability.

Inhibitors of Mg transport.

Amiloride, quinidine and imipramine inhibit both Mg efflux and Mg influx (Figure 3.8 and Table 4.1). The degree of inhibition and the order of potency of these drugs on Mg efflux and influx are similar suggesting that one transporter is involved in at least some of the Mg movement in either direction. This is an important consideration as the experimental conditions under which Mg efflux and influx are measured are very different and each may promote Mg transport through a different route.

Interestingly, of those tested, the drugs which are the most potent inhibitors of Mg transport have already been identified as non-specific blockers of many routes of Na movement across cell membranes. The effectiveness of these agents in blocking Mg transport suggests that either a binding (or access) site of the Mg transporter is similar to a Na site or that the movement of Na is a requirement for the transport of Mg. The latter need not imply that Mg and Na movement are directly coupled. If the transport of Mg (by a carrier mediated process or through a channel) results in a net movement of charge across the membrane, the

cell may move Na to compensate for the charge carried by the Mg ion.

The degree of inhibition (assessed by the K_i) and the order of potency of these drugs is similar to their effects on Mg transport systems in other red cell studies. In all studies, including this one, millimolar concentrations of the drugs are required to produce a measurable inhibition of efflux and no drug tested completely inhibits Mg efflux. The true efficacy of these compounds is difficult to determine as at high concentrations the lysis of ferret red cells becomes quite substantial and the dose-dependent inhibition is masked by a non-specific increase in Mg permeability.

The effects of several divalent cations were tested on Mg efflux (Figure 3.13). Of those tested, Co was the most potent blocker of Mg efflux. The dose-dependent effects of $CoCl_2$ give the clearest indication that not all of the Mg efflux can be inhibited as concentrations above 1 mM $CoCl_2$ do not result in a further reduction of Mg efflux (Figure 3.14). Further, Figure 3.25 shows that the component of Mg efflux which is insensitive to Co is also unaffected by changing the $[Na]_o$. Thus Co reveals a $[Na]_o$-independent component of Mg efflux.

Vanadate, bepridil and SITS have different effects on Mg efflux and Mg influx. Vanadate and bepridil have no effect on Mg efflux in 145 mM [Na] but stimulate Mg influx in 5 mM $[Na]_o$ and 5 mM $[Mg]_o$ (Figures 3.11, 3.13 and Table 4.1) and SITS which stimulates Mg efflux

has no affect on Mg influx (Figure 3.8 and Table 4.1).

Vanadate and bepridil inhibit Ca-pump activity (Nechay *et al*, 1986 and Gill *et al*, 1992). Indeed vanadate is a potent inhibitor of the sodium, calcium and hydrogen pumps (the P-type ATPases). Vanadate and bepridil have no effect on Mg efflux (Figure 3.8 and Table 4.1) indicating that Mg transport in ferret red cells is not mediated by a P-type ATPase. The stimulatory effects of vanadate on Mg influx are dose-dependent and incubation in media with either vanadate or bepridil increases the ferret red cell [ATP] content (Flatman, 1991). As changes in cell [ATP] seem to have complicated effects on Mg transport, the actions of vanadate and bepridil may be secondary to the changes they invoke in the cell [ATP].

SITS depolarises the ferret red cell membrane to 0 mV in 145 mM $[Na]_o$ (Flatman and Smith, 1991). The depolarisation of the membrane potential increases the electrical gradient in favour of Mg efflux. The stimulation in Mg efflux following treatment with SITS indicates that the movement of Mg through this route is sensitive to changes in the membrane potential. Such behaviour would be expected of an electrogenic transporter.

In Na-free (choline chloride) medium, the addition of SITS has complicated effects on the membrane potential (Flatman, personal communication). The cell membrane is at first hyperpolarised but is then depolarised. There is, however, no net change in the membrane potential over the time that influx is

measured and therefore little net change in the driving force for Mg movement. The behaviour of Mg efflux and influx in SITS-containing medium is thus probably an indication of the effects of changes in the membrane potential on Mg transport in these cells.

ATP dependence.

The investigation of the ATP dependence of Mg efflux and influx in ferret red cells has led to anomalous results. Mg efflux is slightly stimulated by the depletion of cellular [ATP] following incubation in a medium containing 2-deoxyglucose while the same treatment inhibits Mg influx (Figures 3.5, 4.6 and 4.7).

The relatively low activation energy for Mg efflux (Figure 3.4) and the insensitivity of Mg efflux to vanadate, indicate that ferret red cells do not rely directly on ATP hydrolysis to provide the energy for Mg transport. Rather than provide the metabolic energy for the movement of Mg, ATP may have other effects on Mg transport. Some membrane transporters only operate when in a phosphorylated state and ATP can affect the activity of such transporters by modulating the proportion of them in the phosphorylated state at any one time. For example the Na-K-Cl cotransporter in ferret red cells is active only when phosphorylated (Flatman, 1991a). Preliminary evidence that phosphorylation may play some role in the regulation of Mg transport has been provided by Günther and Vormann

(1986) who have shown that Mg efflux from Mg-loaded chicken red cells is associated with the phosphorylation of a 230 kDa membrane-bound protein.

Interestingly, Flatman (1991a) has shown that even following a reduction in the cell [ATP] of ferret red cells the Na-K-Cl cotransporter can continue operating for many hours. Ferret red cells seem to have a very low phosphatase activity and dephosphorylation, and hence the inactivation, of a membrane transporter lags behind a reduction in the cell [ATP].

Mg influx is inhibited after the cell [ATP] is depleted by incubation in a medium with 2-deoxyglucose. At first inspection this would seem to suggest that the mechanisms for Mg efflux and influx have very different requirements for cell ATP. However it has already been postulated that under the conditions set to measure Mg influx (high $[Mg]_o$ and low $[Na]_o$) Mg may enter the cell by more than one route. Indeed Mg influx in 145 mM $[Na]_o$ and 5 mM $[Mg]_o$ (where influx occurs passively down a large gradient for Mg) is also inhibited by a reduction in cell [ATP]. Cells which have a higher Mg permeability are more sensitive to changes in the cell [ATP] (Figures 4.6 and 4.7). Cell [ATP] may regulate Mg movement through a passive route (perhaps a channel) rather than through the route responsible for the active transport of Mg.

Depletion of cell [ATP] also increases $[Mg^{2+}]_i$ by reducing the capacity of the intracellular Mg buffers (Figure 3.6). In 3 separate experiments, cell [ATP] was reduced to approximately 4% of the control

concentration. $[Mg^{2+}]_i$ increased by approximately 39% (the final $[Mg^{2+}]_i$ was 1 mM). According to Figure 5.13, where the threshold for an increase in Mg efflux occurs at 0.9 mM, the change in $[Mg^{2+}]_i$ following ATP depletion may also directly stimulate Mg transport.

The effects of increasing $[Mg^{2+}]_i$ on Mg transport.

The effects of increasing $[Mg^{2+}]_i$ on Mg transport are an important consideration in the investigation of Mg transport as in many other studies, where the initial rate of Mg efflux is very low, reliable measurement of Mg transport has necessitated the loading of the cells with Mg.

In this study $[Mg^{2+}]_i$ was increased using 2 methods. Firstly the ionophore, A23187, which has been used extensively for Mg-loading in a number of studies was used to increase the cell [Mg] of ferret red cells (Table 2.2). Secondly the ability of ferret red cells to take up Mg when incubated in a low-$[Na]_o$ medium was exploited to load cells with Mg without the intervention of chemical reagents (Figure 5.7). Both methods have shown that Mg efflux increases when $[Mg^{2+}]_i$ is increased above a threshold level (Figure 5.13). The available data predict that this threshold occurs around 0.9 mM $[Mg^{2+}]_i$ and that the Mg efflux is a linear function of $[Mg^{2+}]_i$ above this concentration. However the Mg efflux from cells loaded using these 2 different techniques has very different properties.

Mg efflux from cells loaded using the ionophore

method is strongly inhibited by amiloride. Very importantly, it is also inhibited by reducing $[Na]_o$. Indeed, these loaded cells can mediate Mg influx against a considerable Mg gradient when $[Na]_o$ is low. This provides further evidence for the presence of Na-Mg exchange in these cells and suggests that Mg efflux occurs through a Na-Mg exchange even when the cells are loaded with Mg. The stimulation in Mg efflux through this route indicates that when the cells contain physiological concentrations of Mg, Na-Mg exchange is operating below its maximum capacity.

Raising $[Mg^{2+}]_i$ (above the threshold value) by incubation in low-$[Na]_o$ and high-$[Mg]_o$ also increases the rate of Mg efflux . However the efflux at any given $[Mg^{2+}]_i$ above the threshold value is considerably greater in these cells than in cells which have been Mg-loaded using the ionophore. This substantial Mg efflux is not inhibited by amiloride and seems to occur through a different route than Mg efflux from cells loaded using the ionophore method.

Control experiments have shown that incubation in low-$[Na]_o$ and a subsequent rise in $[Mg^{2+}]_i$ is not sufficient to reveal this route. The cells must deplete of cell [Na] and increase $[Mg^{2+}]_i$ simultaneously for the Mg permeability to increase.

Changes in Mg permeability following long incubations in some experimental media.

Initial experiments on the effects of incubation in low-$[Na]_o$ media on Mg efflux suggested that this treatment stimulated Mg efflux. However later experiments showed that this was a time dependent phenomenon. Mg efflux is inhibited in low $[Na]_o$ but after 1 hour in this medium there is a large increase in the membrane permeability to Mg and, as a result, a large stimulation in Mg efflux (Figure 3.16). This increase in Mg permeability is dependent on a reduction in the cell [Na] (and/or [K]) as the addition of bumetanide to the medium reduces the loss of these ions from the cell and also delays the increase in Mg permeability. The rise in Mg permeability, although revealed in low-$[Na]_o$, is inhibited by the removal of external K. Montes *et al* (1988) described the movement of Mg coupled to the movement of K in the muscle fibres of the barnacle *Balanus nubilus*. However in their experiments the rise in the [Mg] of the muscle fibres was correlated with a decrease in the cell [K]. In ferret red cells after 1 hour incubation in low-$[Na]_o$, the rise in $[Mg]_o$ (a reduction in cell [Mg]) correlates with an increase in cell [K]. This might suggest the presence of a Mg-K exchanger.

Large movements of an ion through a channel require the movement of other species to allow charge compensation. Under the conditions produced by these experimental procedures K may be the most efficient ion

to move in response to the movement of Mg out of the cell down a considerable Mg gradient.

The time-dependence study of Mg influx similarly reveals that the protocols of these experiments produce changes in the Mg permeability of the red cells. The sigmoidal appearance of the curve measuring Mg uptake over time suggests that over the initial phase of the incubation some cellular event causes a change in the Mg permeability (Figure 4.4). Under the conditions of these (influx) experiments the cells were losing internal Na and simultaneously gaining internal Mg. These factors seem to be able to promote an increase in the cell permeability to Mg.

Mg efflux in ferret red cells is extremely constant even over periods of up to 5 hours. The conditions under which Mg efflux is measured are such that there is little change in the cell [Na] over this time and the cell [Mg] falls very gradually. In Mg influx experiments the simultaneous fall in cell [Na] and rise in cell [Mg], even over much shorter incubation times, may account for the non-linear uptake of Mg into these cells and the variation in the magnitude of influxes measured over the first 40 minutes of incubation.

Loading ferret red cells with Mg using the ionophore does not trigger changes in the cell permeability as ferret red cells contain a high cell [Na]. However when comparing the data from other studies using Mg-loaded red cells it should be borne in mind that most mammalian cells have a low internal [Na]

and thus an increase in cell [Mg] may be sufficient to increase the Mg permeability. Mg transport in Mg-loaded cells may therefore occur through different routes depending on the cell [Na] and the amount by which cell [Mg] has increased.

Consideration of Mg transport *in vivo*.

The experimental protocols in this study have of necessity been chosen so that the small Mg fluxes can be measured as changes in the external or internal [Mg]. Mg efflux was measured under zero-trans conditions. The nominally Mg-free media produced a large outward gradient for Mg. *In vivo*, however, the external [Mg^{2+}] is approximately 0.5 mM (see Introduction) and thus the Mg gradient is inward. These experiments were also routinely performed in Ca-free media. The external Ca was kept at very low levels by the addition of EGTA to the medium. 1 mM Ca inhibits Mg efflux (Figure 3.13). Also the addition of EGTA eradicates the large inward gradient for Ca which exists *in vivo*. Thus, the experimental conditions in this study may favour the transport of Mg on a transporter which, under physiological conditions, would be involved primarily in the transport of another ion. Ca transporters are the obvious candidates for such a mechanism both since Ca and Mg block each others transport and also the conditions in this study will reduce the availability of Ca for transport on its own transporters. Milanick (1989) has shown that

similarly to dog red cells, ferret red cells have a high capacity Na-Ca exchanger which balances Na leak by driving Na out of the cell as Ca moves into the cell down a large gradient. This transporter would only have to switch to Na-Mg exchange occasionally to bring Mg to the equilibrium values seen *in vivo*. La^{3+} had no effect on Mg efflux (Figure 3.13) despite being a potent inhibitor of Na-Ca exchange in a number of different cells (Kaczorowski *et al*, 1989). Thus Na-Mg exchange cannot occur on the Na-Ca exchanger which has been well described in a number of different cells. Féray and Garay (1987) have shown that the $[Na]_o$-dependent Mg transporter in rat red cells can exchange Mn^{2+} for Mg^{2+} in the absence of $[Na]_o$. Thus the Na-Mg exchanger need not be an entirely specific transporter for Mg but may have differing affinities for a range of divalent cations. This need not imply that the regulation of internal Mg would be the secondary function of such a transporter.

Conclusion

Mg transport in ferret red cells is inhibited by a variety of inhibitors including amiloride, quinidine and imipramine. Reducing the $[Na]_o$ can inhibit Mg efflux and if $[Na]_o$ is reduced sufficiently then the direction of Mg transport can be changed and the system can be made to mediate active Mg transport. Active Mg influx can be measured after the outward gradient for Mg is increased by either reducing $[Mg]_o$ or increasing

the cell [Mg]. Changes in membrane potential cannot account for this movement of Mg. This behaviour is strongly indicative of Na-Mg exchange. However this study has not demonstrated the active efflux of Mg. A further requirement for the conclusive identification of Na-Mg exchange is the identification of the Na fluxes which accompany the Mg fluxes. The dissection of these small Na fluxes from the large amount of Na transport in these cells awaits the identification of a potent and specific inhibitor of Mg transport.

The results in this study also indicate that there is more than one route for Mg transport in these cells. As well as Na-Mg exchange it seems that cellular events (a combination of a fall in cell [Na] and a rise in cell [Mg] or an increase in cell [ATP]) may trigger the opening of Mg channels. Changes in the Mg permeability can only be fully elucidated using isotopic tracers.

Na-Mg exchange has been identified as the key regulator of Mg levels in a variety of different cells. However studies using red cells from a number of different species have questioned whether Na-Mg exchange can be a universal regulator of internal [Mg]. In particular, careful studies using human red cells have not been able to change the direction of Mg movement by manipulating the Na gradient (Lüdi and Schatzmann, 1987; Frenkel, Graziani, and Schatzmann, 1989; Schatzmann, 1993). There is no reason why different cell types should not adapt different transport mechanisms to suit their particular

requirements. Indeed red cells eject many of the transport systems of their progenitors before they are released into the circulation (Wiley & Shaller, 1977). Human red cell membranes contain Na-K-ATPase but have no Na-Ca exchanger. Conversely ferret red cells have a high capacity Na-K-Cl cotransporter, little Na-K-ATPase activity and a high capacity Na-Ca exchange (Flatman, 1983). Thus it would not be so surprising if human and ferret red cells have selected different mechanisms for the regulation of cell [Mg].

In ferret red cells, Na-Mg exchange appears to be the transporter which regulates $[Mg^{2+}]_i$. The relatively large fluxes mediated by this transporter have made these cells a useful model in the elucidation of some of the properties of Mg transport.

SCHEMATIC DIAGRAM OF MAGNESIUM TRANSPORT

IN FERRET RED CELLS

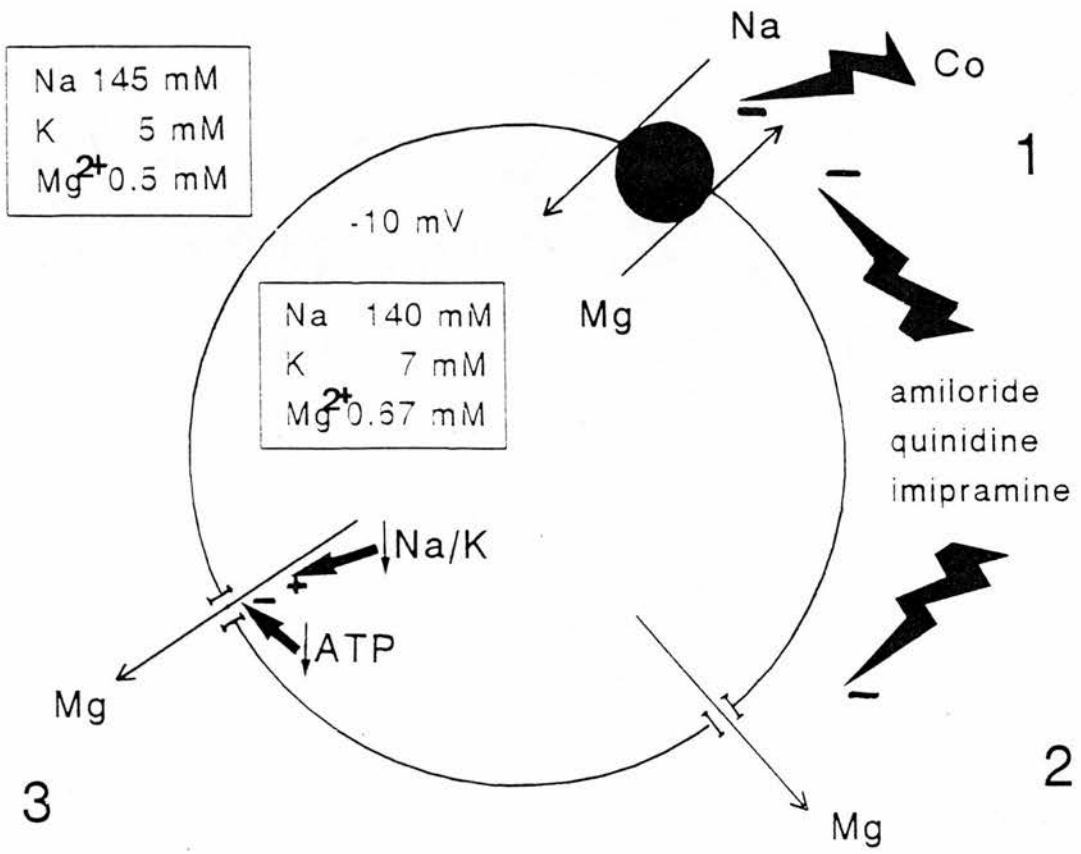

1. Na-Mg exchange. A small inward Na gradient maintains $[Mg^{2+}]_i$ below electrochemical equilibrium. Mg efflux, under zero-trans conditions, is inhibited by Co and physiological $[Na]_o$ and is stimulated when $[Mg^{2+}]_i$ is increased above 0.9 mM.

2. Mg 'leak'. Mg efflux, under zero-trans conditions, is independent of $[Na]_o$.

1 and/or 2. Inhibited by amiloride, quinidine and imipramine.

3. Mg channel. The direction of transport through this route is dictated by the Mg gradient. Stimulated when $[Mg^{2+}]_i$ is increased, particularly when cell [Na] (and/or [K]) is simultaneously reduced. Inhibited by the depletion of cell [ATP].

7. References.

Aikawa, J.K. (1963). 'The role of magnesium in biologic processes.' Charles C. Thomas. Publisher. Springfield, Illinois, USA.

Alcock, N.W. (1969). Development of methods for the determiration of magnesium. *Ann. N.Y.Acad.Sci.*, **162**, 707-715

Alvarez-Leefmans, F.J., Giraldez, F. & Gamiño, S.M. (1987). Intracellular free magnesium in excitable cells: its measurement and its biologic significance. *Can.J.Physiol.*, **65**, 915-925

Ashley, C.C. & Ellory, J.C. (1972). The efflux of magnesium from single crustacean muscle fibres. *J. Physiol.* **226**, 653-674.

Baker, P.F. and Crawford, A.C. (1972). Mobility and transport of magnesium in squid giant axons. *J.Physiol.*, **227**, 855-874

Baylor, S.M., Chandler, W.K. & Marshall, M.W. (1982). Optical measurements of intracellular pH and magnesium in frog skeletal muscle fibres. *J.Physiol.* **331**, 105-137.

Beaven, G.H., Parmar, J., Nash, G.B., Bennett, P.M. & Gratzer, W.B. (1990). Effect of magnesium ions on red cell membrane properties. *J. Membrane Biol.* **118**, 251-257.

Benos, D.J. (1982). Amiloride: a molecular probe of sodium transport in tissues and cells. *Am.J.Physiol.*, **242**, C131-C145

Bergfeld, G. & Forrester, T. (1989). Efflux of adenosine triphosphate from human erythrocytes in response to a brief pulse of hypoxia. *J. Physiol.*, **418**, 88P.

Bernstein, R.E. (1959). Alterations in metabolic energetics and cation transport during aging of red cells. *J.Clin.Invest.* **38**, 1572-1586.

Beyenbach, K.W. (1990) Transport of magnesium across biological membranes. *Magnesium Trace Elem.*, **9**, 233-254.

Bjerrum, P.J. (1979). Hemoglobin-depleted human erythrocyte ghosts: Characterization of morphology and transport function. *J.Membrane Biol.*, **48**, 43-67.

Blatter, L.A. (1990). Intracellular free magnesium in frog skeletal muscle studied with a new type of magnesium-selective microelectrode: interactions between magnesium and sodium in the regulation of $[Mg]_i$. *Pflügers Arch.*, **416**, 238-246.

Blatter, L.A. & McGuigan, J.A.S. (1986). Free intracellular magnesium concentration in ferret ventricular muscle measured with ion selective microelectrodes. *Q.J.Exp.Physiol.*, **71**, 467-473.

Bock, J.L., Wenz, B. & Gupta, R.K. (1985). Changes in intracellular Mg adenosine triphosphate and ionized Mg^{2+} during blood storage: Detection by ^{31}P nuclear magnetic resonance spectroscopy. *Blood*, **65**, 1526-1530.

Borchgrevink, P.C., Bergan, A.S., Bakoy, O.E. & Jynge, P. (1989). Magnesium and reperfusion of ischemic rat heart as assessed by ^{31}P-NMR. *Am.J.Physiol.*, **256**, H195-H204.

Brinley, F.J. & Scarpa, A. (1975). Ionized magnesium concentration in axoplasm of dialyzed squid axons. *FEBS LETTS.*, **50**, 82-85.

Brinley, F.J., Scarpa, A. & Tiffert, T. (1977). The concentration of ionized magnesium in barnacle muscle fibres. *J.Physiol.*, **266**, 545-565.

Brown, A.M. (1982). ATP and ATPase determinations in red blood cells. In 'Red cell membranes - A Methodological Approach' Ed. J.C. Ellory & J.D. Young. Academic Press.

Bunn, H.F., Ransil, B.J. & Chao, A. (1971). The interaction between erythrocyte organic phosphates, magnesium ion, and haemoglobin. *J.biol.Chem.*, **246**, 5273-5279.

Buri, A. & McGuigan, J.A.S. (1990). Intracellular free magnesium and its regulation, studied in isolated ferret ventricular muscle with ion-selective microelectrodes. *Experimental Physiology*, **75**, 751-761.

Caldwell-Violich, M. & Requena, J. (1979). Magnesium content and net fluxes in squid giant axons. *J.Gen.Physiol.*, **74**, 739-752.

Cohen, P., Holmes, C.H.B. & Tsukitani, Y. (1990). Okadaic acid: a new probe for the study of cellular regulation. *Trends in Biochem.Sci.*, **15**, 98-102.

Corkey, B.E., Duszynski, J., Rich, T.L., Matschinsky, B. & Williamson, J.R. (1986). Regulation of free and bound magnesium in rat hepatocytes and isolated mitochondria. *J.Biol.Chem.*, **261**, 2567-2574.

De Weer, P. (1976). Axoplasmic free magnesium levels and magnesium extrusion from squid giant axons. *J.Gen.Physiol.*, **68**, 159-178.

DiPolo, R. & Beaugé, L. (1988). An ATP-dependent Na^{+}/Mg^{2+} countertransport is the only mechanism for Mg extrusion in squid axons. *Biochimica et Biophysica Acta*, **946**, 424-428.

Dunn, M.J. (1974). Red blood cell calcium and magnesium: Effects upon sodium and potassium transport and cellular morphology. *Biochimica et Biophysica Acta*, **352**, 97-116.

Ebel, H. (1990). Intestinal magnesium absorption *in* 'Metal ions in biological systems. Volume 26' *pp* 227-244. Ed. H.Sigel & A.Sigel. Marcel Dekker Inc. New York & Basel.

Ebel , H. & Günther, T. (1980). Magnesium Metabolism: A Review. *J.Clin.Chem.Clin.Biochem.*, **18**, 257-270

Ellory, J.C., Flatman, P.W. & Stewart, G.W. (1983). Inhibition of human red cell sodium and potassium transport by divalent cations. *J.Physiol.*, **340**, 1-17.

Erdos, J.J. & Maguire, M.E. (1983). Hormone-sensitive magnesium transport in murine S49 lymphoma cells: characterization and specificity for magnesium. *J.Physiol.*, **337**, 351-371.

Féray, J-C. & Garay, R. (1986). An Na^+-stimulated Mg^{2+}-transport system in human red blood cells. *Biochimica et Biophysica Acta*, **856**, 76-84.

Féray, J-C. & Garay, R. (1987). A one-to-one Mg^{2+}:Mn^{2+} exchange in rat erythrocytes. *J.Biol.Chem.* **262**, 5763-5768.

Féray, J-C. & Garay, R. (1988). Demonstration of a Na^+:Mg^{2+} exchange in human red cells by its sensitivity to tricyclic antidepressant drugs. *Naunyn-Schmiedeberg's Arch Pharmacol.*, **338**, 332-337.

Féray, J-C., Franck, G., Garay, R. & Henrotte, J-G. (1989). Inter-individual differences in red cell Mg^{2+} contents are related to the activity of a Na^+:Mg^{2+} exchanger. Possible relationship with HLA-associated genetic factors. *Magnesium research*, **2**, 124.

Flatman, P.W. (1980). The effect of buffer composition and deoxygenation of the concentration of ionized magnesium inside human red blood cells. *J.Physiol.*, **300**, 19-30.

Flatman, P.W. (1983). Sodium and potassium transport in ferret red cells. *J.Physiol.*, **341**, 545-557.

Flatman, P.W. (1984). Magnesium transport across cell membranes. *J.Membrane Biol.*, **80**, 1-14.

Flatman, P.W. (1987). The effects of calcium on potassium transport in ferret red cells. *J.Physiol.*, **386**, 407-423.

Flatman, P.W. (1988). The effects of magnesium on potassium transport in ferret red cells. *J.Physiol.* **397**, 471-487.

Flatman, P.W. (1988). The control of red cell magnesium. *Magnesium Research*, **1**, 5-11.

Flatman, P.W. (1989). Stoichiometry of net sodium and potassium fluxes mediated by the Na-K-Cl co-transport system in ferret red cells. *Q.J.Exp.Physiol.*, **74**, 939-941.

Flatman, P.W. (1991a). The effects of metabolism on Na^+-K^+Cl^- co-transport in ferret red cells. *J.Physiol.*, **437**, 495-510.

Flatman, P.W. (1991b). Mechanisms of magnesium transport. *Annu.Rev.Physiol.*, **53**, 259-271.

Flatman, P.W. (1993). The role of magnesium in regulating ion transport. in 'Magnesium and the Cell' ed. N.J. Birch. Academic Press.

Flatman, P.W. & Andrews, P.L.R. (1983). Cation and ATP content of ferret red cells. *Comp.Biochem.Physiol.*, **74A**, 939-943.

Flatman, P.W. & Lew, V.L. (1977). Use of ionophore A23187 to measure and to control free and bound cytoplasmic Mg in intact red cells. *Nature*, **267**, 360-362.

Flatman, P.W. & Lew, V.L. (1978). The magnesium dependence of sodium-potassium and sodium-sodium exchange mediated by the sodium pump in intact human red cells. *J.Physiol.*, **287**, 33-34P.

Flatman, P.W. & Lew, V.L. (1980). Magnesium buffering in intact human red blood cells measured using the ionophore A23187. *J.Physiol.*, **305**, 13-30.

Flatman, P.W. & Lew, V.L. (1981). The magnesium dependence of sodium-pump-mediated sodium-potassium and sodium-sodium exchange in intact human red cells. *J.Physiol.*, **315**, 421-446.

Flatman, P.W. & Smith, L.M. (1990). Magnesium transport in ferret red cells. *J.Physiol.*, **431**, 11-25.

Flatman, P.W. & Smith, L.M. (1991). Sodium-dependent magnesium uptake by ferret red cells. *J.Physiol.*, **443**, 217-230.

Frelin, C., Vigne, P., Barbry, P. & Lazdunski, M. (1987). Molecular properties of amiloride action and of its Na^+ transporting targets. *Kidney International*, **32**, 785-793.

Frenkel, E.J., Graziani, M. & Schatzmann, H.J. (1989). ATP requirement of the sodium-dependent magnesium extrusion from human red blood cells. *J.Physiol.*, **414**, 385-397.

Freudenrich, C.C., Murphy, E., Liu, S. & Lieberman, M. (1992). Magnesium homeostasis in cardiac cells. *Molecular and Cellular Biochemistry*, **114**, 97-103.

Fry, C.H. (1986). Measurement and control of intracellular magnesium ion concentration in guinea pig and ferret ventricular myocardium. *Magnesium*, **5**, 306-316.

Gill, A., Flaim, S.F., Damiano, B.P., Sit, S.P. & Brannan, M.D. (1992). Pharmacology of bepridil. *Am.J.Cardiol.*, **69**, 11D-16D.

Ginsburg, S., Smith, J.G., Ginsburg, F.M., Reardon, J.Z. & Aikawa, J.K. (1962). Magnesium metabolism of human and rabbit erythrocytes. *Blood*, **20**, 722-729

Gonzalez-Serratos, H and Rasgado-Flores, H. (1990). Extracellular magnesium-dependent sodium efflux in squid giant axons. *Am.J.Physiol.*, **259**, C541-C548.

Gonzalez-Serratos, H., Rasgado-Flores, R., Sjodin A. & Montes, J.G. (1988). Evidence for `reverse mode' Na/Mg exchange in dialyzed giant squid axons. *Biophysical Journal*, **53**, 342a.

Grubbs, R.D. & Maguire, M.E. (1986). Regulation of magnesium but not calcium transport by phorbol ester. *J.Biol.Chem.*, **261**, 12550-12554.

Grynkiewicz, G., Poenie, M. & Tsien, R.Y. (1985). A new generation of Ca^{2+} indicators with greatly improved fluorescence properties. *J.Biol.Chem.*, **260**, 3440-3450.

Günther, T. & Vormann, J. (1985). Mg^{2+} efflux is accomplished by an amiloride-sensitive Na^{+}/Mg^{2+} antiport. *Biochem.Biophys.Res.Comm.*, **130**, 540-545.

Günther, T. & Vormann, J. (1986). Probable role of protein phosphorylation in the regulation of Mg^{2+} efflux via Na^{+}/Mg^{2+} antiport. *Magnesium Bulletin*, **8**, 307-309.

Günther, T. & Vormann, J. (1987). Characterization of Na^+/Mg^{2+} antiport by simultaneous $^{28}Mg^{2+}$ influx. *Biochem.Biophys.Res.Comm.*, **148**, 1069-1074.

Günther, T & Vormann, J. (1989a). Na^+-independent Mg^{2+} efflux from Mg^{2+}-loaded human erythrocytes. *FEBS LETTS.*, **247**, 181-184.

Günther, T. & Vormann, J. (1989b). Characterization of Mg^{2+} efflux from human, rat and chicken erythrocytes. *FEBS LETTS.*, **250**, 633-637.

Günther, T., Vormann, J. & Averdunk, R. (1986). Characterization of furosemide-sensitive Mg^{2+} influx in Yoshida ascites tumor cells. *FEBS LETTS.*, **197**, 297-300.

Günther, T., Vormann, J. & Cragoe,Jr, E.J. (1990). Species-specific Mn^{2+}/Mg^{2+} antiport from Mg^{2+}-loaded erythrocytes. *FEBS LETTS.*, **261**, 47-51.

Günther, T., Vormann, J., Cragoe, Jr, E.J. & Höllriegl, V. (1989). Characterization of Na^+-dependent and Na^+-independent Mg^{2+} efflux from erythrocytes by amiloride derivatives. *Magnesium Bulletin*, **11**, 103-107.

Günther, T., Vormann, J. & Forster, R. (1984). Regulation of intracellular magnesium by Mg^{2+} efflux. *Biochem.Biophys.Res.Comm.*, **119**, 124-131.

Günther, T., Vormann, J. & Höllriegl, V. (1990). Characterization of Na^+-dependent Mg^{2+} efflux from Mg^{2+}-loaded rat erythrocytes. *Biochimica et Biophysica Acta*, **1023**, 455-461.

Gupta, R.K., Benovic, J.L. & Rose, Z.B. (1978). Magnetic resonance studies of the binding of ATP and cations to human hemoglobin. *J.Biol.Chem.*, **253**, 6165-6172.

Gupta, R.K. & Moore, R.D. (1980). ^{31}P NMR studies of intracellular free Mg^{2+} in intact frog skeletal muscle. *J.Biol.Chem.*, **255**, 3987-3993.

Halestrap, A.P. (1976). Transport of pyruvate and lactate into human erythrocytes. *Biochem.J.*, **156**, 193-207.

Halperin, J.A., Brugnara, C., Tosteson, M.T., Van Ha, T. & Tosteson, D.C. (1989). Voltage-activated cation transport in human erythrocytes. *Am.J.Physiol.*, **257**, C986-C996.

Harman, A.W., Nieminen, A-L., Lemasters, J.l. & Herman, B. (1990). Cytosolic free magnesium, ATP, and blebbing during chemical hypoxia in cultured rat hepatocytes. *Biochem.Biophys.Res.Comm.*, **170**, 477-483.

Heaton, F.W. (1967). The determination of ionized magnesium in serum and urine. *Clin.Chem.Acta.*, **15**, 139-144.

Heaton, F.W. (1993). Distribution and function of magnesium within the cell. *in* 'Magnesium and the cell.' *pp* 121-136. Ed. N.J.Birch. Academic Press.

Heaton, F.W., Tongyai, S., Motta, C., Rayssiguier, Y. & Gueux, E. (1987). Changes in the erythrocyte membrane during magnesium deficiency. *Nutrition Research*, **7**, 655-663.

Henrotte, J.G. & Franck, G. (1990). Plasma factor(s) inhibiting cell magnesium efflux rapidly determined with a biological assay. *Clin.Chem.*, **36**, 1859-1860.

Henrotte (1993) Genetic regulation of cellular magnesium content *in* 'Magnesium and the cell.' *pp* 177-196 Ed. N.J. Birch. Academic Press.

Hess, P., Metzger, P. & Weingart, R. (1982). Free magnesium in sheep, ferret and frog striated muscle at rest meaasured with ion-selective micro-electrodes. *J.Physiol.*, **333**, 173-188.

Hille, B. (1984). 'Ionic Channels of Excitable Membranes.' Sinauer Associates Inc. Sunderland Massachusetts.

Hmiel, S.P., Snavely, M.D., Miller, C.G. & Maguire, M.E. (1986). Magnesium transport in *Salmonella typhimurium*: Characterization of magnesium influx and cloning of a transport gene. *J.Bacteriol.*, **168**, 1444-1450.

Houslay, M.D. & Stanley, K.K. (1982). 'Dynamics of Biological Membranes.' A Wiley-Interscience publication. John Wiley & sons, 1982.

Iseri, L.T. & French, J.H. (1984). Magnesium: Nature's physiologic calcium blocker. *Am.Heart.J.*, **108**, 188-193.

Jarvis, S.M., McBride, D. & Young, J.D. (1982). Erythrocyte nucleoside transport: asymmetrical binding of nitrobenzylthioinosine to nucleoside permeation sites. *J.Physiol.*, **324**, 31-46.

Jelicks, L.A., Weaver, J., Pollack, S. & Gupta, R.K. (1989). NMR studies of intracellular free calcium, free magnesium and sodium in the guinea pig reticulocyte and mature red cell. *Biochimica et Biophysica Acta*, **1012**, 261-266.

Kaczorowski, G.J., Garcia, M.L., King, F. & Slaughter, R.S. (1989). Developement and use of inhibitors to study sodium-calcium exchange. *in* 'Sodium-Calcium Exchange.' Ed. T.Jeff A. Allen, Denis Noble and Harald Reuter. Oxford University Press, 1989.

Kleyman, T.R. & Cragoe Jr., E.J. (1990). Cation transport probes: the amioride series. *Methods in Enzymology*, **191**, 739-154.

Kobayashi, E., Nakano, H., Morimoto, M. & Tamaoki, T. (1989). Calphostin C (UCN-1028C), a novel microbial compound, is a highly potent and specific inhibitor of protein kinase C. *Biochem.Biophys.Res Comm.*, **159**, 548-553.

Kohlhardt, M., Bauer, B., Krause, H. & Fleckenstein, A. (1972). New selective inhibitors of the transmembrane Ca conductivity in mammalian myocardial fibres. Studies with the voltage clamp technique. *Experientia*, **28**, 288-289.

Kumamoto, J., Raison, J.K. & Lyons, J.M. (1971). Temperature `Breaks' in Arrhenius plots: A thermodynamic consequence of a phase change. *J.theor.Biol.*, **31**, 47-51.

Levitan, I.B. (1985). Phosphorylation of ion channels. *J.Membrane Biol.*, **87**, 177-190.

London, R.E. (1991). Methods for measurememt of intracellular magnesium: NMR and fluorescence. *Annu.Rev.Physiol.*, **53**, 241-258

Lopez, J.R., Alamo, L., Caputo, C., Vergara, J. & DiPolo, R. (1984). Direct measurement of intracellular free magnesium in frog skeletal muscle using magnesium-selective microelectrodes. *Biochimica et Biophysica Acta*, **804**, 1-7.

Lüdi, H. & Schatzmann, H.J. (1987). Some properties of a system for sodium-dependent outward movement of magnesium from metabolizing human red blood cells. *J.Physiol.*, **390**, 367-382.

Lusk, J.E. & Kennedy, E.P. (1969). Magnesium transport in *Escherichia coli*. *J.Biol.Chem.*, **244**, 1653-1655.

Macara, I.G. (1980). Vanadium-an element in search of a role. *Trends in Biochem. Sci.*, **5**, 92-94.

Macey, R.I., Adorante, J.S. & Orme, F.W. (1978). Erythrocyte membrane potentials determined by hydrogen ion distribution. *Biochimica et Biophysica Acta*, **512**, 284-295.

McGuigan,J.A.S., Buri,A., Chen,S., Illner,H & Lüthi,D. (1993). Some theoretical and practical aspects of the measurement of the intracellular free magnesium concentration in heart muscle: Consideration of its regulation and modulation. in 'Magnesium and the Cell' Ed. N.J.Birch, 1993. Academic Press.

Mairbäurl, H. & Hoffman, J.F. (1992). Internal magnesium, 2,3-diphosphoglycerate, and the regulation of the steady-state volume of human red blood cells by the Na/K/2Cl cotransport system. *J.Gen.Physiol.*, **99**, 721-746.

Milanick, M.M. (1989). Na-Ca exchange in ferret red blood cells. *Am.J.Physiol.*, **256**, C390-C398.

Montes, J.G., Sjodin, A., Gonzalez-Serratos, H. & Rasgado-Flores, H. (1988). Evidence for potassium-activated magnesium extrusion in barnacle muscle. *Biophysical Journal*, **53**, 344a.

Mullins, L.J., Brinley, F.J., Spangler, S.G. & Abercrombie, R.F. (1977). Magnesium efflux in dialyzed squid axons. *J.Gen.Physiol.*, **69**. 389-400.

Murphy, E., Freudenrich, C.C., Levy, L.A., London, R.E. & Lieberman, M. (1989). Monitoring cytosolic free magnesium in cultured chicken heart cells by use of the fluorescent indicator Furaptra. *Proc. Natl.Acad.Sci.*, **86**, 2981-2984.

Murphy, E., Freudenrich, C.C. & Lieberman, M. (1991). Cellular magnesium and Na/Mg exchange in heart cells. *Annu.Rev.Physiol.*, **53**, 273-287.

Murphy, J.R. (1960). Erythrocyte metabolism. II. Glucose metabolism and pathways. *J.Lab.Clin.Med.*, **55**, 286-302.

Nakayama, S. & Tomita, T. (1990). Intracellular free magnesium concentration in the taenia isolated from guinea-pig caecum. *in* 'Frontiers in Smooth Muscle Research' *pp* 345-349. Alan R. Liss, Inc, 1990.

Nakayama, S. & Tomita, T. (1991). Regulation of intracellular free magnesium concentration in the taenia of guinea-pig caecum. *J.Physiol.*, **435**, 559-572.

Nanninga, L.B. (1961). Calculation of free magnesium, calcium and potassium in muscle. *Biochim.Biophys.Acta.*, **54**, 338-344.

Nechay, B.R., Nanninga, L.B., Nechay, P.S.E., Post, R.L., Grantham, J.J., Macara, I.G., Kubena, P.S.E., Phillips, T.D. & Nielsen, F.H. (1986). Role of vanadium in biology. *Fed.Proc.*, **45**, 123-132.

Nelson, D.L. & Kennedy, E.P. (1971). Magnesium transport in *Escherichia coli*. *J.Biol.Chem.*, **246**, 3042-3049.

Nishimura, H., Matsubara, T., Ikoma, Y., Nakayama, S. & Sakamoto, N. (1993). Effects of prolonged application of isoprenaline on intracellular free magnesium concentration in isolated heart of rat. *Br.J.Pharmacol.*, **109**, 443-448.

Nishizuka, Y. (1984). The role of protein kinase C in cell surface signal transduction and tumour production. *Nature*, **308**, 693-698.

Page, E. & Polimeni, P.I. (1972). Magnesium exchange in rat ventricle. *J.Physiol.*, **224**, 121-139.

Parker, J.C., Gitelman, H.J. & McManus, T.J. (1989). Role of Mg in the activation of Na-H exchange in dog red cells. *Am.J.Physiol.*, **257**, C1038-C1041.

Quamme, G.A. & Dai, L-J. (1990). Presence of a novel influx pathway for Mg^{2+} in MDCK cells. *Am.J.Physiol.*, **259**, C521-C525.

Quamme, G.A. & de Rouffignac, C. (1993). Transport of magnesium in renal epithelial cells. *in* 'Magnesium and the Cell' Ed. N.J. Birch. Academic Press, 1993.

Quamme, G.A. & Rabkin, S.W. (1990). Cytosolic free magnesium in cardiac myocytes: Identification of a Mg^{2+} influx pathway. *Biochem.Biophysis.Res.Comm.*, **167**, 1406-1412.

Raju, B., Murphy, E., Levy, L.A., Hall, R.D. & London, R.E. (1989). A fluorescent indicator for measuring cytosolic free magnesium. *Am.J.Physiol.*, **256**, C540-C548.

Reed, P.W. & Lardy, H.A. (1972). A23187: A divalent cation ionophore. *J.Biol.Chem.*, **247**, 6970-6977.

Rink, T.J., Tsien, R.Y. & Pozzan, T. (1982). Cytoplasmic pH and free Mg^{2+} in lymphocytes. *J.Cell.Biol.*, **95**, 189-196.

Rogers, T.A. (1961). The exchange of radioactive magnesium in erythrocytes of several species. *J.Cell.Comp.Physiol.*, **57**, 119-121.

Romani, A., Dowell, E. & Scarpa, A. (1991). Cyclic AMP-induced Mg^{2+} release from rat liver hepatocytes, permeabilized hepatocytes, and isolated mitochondria. *J.Biol.Chem.*, **266**, 24376-24384.

Romani, A., Marfella, C. Scarpa, A. (1993). Regulation of magnesium uptake and release in the heart and in isolated ventricular myocytes. *Circulation Res.*, **72**, 1139-1148.

Romani, A. & Scarpa, A. (1990a). Norepinephrine evokes a marked Mg^{2+} efflux from liver cells. *FEBS LETTS.*, **269**, 37-40

Romani, A. & Scarpa, A. (1990b). Hormonal control of Mg^{2+} transport in the heart. *Nature* **346**, 841-844.

Romani, A. & Scarpa, A. (1992). Regulation of cell magnesium. *Archives of Biochemistry and Biophysics*, **298**, 1-12.

Rouilly, M., Rusterholz, B., Spichiger, U.E. & Simon, W. (1990). Neutral ionophore-based selective electrode for assaying the activity of magnesium in undiluted blood serum. *Clin.Chem.*, **36**, 466-469.

Ryan, M.P. (1990). The renal handling of magnesium. *in* 'Metal ions in biological systems. Volume 26.' *pp* 249-264. Ed. H.Sigel & A. Sigel. Marcel Dekker Inc. New York & Basel.

Sachs, C., Ritter, C., Ghahramani, M., Spichiger, U., Kindermans, C., & Marsoner, H.J. (1993). Measurement of ionized magnesium by ISE. *Magnesium Research*, **6**, 59.

Scarpa, A. (1974). Indicators of free magnesium in biological systems. *Biochemistry*, **13**, 2789-2794.

Scarpa, A. & Brinley, F.J. (1981). In situ measurememts of free cytosolic magnesium ions. *Federation Proc.*, **40**, 2646-2652.

Schachter, M., Gallagher, K.L. & Sever, P.S. (1990). Measurement of intracellular magnesium in a vascular smmooth muscle cell line using a fluorescent probe. *Biochimica et Biophysica Acta*, **1035**, 378-380.

Schatzmann, H.J. (1983). The red cell calcium pump. *Ann.Rev.Physiol.*, **45**, 303-312.

Schatzmann, H.J. (1993). Asymmetry of the magnesium sodium exchange across the human red cell membrane. *Biochimica et Biophysica Acta*, **1148**, 15-18.

Schmid-Antomarchi, H., De Weille, J., Fosset, M. & Lazdunski, M. (1987). The receptor for antidiabetic sulfonylureas controls the activity of the ATP-modulated K^+ channel in insulin-secreting cells. *J.Biol.Chem.*, **262**, 15840-15844.

Sha'afi, R.I. & Hajjar, J.J. (1971). Sodium movement in high sodium feline red cells. *J.Gen.Physiol.*, **57**, 684-696.

Sillén, L.G. & Martell, A.E. (1971). Stability constants of metal-ion complexes. The Chemical Society Special Publication No.25. Supplement No.1 to Special Publication No.17. London: The Chemical Society.

Simchowitz, L. & Cragoe Jr.,E.J. (1986). Inhibition of chemotactic factor-activated Na^+/H^+ exchange in human neutophils by analogues of amiloride: structure-activity relationships in the amiloride series. *Molecular Pharmacology*, **30**, 112-120

Simonsen, L.O., Gomme, J. & Lew, V.L. (1982). Uniform ionophore A23187 distribution and cytoplasmic calcium buffering in intact human red cells. *Biochimica et Biophysica Acta*, **692**, 431-440.

Simonsen, L.O. & Lew, V.L. (1980) The correlation between ionophore A23187 content and calcium premeability of ATP-depleted human red blood cells. *In* 'Membrane Transport in Erythrocytes, Alfred Benzon Symposium 14.' Ed. U.V. Lassen, H.H. Ussing & J.O. Wieth, Munksgaard, Copenhagen 1980.

Stewart, G.W., Ellory, J.C. & Klein, R.A. (1980). Increased human red cell cation passive permeability below 12°C. *Nature*, **286**, 403-404.

Thornton, P.C., Wright, P.A., Sacra, P.J. & Goodier, T.E.W. (1979). The ferret *Mustela putorius furo*, as a new species in toxicology. *Laboratory Animals*, **13**, 119-124.

Tsien, R.Y. (1983). Intracellular measurements of ion activities. *Ann.Rev.Biophys.Bioeng.*, **12**, 91-116.

Tsien, R.Y. (1989). Fluorescent probes of cell signaling. *Ann.Rev.Neurosci.*, **12**, 227-53.

Tomov, T.Ch., Tsoneva, I.Ch. & Doncheva, J.Ch. (1988). Electrical stability of erythrocytes in the presence of divalent cations. *Bioscience Reports*, **8**, 421-426.

van Breemen, C. & De Weer, P. (1970). Lanthanum inhibition of ^{45}Ca efflux from the squid giant axon. *Nature (Lond.)*, **226**, 760-761.

Wacker, Warren E.C. (1980). 'Magnesium and Man.' Harvard University Press.

Wacker, W.E.C. (1969). The biochemistry of magnesium. *Ann.N.Y.Acad.Sci.*, **162**, 717-726.

Walser, M. (1961). Ion association. VI. Interactions between calcium, magnesium, inorganic phosphate, citrate and protein in normal human plasma. *J.Clin.Invest.*, **40**, 723-729

Walser, M. (1967). Magnesium Metabolism. *Ergeben. Physiol.*, **59**, 185-296.

Walsh, A. (1955). The application of atomic absorption spectra to chemical analysis. *Spectrochimica Acta*, **7**, 108-117.

Whittam, R. (1964). 'Transport and diffusion in Red Blood Cells.' Edward Arnold (Publishers) Ltd.

Wiater, L.A. & Dunham, P.B. (1983). Passive transport of K^+ and Na^+ in human red blood cells: sulfhydryl binding agents and furosemide. *Am.J.Physiol.*, **245**, C348-C356.

Wiley, J.S. & Shaller, C.C. (1977). Selective loss of calcium permeability on maturation of reticulocytes. *J.Clin.Invest.*, **59**, 1113-1119

Williams, R.J.P. (1993). Magnesium: An introduction to its biochemistry. *in* 'Magnesium and the cell. ed. N.J. Birch, Academic press, 1993.

Willis, J.S., Xu, W. & Zhao, Z. (1992). Diversities of transport of sodium in rodent red cells. *Comp.Biochem.Physiol.*, **102A**, 609-614.

Wu, S.T., Pieper, G.M., Salhany, J.M. & Eliot, R.S. (1981). Measurement of free magnesium in perfused and ischaemic arrested heart muscle. A quantitative phosphorus-31 nuclear magnetic resonance and multiequilibria analysis. *Biochemistry*, **20**, 7399-7403.

Xu, W. & Willis, J.S. (1991). Amiloride-sensitive Na influx in hamster red cells is due to Na-Mg exchange. *FASEBJ*, **5**, A686 (1853).

Zhao, Z. & Willis, J.S. (1993). Cold activation of Na influx through the Na-H exchange pathway in guinea pig red cells. *J.Membrane Biol.*, **131**, 43-53.

APPENDIX

Parts of the work described in this thesis have appeared in the publications listed below. Copies of the papers appearing in the Journal of Physiology are attached.

Flatman, P.W. & Smith, L.M. (1990). Magnesium transport in red cells. Magnesium Research **3**, 63.

Flatman, P.W. & Smith, L.M. (1990). Magnesium transport in ferret red cells. Journal of Physiology **431**, 11-25.

Flatman, P.W. & Smith, L.M. (1991). Magnesium transport in red cells. In "Magnesium, a relevant ion", pp 191-199. Ed. Lassere,B. & Durlach,J. London: John Libbey.

Flatman, P.W. & Smith, L.M. (1991). Sodium-dependent magnesium uptake by ferret red cells. Journal of Physiology **443**, 217-230.

Flatman, P.W. & Smith, L.M. (1993). Sodium-dependent magnesium transport in ferret red cells. Abstracts of the 32nd Congress of the International Union of Physiological Sciences, 221.1/O.

Journal of Physiology (1990), **431**, *pp.* 11–25
With 10 figures
Printed in Great Britain

MAGNESIUM TRANSPORT IN FERRET RED CELLS

BY PETER W. FLATMAN AND LORRAINE M. SMITH
From the Department of Physiology, University Medical School, Teviot Place, Edinburgh EH8 9AG

(*Received 19 April 1990*)

SUMMARY

1. Mg^{2+} efflux from ferret red cells into a nominally Mg^{2+}-free medium is 41 ± 2 μmol (l cell)$^{-1}$ h^{-1}. The properties of Mg^{2+} transport can be measured in these cells without the need for Mg^{2+} loading.

2. Amiloride, quinidine, imipramine and external divalent cations partially inhibit Mg^{2+} efflux. Maximal inhibition by these agents is about 60–70% suggesting that at least two Mg^{2+} transport pathways exist.

3. As external Na^+ is replaced by choline or *N*-methyl-D-glucamine Mg^{2+} efflux is first stimulated, reaching a peak when external [Na^+] ($[Na^+]_o$) is about 10 mM, and then inhibited. Mg^{2+} transport reverses direction so net Mg^{2+} uptake occurs when $[Na^+]_o$ is reduced below 1 mM.

4. Mg^{2+} efflux is stimulated when 0·1 mM-EDTA is added to the medium only when $[Na^+]_o$ is low.

5. Reduction of cell ATP content to about 20 μmol (l cell)$^{-1}$ by treating cells with 2-deoxyglucose stimulates Mg^{2+} efflux measured over the 2 h period following depletion.

6. Substantial Mg^{2+} influx can be observed in ferret red cells when they are incubated in media containing 10 mM-Mg^{2+}. Influx is stimulated by reducing $[Na^+]_o$ to 10 mM. Further reduction of $[Na^+]_o$ to below 1 mM reduces Mg^{2+} uptake. A component of uptake is inhibited by external Co^{2+}.

7. Na^+–Mg^{2+} antiport may account for a substantial component of Mg^{2+} transport in ferret red cells. The direction of transport can be reversed by sufficiently lowering $[Na^+]_o$ or by increasing external [Mg^{2+}]. Analysis of the conditions at which transport reverses direction suggests transport with a stoichiometry of 1 Na^+:1 Mg^{2+}. Antiport with this stoichiometry would also explain maintenance of the physiological level of intracellular ionized Mg^{2+} in these cells.

INTRODUCTION

Intracellular ionized Mg ($[Mg^{2+}]_i$) is maintained below electrochemical equilibrium with external ionized Mg ($[Mg^{2+}]_o$), and cell Mg content probably falls with age in human red cells. These observations suggest the presence of a system capable of active Mg^{2+} extrusion (Flatman & Lew, 1980; see Flatman, 1988*a*). This prediction was confirmed by Féray & Garay (1986) and Lüdi & Schatzmann (1987) who

MS 8427

demonstrated that human red cells contain a Na^+-dependent Mg^{2+} transport system capable of moving Mg^{2+} out of the cells against a considerable electrochemical gradient. In order to study transport characteristics the cells had to be loaded with Mg^{2+} using either parachloromercuribenzene sulphonate (PCMBS) or A23187 as Mg^{2+} fluxes in these cells are very small at physiological $[Mg^{2+}]_i$. The system is activated by external Na^+ ($[Na^+]_o$) with a $K_{\frac{1}{2}}$ of about 16–20 mM (Féray & Garay, 1986; Lüdi & Schatzmann, 1987) which may be transported into the cell in exchange for Mg^{2+} (Féray & Garay, 1988). It is also activated by $[Mg^{2+}]_i$ either binding to a single site with a $K_{\frac{1}{2}}$ of 2·6 mM (Féray & Garay, 1986) or binding to two or more sites with a $K_{\frac{1}{2}}$ of 1·3 mM (Lüdi & Schatzmann, 1987). Mg^{2+} efflux is reduced by metabolic depletion (Féray & Garay, 1986; Lüdi & Schatzmann, 1987) and is activated by internal ATP with a $K_{\frac{1}{2}}$ of 0·15 mmol (l cells)$^{-1}$ (Frenkel, Graziani & Schatzmann, 1989). Non-hydrolysable analogues of ATP such as adenylyl (β, γ-methylene) diphosphonate do not support Mg^{2+} extrusion indicating that ATP hydrolysis is necessary to activate transport (Frenkel *et al.* 1989).

On the surface these observations suggest that Mg^{2+} efflux occurs via a Na^+–Mg^{2+} antiport, which obtains energy for active Mg^{2+} transport from the transmembrane Na^+ gradient, and is activated by phosphorylation. In addition, Na^+–Mg^{2+} antiport with a stoichiometry of 1 Na^+:1 Mg^{2+} could provide more than enough energy to maintain $[Mg^{2+}]_i$ at the physiological level. However, there is evidence that the Na^+ gradient may not supply the energy needed. Reversal of the Na^+ gradient reduces but does not reverse the direction of Mg^{2+} movement (Lüdi & Schatzmann, 1987) and abolition of the Na^+ gradient produces a rather small change in Mg^{2+} efflux rate (Frenkel *et al.* 1989). Frenkel *et al.* (1989) suggest that at least part of the energy for Mg^{2+} transport is provided by a linked chemical reaction, for instance the hydrolysis of ATP or some other high energy source. These findings appear to favour a Mg^{2+} pump though it is not clear why the pump should fruitlessly dissipate the Na^+ gradient. A similar Na^+-dependent Mg^{2+} transport system has been reported in chicken red cells (Günther, Vormann & Förster, 1984; Günther & Vormann, 1985, 1987) where again it appears that the Na^+ gradient does not supply the energy for transport. A Na^+- and ATP-dependent Mg^{2+} transport system has recently been reported in rat red cells (Féray & Garay, 1987).

Experiments on the energetics of transport in human and chicken red cells were carried out on cells pretreated with PCMBS (Günther & Vormann, 1985; Lüdi & Schatzmann, 1987; Frenkel *et al.* 1989). As the effects of this reagent may not be entirely reversible the transporter's properties may have been altered. In this paper we will demonstrate that Mg^{2+} fluxes in ferret red cells are large enough to study in cells which have not been previously treated with A23187 or PCMBS. In addition it is possible to exploit these cells' high Na^+ content (Flatman & Andrews, 1983) to explore aspects of the system not easily studied in other red cells. We will show that the properties of Mg^{2+} transport in ferret red cells are consistent with Na^+:Mg^{2+} antiport and that the physiological $[Mg^{2+}]_i$ in these cells can be explained by an antiport transporting a single Na^+ ion with each Mg^{2+} ion. A preliminary account of this work was given to the 3rd European Congress on Magnesium (Flatman & Smith, 1990).

METHODS

Blood samples were taken into EDTA from adult ferrets anaesthetized with intraperitoneal urethane, 1·5 g kg^{-1} body weight. Red cells were washed by centrifugation and resuspension in an ice-cold medium (FBM: 145 mM-NaCl, 5 mM-KCl, 10 mM-Na–HEPES buffer, pH 7·5 at 38 °C) containing 0·05 mM-Tris–EGTA. Cells were stored packed in this medium at about 70% haematocrit at 5 °C until used (usually the day after collection). All tubes had been sterilized with ethanol and all solutions were passed through a 0·22 μm filter before use. Unless otherwise stated, flux experiments were carried out at 38 °C with cells suspended at 5–8% haematocrit. Haematocrit, cell lysis and original cell volume were usually calculated from the absorbance at 540 nm of samples diluted in Van Kampen & Ziljstra's reagent, assuming a packed cell absorbance of 230 (Flatman & Andrews, 1983). Samples containing Co^{2+} or Mn^{2+} were diluted in 0·05% Triton X-100 as these ions interfere with the determination in Van Kampen & Ziljstra's reagent. The packed cell absorbance in Triton was 285 ± 1 ($n = 14$).

Cell Mg content ($[Mg]_i$) was measured after the cells had been separated from the medium by rapid centrifugation through di-*n*-butylphthalate following the method of Flatman & Lew (1980) with the following modification. The cell pellet was lysed in 1·19 ml distilled water. Mg was measured in this lysate by atomic absorption spectroscopy (AAS) with background correction. Controls showed that the omission of trichloracetic acid from the procedure does not affect measured levels. Cell Na and K were measured in a similar way. A 0·1 ml suspension was transferred to a 1·4 ml centrifuge tube containing 1·0 ml ice-cold 150 mM-choline chloride, 0·1 mM-bumetanide and 0·3 ml-di-*n*-butylphthalate. The tube was capped, shaken and then spun at 15000 *g* for 1 min to reduce the extracellular space in the pellet to a reproducible 2%. After removal of the supernatant and oil and the cleaning of the tube walls, the pellets were lysed in 1·2 ml distilled water containing 1 g l^{-1} LiCl. Na and K were measured in these lysates by AAS against standards prepared in LiCl. Mg, Na and K in the medium were measured by AAS after suitable dilution with distilled water or LiCl. Cell ATP was measured by the fire-fly assay as described previously (Flatman, 1988*b*).

Mg^{2+} fluxes were usually measured as the appearance of Mg in the external medium. The fluxes are small and need to be carefully corrected for Mg lost into the medium by lysis and for any changes in concentration due to evaporation. The following protocol was therefore adopted. At each time point samples were taken to measure haematocrit and cell Mg content. A sample was also transferred to a centrifuge tube and spun at 15000 *g* for 30 s. The supernatant was transferred to a separate tube taking great care not to disturb the cell pellet. Aliquots of the supernatant were used to determine external Mg, Na and K concentrations and the degree of lysis. The amount of Mg released by lysis was calculated from:

$$[Mg]_{lysis} = [Mg]_i(hct_2/(1-hct_1+hct_2)),$$

where hct_1 and hct_2 are the apparent haematocrits of the total suspension and supernatant and $[Mg]_i$ is the cell Mg content. The calculation assumes that cells which lyse have the same Mg content as the average population and that these cells lose all their Mg on lysis. The Mg^{2+} efflux was then calculated from the slope of the line relating $[Mg]_o$ to time. The fluxes are expressed per litre of original cells.

Solutions were prepared in double glass-distilled water with Analar grade reagents (BDH Ltd, Poole) where possible. HEPES, Tris base, EGTA, *N*-methyl-D-glucamine (NMDG), ouabain, EDTA, imipramine, quinidine, Triton X-100 and choline chloride were obtained from Sigma Chemical Co. Ltd. Choline chloride was recrystallized from ethanol before use. Bumetanide and amiloride were gifts from Leo Laboratories Ltd (Aylesbury) and Merck, Sharp & Dohme Ltd (Hoddesdon) respectively. Purified fire-fly enzyme was obtained from LKB Ltd (Turku, Finland) (product 1243–200). All plastic tubes used in the preparation of samples for AAS were soaked in dilute nitric acid and then rinsed several times with double distilled water before use.

RESULTS

Mg^{2+} efflux from fed, intact ferret red cells incubated in a medium containing physiological concentrations of Na^+ and K^+ but no added Mg^{2+} is shown in Fig. 1.

Figure 1*A* shows accumulation of Mg in the medium and has been corrected for Mg release due to cell lysis. Mg^{2+} efflux, 39 μmol (l cell^{-1}) h^{-1} in this experiment, is constant over the 5 h period. Mg^{2+} efflux can also be determined from the change in $[Mg]_i$ as shown in Fig. 1*B*. Although both methods give comparable results over a

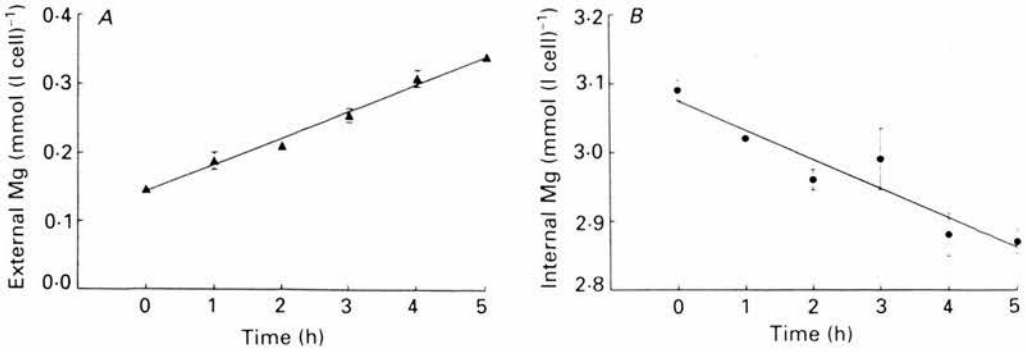

Fig. 1. Mg^{2+} fluxes in fed, intact ferret red cells. Points show the mean of three measurements with S.E.M. if this is larger than point size. Lines are drawn through data by linear regression analysis. Mg^{2+} efflux is obtained from the slope (±S.E. slope, $n = 18$). *A* shows the accumulation of Mg in the medium expressed in terms of the volume of cells in the suspension. The data have been corrected for Mg released by cell lysis which was 0·30% initially and increased linearly to 0·74% after 5 h. Mg^{2+} efflux is 39±2 μmol (l cell)$^{-1}$ h^{-1}. *B* shows $[Mg]_i$ plotted as a function of time for the same experiment. Mg^{2+} efflux is 42±7 μmol (l cell)$^{-1}$ h^{-1}.

5 h period (in six experiments the ratio of fluxes obtained by following $[Mg]_i$ or $[Mg]_o$ was 1:1·01±0·17 (S.E.M.)), it is not possible to determine fluxes accurately over 0·5 or 1 h periods by following $[Mg]_i$. In many experiments it was necessary to measure Mg^{2+} fluxes quickly so Mg^{2+} fluxes were usually estimated from the accumulation of extracellular Mg. This method has the drawback that it is not possible to examine the effects of $[Mg^{2+}]_o$ on transport.

Mg^{2+} efflux from ferret red cells into a nominally Mg^{2+}-free medium shows little variation between individuals (42±2 μmol (l cell)$^{-1}$ h^{-1}. mean±S.E.M., $n = 22$ ferrets). No significant difference could be found between fluxes in cells from males and females or from fitch and albino ferrets (Table 1A). Storage of blood in FBM at 5 °C for up to 21 days has no discernible effect on efflux (Table 1B).

Figure 2*A* shows that Mg^{2+} efflux increases slowly as temperature is increased from 25–40 °C. In a separate experiment measurement of efflux at intervals of 2–3 °C between 30 and 42 °C shows that flux increases rapidly above 40 °C. An Arrhenius plot of the data (Fig. 2*B*) yields an activation energy of only 24 kJ mol^{-1} between 25 and 40 °C.

In order to compare the properties of Mg^{2+} transport in ferret red cells with those of Mg^{2+} transport in other red cells the effects of external divalent cations and a range of transporter inhibitors were tested. Figure 3 shows that Mg^{2+} efflux is inhibited by the presence of other divalent cations in the medium. The most effective is Co^{2+} which inhibits about 55% of the flux at a concentration of 1 mM. Figure 3 also shows the effects of various transport inhibitors. High concentrations (0·5 mM) of ouabain

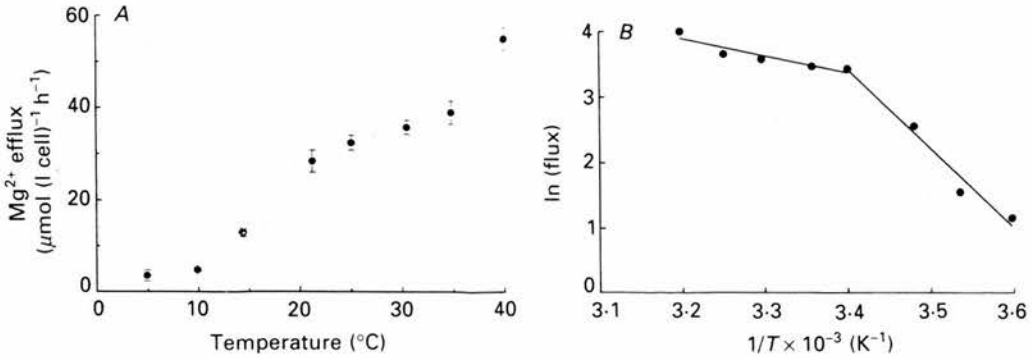

Fig. 2. Temperature dependence of Mg^{2+} efflux. *A*, points represent the mean (±S.E.M.) of three measurements of Mg^{2+} efflux at each temperature (*T*). The pHs of the suspensions were adjusted to 7·5 at each temperature by addition of HCl. Fluxes were measured over the following times: 5–15 °C, 2 h; 20–30 °C, 1 h; above 30 °C, 30 min. *B*, Arrhenius plot of data shown in *A*. The data are best fitted by assuming that there is a break at 25 °C. Activation energies (with standard errors) calculated from the slopes (and standard errors of the slopes) of these lines by linear regression analysis are: 5–25 °C, 96±11 kJ mol^{-1} and 25–40 °C, 25±4 kJ mol^{-1}.

TABLE 1. Mg^{2+} fluxes in ferret red cells

A

	Mg^{2+} flux (μmol (l cell)$^{-1}$ h^{-1})	
	Male	Female
Albino	41±3 (n = 5)	46±5 (n = 7)
Fitch	31±3 (n = 2)	39±5 (n = 8)

B

Days in storage	Mg^{2+} flux (μmol (l cell)$^{-1}$ h^{-1})
1	41±2 (n = 22)
2	37±3 (n = 5)
3	46±11 (n = 4)
8	39
11	34
21	45

A, Mg^{2+} efflux from ferret red cells incubated at 38 °C in FBM on the day after collection. Values given are the mean±S.E.M. with the number of ferrets in brackets. B shows the effects of storage of cells in FBM at 5 °C on mean Mg^{2+} efflux measured at 38 °C. For the longer storage periods only data from single ferrets are available.

and bumetanide do not affect Mg^{2+} efflux. However, amiloride, quinidine and imipramine, all of which inhibit Mg^{2+} efflux in other red cells, produe substantial inhibition in ferret red cells too. Quinine (0·5 mM) reduces transport to 64±5% (S.E.M., n = 4) of control. The anion exchange inhibitor 4-acetamido-4′-isothiocyanatostilbene-2,2′-disulphonic acid (SITS) stimulates Mg^{2+} efflux by about 23%. Neither 0·3 mM-α-cyano-4-hydroxycinnamate (which inhibits lactate and pyruvate transport (Aronson, 1989)) nor 10 nM-*S*-(*p*-nitrobenzyl)-6-thioinosine (which inhibits ATP efflux from human red cells (Bergfeld & Forrester, 1989)) had any significant effect on Mg^{2+} transport.

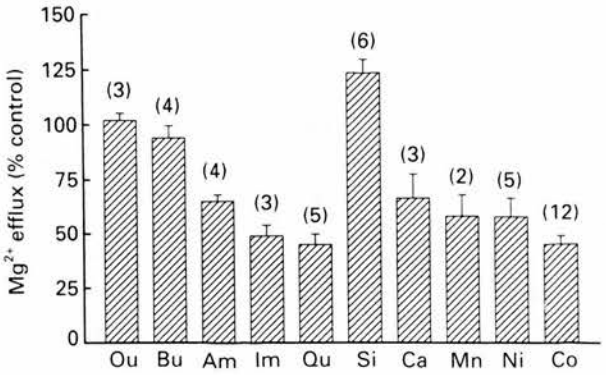

Fig. 3. Effect of divalent cations and transport inhibitors on Mg^{2+} efflux. Mg^{2+} efflux was measured into FBM containing (mM): ouabain (Ou), 0·5; bumetanide (Bu), 0·5; amiloride (Am), 1; imipramine (Im), 0·5; quinidine (Qu), 0·5; SITS (Si), 0·1. $CaCl_2$ (Ca), 1; $MnCl_2$ (Mn), 1; $NiCl_2$ (Ni), 1; $CoCl_2$ (Co), 1. Each bar represents the mean with S.E.M. (n) of the fluxes in the presence of the agent expressed as percentages of the control fluxes.

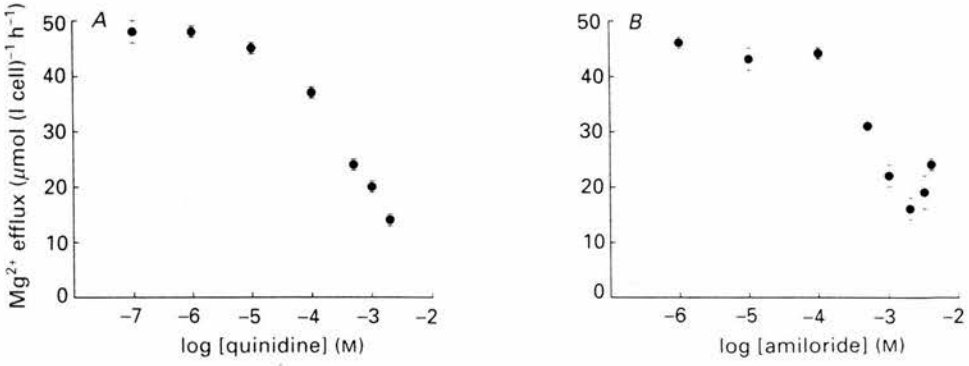

Fig. 4. Mg^{2+} efflux plotted as a function of quinidine (*A*) and amiloride (*B*) concentrations. Fluxes were measured over a 2 h period and the points show the mean of three measurements with S.E.M. if this is larger than point size. Control fluxes in the absence of quinidine and amiloride were 45 ± 2 and 39 ± 5 μmol (l cell)$^{-1}$ h^{-1} respectively. At the end of the experiment lysis was less than 0·7% with the quinidine concentrations shown. It was less than 2% when 1 mM or less amiloride was present but rose to 4 or 6% when 2 or 4 mM-amiloride were present.

Both quinidine and amiloride have been used to define components of Mg^{2+} transport in red cells. Their effects in ferret red cells are shown in Fig. 4. Quinidine in concentrations from 10^{-7} to 10^{-5} M has little effect on transport. At concentrations above 10^{-5} M, quinidine inhibits transport with maximal inhibition (70%) occurring at 2 mM (Fig. 4*A*). Further increase in concentration stimulates Mg^{2+} loss from the cells. This stimulation is far less reproducible than the inhibition seen at lower concentrations. Stimulation is associated with increased cell lysis which may indicate that high quinidine concentrations damage cells and release Mg^{2+}. Thus it is difficult to obtain a K_i from the data of Fig. 4*A*. K_is ranging from 0·2 to 0·6 mM are obtained depending whether it is assumed that quinidine inhibits 70 or 100% of Mg^{2+} efflux.

Similar effects are seen with amiloride (Fig. 4*B*). Inhibition of efflux is seen with concentrations above 10^{-4} M and inhibition is maximal (65%) with 2 mM-amiloride. Above this level both efflux and haemolysis increase. Once again it is not possible to obtain an accurate K_i. Values range between 0·5 and 1 mM depending on whether it is assumed that amiloride inhibits 65 or 100% Mg^{2+} efflux.

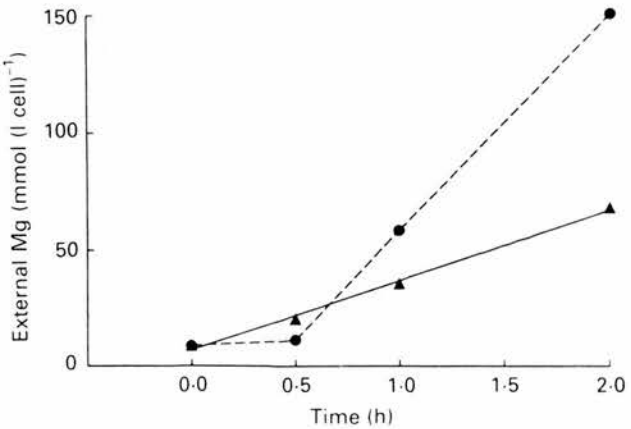

Fig. 5. The effect of replacing Na_o^+ on Mg^{2+} efflux from ferret red cells. Mean Mg accumulation in the media (expressed in terms of cell volume) was measured at different times after adding cells. In both experiments media contained (mM): KCl, 5; Tris HEPES, 10 (pH 7·5 at 38 °C); glucose, 11; Tris EGTA, 0·05. In addition the control medium, ▲, contained 145 mM-NaCl whereas the replacement medium, ●, contained 145 mM-choline Cl and 20 mM-sucrose. The control flux was 30 μmol (l cell)$^{-1}$ h^{-1} over the entire period. In the absence of Na^+, efflux was 4·8 μmol (l cell)$^{-1}$ h^{-1} for the first 30 min and increased to 92·9 μmol (l cell)$^{-1}$ h^{-1} over the next 90 min.

The effect of replacing Na_o^+ with choline is seen in Fig. 5. Mg^{2+} efflux is reduced from a control value of 30 to 5 μmol (l cell)$^{-1}$ h^{-1} for the 30 min period immediately following cell addition. After this time Mg^{2+} efflux increased to 93 μmol (l cell)$^{-1}$ h^{-1}, well above the control value and the cells shrank substantially. Similar results were obtained when Na^+ was replaced by NMDG indicating that the effects were due to the removal of Na^+ and not to the presence of choline. Mg^{2+} efflux after removal of Na_o^+ can thus be divided into two phases. The duration of the first phase varied from 30 min to over 2 h depending on the leakiness of the cells to Na^+ and was longer when Na^+ was lost more slowly from the cells. This first phase could be prolonged by adding 10 μM-bumetanide to the medium. It will be shown later that Mg^{2+} efflux is very sensitive to $[Na^+]_o$. The large increase in Mg^{2+} efflux during the second phase is probably due largely to the progressive accumulation of Na^+ in the medium, though cell shrinkage and changes in membrane potential may also play a role. In many later experiments 10 μM-bumetanide was added to the medium to inhibit the Na^+, K^+, Cl^- co-transporter (the main route for Na^+ and K^+ movements in these cells (Flatman, 1983)) and thus reduce the loss of cell Na^+ and K^+ (Fig. 6) and the accumulation of Na^+ in the medium. Bumetanide also prevents cell shrinkage and changes in membrane potential for at least 30 min. Analysis of many experiments shows that bumetanide does not have a direct effect on Mg^{2+} transport in ferret red cells. All

observed effects of bumetanide could be attributed to its inhibition of Na^+, K^+, Cl^- co-transport.

In order to study the Na^+ dependence of Mg^{2+} efflux the following protocol was adopted. Mg^{2+} efflux was measured over the first 30 min of incubation in media in

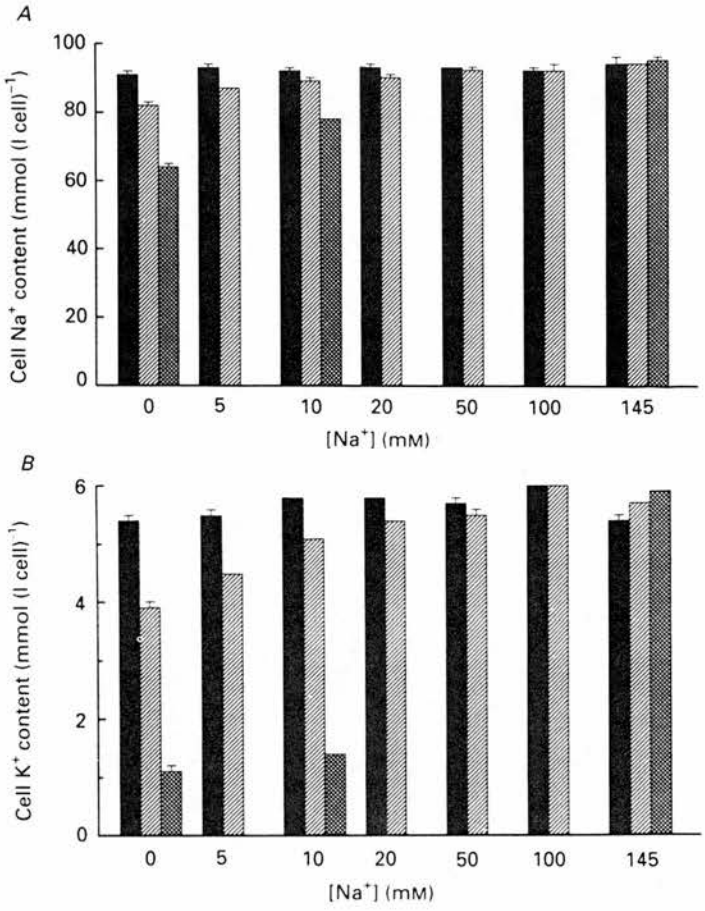

Fig. 6. Mean Na^+ (*A*) and K^+ (*B*) contents ($\pm$S.E.M., $n = 3$) of ferret red cells are shown as a function of $[Na^+]_o$. Media contained (mM): Tris–Hepes, 10; glucose, 11; Tris EGTA, 0·05; KCl, 5 and the initial $[Na^+]$ indicated. NaCl was replaced by equimolar choline Cl so that the sum, [NaCl] + [choline Cl], equalled 145 mM. When present bumetanide was at a concentration of 10 μM. Ion contents were measured initially (filled bars) and after 30 min incubation with bumetanide (hatched bars) and without (cross-hatched bars). Data from same experiment as Fig. 7.

which Na^+ was replaced to varying extents with either choline or NMDG. Fluxes were measured both in the presence and absence of 10 μM-bumetanide. Cell and medium $[Na^+]$ and $[K^+]$ were also measured at the start and end of the flux.

Figure 7 shows Mg^{2+} flux plotted as a function of measured $[Na^+]_o$ both in the presence and absence of bumetanide. Reduction of $[Na^+]_o$ from 145 to 10 mM stimulates Mg^{2+} efflux. Stimulation was seen both in the presence (78$\pm$24%,

mean $\pm$ S.E.M., $n = 3$) and absence ($82 \pm 6\%$, $n = 3$) of bumetanide. In a number of other experiments stimulation varied between 50 and 130%. Reduction of $[Na^+]_o$ below 10 mM inhibited Mg^{2+} efflux. In this experiment incubation of cells in a nominally Na^+-free medium resulted in a much reduced level of Mg^{2+} efflux in the

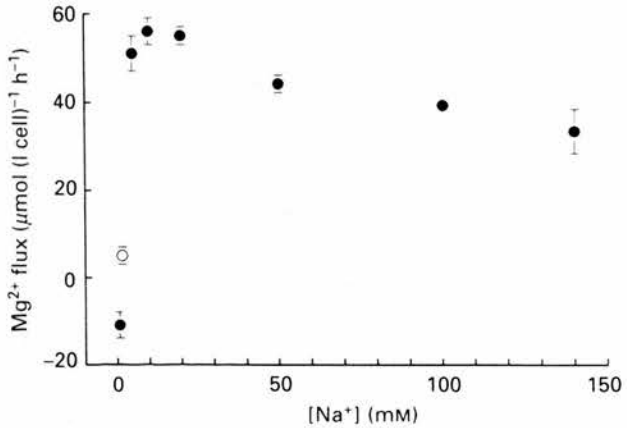

Fig. 7. Mg^{2+} flux is plotted as a function of measured $[Na^+]_o$. Mg^{2+} fluxes were measured over a 30 min period after adding cells to media. Composition of media is described in legend to Fig. 6. ●, fluxes in presence and ○, in the absence of 10 μM-bumetanide. Points indicate the mean of three measurements with S.E.M. if this is larger than point size. Fluxes measured without bumetanide in media containing 145 or 10 mM-Na^+ were $31{\cdot}7 \pm 0{\cdot}3$ and $57{\cdot}9 \pm 2{\cdot}1$ μmol (l cell)$^{-1}$ h^{-1} respectively. $[Na^+]_o$ measured in the 'Na^+-free' media were as follows (mM. $\pm$S.E.M., $n = 3$): no bumetanide, initially $0{\cdot}37 \pm 0{\cdot}04$ rising to $2{\cdot}83 \pm 0{\cdot}15$ after 30 min incubation; and in the presence of 10 μM-bumetanide, initially $0{\cdot}21 \pm 0{\cdot}01$ rising to $1{\cdot}42 \pm 0{\cdot}34$.

absence of bumetanide and Mg^{2+} uptake in its presence. Mg^{2+} uptake occurs against a considerable electrochemical gradient as $[Mg^{2+}]_o$ and $[Mg^{2+}]_i$ are about 2 and 650 μM respectively. As Mg^{2+} influx was only observed in the presence of bumetanide in this experiment it suggests that Mg^{2+} transport reverses direction only if a sufficiently low $[Na^+]_o$ is maintained. In the presence of bumetanide the average level of $[Na^+]_o$ was 0·8 mM during the flux period whereas it was 1·6 mM in its absence. Mg^{2+} uptake (14 ± 2 μmol (l cell)$^{-1}$ h^{-1}, mean $\pm$ S.E.M., $n = 3$) has also been seen in an experiment where bumetanide was not used but the average $[Na^+]_o$ was only about 0·9 mM during the flux measurement. This clearly shows that bumetanide need not be present for Mg^{2+} influx to be seen. As Mg^{2+} uptake is against a large electrochemical gradient this also indicates that bumetanide does not induce Mg^{2+} influx directly (for instance by increasing cell leakiness). Incubation in low-Na^+ media also results in loss of cell K^+ and although bumetanide reduces this loss it does not abolish it (Fig. 6*B*). However, no correlation or consistent pattern could be established between $[K^+]_i$ and Mg^{2+} fluxes. This does not rule out the possibility that K^+ influences Mg^{2+} fluxes, however, it does show that K^+ is not the primary determinant of Mg^{2+} transport.

Figure 8 shows the effect of reducing $[Mg^{2+}]_o$ from its usual 2 μM to 10^{-8} M by chelating Mg^{2+} with 0·1 mM-EDTA. It can be seen that reduction of $[Mg^{2+}]_o$ to about 10^{-8} M stimulates Mg^{2+} efflux substantially only when $[Na^+]_o$ is low. Unlike the

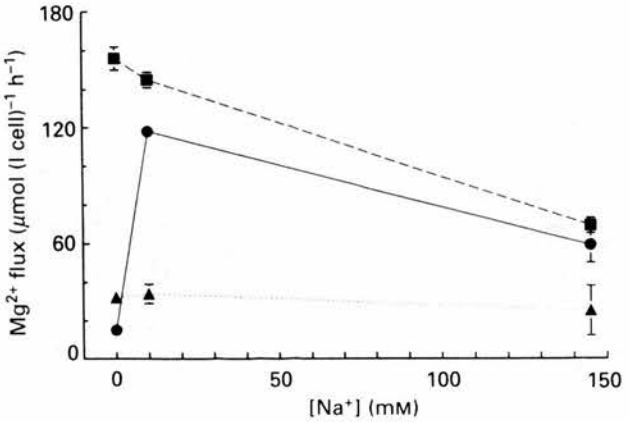

Fig. 8. Effect of EDTA and Co^{2+} on Mg^{2+} transport. Cells were incubated in media containing (mM): K^+, 5; Tris EGTA, 0·05; glucose, 11; HEPES, 8 and the initial [Na^+] shown. NaCl was replaced by equimolar choline Cl so that the sum, [NaCl]+[choline Cl], equalled 145 mM. $CoCl_2$ (1 mM) and Tris EDTA (0·1 mM) were added as indicated. Each point is the mean of three flux measurements with S.E.M. if this is larger than point size. ●, control; ▲, +Co^{2+}; ■, +EDTA.

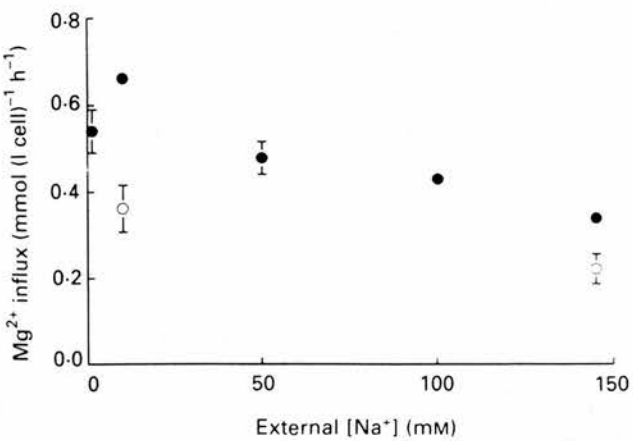

Fig. 9. Mg^{2+} uptake as a function of $[Na^+]_o$ in the presence of bumetanide. The media are as described in Fig. 8 with the addition of 10 mM-$MgCl_2$ and 10 μM-bumetanide; 1 mM-$CoCl_2$ was added as indicated. Mg^{2+} influx was determined over a 30 min period after adding cells to medium (haematocrit in this experiment was about 13%). Points show the mean of three measurements with S.E.M. if this is larger than point size. ●, total flux and ○, flux in the presence of Co^{2+}. $[Na^+]_o$ in the 'Na^+-free' media was 0·35±0·07 mM (mean±S.E.M., $n = 3$) initially rising to 1·26±0·09 mM after 30 min.

control condition Mg^{2+} efflux in the presence of EDTA increases steadily as $[Na^+]_o$ is reduced and there is no reduction of efflux (nor is influx seen) at the lowest [Na^+]. In a separate experiment the effects of EDTA were shown to be identical in the presence and absence of 10 μM-bumetanide. Figure 8 also shows that Mg^{2+} efflux in the presence of 1 mM-Co^{2+} is not affected by reducing $[Na^+]_o$ suggesting that Co^{2+} inhibits the Na^+-dependent component.

The observation that reducing $[Na^+]_o$ sufficiently can reverse the direction of Mg^{2+} transport is unique in red cell experiments. Taken with the data of Fig. 7 this suggests a substantial component of Mg^{2+} transport occurs through Na^+–Mg^{2+} antiport. If this is so it should be possible to stimulate Mg^{2+} uptake (down an

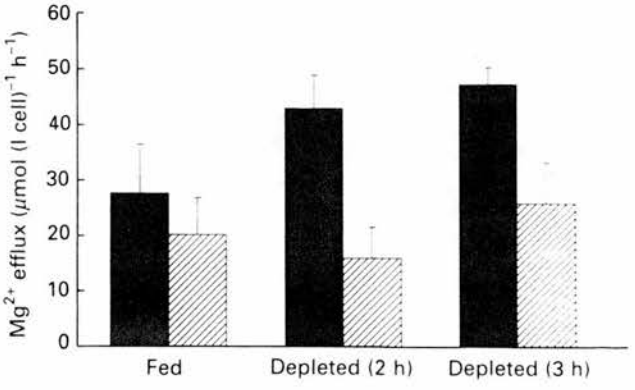

Fig. 10. Effect of metabolic depletion on Mg^{2+} efflux. Ferret red cells were either incubated for 1 h in FBM containing 11 mM-glucose or for 2 or 3 h in media containing 11 mM-2-deoxyglucose. The cells were then washed twice and resuspended either in FBM + glucose (fed cells) or in FBM (depleted cells). Mg^{2+} efflux was determined in these media over a 30 min period both in the presence and absence of 1 mM-Co^{2+}. Cell ATP content was measured in the middle of the flux period. Bars show the mean of three measurements with S.E.M. Filled bars represent total flux and hatched bars the flux in the presence of Co^{2+}. Cell ATP contents were (mean ± S.E.M., $n = 6$, μmol (l cell)$^{-1}$): fed 635 ± 23; 2 h depleted, 25 ± 1; 3 h depleted, 21 ± 1.

electrochemical gradient) by reducing $[Na^+]_o$. Figure 9 shows that mean Mg^{2+} uptake from a medium containing 10 mM-Mg^{2+} and 10 μM-bumetanide is stimulated 96% by reducing $[Na^+]_o$ from 145 to 10 mM. This behaviour is consistent with Na^+–Mg^{2+} antiport. However, as $[Na^+]_o$ is reduced further Mg^{2+} influx begins to fall. Mg^{2+} influx at 0·8 mM $[Na^+]_o$ is only about 60% greater than that at 145 mM. This may indicate the presence of an external Na^+ site which regulates Mg^{2+} transport. Figure 9 also shows that 1 mM-Co^{2+} not only reduces Mg^{2+} influx but also reduces its sensitivity to Na^+ removal. Substantial Mg^{2+} influx, stimulated by reducing $[Na^+]_o$, is also observed in ferret red cells in the absence of bumetanide.

Mg^{2+} uptake by human, chicken and rat red cells in inhibited when the ATP level in the cells is reduced by starvation or treatment with iodoacetamide. Figure 10 shows that Mg^{2+} efflux increases when the ATP content of ferret red cells is reduced to 25 or 21 μmol (l cell)$^{-1}$ (less than 4% initial content) by incubating them for 2 or 3 h in 2-deoxyglucose. Both the total and cobalt-sensitive components of efflux are stimulated.

DISCUSSION

Mg^{2+} efflux from ferret red cells into a nominally Mg^{2+}-free medium is about 41 μmol (l cell)$^{-1}$ h^{-1}. Fluxes are large enough to study without the need for loading so Mg^{2+} transport can be studied in cells not treated with A23187 or PCMBS. In some

respects Mg^{2+} transport in ferret red cells is similar to Mg^{2+} transport in other red cells. Efflux is inhibited by quinidine, amiloride, imipramine, and high concentrations of external divalent cations but not by ouabain, bumetanide or SITS. Maximum inhibition with quinidine, amiloride, Co^{2+} and imipramine is about 60–70% of the total flux. High concentrations of these agents increase Mg^{2+} efflux and usually increase haemolysis. The data suggest, however, that there are at least two pathways for Mg^{2+} transport. The inhibitory effects of amiloride and quinidine are quantitatively similar to those seen in other red cells. Quinidine inhibits Mg^{2+} efflux from human red cells with a K_i of 50 μM (Féray & Garay, 1986) and that from rat red cells with a K_i of about 400 μM. The latter value is difficult to assess as quinidine causes substantial lysis in these cells (Féray & Garay, 1987). Amiloride inhibits Na^+-dependent Mg^{2+} efflux in human red cells with a K_i of 0·4 mM (Lüdi & Schatzmann, 1987) and total Mg^{2+} efflux in chicken red cells with a K_i of 0·6 mM (Günther & Vormann, 1985). Recently Féray & Garay (1988) working with human red cells have suggested that imipramine is a useful Mg^{2+} transport inhibitor as it appears to be more selective than either quinidine or amiloride. Results reported above show that imipramine is also an effective inhibitor of Mg^{2+} transport in ferret red cells, though high concentrations cause haemolysis.

Many of the features of Mg^{2+} transport in red cells can be explained in terms of either a carrier or a channel. However, the finding that the system is capable of taking up Mg^{2+} against a substantial electrochemical gradient (Fig. 7) favours a carrier-mediated process. Currently two models are used to describe active Mg^{2+} transport in red cells. In one model, Na^+–Mg^{2+} exchange, active Mg^{2+} transport is driven by the energy in the Na^+ gradient. In the other, Na^+-dependent Mg^{2+} pump, energy is derived from a linked chemical reaction. At present the Mg^{2+} pump is the favoured model for Mg^{2+} transport in chicken and human red cells (Günther & Vormann, 1985; Lüdi & Schatzmann, 1987) mainly because alterations to the Na^+ gradient do not have the expected effects on Mg^{2+} transport (see Introduction). There is little direct evidence for a pump.

Mg^{2+} transport in ferret red cells does, however, respond to changes in Na^+ gradient as predicted for Na^+–Mg^{2+} exchange. Reduction of $[Na^+]_o$ to a sufficiently low level reverses the direction of Mg^{2+} transport (Fig. 7). Substantial Mg^{2+} influx, which increases as $[Na^+]_o$ is reduced, can also be observed (Fig. 9) when ferret red cells are incubated in media containing greater than physiological $[Mg^{2+}]_o$. These phenomena, which have not been seen in other red cells, are consistent with Na^+–Mg^{2+} antiport. The finding that Mg^{2+} efflux is stimulated by chelating Mg^{2+} with EDTA only when $[Na^+]_o$ is low also favours antiport. EDTA not only increases the outward Mg^{2+} gradient but would also reduce Mg^{2+} uptake by reverse Na^+–Mg^{2+} exchange (only seen at low $[Na^+]_o$). It is not clear how Mg^{2+} chelation could stimulate a Mg^{2+} pump only when $[Na^+]_o$ is low. Thus ferret red cells either have a different Mg^{2+} transport system from human or chicken red cells or the same transporter is present and the differences are due to experimental conditions. In ferret red cells it was possible to manipulate the Na^+ gradient without using PCMBS and to generate far larger outward Na^+ gradients than have been used in previous studies of Mg^{2+} transport.

There is considerable evidence that phosphorylation plays an important role in

Na^+-dependent Mg^{2+} transport. Günther & Vormann (1986) have shown that phosphorylation of a 230 kDa membrane protein is associated with increased Mg^{2+} transport in chicken red cells. In human red cells Mg^{2+} efflux is inhibited by metabolic depletion which can be restored by ATP but not by non-hydrolysable ATP analogues (Frenkel *et al.* 1989). Recent work suggests that Mg^{2+} transport in squid axons is mainly via a Na^+–Mg^{2+} antiport which is activated by ATP (Baker & Crawford, 1972; Mullins, Brinley, Spangler & Abercrombie, 1977; DiPolo & Beaugé, 1988). However, Mg^{2+} efflux is stimulated (at least in the short run) when the ATP content of ferret red cells is rapidly reduced by incubating them in 2-deoxyglucose (Fig. 10). The finding that Mg^{2+} transport can persist for several hours in the presence of only 25 μmol (l cell)$^{-1}$ ATP argues against a Mg^{2+} pump though it does not rule out the possibility that phosphorylation of the transporter (or an activator) influences Mg^{2+} transport. The level of the crucial phosphorylated form may decline only slowly during metabolic depletion. As [ATP] falls, altering Mg^{2+} buffering, loss of activity due to dephosphorylation may be more than offset by stimulation due to increased $[Mg^{2+}]_i$. Efflux through alternative (leak) pathways may also increase as [ATP] declines (Frenkel *et al.* 1989). Movement through these routes could easily come to dominate total flux as it represents a much larger fraction of total flux in ferret than in other red cells.

The moderate increase in Mg^{2+} efflux as temperature is increased (between 25 and 40 °C) and the low activation energy also argue against a Mg^{2+} pump. The activation energies of the Na^+ and Ca^{2+} pumps are both much greater (Inesi, Millman & Eletr, 1973; Stewart, Ellory & Klein, 1980). Activation energies of co-transport systems range widely. The values reported here, which are similar to those obtained for the Na^+, K^+, Cl^- co-transport system (Stewart *et al.* 1980), are consistent with the antiport model. They contrast with the higher values reported for Mg^{2+} transport in human red cells (Féray & Garay, 1986).

The high Na^+ content and Na^+ permeability of ferret red cells make it difficult to assess directly whether Na^+ is exchanged across the membrane for Mg^{2+}. Strictly, the data presented only indicate the presence of a Na^+-dependent Mg^{2+} transport system. However, if it is assumed that Mg^{2+} is transported on a Na^+–Mg^{2+} antiport which obtains energy solely from the Na^+ and Mg^{2+} gradients then it is possible to assess transport stoichiometry. The technique requires estimation of the conditions under which there is no net Mg^{2+} transport through the system. Na^+–Mg^{2+} antiport is at equilibrium when:

$$\left(\frac{[Mg^{2+}]_o}{[Mg^{2+}]_i}\right) = \left(\frac{[Na^+]_o}{[Na^+]_i}\right)^r \exp\left(EF(2-r)/RT\right). \quad (1)$$

where E is the membrane potential and r is the number of Na^+ ions transported with each Mg^{2+} ion. For the experiment shown in Figs 6 and 7 there is no net Mg^{2+} movement when $[Na^+]_o$ is about 1 mM though estimation of the exact value is complicated by Mg^{2+} efflux through other routes. The other values, measured or reliably estimated are: $[Mg^{2+}]_i$, 0·65 mM for oxygenated ferret red cells (Flatman, 1987); average $[Na^+]_i$, 130 mM; $[Mg^{2+}]_o$, 2 μM; E, −10 mV. Solution of eqn (1) gives $r = 1{\cdot}1$ suggesting that a single Na^+ ion is transported with each Mg^{2+} ion. The data would have to be very seriously in error (for instance a tenfold overestimate of

$[Mg^{2+}]_o$) before a stoichiometry of 2 Na^+:1 Mg^{2+} becomes viable. A similar approach may be used to see whether Na^+:Mg^{2+} exchange could account for the maintenance of $[Mg^{2+}]_i$ below electrochemical equilibrium under physiological conditions. Physiological values for $[Mg^{2+}]_o$, $[Mg^{2+}]_i$, $[Na^+]_o$, $[Na^+]_i$ and the membrane potential are about 0·5 mM, 0·65 mM, 149 mM, 137 mM and −10 mV respectively (see Thornton, Wright, Sacra & Goodier, 1979; Flatman & Andrews, 1983; Flatman, 1987). Solution of eqn (1) yields a value for r of 1·06 suggesting that antiport of 1 Na^+:1 Mg^{2+} can account for the physiological regulation of $[Mg^{2+}]_i$ in these cells.

Mg^{2+} transport in ferret red cells has another interesting feature. High $[Na^+]_o$ inhibits transport. This behaviour has not been observed in Mg^{2+} transport systems before. It may indicate substrate inhibition or that Na^+ competes with another activating ion (or molecule) at the outer surface of the membrane. These possibilities are being investigated.

In conclusion, it is suggested that Na^+–Mg^{2+} antiport is a viable model for Mg^{2+} transport in ferret red cells as it is in squid axon (DiPolo & Beaugé, 1988). Antiport of 1 Na^+:1 Mg^{2+} not only explains the transport data presented in this paper but also accurately accounts for the physiological level of $[Mg^{2+}]_i$ found in ferret red cells and explains how this is maintained below electrochemical equilibrium with $[Mg^{2+}]_o$. The data do not rule out the existence of a Mg^{2+} pump which may operate alongside the antiport. They suggest, however, that if the pump exists it only plays a minor role in ferret red cells.

We should like to thank The Wellcome Trust for support.

REFERENCES

ARONSON, P. S. (1989). The renal proximal tubule: a model for diversity of anion exchangers and stilbene-sensitive anion transporters. *Annual Review of Physiology* **51**, 419–441.

BAKER, P. F. & CRAWFORD, A. C. (1972). Mobility and transport of magnesium in squid giant axons. *Journal of Physiology* **227**, 855–874.

BERGFELD, G. & FORRESTER, T. (1989). Efflux of adenosine triphosphate from human erythrocytes in response to a brief pulse of hypoxia. *Journal of Physiology* **418**, 88*P*.

DIPOLO, R. & BEAUGÉ, L. (1988). An ATP-dependent Na^+/Mg^{2+} countertransport is the only mechanism for Mg extrusion in squid axons. *Biochimica et biophysica acta* **946**, 424–428.

FÉRAY, J.-C. & GARAY, R. (1986). An Na^+-stimulated Mg^{2+}-transport system in human red blood cells. *Biochimica et biophysica acta* **856**, 76–84.

FÉRAY, J.-C. & GARAY, R. (1987). A one-to-one Mg^{2+}:Mn^{2+} exchange in rat erythrocytes. *Journal of Biological Chemistry* **262**, 5763–5768.

FÉRAY, J.-C. & GARAY, R. (1988). Demonstration of a Na^+:Mg^{2+} exchange in human red cells by its sensitivity to tricyclic antidepressant drugs. *Naunyn-Schmiedeberg's Archives of Pharmacology* **338**, 332–337.

FLATMAN, P. W. (1983). Sodium and potassium transport in ferret red cells. *Journal of Physiology* **341**, 545–557.

FLATMAN, P. W. (1987). The effects of calcium on potassium transport in ferret red cells. *Journal of Physiology* **386**, 407–423.

FLATMAN, P. W. (1988*a*). The control of red cell magnesium. *Magnesium Research* **1**, 5–11.

FLATMAN, P. W. (1988*b*). The effects of magnesium on potassium transport in ferret red cells. *Journal of Physiology* **397**, 471–487.

FLATMAN, P. W. & ANDREWS, P. L. R. (1983). Cation and ATP content of ferret red cells. *Comparative Biochemistry and Physiology* **74**A, 939–943.

FLATMAN, P. W. & LEW, V. L. (1980). Magnesium buffering in intact human red blood cells measured using the ionophore A23187. *Journal of Physiology* **305**, 13–30.

FLATMAN, P. W. & SMITH, L. M. (1990). Magnesium transport in red cells. *Magnesium Research* **3**, 63.

FRENKEL, E. J., GRAZIANI, M. & SCHATZMANN, H. J. (1989). ATP requirement of the sodium-dependent magnesium extrusion from human red blood cells. *Journal of Physiology* **414**, 385–397.

GÜNTHER, T. & VORMANN, J. (1985). Mg^{2+} efflux is accomplished by an amiloride-sensitive Na^+/Mg^{2+} antiport. *Biochemical and Biophysical Research Communications* **130**, 540–545.

GÜNTHER, T. & VORMANN, J. (1986). Probable role of protein phosphorylation in the regulation of Mg^{2+} efflux via Na^+/Mg^{2+} antiport. *Magnesium Bulletin* **8**, 307–309.

GÜNTHER, T. & VORMANN, J. (1987). Characterization of Na^+/Mg^{2+} antiport by simultaneous $^{28}Mg^{2+}$ influx. *Biochemical and Biophysical Research Communications* **148**, 1069–1074.

GÜNTHER, T., VORMANN, J. & FÖRSTER, R. (1984). Regulation of intracellular magnesium by Mg^{2+} efflux. *Biochemical and Biophysical Research Communications* **119**, 124–131.

INESI, G., MILLMAN, M. & ELETR, S. (1973). Temperature-induced transitions of function and structure in sarcoplasmic reticulum membranes. *Journal of Molecular Biology* **81**, 483–504.

LÜDI, H. & SCHATZMANN, H. J. (1987). Some properties of a system for sodium-dependent outward movement of magnesium from metabolizing human red blood cells. *Journal of Physiology* **390**, 367–382.

MULLINS, L. J., BRINLEY, F. J. JR, SPANGLER, S. G. & ABERCROMBIE, R. F. (1977). Magnesium efflux in dialyzed squid axons. *Journal of General Physiology* **69**, 389–400.

STEWART, G. W., ELLORY, J. C. & KLEIN, R. A. (1980). Increased human red cell cation passive permeability below 12 °C. *Nature* **286**, 403–404.

THORNTON, P. C., WRIGHT, P. A., SACRA, P. J. & GOODIER, T. E. W. (1979). The ferret, *Mustela putorius furo*, as a new species in toxicology. *Laboratory Animals* **13**, 119–124.

Journal of Physiology (1991), **443**, *pp.* 217–230
With 6 figures
Printed in Great Britain

SODIUM-DEPENDENT MAGNESIUM UPTAKE BY FERRET RED CELLS

BY PETER W. FLATMAN AND LORRAINE M. SMITH

From the Department of Physiology, University Medical School, Teviot Place, Edinburgh EH8 9AG

(*Received 12 March 1991*)

SUMMARY

1. Magnesium uptake can be measured in ferret red cells incubated in media containing more than 1 mM-magnesium. Uptake is substantially increased if the sodium concentration in the medium is reduced.

2. Magnesium uptake is half-maximally activated by 0·37 mM-external magnesium when the external sodium concentration is 5 mM. Increasing the external sodium concentration increases the magnesium concentration needed to activate the system.

3. Magnesium uptake is increased by reducing the external sodium concentration. Uptake is half-maximum at sodium concentrations of 17, 22 and 62 mM when the external magnesium concentrations are 2, 5 and 10 mM respectively.

4. Replacement of external sodium with choline does not affect the membrane potential of ferret red cells over a 45 min period.

5. Magnesium uptake from media containing 5 mM-sodium is inhibited by amiloride, quinidine and imipramine. It is not affected by ouabain or bumetanide. Vanadate stimulates magnesium uptake but has no effect on magnesium efflux.

6. When cell ATP content is reduced to 19 μmol (l cell)$^{-1}$ by incubating cells for 3 h with 2-deoxyglucose, magnesium uptake falls by 50% in the presence of 5 mM-sodium and is completely abolished in the presence of 145 mM-sodium. Some of the inhibition may be due to the increase in intracellular ionized magnesium concentration ($[Mg^{2+}]_i$) from 0·7 to 1·0 mM which occurs under these conditions.

7. Magnesium uptake can be driven against a substantial electrochemical gradient if the external sodium concentration is reduced sufficiently.

8. These findings are discussed in terms of several possible models for magnesium transport. It is concluded that the majority of magnesium uptake observed in low-sodium media is via sodium–magnesium antiport. A small portion of uptake is through a parallel leak pathway. It is believed that the antiport is responsible for maintaining $[Mg^{2+}]_i$ below electrochemical equilibrium in these cells at physiological external sodium concentration. Thus in ferret red cells the direction of magnesium transport can be reversed by reversing the sodium gradient.

INTRODUCTION

Magnesium moves only slowly across the membranes of red cells with physiological magnesium contents. Net efflux of magnesium from human red cells into nominally

magnesium-free media is about 4–8 μmol (l cells)$^{-1}$ h^{-1} (Féray & Garay, 1986; Lüdi & Schatzmann, 1987). It is higher in ferret red cells, at about 41 μmol (l cell)$^{-1}$ h^{-1} (Flatman & Smith, 1990) and higher still in rat red cells at 220 μmol (l cell)$^{-1}$ h^{-1} (Féray & Garay, 1987). Efflux is substantially increased by loading cells with magnesium using A23187 or *p*-chloromercuribenzene sulphonic acid (Günther, Vormann & Förster, 1984; Féray & Garay, 1986; Lüdi & Schatzmann, 1987). Until recently net magnesium uptake had not been observed in red cells. The magnesium content of human, rat and chicken red cells does not change significantly when cells are incubated in media with high magnesium concentrations (Günther & Vormann, 1985*a*; Günther & Ebel, 1990), nor is influx induced by reducing the initial magnesium content by treatment of cells with A23187 and EDTA or by obtaining cells from magnesium-deficient animals. It has been suggested that non-proliferating cells may not possess mechanisms capable of mediating net magnesium uptake (Günther & Ebel, 1990), but there is recent evidence to the contrary. Deoxygenation and sickling of red cells from humans with sickle-cell disease produces a large increase in magnesium permeability which can result in rapid and significant magnesium uptake if the magnesium gradient is inward (Ortiz, Lew, Bookchin, 1990). In ferret red cells replacement of external sodium with choline can also result in substantial magnesium uptake (Flatman & Smith, 1990).

This paper examines the properties of magnesium uptake observed in ferret red cells incubated in low-sodium media. It shows that magnesium uptake probably occurs by reversal of sodium magnesium antiport, the mechanism which normally keeps the ionized magnesium concentration ($[Mg^{2+}]_i$) in these cells below electrochemical equilibrium (Flatman & Smith, 1990).

METHODS

Washed red cells were separated from blood taken from anaesthetized (1·5 g urethane (kg body weight)$^{-1}$: I.P.) adult ferrets as described previously (Flatman & Smith, 1990). Cells were stored at about 80% haematocrit at 5 °C in FBM (ferret basic medium: 145 mM-NaCl, 5 mM-KCl, 10 mM-HEPES, titrated to pH 7·6 at 38 °C with about 6·5 mM-NaOH) containing 0·05 mM-Tris–EGTA until used (usually within 3 days). Fluxes were measured at 38 °C in 5–10% suspensions of washed cells. The initial pHs of these suspensions were 7·5. Usually cells were incubated in the test medium for 10 min and then magnesium uptake was followed over the next 30 min. Each experiment was carried out in triplicate and values are given as means with standard error of the mean. Unless otherwise stated the media for flux experiments were prepared by mixing suitable amounts of media containing (mM): KOH, 5; Tris–EGTA, 0·05; glucose, 11; and either NaCl, 145 or choline chloride, 145. The pHs of these solutions were adjusted to 7·6 at 38 °C with approximately 7·4 mM-HEPES. $MgCl_2$ was added to obtain the desired magnesium concentration. Bumetanide (0·1 mM) was often included in the media to prevent cells losing excessive sodium when incubated in low-sodium media (Flatman & Smith, 1990). Sources of materials, preparation of solutions, and methods to measure haematocrit, haemolysis, cell sodium content, potassium content and magnesium efflux have been described previously (Flatman & Smith, 1990). Cell magnesium, potassium and sodium contents are expressed per litre of original cells to facilitate assessment of ion fluxes across the membrane.

The method used to measure cell magnesium content (Flatman & Smith, 1990) was slightly modified in order to obtain accurate measurements of magnesium uptake which may appear as very small percentage changes in total cell magnesium content. Cells were separated from medium by centrifuging a diluted sample of the suspension in a tube containing a layer of di-*n*-butylphthalate at about 15000*g*. Cells pass through the oil whereas the medium remains above. A small volume of extracellular medium passes through the oil with the cells and any magnesium in

this is measured together with that genuinely contained within the cells. The volume of the trapped extracellular space is sensitive to the duration of centrifugation particularly with spins of less than 30 s, but can be reduced to a reproducibly stable level with spins of 1 min or longer. When cells are incubated in media containing a low magnesium concentration, trapped extracellular magnesium represents such a small fraction of total cell magnesium that it can be safely neglected and short spin times can be used. However, as magnesium uptake is often measured in the presence of high external magnesium concentrations variations in trapped extracellular magnesium can cause problems in assessing magnesium fluxes. These variations can be reduced by prolonged centrifugation. In the experiments described below a 2 min spin was used.

Ferret red cell membrane potential was assessed from the distribution of hydrogen ions across the membrane of cells suspended in a buffer-free medium containing the protonophore carbonyl cyanide *m*-chlorophenylhydrazone (CCCP). The method used is a modification (Halperin, Brugnara, Tosteson, Van Ha & Tosteson, 1989; see also Frenkel, Graziani & Schatzmann, 1989) of that first developed by Macey, Adorante & Orme (1978). Cells were washed twice in a buffer-free medium of the desired composition and then suspended in the medium at about 6–7% haematocrit. The pH of the suspension was measured with an Orion Ross combination electrode (Orion Research Inc., Boston, MA, USA). Sufficient stock CCCP (50 mM in dimethyl sulphoxide) was added to give a final concentration of 200 μM. Under these conditions the distribution of hydrogen ions across the membrane comes quickly into equilibrium with the membrane potential. External pH was adjusted to approximately 7·4 by adding a small quantity of 0·27 M-tetramethylammonium hydroxide solution. The pH was recorded when it had reached a steady level and then the cells were lysed by adding Triton X-100 to a final concentration of 0·2%. The pH of the lysate was recorded. It is equivalent to the internal pH of the cells before lysis. Initially, intracellular pH was measured in a lysate produced by freezing and thawing a pellet of cells spun out of the suspension through di-*n*-butylphthalate (trapped extracellular space about 2%). The values for intracellular pH measured by this method were identical to the values obtained with Triton. The latter method was adopted for most later experiments as it is simpler and more reliable. The membrane potential (in mV) was calculated as:

$$E_m = 61{\cdot}7 \times (pH_i - pH_o),$$

where pH_o and pH_i are the pHs of the suspension before and after lysis respectively.

RESULTS

It has been shown previously that ferret red cells take up magnesium when incubated in a medium containing magnesium, and that this uptake is stimulated when the external sodium concentration is reduced (Flatman & Smith, 1990). Figure 1 shows an example of the time-dependent changes in the magnesium content of ferret red cells incubated in media containing 5 mM-magnesium. Magnesium uptake is linear over a 2 h period when media contain 145 mM-sodium. Decreasing sodium concentration to 5 mM causes cell magnesium content to rise far more rapidly to a plateau after about 90 min.

In order to minimize changes in cell volume and composition seen with prolonged incubation of ferret red cells in low-sodium media (Flatman & Smith, 1990) incubation time was limited and bumetanide was added to the media. Bumetanide reduces loss of cell sodium and potassium but does not affect magnesium fluxes (Flatman & Smith, 1990; and later). In most experiments uptake was determined by measuring cell magnesium content 10 and 40 min after the start of incubation. Uptake over this period was usually linear and large enough to be measured with precision.

Figure 2 shows the magnesium-dependence of uptake. Magnesium uptake in media containing 145 mM-sodium is slow but detectable and reaches a maximum rate of

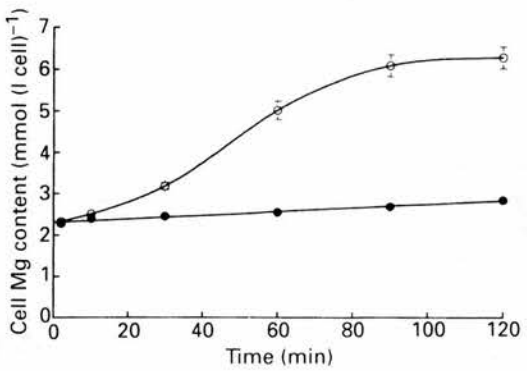

Fig. 1. Time-dependent changes in magnesium content of ferret red cells incubated in media (see Methods) containing (mM): $MgCl_2$, 5; bumetanide, 0·1 and NaCl either 5 (○) or 145 (●). Symbols show mean of three determinations with S.E.M. if larger than symbol size. Lines through symbols are drawn by eye. Cells incubated in the 5 mM-sodium media shrank substantially and their sodium and potassium contents (mmol (l original cell)$^{-1}$) fell from 98±1 to 40±1 and from 6·4±0·03 to 5·6±0·1 after 2 h incubation. There were no significant changes in the volume or in the sodium and potassium contents of cells incubated in 145 mM-sodium media.

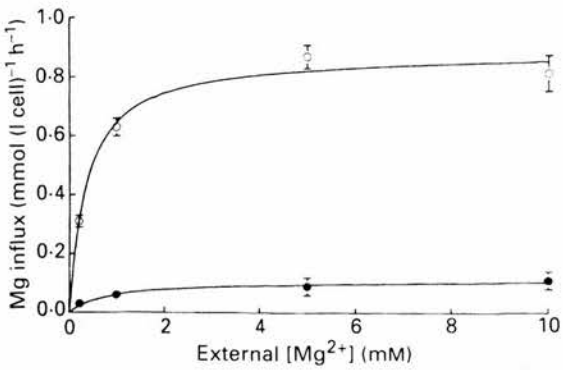

Fig. 2. Magnesium uptake as a function of $[Mg^{2+}]_o$ in the presence of 0·1 mM-bumetanide. Cells were incubated in media (see Methods) containing (mM): bumetanide, 0·1; $MgCl_2$ as indicated and NaCl either 145 (●) or 5 (○). After a 10 min pre-incubation in these media the fluxes were measured over the next 30 min. Symbols show the mean value of three measurements with S.E.M. if larger than symbol size. Lines are drawn assuming Michaelis–Menten kinetics and are fitted to the data by non-linear regression analysis (Marquardt method). The parameters used (with standard errors) are for 145 mM-NaCl: maximal uptake rate (V_{max}), 0·113±0·019 mmol (l cell)$^{-1}$ h^{-1}; K_m, 0·873±0·583 mM; and for 5 mM-NaCl: V_{max}, 0·881±0·033 mmol (l cell)$^{-1}$ h^{-1}; K_m, 0·369±0·069 mM.

about 0·1 mmol (l cell)$^{-1}$ h^{-1} when the magnesium concentration is more than 5 mM. In this experiment a small uptake (0·027±0·003 mmol (l cell)$^{-1}$ h^{-1}) was observed with only 0·2 mM-magnesium in the medium. It is usually difficult to measure any significant change in the magnesium content of cells incubated in media containing physiological sodium unless the magnesium concentration is more than 1 mM. For instance there is a slight fall in mean magnesium content (−0·06±0·04 mmol (l cell)$^{-1}$ h^{-1}, $n = 5$ ferrets) with between 0·2 and 0·4 mM-external magnesium and

there is little change ($0{\cdot}01 \pm 0{\cdot}02$ mmol (l cell)$^{-1}$ h^{-1}. $n = 5$ ferrets) with 1 mM. Reducing external sodium concentration to 5 mM strongly stimulates magnesium uptake. Under these conditions magnesium uptake is clearly revealed to be a saturating function of the external ionized magnesium concentration ($[Mg^{2+}]_o$) and can be described by Michaelis–Menten kinetics. Maximal uptake rate in this batch of cells is 0·88 mmol (l cell)$^{-1}$ h^{-1} and the Michaelis–Menten constant (K_m) is 0·37 mM. In experiments with low-sodium media magnesium uptake is often less with 10 mM-than with 5 mM-magnesium in the medium. In Fig. 2 the mean magnesium uptake at 10 mM-magnesium is less than at 5 mM. In this case the difference does not reach significance but in a separate experiment uptake at 10 mM-magnesium was 0·45 ($\pm 0{\cdot}03$) whereas at 5 mM-magnesium it was 0·63 ($\pm 0{\cdot}08$) mmol (l cells)$^{-1}$ h^{-1}.

Maximal uptake is difficult to quantify as it is not possible to maintain very low sodium concentrations in the media. Ferret red cells have a high sodium content (Flatman & Andrews, 1983). Even in the presence of bumetanide, sodium is lost from cells incubated in media initially containing very low sodium concentrations. This can markedly affect magnesium transport. However, fluctuations in sodium levels can be minimized at little cost to magnesium uptake by using media containing 5 mM-sodium. Thus, in experiments where it was necessary to produce substantial yet reproducible magnesium uptake, media containing 5 mM-magnesium and 5 mM-sodium were used. Fluxes measured under these conditions ranged from 0·55 to 3·55 mmol (l cells)$^{-1}$ h^{-1} (mean $\pm$ S.E.M., $1{\cdot}65 \pm 0{\cdot}25$. $n = 13$) (see also Table 1). This represents a 3·5- to 21·2-fold ($8{\cdot}8 \pm 1{\cdot}7$. $n = 13$) stimulation of magnesium uptake when sodium is reduced from 145 to 5 mM. Fluxes with cells from individual ferrets were very reproducible during each experiment. There was, however, substantial variation in maximum magnesium transport rate seen in cells from different animals. Some variation in rate also occurred during storage, though this showed no systematic pattern.

The relationship between external sodium concentration and magnesium uptake was more fully explored by incubating cells in media containing 5 mM-magnesium and variable sodium concentrations. Figure 3*A* shows that reducing external sodium stimulates magnesium uptake. The data can be described by Michaelis–Menten kinetics assuming that sodium binds to an external saturable site with a K_m of about 22 mM to inhibit magnesium uptake. In an experiment using cells from a different ferret half-maximal inhibition was observed with 25 mM-sodium and magnesium uptake increased only marginally (from 2·14 to 2·3 mmol (l cell)$^{-1}$ h^{-1}) as the sodium concentration was reduced from 10 to 0·9 mM. This increase is far less than expected from a model where removal of sodium simply activates influx. The concentration of sodium at which magnesium uptake is half its maximal value depends on the magnesium concentration. Figure 3*B* shows that half-maximal activity occurs at 17 mM-sodium with 2 mM-magnesium and at about 62 mM with 10 mM-magnesium (see also Flatman & Smith, 1990).

The possibility that the magnesium uptake system is capable of active magnesium transport was explored by incubating ferret red cells in a nominally sodium-free medium containing 0·1 mM-bumetanide and 0·2 mM added magnesium. Under these conditions the magnesium concentration gradient is outward ($[Mg^{2+}]_i = 0{\cdot}67$ mM). The internal and external magnesium and the external sodium concentrations were

measured over a 30 min period. A substantial magnesium uptake of 1·10 ± 0·04 mmol (l cells)$^{-1}$ h^{-1} ($n = 3$) was observed. Measured external magnesium concentration fell from 0·22 (±0·01) to 0·17 (±0·01) and the sodium concentration rose from 0·13 (±0·00) to 0·70 (±0·03) mM.

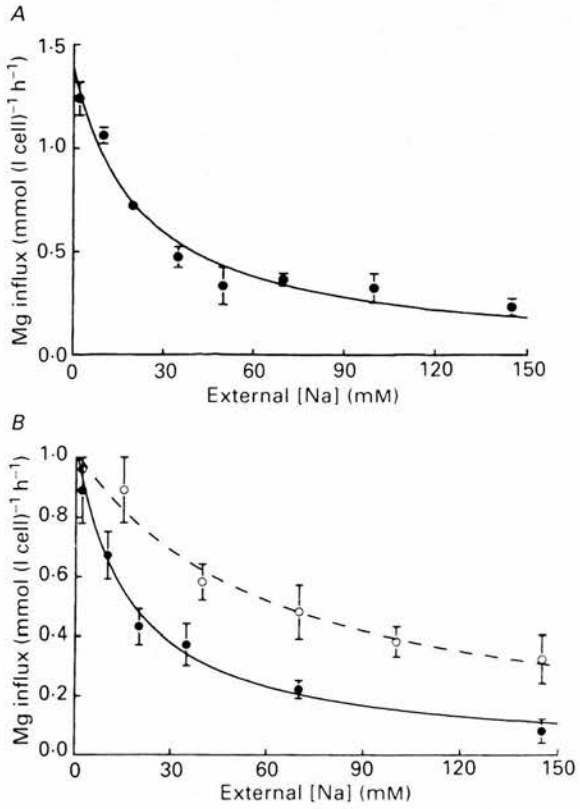

Fig. 3. Magnesium uptake as a function of external sodium concentration in the presence of 0·1 mM-bumetanide. Cells were incubated in media containing (mM): KOH, 5; Tris–EGTA, 0·05; glucose, 11; HEPES, 7·4; bumetanide, 0·1; $MgCl_2$, 2–10; the initial NaCl concentration shown and sufficient choline chloride to maintain the sum, [NaCl] + [choline chloride] = 145 mM. Fluxes were measured over a 30 min period after a 10 min pre-incubation. Symbols show the mean of three measurements with S.E.M. if larger than symbol size. The lines are drawn according to Michaelis–Menten kinetics and are fitted by non-linear regression analysis. The model assumes sodium binds to an external site to inhibit magnesium uptake. *A*. $MgCl_2 = 5$ mM. Curve fit parameters: $K_m = 22$ mM. maximum magnesium uptake = 1·39 mmol (l cell)$^{-1}$ h^{-1}. *B*. $MgCl_2 = 2$ mM (●). $K_m = 17$ mM. maximum magnesium uptake = 1·04 mmol (l cell)$^{-1}$ h^{-1}. $MgCl_2 = 10$ mM (○). $K_m = 62$ mM. maximum magnesium uptake = 1·02 mmol (l cell)$^{-1}$ h^{-1}.

Knowledge of the membrane potential is crucial to the analysis of this experiment. Removal of external sodium may have substantially hyperpolarized these high-sodium cells so that although the chemical gradient for magnesium may have been outward the electrochemical gradient may have been inward. Calculations show that the electrochemical gradient is inward if the membrane potential is more negative

than −16 mV. An experiment was therefore carried out to see whether incubation of ferret red cells in choline chloride affects membrane potential. The membrane potential of control cells suspended in a medium containing 145 mM-sodium and 5 mM-potassium was −10·0 (±1·3, $n = 4$) mV. The experimental group of cells were incubated at about 10% haematocrit in a medium containing (mM): choline chloride.

TABLE 1. Effect of transport inhibitors on magnesium uptake from media containing 5 mM-NaCl

Inhibitor	Magnesium uptake (mmol (l cell)$^{-1}$ h^{-1}) Mean ± S.E.M.	Mean as % of control
Group A		
Control	2·50 ± 0·05	100 ± 2
Quinidine (0·5 mM)	0·56 ± 0·02	22 ± 1
Imipramine (0·5 mM)	0·47 ± 0·06	19 ± 2
Amiloride (1 mM)	0·55 ± 0·07	22 ± 3
Group B		
Control	3·55 ± 0·14	100 ± 4
Ouabain (0·5 mM)	3·57 ± 0·23	101 ± 7
SITS (0·1 mM)	3·53 ± 0·22	99 ± 6
Group C		
Control	0·94 ± 0·02	100 ± 2
Vanadate (0·05 mM)	1·37 ± 0·05	146 ± 5
Vanadate (0·20 mM)	2·78 ± 0·05	296 ± 5
Group D		
Control	1·30 ± 0·05	100 ± 4
Bumetanide (0·1 mM)	1·34 ± 0·05	103 ± 4

Magnesium uptake was measured over a 30 min period in cells incubated in media (see Methods) containing 5 mM-NaCl, 5 mM-$MgCl_2$ and the additions shown. In groups A and C (including controls) 0·1 mM-bumetanide was also present. The groups represent experiments carried out with blood from different ferrets. The table gives the mean uptake and S.E.M. of three measurements.

145; KOH, 5; HEPES, 7·4, bumetanide, 0·1, $MgCl_2$, 0·2, glucose, 11 and Tris EGTA, 0·05. Samples of the suspension were taken at 15 or 45 min after the start of the incubation. Cells were spun down, washed twice and then suspended in a similar medium but lacking HEPES and with KOH replaced by KCl. The membrane potential scarcely changed (−9·3 ± 0·9 mV at 15 min and −9·7 ± 0·8 mV at 45 min). Thus the magnesium electrochemical gradient is outward when cells are incubated in low-sodium media containing less than 0·3 mM-magnesium. Magnesium uptake observed under these conditions must be active.

Magnesium uptake was also measured under more stringent conditions. External sodium concentration was increased to 10 mM to limit any changes in cell and medium composition. The outward electrochemical gradient for magnesium was increased by reducing the external magnesium concentration to 0·11 mM. Under these conditions an active magnesium uptake of 0·12 ± 0·05 mmol (l cells)$^{-1}$ h^{-1} was observed.

The sensitivity of sodium-dependent magnesium uptake to a variety of transport inhibitors was investigated in order to test the idea that both magnesium influx and

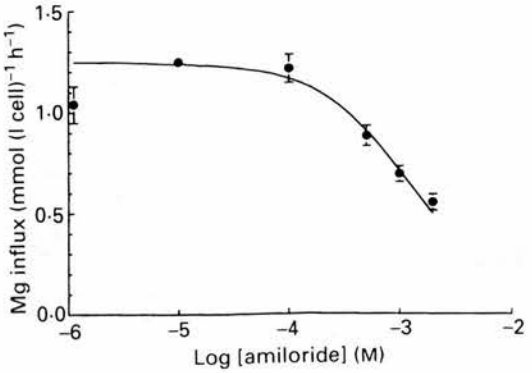

Fig. 4. The effect of amiloride on magnesium uptake by cells incubated in media (see Methods) containing 5 mM-NaCl, 0·1 mM-bumetanide and 5 mM-$MgCl_2$. The symbols show the mean with S.E.M. of three measurements of uptake. Uptake in the absence of amiloride was 1·18±0·07 mmol (l cell)$^{-1}$ h^{-1}. The line is drawn assuming that amiloride inhibits all magnesium uptake and that the K_i is 1·3 mM.

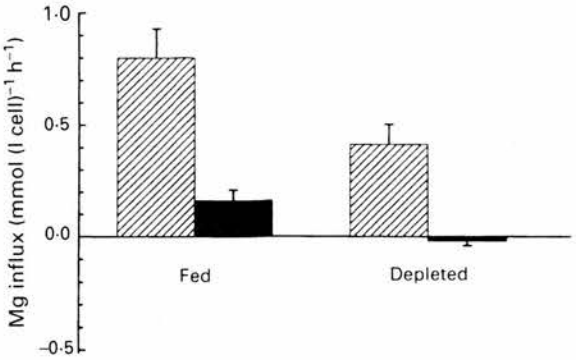

Fig. 5. Magnesium uptake by fed and depleted ferret red cells. The bars show the mean (with S.E.M.) of three measurements of magnesium uptake. The media (see Methods) contained (mM): $MgCl_2$, 5; bumetanide, 0·1 and either NaCl, 5 (hatched bars) or 145 (filled bars). Glucose was omitted from media used to suspend depleted cells. Fed cells had been pre-incubated for 1 h in FBM containing 11 mM-glucose. Their ATP content, measured in the middle of the flux period by the fire-fly assay (Flatman, 1988) was 0·61±0·01 mmol (l cell)$^{-1}$. The ATP content of depleted cells was reduced to 19±0·2 μmol (l cell)$^{-1}$ by incubation for 3 h in FBM containing 11 mM-2-deoxyglucose. Depletion produced no change in water content (0·63 g water (g wet weight)$^{-1}$ over entire period), a small change in chloride distribution ratio ($[Cl]_o/[Cl]_i$, 1·37±0·01 to 1·42±0·03), and a small fall in cell magnesium content (2·58±0·01 to 2·47±0·02 mmol (l cell)$^{-1}$).

magnesium efflux in ferret red cells are mediated by the same transport system. Table 1 shows that magnesium uptake from a medium containing 5 mM-sodium is substantially inhibited by quinidine, imipramine and amiloride, but is not affected by ouabain, bumetanide or 4-acetamido-4′-isothiocyanatostilbene-2,2′-disulphonic acid (SITS). Of these agents only quinidine significantly inhibits magnesium uptake measured in 145 mM-sodium (data not shown). The effects of a range of amiloride concentrations on magnesium uptake in 5 mM-sodium are shown in Fig. 4. Assuming

that amiloride inhibits all the magnesium uptake, the dissociation constant (K_i) for amiloride is 1·3 mM. Unfortunately it is not possible to assess the maximum inhibitory effect of the drug as concentrations above 2 mM caused significant lysis. Thus the sensitivity of magnesium uptake to transport inhibitors is indeed very similar to that reported for magnesium efflux (Flatman & Smith, 1990).

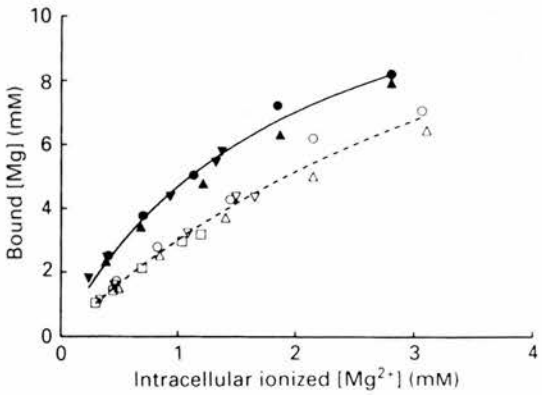

Fig. 6. Magnesium buffering by fed and depleted ferret red cells incubated in FBM. The concentration of bound magnesium in both fed (filled symbols) and depleted (open symbols) cells is plotted as a function of intracellular ionized magnesium concentration determined by the methods of Flatman & Lew (1980) and Flatman (1988). Equilibration of magnesium across the membrane was achieved by adding 10 μM-A23187 to the medium. Fed and depleted cells were produced as described in the legend to Fig. 5. The ATP contents (means ± S.E.M.) of fed and depleted cells were 674 ± 37 ($n = 3$) and 30 ± 7 ($n = 4$) μmol (l cell)$^{-1}$ respectively. The figure shows results of four experiments each represented by a different symbol. Lines are drawn through the data using non-linear regression analysis (Marquardt method) assuming that magnesium binds to a single saturable site. Parameters used for fed cells (continuous line) are: binding capacity, 13·5 ± 0·8 mM: K_m, 1·9 ± 0·2 mM; and for depleted cells (dashed line): binding capacity, 18 ± 2 mM: K_m, 5 ± 1 mM.

Vanadate substantially stimulates magnesium uptake in 5 mM-sodium (Table 1) and at the same time increases cell ATP content. In the experiment shown in Table 1 ATP content increased from a control of 337 (± 5) to 377 (± 8) and 479 (± 13) μmol (l cells)$^{-1}$ 30 min after the addition of 50 and 200 μM-vanadate respectively. Vanadate does not affect the efflux of magnesium into a medium, nominally magnesium-free but containing 145 mM-NaCl (fluxes (μmol (l cells)$^{-1}$ h^{-1}: control, 31 ± 4; 50 μM-vanadate, 30 ± 3; 200 μM-vanadate, 29 ± 5).

Cell ATP content influences the activity of magnesium transport systems in red cells from a variety of species (Günther *et al.* 1984; Féray & Garay, 1986, 1987; Lüdi & Schatzmann, 1987; Frenkel *et al.* 1989). Figure 5 shows the effects of reducing ferret red cell ATP content from its normal value of 610 to 19 μmol (l cells)$^{-1}$ by incubating the cells in 2-deoxyglucose for 3 h. This treatment does not affect cell sodium, potassium or water content or the membrane potential as indicated by the chloride distribution ratio (Flatman, 1991*a*; and see legend to Fig. 5) but it does cause a small reduction in cell magnesium content. Magnesium uptake in both 5 and 145 mM-sodium is reduced significantly. This inhibition may be due to a variety of

factors acting either alone or in combination. The transport system may be ATP-dependent. Inhibition may also reflect an increase in $[Mg^{2+}]_i$ as the concentration of ATP, a major intracellular magnesium buffer, is reduced.

Magnesium buffering curves were constructed for fed and depleted cells to pursue this last idea. Figure 6 shows composite data for a number of experiments. Magnesium buffering is significantly altered in cells treated with 2-deoxyglucose. The cytoplasm behaves as though its affinity for magnesium is much reduced but its capacity is increased. Analysis of these data by the method of Flatman & Lew (1980) indicate that $[Mg^{2+}]_i$ increases from $0{\cdot}73 \pm 0{\cdot}05$ to $1{\cdot}01 \pm 0{\cdot}07$ ($n = 3$) mM following depletion, in spite of a small fall in total cell magnesium. The increase in $[Mg^{2+}]_i$ may contribute to the inhibition of magnesium uptake.

DISCUSSION

Ferret red cells can take up magnesium from the external medium. Uptake is observed when the medium contains more than 1 mM-magnesium and is stimulated by reducing the external sodium concentration. This paper examines the properties of magnesium uptake measured within 40 min of changing external sodium concentration, usually in the presence of bumetanide. Under these conditions cell sodium and potassium content, cell volume and membrane potential change very little.

Magnesium uptake increases to a maximum as the external magnesium concentration is increased. The magnesium concentration required to half-maximally activate the system increases with external sodium concentration. This suggests that raising the concentration of sodium in the medium lowers the affinity of the external magnesium site on the transporter. In addition, very high magnesium concentrations may inhibit magnesium uptake when media contain little sodium.

Magnesium uptake is stimulated by reducing the concentration of external sodium. The concentration of sodium required to produce half-maximal uptake rises with magnesium concentration. Thus increasing the external magnesium concentration reduces the affinity of the external sodium site on the transporter.

Many of the properties of magnesium uptake in ferret red cells are consistent with either of two simple models. One possibility is that all magnesium uptake is via a magnesium channel activated by the removal of external sodium, but this can be ruled out because such a system would not be capable of active magnesium transport. Active transport was demonstrated in ferret red cells incubated in low-sodium media after it had been established that removal of external sodium did not hyperpolarize the membrane potential. The simplest remaining explanation of magnesium uptake is that it occurs via two routes operating in parallel with each other. The majority occurs through sodium–magnesium antiport which can produce active magnesium uptake given a sufficiently large outward sodium gradient. The rest is through a leak pathway which is revealed in the presence of inhibitors.

The interactions between external sodium and magnesium described here are consistent with the expected properties of sodium–magnesium antiport. It is believed that a sodium–magnesium antiport is normally responsible for most of the magnesium efflux observed in these cells (Flatman & Smith, 1990). In principal this system should reverse direction to produce magnesium influx at physiological

sodium concentrations if the external magnesium concentrations exceeds 0·5 mM, assuming a stoichiometry of 1 Na^+:1 Mg^{2+} and a membrane potential of −10 mV. Magnesium uptake was in fact reproducibly observed when there was more than 1 mM-magnesium in the medium. The exact reversal point of the antiport is difficult to assess as some magnesium movement occurs through the leak pathway, whose contribution varies with cells from different ferrets. Movement through the leak, together with slight differences in $[Mg^{2+}]_i$ and membrane potential may explain some of the uptake seen with 0·2 mM-magnesium in Fig. 2. Further evidence that both magnesium influx and efflux occur through the same system is provided by the finding that they have a similar sensitivity to transport inhibitors. Thus influx is significantly reduced by amiloride, quinidine and imipramine but not by ouabain or bumetanide (see Flatman & Smith, 1990).

Transport via sodium–magnesium antiport with a stoichiometry of 1 Na^+:1 Mg^{2+} should be influenced by the membrane potential. There is some evidence for this. The anion-exchange inhibitor SITS stimulates magnesium efflux into a medium containing physiological sodium (Flatman & Smith, 1990) but has little influence on magnesium uptake observed in 5 mM-sodium. Measurements of membrane potential show that SITS depolarizes the membrane potential to about 0 mV when physiological sodium is present but has little effect when the external sodium concentration is low (data not shown).

External magnesium may have a further effect on magnesium uptake at very low external sodium concentrations. For instance, uptake from media containing 10 mM-magnesium is less at 0·8 mM than at 10 mM-sodium (Fig. 9, Flatman & Smith, 1990). This inhibition at very low sodium concentrations is not seen with 5 mM-magnesium (Fig. 3*A*), though the increase in uptake rate as sodium concentration is reduced is often less than expected. In addition, uptake seen with 10 mM-magnesium is often less than with 5 mM-magnesium. It seems that when the external sodium concentration is low, high external magnesium may reduce the turnover of the transporter, perhaps by slowing the rate at which it returns to the initial conformation or by impeding sodium loss. A similar explanation may account for the reduction of magnesium efflux caused by high external sodium when media contain very little magnesium (Flatman & Smith, 1990). In this case sodium may slow the return of the carrier to the original conformation or impede magnesium loss.

Without a reasonably specific inhibitor of sodium–magnesium antiport it is difficult to demonstrate a direct effect of intracellular ATP on uptake through the transporter. It is evident, however, that total uptake continues, albeit at a reduced rate, for several hours in cells containing very little ATP. Analysis is complicated by the possibility that transport via both antiport and leak pathways is affected by changes in ATP levels. At least part of the inhibitory effect of reducing cell ATP might be attributed to the increased $[Mg^{2+}]_i$ seen under these conditions.

Magnesium transport in a variety of cells has a demonstrable requirement for ATP (DiPolo & Beaugé, 1988; Frenkel *et al.* 1989) and it has been suggested that the magnesium transporter may be an ATPase or be activated by phosphorylation. The results described here do not exclude the idea that phosphorylation of the transporter may change its activity perhaps by changing ion binding affinities.

Vanadate has a wide range of effects on membrane transport and cell function (Ramasarma & Crane, 1981; Nechay, 1984). Micromolar concentrations potently

inhibit plasma membrane sodium, calcium and hydrogen pumps (O'Neal, Rhoads & Racker, 1979; Beaugé, Cavieres, Glynn & Grantham, 1980; Rossi, Garrahan & Rega, 1981; Faller, Jackson, Malinowska, Mukidjam, Rabon, Saccomani, Sachs & Smolka, 1982). However, 200 μM-vanadate did not inhibit magnesium efflux from ferret red cells. Frenkel *et al.* (1989) have reported that sodium-dependent magnesium efflux from human red cells is also insensitive to vanadate. These findings support the idea that magnesium efflux from these cells is not mediated by a magnesium pump belonging to the same family as the sodium, calcium or hydrogen pumps.

Vanadate stimulates magnesium uptake from low-sodium media and at the same time increases cell ATP content. The changes in ATP content are similar to those seen when ferret red cells incubated in media containing 145 mM-sodium are treated with vanadate (Flatman, 1991*a*). Transport stimulation may result from both a direct effect of vanadate on the transporter and via the changes in ATP concentration. This stimulation may also be modified by changes in $[Mg^{2+}]_i$ due to altered magnesium buffering. Vanadate may directly stimulate sodium–magnesium antiport, as it does sodium–calcium exchange (DiPolo, 1989). If this comparison is appropriate then vanadate should also stimulate magnesium efflux on the antiport. The absence of any effect of vanadate on magnesium efflux indicates either that in efflux mode the transporter is insensitive to vanadate or that any stimulation is offset by a reduction in $[Mg^{2+}]_i$. Experiments are now under way to clarify some of these possibilities.

The source of energy for active magnesium transport has received much recent attention (Flatman, 1991*b*). It seems likely that sodium–magnesium antiport mediates most of the active magnesium transport seen in squid axons under physiological conditions (DiPolo & Beaugé, 1988). Sodium–magnesium antiport has also been proposed as the magnesium regulator in guinea-pig ventricle (Fry, 1986), frog skeletal muscle (Blatter, 1990) and in guinea-pig taenia caeci (Nakayama & Tomita, 1991), though in the latter case it may be operating in parallel with a magnesium pump. Buri & McGuigan (1990) believe that $[Mg^{2+}]_i$ is regulated by a sodium-dependent magnesium pump in ferret papillary muscle. Magnesium transport in human red cells has been described as a sodium–magnesium pump which probably obtains energy from ATP or a related compound (Frenkel *et al.* 1989). Magnesium transport in chicken red cells has been described as electroneutral 2 Na^+:1 Mg^{2+} antiport (Günther & Vormann, 1985*b*). However, this system, like that in human cells, is though to be incapable of using energy stored in the sodium gradient.

This paper adds support to the idea that magnesium transport in ferret red cells is largely the result of the activity of a sodium–magnesium antiport. The system is reversible and at low external sodium concentrations can carry large amounts of magnesium into the cell. The system is capable of active magnesium transport provided there is a suitable sodium gradient. ATP does not appear to provide energy for this process, but may have some other role.

There is still speculation that magnesium and calcium share the same transporter, at least in some situations (see Flatman, 1991*b*). Milanick (1989) has demonstrated substantial calcium uptake in ferret red cells when the calcium pump is inhibited with vanadate. The properties of transport are consistent with sodium–calcium exchange. The system is capable of active calcium transport using energy from the

sodium gradient. ATP and possibly vanadate activate calcium uptake (Frame & Milanick, 1990). Thus ferret red cells show both sodium–calcium and sodium–magnesium antiport activity with strikingly similar properties. One avenue for future work is to see whether this is one and the same transporter.

We should like to thank the Wellcome Trust for support and J. Morris for reading the manuscript.

REFERENCES

BEAUGÉ, L. A., CAVIERES, J. D., GLYNN, I. M. & GRANTHAM, J. J. (1980). The effects of vanadate on the fluxes of sodium and potassium ions through the sodium pump. *Journal of Physiology* **301**, 7–23.

BLATTER, L. A. (1990). Intracellular free magnesium in frog skeletal muscle studied with a new type of magnesium-selective microelectrode: interactions between magnesium and sodium in the regulation of $[Mg]_i$. *Pflügers Archiv* **416**, 238–246.

BURI, A. & MCGUIGAN, J. A. S. (1990). Intracellular free magnesium and its regulation, studied in isolated ferret ventricular muscle with ion-selective microelectrodes. *Experimental Physiology* **75**, 751–761.

DIPOLO, R. (1989). The sodium–calcium exchange in intact cells. In *Sodium–Calcium Exchange*, ed. ALLEN, T. J. A., NOBLE, D. & REUTER, H., pp. 5–26. Oxford University Press, Oxford.

DIPOLO, R. & BEAUGÉ, L. (1988). An ATP-dependent Na^+/Mg^{2+} countertransport is the only mechanism for Mg extrusion in squid axons. *Biochimica et Biophysica Acta* **946**, 424–428.

FALLER, L., JACKSON, R., MALINOWSKA, D., MCKIDJAM, E., RABON, E., SACCOMANI, G., SACHS, G. & SMOLKA, A. (1982). Mechanistic aspects of gastric $(H^+ + K^+)$-ATPase. *Annals of the New York Academy of Sciences* **402**, 146–163.

FÉRAY, J.-C. & GARAY, R. (1986). An Na^+-stimulated Mg^{2+}-transport system in human red blood cells. *Biochimica et Biophysica Acta* **856**, 76–84.

FÉRAY, J.-C. & GARAY, R. (1987). A one-to-one $Mg^{2+}:Mn^{2+}$ exchange in rat erythrocytes. *Journal of Biological Chemistry* **262**, 5763–5768.

FLATMAN, P. W. (1988). The effects of magnesium on potassium transport in ferret red cells. *Journal of Physiology* **397**, 471–487.

FLATMAN, P. W. (1991*a*). The effects of metabolism on Na^+–K^+–Cl^- co-transport in ferret red cells. *Journal of Physiology* **437**, 495–510.

FLATMAN, P. W. (1991*b*). Mechanisms of magnesium transport. *Annual Review of Physiology* **53**, 259–271.

FLATMAN, P. W. & ANDREWS, P. L. R. (1983). Cation and ATP content of ferret red cells. *Comparative Biochemistry and Physiology* **74A**, 939–943.

FLATMAN, P. W. & LEW, V. L. (1980). Magnesium buffering in intact human red blood cells measured using the ionophore A23187. *Journal of Physiology* **305**, 13–30.

FLATMAN, P. W. & SMITH, L. M. (1990). Magnesium transport in ferret red cells. *Journal of Physiology* **431**, 11–25.

FRAME, M. D. & MILANICK, M. A. (1990). ATP increases Na/Ca and Na/Mn exchange in resealed ferret red blood cell ghosts. *Biophysical Journal* **57**, 180*a*.

FRENKEL, E. J., GRAZIANI, M. & SCHATZMANN, H. J. (1989). ATP requirement of the sodium-dependent magnesium extrusion from human red blood cells. *Journal of Physiology* **414**, 385–397.

FRY, C. H. (1986). Measurement and control of intracellular magnesium ion concentration in guinea pig and ferret ventricular myocardium. *Magnesium* **5**, 306–316.

GÜNTHER, T. & EBEL, H. (1990). Membrane transport of magnesium. In *Metal Ions in Biological Systems*, vol. 26, ed. SIGEL, H. & SIGEL, A., pp. 215–225. Marcel Dekker, New York.

GÜNTHER, T. & VORMANN, J. (1985*a*). Removal and reuptake of intracellular magnesium. *Magnesium Bulletin* **2**, 66–69.

GÜNTHER, T. & VORMANN, J. (1985*b*). Mg^{2+} efflux is accomplished by an amiloride-sensitive Na^+/Mg^{2+} antiport. *Biochemical and Biophysical Research Communications* **130**, 540–545.

GÜNTHER, T., VORMANN, J. & FÖRSTER, R. (1984). Regulation of intracellular magnesium by Mg^{2+} efflux. *Biochemical and Biophysical Research Communications* **119**, 124–131.

HALPERIN, J. A., BRUGNARA, C., TOSTESON, M. T., VAN HA, T. & TOSTESON, D. C. (1989). Voltage-activated cation transport in human erythrocytes. *American Journal of Physiology* **257**, C986–996.

LÜDI, H. & SCHATZMANN, H. J. (1987). Some properties of a system for sodium-dependent outward movement of magnesium from metabolizing human red blood cells. *Journal of Physiology* **390**, 367–382.

MACEY, R. I., ADORANTE, J. S. & ORME, F. W. (1978). Erythrocyte membrane potentials determined by hydrogen ion distribution. *Biochimica et Biophysica Acta* **512**, 284–295.

MILANICK, M. A. (1989). Na–Ca exchange in ferret red blood cells. *American Journal of Physiology* **256**, C390–398.

NAKAYAMA, S. & TOMITA, T. (1991). Regulation of intracellular free magnesium concentration in the taenia of guinea-pig caecum. *Journal of Physiology* **435**, 559–572.

NECHAY, B. R. (1984). Mechanisms of action of vanadium. *Annual Review of Pharmacology and Toxicology* **24**, 501–524.

O'NEAL, S. G., RHOADS, D. B. & RACKER, E. (1979). Vanadate inhibition of sarcoplasmic reticulum Ca^{2+}-ATPase and other ATPases. *Biochemical and Biophysical Research Communications* **89**, 845–850.

ORTIZ, O. E., LEW, V. L. & BOOKCHIN, R. M. (1990). Deoxygenation permeabilizes sickle cell anaemia red cells to magnesium and reverses its gradient in the dense cells. *Journal of Physiology* **427**, 211–226.

RAMASARMA, T. & CRANE, F. L. (1981). Does vanadium play a role in cellular regulation? *Current Topics in Cellular Regulation* **20**, 247–301.

ROSSI, J. P. F. C., GARRAHAN, P. J. & REGA, A. F. (1981). Vanadate inhibition of active Ca^{2+} transport across human red cell membranes. *Biochimica et Biophysica Acta* **648**, 145–150.